MOSCOW CENTER
FOR DIAGNOSTICS & TELEMEDICINE

ISSN 2712-8490 (Print)
ISSN 2712-8962 (Online)

DIGITAL DIAGNOSTICS

A peer-reviewed scientific medical journal

5 Volume 1 Issue

Artificial intelligence in medicine

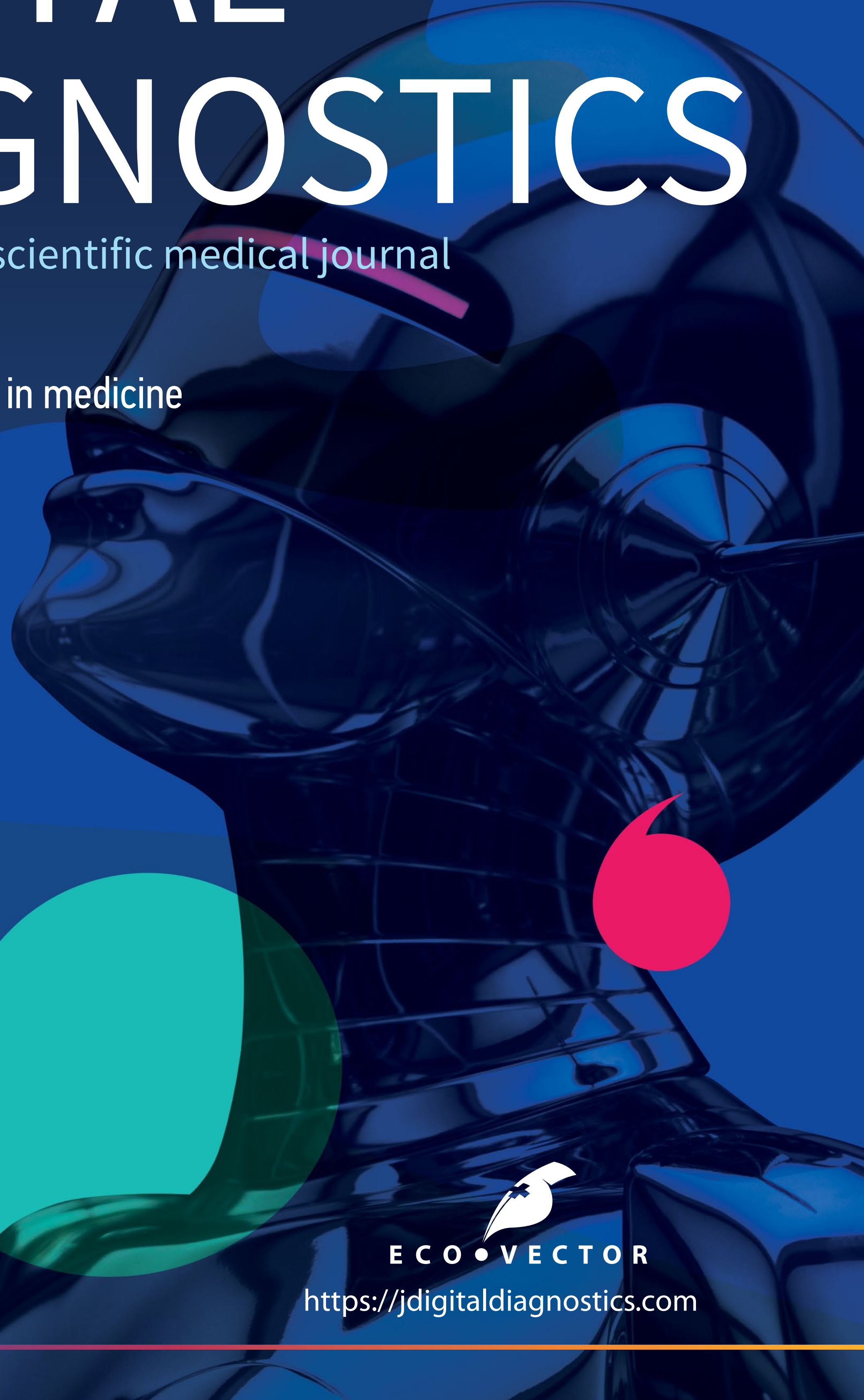

ECO•VECTOR

2024

https://jdigitaldiagnostics.com

УЧРЕДИТЕЛИ

- ГБУЗ «Научно-практический клинический центр диагностики и телемедицинских технологий ДЗМ»
- ООО «Эко-Вектор»

Свидетельство о регистрации СМИ ПИ
ПИ № ФС 77 - 79539 от 09.11.2020

ИЗДАТЕЛЬ

ООО «Эко-Вектор»
Адрес: 191186, Санкт-Петербург, Аптекарский переулок, д. 3, литера А, помещение 1Н
E-mail: info@eco-vector.com
WEB: https://eco-vector.com

РЕКЛАМА

Отдел рекламы
Тел.: +7 (968) 545 78 20
E-mail: adv2@eco-vector.com

РЕДАКЦИЯ

Зав. редакцией
Елена Андреевна Филиппова
E-mail: ddjournal@eco-vector.com
Тел: +7 (965) 012 70 72
Адрес: 125040, г. Москва,
ул. Расковой, д. 16/26, стр. 1

ПОДПИСКА

Подписка на печатную версию через интернет:
www.journals.eco-vector.com/
www.akc.ru
www.pressa-rf.ru

OPEN ACCESS

В электронном виде журнал распространяется бесплатно —
в режиме немедленного открытого доступа

ИНДЕКСАЦИЯ

- SCOPUS
- РИНЦ
- Google Scholar
- Ulrich's International Periodicals Directory
- WorldCat

Оригинал-макет
подготовлен в издательстве «Эко-Вектор».
Литературный редактор: *А.А. Ридэль*
Корректор: *А.А. Ридэль*
Вёрстка: *Ф.А. Игнащенко*
Обложка: *Е.Д. Бугаенко*

Сдано в набор 14.03.2024. Подписано в печать 29.03.2024.
Выход в свет 20.04.2024. Формат 60 × 88⅛.
Печать офсетная. Печ. л. 17. Усл. печ. л. 15,8.
Уч.-изд. л. 9,3. Тираж 5000 экз.
Цена свободная.

Отпечатано в ООО «Типография Фурсова».
196105, Санкт-Петербург, ул. Благодатная, 69.
Тел.: +7 (812) 646-33-77

16+

ISSN 2712-8490 (Print)
ISSN 2712-8962 (Online)

Digital Diagnostics

Том 5 | Выпуск 1 | 2024

ЕЖЕКВАРТАЛЬНЫЙ РЕЦЕНЗИРУЕМЫЙ НАУЧНЫЙ МЕДИЦИНСКИЙ ЖУРНАЛ

ЭКО • ВЕКТОР

FOUNDERS
- Moscow Center for Diagnostics and Telemedicine
- Eco-Vector

PUBLISHER
Eco-Vector
Address: 3 liter A, 1H, Aptekarsky pereulok, 191186, Saint Petersburg, Russian Federation
E-mail: info@eco-vector.com
WEB: https://eco-vector.com

ADVERTISE
Adv. department
Phone: +7 (968) 545 78 20
E-mail: adv2@eco-vector.com

EDITORIAL OFFICE
Executive editor
Elena A. Philippova
E-mail: ddjournal@eco-vector.com
Phone: +7 (965) 012 70 72

SUBSCRIPTION
For print version:
www.journals.eco-vector.com/

PUBLICATION ETHICS
Journal's ethic policies are based on:
- ICMJE
- COPE
- ORE
- CSE
- EASE

OPEN ACCESS
Immediate Open Access is mandatory for all published articles

INDEXATION
- SCOPUS
- Russian Science Citation Index
- Google Scholar
- Ulrich's International Periodicals Directory
- WorldCat

TYPESET
completed in Eco-Vector
Copyeditor: *A.A. Ridel*
Proofreader: *A.A. Ridel*
Layout editor: *Ph. Ignashchenko*
Cover: *E. Bugaenko*

16+

ISSN 2712-8490 (Print)
ISSN 2712-8962 (Online)

Digital Diagnostics

Volume 5 | Issue 1 | 2024

QUARTERLY PEER-REVIEWED MEDICAL JOURNAL

ECO•VECTOR

В ВЫПУСКЕ

материалы лучших докладов конференции

ВТОРОЙ ВСЕРОССИЙСКИЙ САММИТ С МЕЖДУНАРОДНЫМ УЧАСТИЕМ

по использованию алгоритмов искусственного интеллекта
для решения научных и прикладных задач
в области офтальмологии

ИСКУССТВЕННЫЙ ИНТЕЛЛЕКТ В ОФТАЛЬМОЛОГИИ

9 декабря 2023 года

город Москва

WEB: https://aio-summit.ru/

IT THE ISSUE

conference proceedings articles

SECOND ALL-RUSSIAN SUMMIT WITH INTERNATIONAL PARTICIPATION

artificial intelligence algorithms
to solve scientific and applied problems
in the field of ophthalmology

ARTIFICIAL INTELLIGENCE IN OPHTHALMOLOGY

9 December 2023
Moscow
WEB: https://aio-summit.ru/

СОДЕРЖАНИЕ

ОРИГИНАЛЬНЫЕ ИССЛЕДОВАНИЯ

СИСТЕМАТИЧЕСКИЕ ОБЗОРЫ

НАУЧНЫЕ ОБЗОРЫ

CONTENTS

ORIGINAL STUDY ARTICLES

SYSTEMATIC REVIEWS

REVIEWS

DOI: https://doi.org/10.17816/DD623801

Классификация снимков оптической когерентной томографии с использованием методов глубокого машинного обучения

А.А. Арзамасцев[1,2], О.Л. Фабрикантов[2], Е.В. Кулагина[2], Н.А. Зенкова[3]

[1] Воронежский государственный университет, Воронеж, Россия;
[2] Национальный медицинский исследовательский центр «Межотраслевой научно-технический комплекс “Микрохирургия глаза” имени академика С.Н. Фёдорова», Тамбов, Россия;
[3] Тамбовский государственный университет имени Г.Р. Державина, Тамбов, Россия

АННОТАЦИЯ

Обоснование. Оптическая когерентная томография — современный высокотехнологичный и информативный метод выявления патологии сетчатки глаза и преретинальных слоёв стекловидного тела. Однако описание и интерпретация результатов исследования требуют высокой квалификации и специальной подготовки врача-офтальмолога, а также значительных временных затрат врача и пациента. Вместе с тем использование математических моделей на основе аппарата искусственных нейронных сетей в настоящее время позволяет автоматизировать многие процессы, связанные с обработкой изображений. Именно поэтому актуально решение задач, связанных с автоматизацией процесса классификации снимков оптической когерентной томографии на основе глубокого обучения моделей искусственных нейронных сетей.

Цель — разработать архитектуры математических (компьютерных) моделей на основе глубокого обучения свёрточных нейронных сетей, предназначенных для классификации снимков оптической когерентной томографии сетчатки глаза; сравнить результаты вычислительных экспериментов, проведённых с использованием средств Python в Google Colaboratory при одно- и многомодельном подходах, и выполнить оценки точности классификации; сделать выводы об оптимальной архитектуре моделей искусственных нейронных сетей и значениях используемых гиперпараметров.

Материалы и методы. Исходный датасет, представляющий собой обезличенные снимки оптической когерентной томографии реальных пациентов, включал более 2000 изображений, полученных непосредственно с прибора в разрешении 1920×969×24 BPP. Количество классов изображений — 12. Для создания обучающего и валидационного наборов данных осуществляли «вырезание» предметной области 1100×550×24 BPP. Изучали различные подходы: возможность использования предобученных свёрточных нейронных сетей с переносом обучения, методики изменения размера и аугментации изображений, а также различные сочетания гиперпараметров моделей искусственных нейронных сетей. При компиляции модели использовали следующие параметры: оптимизатор Adam, функцию потерь categorical_crossentropy, метрику accuracy. Все технологические процессы с изображениями и моделями искусственных нейронных сетей проводили с использованием средств языка Python в Google Colaboratory.

Результаты. Предложены одно- и многомодельный принципы классификации изображений оптической когерентной томографии сетчатки глаза. Вычислительные эксперименты по автоматизированной классификации таких изображений, полученных с томографа DRI OCT Triton, с использованием различных архитектур моделей искусственных нейронных сетей показали точность при обучении и валидации 98–100%, и на дополнительном тесте — 85%, что является удовлетворительным результатом. Выбрана оптимальная архитектура модели искусственной нейронной сети — 6-слойная свёрточная сеть, — и определены значения её гиперпараметров.

Заключение. Результаты глубокого обучения моделей свёрточных нейронных сетей с различной архитектурой, их валидации и тестирования показали удовлетворительную точность классификации снимков оптической когерентной томографии сетчатки глаза. Данные разработки могут быть использованы в системах поддержки принятия решений в области офтальмологии.

Ключевые слова: искусственный интеллект; медицинские данные; датасет; машинное обучение; свёрточные нейронные сети; оптическая когерентная томография.

Как цитировать:
Арзамасцев А.А., Фабрикантов О.Л., Кулагина Е.В., Зенкова Н.А. Классификация снимков оптической когерентной томографии с использованием методов глубокого машинного обучения // Digital Diagnostics. 2024. Т. 5, № 1. С. 5–16. DOI: https://doi.org/10.17816/DD623801

Рукопись получена: 24.11.2023 **Рукопись одобрена:** 12.02.2024 **Опубликована online:** 11.03.2024

DOI: https://doi.org/10.17816/DD623801

Classification of optical coherence tomography images using deep machine-learning methods

Alexander A. Arzamastsev[1, 2], Oleg L. Fabrikantov[2], Elena V. Kulagina[2], Natalia A. Zenkova[3]

[1] Voronezh State University, Voronezh, Russia;
[2] The S. Fyodorov Eye Microsurgery Federal State Institution, Tambov, Russia;
[3] Derzhavin Tambov State University, Tambov, Russia

ABSTRACT

BACKGROUND: Optical coherence tomography is a modern high-tech, insightful approach to detecting pathologies of the retina and preretinal layers of the vitreous body. However, the description and interpretation of study findings require advanced qualifications and special training of ophthalmologists and are highly time-consuming for both the doctor and the patient. Moreover, mathematical models based on artificial neural networks now allow for the automation of many image processing tasks. Therefore, addressing the issues of automated classification of optical coherence tomography images using deep learning artificial neural network models is crucial.

AIM: To develop architectures of mathematical (computer) models based on deep learning of convolutional neural networks for the classification of retinal optical coherence tomography images; to compare the results of computational experiments conducted using Python tools in Google Colaboratory with single-model and multimodel approaches, and evaluate classification accuracy; and to determine the optimal architecture of models based on artificial neural networks, as well as the values of the hyperparameters used.

MATERIALS AND METHODS: The original dataset included >2,000 anonymized optical coherence tomography images of real patients, obtained directly from the device with a resolution of 1,920×969×24 BPP. The number of image classes was 12. To create the training and validation datasets, a subject area of 1,100×550×24 BPP was “cut out”. Various approaches were studied: the possibility of using pretrained convolutional neural networks with transfer learning, techniques for resizing and augmenting images, and various combinations of the hyperparameters of models based on artificial neural networks. When compiling a model, the following parameters were used: Adam optimizer, categorical_crossentropy loss function, and accuracy. All technological operations involving images and models based on artificial neural networks were performed using Python language tools in Google Colaboratory.

RESULTS: Single-model and multimodel approaches to the classification of retinal optical coherence tomography images were developed. Computational experiments on the automated classification of such images obtained from a DRI OCT Triton tomograph using various architectures of models based on artificial neural networks showed an accuracy of 98–100% during training and validation, and 85% during an additional test, which is a satisfactory result. The optimal architecture of the model based on an artificial neural network, a six-layer convolutional network, was selected, and the values of its hyperparameters were determined.

CONCLUSION: Deep training of convolutional neural network models with various architectures, as well as their validation and testing, resulted in satisfactory classification accuracy of retinal optical coherence tomography images. These findings can be used in decision support systems in ophthalmology.

Keywords: artificial intelligence; medical data; dataset; machine learning; convolutional neural networks; optical coherence tomography.

To cite this article:
Arzamastsev AA, Fabrikantov OL, Kulagina EV, Zenkova NA. Classification of optical coherence tomography images using deep machine-learning methods. *Digital Diagnostics*. 2024;5(1):5–16. DOI: https://doi.org/10.17816/DD623801

Submitted: 24.11.2023 **Accepted:** 12.02.2024 **Published online:** 11.03.2024

ECO•VECTOR

DOI: https://doi.org/10.17816/DD623801

利用深度机器学习技术对光学相干断层扫描图片进行分类

Alexander A. Arzamastsev[1, 2], Oleg L. Fabrikantov[2], Elena V. Kulagina[2], Natalia A. Zenkova[3]

[1] Voronezh State University, Voronezh, Russia;
[2] The S. Fyodorov Eye Microsurgery Federal State Institution, Tambov, Russia;
[3] Derzhavin Tambov State University, Tambov, Russia

摘要

论证。光学相干断层扫描是一种现代高科技和信息丰富的方法，用于检测视网膜和玻璃体视网膜前层的病理。然而，对研究结果的描述和解释需要眼科医生的高技能和专业培训，还需要医生和病人花费大量时间。与此同时，如今使用基于人工神经网络设备的数学模型可以实现许多图片处理过程的自动化。因此，在人工神经网络模型深度学习的基础上解决光学相干断层扫描图片分类过程的自动化问题具有现实意义。

目的。本研究的目的是开发基于卷积神经网络深度学习的数学（计算机）模型结构，此类网络设计被用于视网膜光学相干断层扫描的的图像分类；使用Google Colaboratory的Python工具，比较单一模型和多模型方法的计算实验结果，并评估分类准确性；就人工神经网络模型的最佳架构和所使用的超参数值得出结论。

材料与方法。原始数据集是真正患者的匿名光学相干断层扫描图像，其中包括2000多张图像。图像直接从设备中获取，分辨率为1920×969×24 BPP。图像类别数量为12个。为了创建训练和验证数据集，对1100×550×24 BPP主题区域进行了“切割”。研究了不同的方法：使用带学习转移的预训练卷积神经网络的可能性、图像缩放和增强技术，以及人工神经网络模型超参数的不同组合。在编制模型时，使用了以下参数：Adam优化器、categorical_crossentropy损失函数、accuracy指标。所有图像和人工神经网络模型的技术处理都是通过Google Colaboratory的Python语言工具进行的。

结果。提出了视网膜光学相干断层扫描图片分类的单模型和多模型原理。使用不同的人工神经网络模型架构对来自DRI OCT Triton断层扫描仪的此类图像进行自动分类的计算实验表明了，训练和验证期间的准确率为98%-100%，额外测试的准确率为85%。这是一个令人满意的结果。人工神经网络模型的最佳架构是6层卷积网络，并确定了其超参数值。

结论。对不同结构的卷积神经网络模型进行深度学习、验证和测试的结果表明，视网膜光学相干断层扫描图片分类的准确度令人满意。这些研制成果可被用于眼科领域的决策支持系统。

关键词：人工智能；医学数据；数据集；机器学习；卷积神经网络；光学相干断层扫描。

引用本文：
Arzamastsev AA, Fabrikantov OL, Kulagina EV, Zenkova NA. 利用深度机器学习技术对光学相干断层扫描图片进行分类. *Digital Diagnostics*. 2024;5(1):5–16. DOI: https://doi.org/10.17816/DD623801

收到：24.11.2023 **接受：**12.02.2024 **发布日期：**11.03.2024

BACKGROUND

Optical coherence tomography (OCT) is a modern, high-tech, conclusive method for detecting retinal and preretinal vitreous abnormalities [1]. However, describing and interpreting the examination results requires highly skilled and trained HCPs and a considerable duration on the part of ophthalmologists and patients. Therefore, we must solve issues associated with the automation of OCT image classification.

Computerized tools and technologies are rapidly evolving to build artificial intelligence (AI) systems based on neural networks with various architectures, for medical [2, 3] and general use [4–6]. In the past decades, advanced ophthalmology centers have created repositories of patient data with hundreds of thousands of OCT images, paving the pathway to (i) search for generalized dependencies and relationships between individual parameters and (ii) construct fundamentally new, science-based approaches for identification, classification, calculation, and prediction, all of which are almost always centered on a mathematical model.

In one of our papers, we have already described computerized methods for the examination of the vitreous body, identification and approximation of the retinal border, determination of its curvature, calculation of average retinal thickness, among others; one of these methods include artificial neural networks (ANNs) [7]. This study is a logical continuation of that research and presents results of OCT image classification achieved via convolutional neural networks (CNNs) using single- and multi-model approaches.

There have been many publications on similar topics. For example, Yu. A. Vasiliev et al. [8] developed a general, AI-based methodology for software testing and monitoring in medical diagnostics. The methodology enhanced the quality of this software and implementation in clinical practice. It consisted of seven steps: self-testing, functional testing, calibration testing, process monitoring, clinical monitoring, feedback, and improvement. The methodology was characterized by the cyclical phases of testing, monitoring, and improving the software for continuous improvement of software quality, detailed requirements for outcomes, and involvement of HCPs in software evaluation. The methodology allowed software developers to achieve remarkable results in various areas and enabled users to make informed and confident choices from programs that passed an independent and comprehensive quality check.

Katalevskaya et al. [9] developed algorithms for segmentation of visual signs of diabetic retinopathy and diabetic macular edema in digital fundus images acquired using a fundus camera. Features included in the International Classification were selected for segmentation: microaneurysms, hard exudates, soft exudates, intraretinal hemorrhages, retinal and optic disc neovascularization, preretinal hemorrhages, epiretinal membranes, and laser coagulates. Neural networks were implemented and trained using the deep-learning framework TensorFlow (Google Brain, USA). The training database contained 1,200 images, and 310 fundus images were used for validation. The accuracy of identifying these features by the trained model ranged from 86% to 96%.

T. Kerr et al. [10] described a home monitoring system for age-related macular degeneration. CNNs were used to segment the entire retina and pigment epithelial detachments. The dataset of 711 images was divided into training/validation/test image sets in the ratio of 60%:20%:20%. The CNN-based approach reportedly provided accurate retinal segmentation.

Sakhnov et al. [11] developed a cataract screening model based on an open dataset to validate the model based on clinical data. The open dataset comprised 9,668 images acquired using a smartphone camera, of which 4,514 were for "cataract" eyes and 5,154 for "healthy" eyes. The external validation set included 51 cataract and normal images. A machine learning model was built using CNN. The accuracy of data classification was 97% for the internal validation set and 75% for the external validation set. These authors noted predictive value to be low and concluded that they needed to refine their model to meet the performance metrics.

Shukhaev et al. [12] employed the pretrained networks ResNet-18, ResNet-50, VGG16, VGG19, and GoogleNet to solve the problem of using CNNs for automatic detection of Fuchs' dystrophy. A random sample (n = 700) of corneal biomicroscopic images was obtained using a Tomey EM-3000 endothelial microscope (Tomey Corporation, Japan). In the first step, the images were categorized into two groups: the first group included images showing Fuchs' dystrophy, whereas the other one included normal images or images of other abnormalities. The images of the endothelial cell density were arranged into three categories: training, validation, and test datasets. The following F-metric values were obtained while testing the neural network on a test sample for various CNN architectures: ResNet-18, 0.985; ResNet-50, 1.000; VGG16, 0.940; VGG19, 0.990; and GoogleNet, 0.987. ResNet-50 demonstrated the optimum performance with ImageNet data that had frozen layers, Adam optimization algorithm, and cross-entropy as the loss function.

Therefore, a brief analysis of the abovementioned studies allowed us to conclude the prospects of use of CNN-based ANN models for retinal OCT image classification.

AIMS

Our objectives were:

1. to develop architectures of mathematical (computerized) models based on deep-learning CNN for classifying OCT images using the libraries Python Keras and TensorFlow in Google Colaboratory,
2. to compare the results of computational experiments to classify OCT images obtained using single- and multi-model approaches and to evaluate the accuracy of such classifications, and

3. to conclude on the optimal architecture of ANN models regarding classification accuracy and the hyperparameter values used.

MATERIALS AND METHODS

The initial dataset comprised anonymized OCT images of real patients and included 1,004 images directly obtained as JPG files from the DRI-OCT Triton tomograph (Topcon Corporation, Japan) at a resolution of 1,920 × 969 × 24 BPP. For classification purposes, the entire dataset was categorized into the following 12 classes by experienced ophthalmologists:

1. Normal
2. Cystoid macular edema
3. Neuroepithelial detachment
4. Pigment epithelial detachment
5. Hard exudates
6. Epiretinal membranes
7. Vitreomacular adhesion
8. Posterior vitreous detachment
9. Full-thickness macular hole + epiretinal membrane
10. Hard exudates + cystoid macular edema
11. Pigment epithelial drusen
12. Lamellar macular hole + epiretinal membrane

The number of images in each class corresponded to the incidence of the corresponding abnormality in the patients. In subsequent computational experiments, new OCT images were added to the dataset, following which the total number of images exceeded 2,000. A fragment of 1,100 × 550 × 24 BPP was cropped from the entire subject area image to create the training, validation, and test datasets. In computational experiments, the entire data set was usually divided into training, validation, and test sets in the ratio of 70%:20%:10%.

The following technological methods were also used:

- Image rescaling using filters NEAREST, BILINEAR, BICUBIC, and LANCZOS
- Data augmentation via various options, such as image rotation by a given angle, shifting the image along the X and Y axes, horizontal and vertical rotation, and changing the brightness of the image channel

The optimum results in this study were obtained with the simplest NEAREST filter, which uses the parameters of nearest pixel. More complex filters that approximate the region using different methods gave poorer results, apparently because small image details important for classification were lost during the smoothing process.

The following parameters were used while compiling the model:

- Adam optimizer as one of the most effective optimization algorithms
- Categorical_crossentropy loss function
- Accuracy metric as percentage of correct answers given by the algorithm

The accuracy metric is usually used to solve classification problems when the number of images between the groups is balanced. Herein, we estimated an overall average because of the small number of images in the training and test sets. Python language tools were used in Google Colaboratory for all technological processes with the models.

RESULTS

Preliminary computational experiments

Herein, we evaluated the effectiveness of various approaches to OCT image classification (such as the possibility of employing pretrained networks and transfer learning), image rescaling and augmentation techniques, and combinations of ANN model hyperparameters (number of convolutional and fully connected layers, batch size, among others).

For pretrained neural networks based on MobileNetV2 and MobileNetV3, the accuracies were 95%–98%, 61%–80%, and 41%–59% on the training, validation, and test sets, respectively. The image was scaled to 224 × 224 pixels to fit MobileNet.

Moreover, the abilities of different pretrained neural networks to learn using the given dataset were compared with transfer learning. The validation results were 80%, 81%, 79%, and 80% for MobileNetV2, ResNet101V2, InceptionResNetV2, and NASNetLarge, respectively.

For multilayer CNNs with traditional architecture (several Conv2D convolutional layers, each with a MaxPooling2D subsampling function, transforming the data pools into a one-dimensional Flatten tensor and several fully connected Dense layers), the accuracy of 70%–100% was achieved on the training set with a reasonable selection of epoch number. Comparatively, in the validation set, this number was considerably lower and had a wider range (35%–94%). In both cases, the validation accuracy was higher than the training accuracy, which may be ascribed to considerable heterogeneity in the training and validation datasets. The test accuracy was even lower, ranging from 27% to 59%, which is obviously not a satisfactory result.

The following conclusions were drawn after the preliminary experiments:

- The training set was unbalanced and heterogeneous and required correction and supplementation with new images.
- Although transfer learning models showed slightly better classification results, these results were inappropriate for ophthalmology practice. In addition, there were not many opportunities for improvement because of the freezing of the first hidden layers.
- The hyperparameters and the classification approach must be optimized to achieve acceptable classification accuracy.

Computational experiments: a single-model approach

Based on the preliminary experiments, new OCT images were added to the dataset, after which the total number of images increased to >2,000. The experiments tested various architectures of multilayer sequential CNNs, such as Several Conv2D convolutional layers, each with a MaxPooling2D subsampling layer and a layer that transformed into a one-dimensional Flatten tensor, and two fully connected Dense layers, the latter featuring the Softmax neuron transfer function suitable for solving classification problems.

The maximum number of convolutional layers is seven for a normalized image resolution of 512 × 512 pixels. All images in the dataset were rescaled using the Rescale tool. We tested CNN structures with two–seven such layers (Table 1) with simultaneous selection of the size and number of filters in the layers. Training was performed (typically with epochs = 15, BATCH_SIZE = 50, optimizer = "Adam," loss = "categorical_crossentropy," and metric = ["accuracy"]) for all computational experiments, as well as for validation and additional testing with images not previously included in the dataset.

Acceptable training and validation accuracies were achieved for almost all ANN models, except for the two-layer model (Table 1). However, the additional testing accuracy first increased with increasing number of convolutional layers, reaching a maximum value of 85% for the six-layer model and decreasing for the seven-layer model. Notably, the models presented here are currently positioned solely as a decision support system for an ophthalmologist. Considering that the dataset contained a limited number of images of various abnormalities, we accepted the level of 85% as sufficient for images to be classified by an ophthalmologist with limited experience. We concluded that an optimal number of layers was required for accuracy, which in this case was 6. However, this value may later change because new data will be added to the dataset and models will be retrained.

Fig. 1 shows the processes of ANN model training and validation with four to seven convolutional layers. The training process was completed in 9 epochs when four and five convolutional layers were used, achieving 100% training and validation accuracies. However, the accuracy of the additional test was only 65%–70% (Table 1). The training process was longer and consisted of 15 epochs when using a model with six convolutional layers, achieving 100% training and validation accuracies. However, accuracy in the additional test increased to 85%, which was considered satisfactory. Upon further increasing the number of convolutional layers to seven, the process for ANN model training and validating consisted of >15 epochs, while the training accuracy was 100%, and the validation and testing accuracies decreased to 89% and 74% (Fig. 1 and Table 1).

Fig. 2 shows the architecture of the optimal ANN model concerning the accuracy of retinal OCT image classification. It includes six Conv2D convolutional layers with MaxPooling2D subsampling, a Flatten layer, and two fully connected Dense layers that act as classifiers, the latter featuring the Softmax neuron transfer function.

The lower classification accuracy in testing (compared with training and validation accuracies) is explained as follows: relatively small datasets of ~2,000 images were used to train the models, which did not contain a full set of graphical details characteristic of a particular abnormality. If such details are found in the test dataset, the classification

Table 1. Comparison of various sequential artificial neural network models

Number of convolutional layers	Number of parameters to be optimized	Training accuracy, %	Validation accuracy, %	Additional testing accuracy, %	Note
2	31 844 921	13	0	0	The ANN model is not trained well.
3	13 401 045	97	100	55	Number of ANN model training epochs: >15; number of filters in CNN layers: 3/8/16
3	15 215 889	100	100	62	Number of ANN model training epochs: 9; number of filters in CNN layers: 4/8/16
3	13 401 933	100	100	64	Number of ANN model training epochs: 12; number of filters in CNN layers: 5/8/16
4	6 929 729	100	100	65	Number of ANN model training epochs: 12
5	1 430 977	100	100	70	Number of ANN model training epochs: 9
6	556 673	100	100	85	Number of ANN model training epochs: 15
7	132 801	100	89	74	Number of ANN model training epochs: >15
8	–	–	–	–	8 CNN layers cannot be used for the accepted image size

Note. ANN, artificial neural network; CNN, convolutional neural network

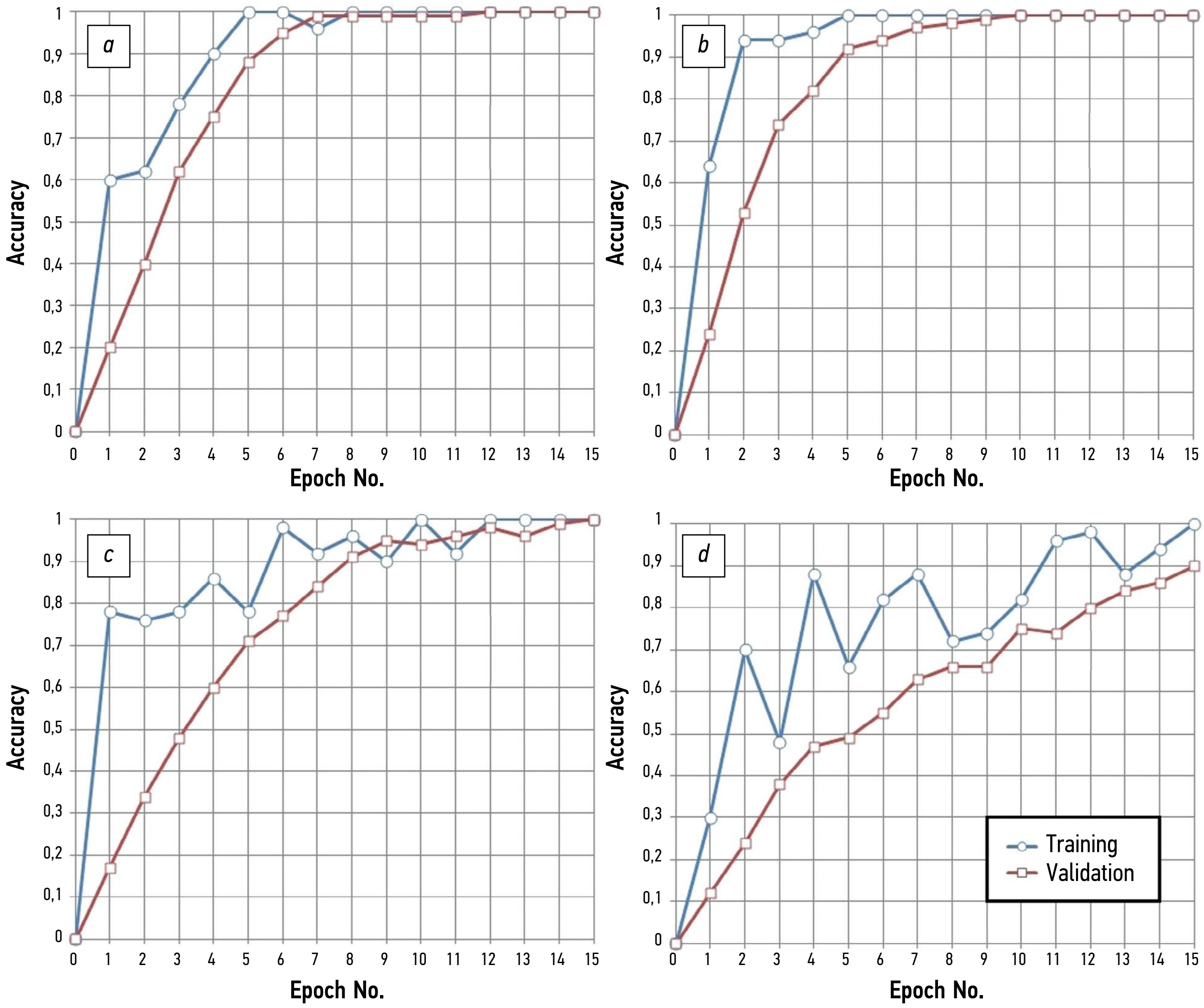

Fig. 1. Training and validation of convolutional neural network models with: *a* — four, *b* — five, *c* — six, and *d* — seven convolutional layers.

```
[ ]  model = tf.keras.models.Sequential([
         tf.keras.layers.Conv2D(4, (9,9), activation='relu', input_shape=(IMG_SHAPE, IMG_SHAPE, 3)),
         tf.keras.layers.MaxPooling2D(2, 2),

         tf.keras.layers.Conv2D(8, (5, 5), activation='relu'),
         tf.keras.layers.MaxPooling2D(2, 2),

         tf.keras.layers.Conv2D(16, (3, 3), activation='relu'),
         tf.keras.layers.MaxPooling2D(2, 2),

         tf.keras.layers.Conv2D(32, (3, 3), activation='relu'),
         tf.keras.layers.MaxPooling2D(2, 2),

         tf.keras.layers.Conv2D(32, (3, 3), activation='relu'),
         tf.keras.layers.MaxPooling2D(2, 2),

         tf.keras.layers.Conv2D(64, (3, 3), activation='relu'),
         tf.keras.layers.MaxPooling2D(2, 2),

         tf.keras.layers.Flatten(),
         tf.keras.layers.Dense(225, activation='relu'),
         tf.keras.layers.Dense(12, activation='softmax')
     ])
```

Fig. 2. Architecture and parameters of a six-layer convolutional artificial neural network model: the first number in Conv2D denotes the number of filters to be used in the convolution layer. The next two numbers represent the size (in pixels) of the filters. The activation functions of the network neurons are *Relu* and *Softmax* in the output classification layer. The first number in the fully connected Dense layer represents the number of neurons.

may be deemed incorrect even when the ANN model validation accuracy is 100%.

Preliminary computational experiments: a multimodel approach

Following the general logic of the study and considering the need to increase the accuracy of additional testing, O.L. Fabrikantov and Ye.V. Kulagina proposed a sequential scheme that usually imitates the process of identifying a retinal OCT image by an ophthalmologist. Accordingly, a computer algorithm was developed (Fig. 3).

This algorithm is based on the sequential implementation of multiple models (Fig. 3). In Step 1, images were preprocessed (Blocks 1–3). In Block 4, ANN Model 1 was used, which was designed for a preliminary classification to distinguish between normal and abnormal images. The result of this classification was saved (S1). Such a model should be trained and validated on a special dataset 1 containing only two corresponding image classes. When no abnormality was detected (Block 5), we proceeded to Step 4 (examination of the vitreous body), bypassing all intermediate steps. As in Block 6, ANN model 2 was used, which is trained on a special dataset 2, to detect a macular hole. The result was saved (S2). If there was a macular hole (Block 7), then in Block 8, based on ANN model 3, also trained using a special dataset 3, we determined whether there was a full-thickness or lamellar macular hole. The results were saved (S3), after which we proceeded to Step 2.

If there was no macular hole (Block 7), we proceeded to Block 9, which used ANN model 4 trained on a special dataset 4 to detect one of the following three: cystoid macular

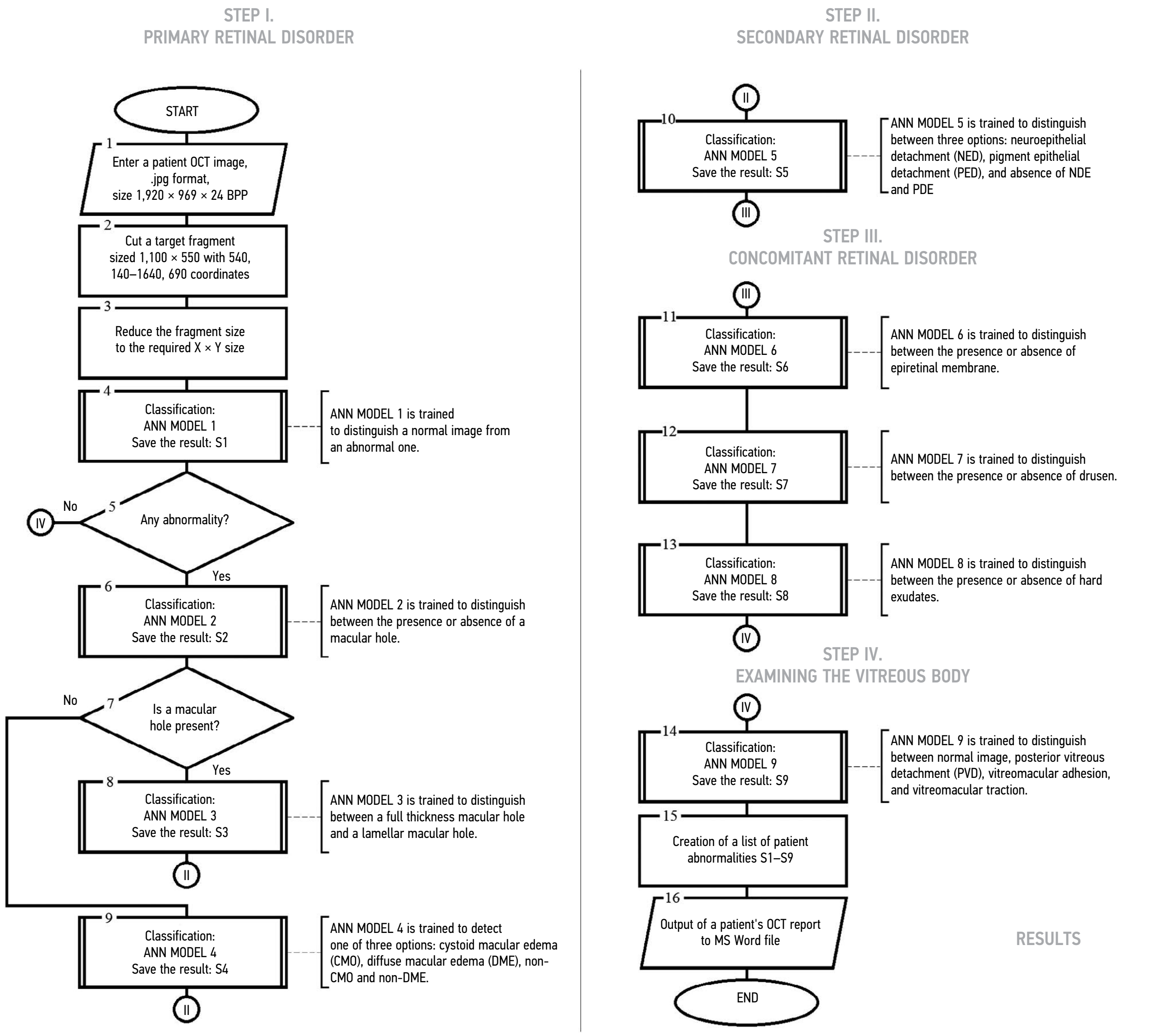

Fig. 3. Flowchart of a multimodel algorithm for optical coherence tomography image identification; ANN, artificial neural network; OCT, optical coherence tomography.

edema, diffuse macular edema, or their absence. The result was saved (S4), after which we proceeded to Step 2.

Step 2 used ANN model 5 (Block 10) trained on a special dataset 5 to detect one of the following three: neuroepithelial detachment, pigment epithelial detachment, or their absence. The result was saved (S5), and we proceeded to Step 3 for the analysis and classification of OCT images.

In Step 3, ANN models 6, 7, and 8 were sequentially used.

- ANN model 6 (Block 11) was trained on a special dataset 6 to detect the presence or absence of epiretinal membranes.
- ANN model 7 (Block 12) was trained on a special dataset 7 to detect the presence or absence of drusen.
- ANN model 8 (Block 13) was trained on a special dataset 8 to detect the presence or absence of exudates.

The corresponding results were also saved (S6–S8) in Blocks 11–13, after which we proceeded to Step 4.

In Step 4, ANN model 9 (Block 14) was used, trained on a special dataset 9 to detect normal images, posterior vitreous detachment, vitreomacular adhesion, and vitreomacular traction, and the results were saved (S9). In Blocks 15 and 16, a general list of abnormalities was generated based on the previously saved S1–S9 data, and a report describing an OCT map was generated as a file.

DISCUSSION

In the described approach, nine different ANN models are used to classify abnormalities in OCT images, each model trained in its unique dataset (1–9). In the final step of examination of the vitreous body, the algorithm described earlier [7] can be used rather than the ANN model 9. It includes:

- vertical scanning of the image and determining the X and Y coordinates of the vitreous body borders,
- smoothing Y coordinates via the moving-average method with a base corresponding to minimum details of the image (10 pixels in our case), via approximation of the vitreous body border with a spline or parabola of the appropriate order, and
- calculating maximum border curvature and the corresponding distances to identify posterior vitreous detachment, vitreomacular adhesion, and vitreomacular traction.

Herein, a multimodel algorithm (Figure 3) was tested with an increasing number of OCT images in the datasets and optimized hyperparameters of ANN models. Preliminary computational experiments conducted for several steps of this algorithm indicated that 98%–100% accuracy can be achieved on training and validation sets with increased additional testing accuracy compared with the single-model approach, owing to the reduced number of factors classified at each step. Contextually, a single architecture with seven convolutional layers was used for all ANN models 1–9. The only difference is that they were trained on unique datasets and had different sets of coefficients of interneuronal synaptic junctions.

CONCLUSION

Single- and multi-model approaches were proposed for the classification of retinal OCT images. Computational experiments on automatic classification of such images obtained using a DRI-OCT Triton tomograph with various ANN model architectures indicated 100% accuracy on training and validation datasets and 85% for additional testing. This result is considered satisfactory. The ANN model with optimal architecture (6-layer CNN) was selected, and values of the corresponding hyperparameters were determined, further developing decision support systems for use in ophthalmology.

ADDITIONAL INFORMATION

Funding source. This study was not supported by any external sources of funding.

Competing interests. The authors declare that they have no competing interests.

Authors' contribution. All authors made a substantial contribution to the conception of the work, acquisition, analysis, interpretation of data for the work, drafting and revising the work, final approval of the version to be published and agree to be accountable for all aspects of the work.
A.A. Arzamastsev — development of the concept, preliminary processing of OCT images, conducting research, writing programs, conducting computational experiments, multi-model approach to image classification, preparation of the manuscript; O.L. Fabrikantov — development of the concept, collection and preparation of OCT images, multi-stage classification scheme for OCT images, discussion and approval of the final version of the manuscript; E.V. Kulagina — development of a methodology for collecting and preparing OCT images, conducting research, a multi-stage classification scheme for OCT images, approval of the final version of the manuscript; N.A. Zenkova — concept development, research, editing and approval of the final version of the manuscript, analysis of literature data, editing the text of the article.

Acknowledgments. The work was carried out in accordance with the agreement on scientific and technical cooperation between Voronezh State University and the Federal State Autonomous Institution "National Medical Research Center" Interindustry Scientific and Technical Complex "Eye Microsurgery" named after Academician S.N. Fedorov"", Tambov branch dated November 28, 2022.
Master's degree students from the Faculty of Applied Mathematics, Informatics and Mechanics of Voronezh State University took part in the preliminary computational experiments: E.P. Galizina, V.A. Gushchina, I.O. Zavyalova, V.Yu. Kolupaev, N.M. Kushnarev, I.Yu. Novoskoltsev, E.A. Strukova, N.M. Chernyshov, I.D. Chikunov, A.A. Shcheglevatykh, as well as a diploma student M.A. Kuprin. These works were carried out under the guidance of one of the authors of the article.

REFERENCES

1. Daker DS, Vekhid NK, Goldman DR, editors. *Optical coherence tomography of the retina.* Moscow: MEDpress-inform; 2021. (In Russ).

2. Oakden-Rayner L, Palme LJ. Artificial intelligence in medicine: Validation and study design. In: Ranschart E, Morozov S, Algra P, editors. *Artificial intelligence in medical imaging*. Cham: Springer; 2019. P:83–104. doi: 10.1007/978-3-319-94878-2_8

3. Ramsundar B, Istman P, Uolters P, Pande V. *Deep learning in biology and medicine*. Moscow: DMK Press; 2020. (In Russ).

4. Buduma N, Lokasho N. *Foundations of deep learning. Creating Algorithms for Next Generation Artificial Intelligence*. Moscow: Mann, Ivanov i Ferber; 2020. (In Russ).

5. Foster D. *Generative deep learning. Creative potential of neural networks*. Saint Petersburg: Piter; 2020. (In Russ).

6. Postolit AV. *Fundamentals of Artificial Intelligence in Python examples*. Saint Petersburg: BKhV-Peterburg; 2021. (In Russ).

7. Arzamastsev AA, Fabrikantov OL, Zenkova NA, Kulagina EV. Software development for analysing the optical coherence tomography protocols of the retina and automatic composition of their descriptions. *Sovremennye problemy nauki i obrazovaniya.* 2021;(6). EDN: PCVMRX doi: 10.17513/spno.31208

8. Vasiliev YA, Vlazimirsky AV, Omelyanskaya OV, et al. Methodology for testing and monitoring artificial intelligence-based software for medical diagnostics. *Digital Diagnostics.* 2023;4(3):252–267. doi: 10.17816/DD321971

9. Katalevskaya EA, Katalevsky DYu, Tyurikov MI, Shaykhutdinova EF, Sizov AYu. Algorithm for segmentation of visual signs of diabetic retinopathy (DR) and diabetic macular edema (DME) in digital fundus images. *Russian Journal of Telemedicine and e-health.* 2021;7(4):17–26. EDN: PPSPAL doi: 10.29188/2712-9217-2021-7-4-17-26

10. Kepp T, Sudkamp H, Burchard C, et al. Segmentation of retinal low-cost optical coherence tomography images using deep learning. *Medical Imaging 2020: Computer-Aided Diagnosis.* 2020;11314:389–396. doi: 10.48550/arXiv.2001.08480

11. Sakhnov SN, Axenov KD, Axenova LE, et al. Development of a cataract screening model using an open dataset and deep machine learning algorithms. *Fyodorov Journal of Ophthalmic Surgery.* 2022;(4S):13–20. EDN: VEGPAW doi: 10.25276/0235-4160-2022-4S-13-20

12. Shukhaev SV, Mordovtseva EA, Pustozerov EA, Kudlakhmedov SS. Application of convolutional neural networks to define Fuchs endothelial dystrophy. *Fyodorov Journal of Ophthalmic Surgery.* 2022;(4S):70–76. EDN: WEZTKV doi: 10.25276/0235-4160-2022-4S-70-76

СПИСОК ЛИТЕРАТУРЫ

1. Оптическая когерентная томография сетчатки / под ред. Дж.С. Дакера, Н.К. Вэхид, Д.Р. Голдмана. Москва : МЕДпресс-информ, 2021.

2. Oakden-Rayner L., Palme L.J. Artificial intelligence in medicine: Validation and study design. In: Ranschart E., Morozov S., Algra P., editors. Artificial intelligence in medical imaging. Cham : Springer, 2019. P. 83–104. doi: 10.1007/978-3-319-94878-2_8

3. Рамсундар Б., Истман П., Уолтерс П., Панде В. Глубокое обучение в биологии и медицине. Москва : ДМК Пресс, 2020.

4. Будума Н., Локашо Н. Основы глубокого обучения. Создание алгоритмов для искусственного интеллекта следующего поколения. Москва : Манн, Иванов и Фербер, 2020.

5. Фостер Д. Генеративное глубокое обучение. Творческий потенциал нейронных сетей. Санкт-Петербург : Питер, 2020.

6. Постолит А.В. Основы искусственного интеллекта в примерах на Python. Санкт-Петербург : БХВ-Петербург, 2021.

7. Арзамасцев А.А., Фабрикантов О.Л., Зенкова Н.А., Кулагина Е.В. Разработка программного обеспечения для анализа протоколов оптической когерентной томографии сетчатки глаза и автоматизированного составления их описаний // Современные проблемы науки и образования. 2021. № 6. EDN: PCVMRX doi: 10.17513/spno.31208

8. Васильев Ю.А., Владзимирский А.В., Омелянская О.В., и др. Методология тестирования и мониторинга программного обеспечения на основе технологий искусственного интеллекта для медицинской диагностики // Digital Diagnostics. 2023. Т. 4, № 3. С. 252–267. doi: 10.17816/DD321971

9. Каталевская Е.А., Каталевский Д.Ю., Тюриков М.И., Шайхутдинова Э.Ф., Сизов А.Ю. Алгоритм сегментации визуальных признаков диабетической ретинопатии (ДР) и диабетического макулярного отёка (ДМО) на цифровых фотографиях глазного дна // Российский журнал телемедицины и электронного здравоохранения. 2021. Т. 7, № 4. С. 17–26. EDN: PPSPAL doi: 10.29188/2712-9217-2021-7-4-17-26

10. Kepp T., Sudkamp H., Burchard C., et al. Segmentation of retinal low-cost optical coherence tomography images using deep learning // Medical Imaging 2020: Computer-Aided Diagnosis. 2020. Vol. 11314. P. 389–396. doi: 10.48550/arXiv.2001.08480

11. Сахнов С.Н., Аксенов К.Д., Аксенова Л.Е., и др. Разработка модели скрининга катаракты с использованием открытого набора данных и алгоритмов глубокого машинного обучения // Офтальмохирургия. 2022. № 4S. С. 13–20. EDN: VEGPAW doi: 10.25276/0235-4160-2022-4S-13-20

12. Шухаев С.В., Мордовцева Е.А., Пустозеров Е.А., Кудлахмедов Ш.Ш. Применение сверточных нейронных сетей для определения эндотелиальной дистрофии Фукса // Офтальмохирургия. 2022. № 4S. С. 70–76. EDN: WEZTKV doi: 10.25276/0235-4160-2022-4S-70-76

AUTHORS' INFO

*** Alexander A. Arzamastsev,** Dr. Sci. (Engineering), Professor;
address: 24 Lavrov street, 392000 Tambov, Russia;
ORCID: 0000-0001-6795-2370;
eLibrary SPIN: 4410-6340;
e-mail: arz_sci@mail.ru

Oleg L. Fabrikantov, MD, Dr. Sci. (Medicine), Professor;
ORCID: 0000-0003-0097-991X;
eLibrary SPIN: 9675-9696;
e-mail: fabr-mntk@yandex.ru

Elena V. Kulagina, MD;
ORCID: 0009-0006-0026-0832;
eLibrary SPIN: 8785-4949;
e-mail: irina-kulagin2015@yandex.ru

Natalia A. Zenkova, Cand. Sci. (Psychology), Assistant Professor;
ORCID: 0000-0002-2325-1924;
eLibrary SPIN: 2266-4168;
e-mail: natulin@mail.ru

ОБ АВТОРАХ

*** Арзамасцев Александр Анатольевич,** д-р техн. наук, профессор;
адрес: Россия, 392000, г. Тамбов, ул. Лаврова, д. 24;
ORCID: 0000-0001-6795-2370;
eLibrary SPIN: 4410-6340;
e-mail: arz_sci@mail.ru

Фабрикантов Олег Львович, д-р мед. наук, профессор;
ORCID: 0000-0003-0097-991X;
eLibrary SPIN: 9675-9696;
e-mail: fabr-mntk@yandex.ru

Кулагина Елена Валерьевна;
ORCID: 0009-0006-0026-0832;
eLibrary SPIN: 8785-4949;
e-mail: irina-kulagin2015@yandex.ru

Зенкова Наталья Александровна, канд. психол. наук, доцент;
ORCID: 0000-0002-2325-1924;
eLibrary SPIN: 2266-4168;
e-mail: natulin@mail.ru

* Corresponding author / Автор, ответственный за переписку

DOI: https://doi.org/10.17816/DD624131

Изучение возможностей программы искусственного интеллекта в диагностике заболеваний макулярной области

М.Р. Хабазова[1], Е.Н. Пономарева[1], И.А. Лоскутов[2], Е.А. Каталевская[3], А.Ю. Сизов[3, 4], Г.М. Габараев[1]

[1] Федеральный научно-клинический центр специализированных видов медицинской помощи и медицинских технологий, Москва, Россия;
[2] Московский областной научно-исследовательский клинический институт имени М.Ф. Владимирского, Москва, Россия;
[3] ООО «Диджитал Вижн Солюшнс», Москва, Россия;
[4] Нижегородский государственный технический университет им. Р.Е. Алексеева, Нижний Новгород, Россия

АННОТАЦИЯ

Обоснование. Заболевания макулярной области представляют собой большую группу патологических состояний, приводящих к потере зрения и слабовидению. Ранняя диагностика таких изменений играет большую роль в выборе тактики лечения и является одной из определяющих в прогнозировании результатов.

Цель — изучить возможности программы искусственного интеллекта в диагностике заболеваний макулярной области на основе анализа сканов структурной оптической когерентной томографии.

Материалы и методы. В исследование были включены пациенты, проходившие обследование и лечение в Федеральном научно-клиническом центре специализированных видов медицинской помощи и медицинских технологий и Московского областного научно-исследовательского клинического института им. М.Ф. Владимирского. Обследовано 200 глаз с заболеваниями макулярной области, а также глаза без макулярной патологии. Проведён сравнительный клинический анализ сканов структурной оптической когерентной томографии, выполненных на офтальмологическом томографе RTVue XR 110-2. Для анализа сканов оптической когерентной томографии использовалось программное обеспечение Retina.AI.

Результаты. В ходе анализа сканов оптической когерентной томографии с помощью программы были выявлены различные патологические структуры макулярной области, а затем сформулировано заключение о вероятной патологии. Полученные результаты сравнивались с заключениями врачей-офтальмологов. Чувствительность метода составила 95,16%; специфичность — 97,76%; точность — 97,38%.

Заключение. Платформа Retina.AI позволяет офтальмологам успешно проводить автоматизированный анализ сканов структурной оптической когерентной томографии и выявлять различные патологические состояния глазного дна.

Ключевые слова: оптическая когерентная томография; искусственный интеллект; витреомакулярный интерфейс; диагностика; диабетический макулярный отёк; возрастная макулярная дегенерация.

Как цитировать:
Хабазова М.Р., Пономарева Е.Н., Лоскутов И.А., Каталевская Е.А., Сизов А.Ю., Габараев Г.М. Изучение возможностей программы искусственного интеллекта в диагностике заболеваний макулярной области // Digital Diagnostics. 2024. Т. 5, № 1. С. 17–28. DOI: https://doi.org/10.17816/DD624131

Рукопись получена: 30.11.2023 **Рукопись одобрена:** 02.02.2024 **Опубликована online:** 11.03.2024

DOI: https://doi.org/10.17816/DD624131

Exploring the possibilities of an artificial intelligence program in the diagnosis of macular diseases

Margarita R. Khabazova[1], Elena N. Ponomareva[1], Igor A. Loskutov[2], Evgenia A. Katalevskaya[3], Aleksandr Yu. Sizov[3, 4], Georgy M. Gabaraev[1]

[1] Federal Research and Clinical Center of Specialized Medical Care and Medical Technologies, Moscow, Russia;
[2] Moscow Regional Research and Clinical Institute, Moscow, Russia;
[3] Digital Vision Solutions LLC, Moscow, Russia;
[4] Nizhny Novgorod State Technical University n.a. R.E. Alekseev, Nizhny Novgorod, Russia

ABSTRACT

BACKGROUND: Macular diseases are a large group of pathological conditions that cause vision loss and visual impairment. Early diagnosis of such changes plays an important role in treatment selection and is one of the crucial factors in predicting outcomes.

AIM: To examine the potential of an artificial intelligence program in the diagnosis of macular diseases using structural optical coherence tomography scans.

MATERIALS AND METHODS: The study included patients examined and treated at the Federal Research and Clinical Center of Specialized Medical Care and Medical Technologies and Moscow Regional Research and Clinical Institute. In total, 200 eyes with macular diseases were examined, as well as eyes without macular pathologies. A comparative clinical analysis of structural optical coherence tomography scans obtained using an RTVue XR 110-2 tomograph was conducted. The Retina.AI software was used to analyze optical coherence tomography scans.

RESULTS: In the analysis of optical coherence tomography scans using Retina.AI, various pathological structures of the macula were identified, and a probable pathology was then determined. The results were compared with the diagnoses made by ophthalmologists. The sensitivity, specificity, and accuracy of the method were 95.16%, 97.76%, and 97.38%, respectively.

CONCLUSION: Retina.AI allows ophthalmologists to automatically analyze optical coherence tomography scans and identify various pathological conditions of the fundus.

Keywords: optical coherence tomography; artificial intelligence; diagnosis; macular edema; age-related macular degeneration.

To cite this article:
Khabazova MR, Ponomareva EN, Loskutov IA, Katalevskaya EA, Sizov AYu, Gabaraev GM. Exploring the possibilities of an artificial intelligence program in the diagnosis of macular diseases. *Digital Diagnostics*. 2024;5(1):17–28. DOI: https://doi.org/10.17816/DD624131

Submitted: 30.11.2023 **Accepted:** 02.02.2024 **Published online:** 11.03.2024

DOI: https://doi.org/10.17816/DD624131

人工智能程序在黄斑疾病诊断中的可行性研究

Margarita R. Khabazova[1], Elena N. Ponomareva[1], Igor A. Loskutov[2],
Evgenia A. Katalevskaya[3], Aleksandr Yu. Sizov[3, 4], Georgy M. Gabaraev[1]

[1] Federal Research and Clinical Center of Specialized Medical Care and Medical Technologies, Moscow, Russia;
[2] Moscow Regional Research and Clinical Institute, Moscow, Russia;
[3] Digital Vision Solutions LLC, Moscow, Russia;
[4] Nizhny Novgorod State Technical University n.a. R.E. Alekseev, Nizhny Novgorod, Russia

摘要

论证。黄斑疾病是一大类病症。它们会导致视力丧失和视力低下。对这些病变的早期诊断对治疗策略的选择起着重要作用，它是疗效预测的决定性因素之一。

目的。本研究的目的是研究人工智能程序在基于对结构光学相干断层扫描图片的分析诊断黄斑疾病方面的可行性。

材料与方法。本研究对象包括在俄罗斯联邦医疗和生物局联邦专业医疗救护和医疗技术科学与临床中心以及以M.F.弗拉基米尔斯基莫斯科州临床研究所接受检查和治疗的患者。对200只有黄斑病变的眼和无黄斑病变的眼进行了检查。对RTVue XR 110-2眼科断层扫描仪上的结构光学相干断层扫描进行了临床对比分析。利用Retina.AI软件对光学相干断层扫描进行分析。

结果。使用该程序分析光学相干断层扫描图片时，确定了黄斑区的各种病理结构。此外，还得出了关于可能病理的结论。对获得的结果与眼科医生的结论进行了比较。该方法的灵敏度为95.16%；特异性为97.76%；准确率为97.38%。

结论。Retina.AI平台使眼科医生能够成功地对结构光学相干断层扫描图片进行自动分析，并检测眼底的各种病理状态。

关键词：光学相干断层扫描；人工智能；玻璃体黄斑界面；诊断；糖尿病性黄斑水肿；老年性黄斑变性。

引用本文：
Khabazova MR, Ponomareva EN, Loskutov IA, Katalevskaya EA, Sizov AYu, Gabaraev GM. 人工智能程序在黄斑疾病诊断中的可行性研究. *Digital Diagnostics*. 2024;5(1):17–28. DOI: https://doi.org/10.17816/DD624131

收到：30.11.2023 **接受：**02.02.2024 **发布日期：**11.03.2024

BACKGROUND

According to the World Health Organization, approximately 2.2 billion people in the world suffer from visual impairment, and the largest group include patients aged >50 years [1]. Macular diseases, particularly age-related macular degeneration (AMD) and diabetic macular edema (DME), are significant causes of irreversible blindness and low vision quality [2].

As of 2020, 196 million patients have AMD worldwide, and this figure is expected to reach 288 million by 2040 [3]. Clinically, AMD may present with drusenoid deposits, retinal pigment epithelial changes, macular neovascularization, exudation, and hemorrhage. At advanced stages, geographic atrophy of the retinal pigment epithelium occurs [4]. These manifestations lead to severe visual impairment.

The number of patients with diabetes mellitus is increasing steadily, including its ocular manifestations. By 2045, the number of cases of diabetic retinopathy (DR) is predicted to reach 160.50 million, and the number of patients with sight-threatening DR will reach 44.82 million [5]. DME, which occurs at various stages of DR, is the most common cause of vision loss in patients with diabetes, and nearly 75,000 patients are newly diagnosed in the United States each year [6]. A direct correlation was found between the prevalence of DME and DR severity, and 70% of the cases are at the proliferative stage. Among patients with type 1 diabetes mellitus, DME develops in 27% within 9 years of disease onset [7]. In Russia, >630,000 patients have various stages of DR, and its prevalence in patients with type 1 diabetes mellitus is twice as high [8].

Central serous chorioretinopathy is the fourth macular disease that causes decreased visual acuity, characterized by serous detachment of the neuroepithelium above the area of leakage from the choriocapillaris. Central serous chorioretinopathy affects 9.9 individuals per 100,000 of population. The process is often unilateral; however, bilateral involvement was observed in 40% of cases [9]. The process has a chronic nature in 5% of cases, and central serous chorioretinopathy relapses within 12 months in 30%–50% of the patients [10].

Abnormalities of the vitreomacular interface include full-thickness and lamellar macular holes, vitreomacular traction, and epiretinal membrane. In some cases, vitreomacular interface changes may not cause significant functional impairment but have a significant effect on the macular area; the symptoms are accompanied by significant vision loss and negatively affect the patient's quality of life. Macular holes affect 3.3 individuals per 1,000 patients aged >55 years [11]. Annual incidence ranges from 4.71 to 8.5 individuals per 100,000 populations [12].

During the 20-year follow up in the Beaver Dam Eye Study (BDES), optical coherence tomography (OCT) detected an epiretinal membrane in 34.1%. Despite the different pathogenesis mechanisms, the clinical manifestations may be identical. An epiretinal membrane may develop as an idiopathic disease or as a concomitant pathology in previous eye diseases, such as DR, retinal vein occlusion, or previous cataract surgery [13]. Epiretinal membrane without posterior vitreous detachment may be a prerequisite for macular edema and lamellar macular holes caused by tangential traction syndrome [14].

At present, with the increasing life expectancy of the population, early detection of age-related diseases is relevant. Timely disease detection plays a major role in its treatment and is one of the keys to reducing the incidence rate. Because DME and AMD remain the leading causes of low visual acuity, regular ophthalmological screening for these pathologies is necessary to identify patients in need of specialized ophthalmological treatment. This strategy will prevent progression to blindness at the early stages [15]. Timely treatment initiation is often central to a favorable outcome with positive morphological and functional results (primarily visual acuity).

The use of vascular endothelial growth factor inhibitors (anti-VEGFs) is the gold standard treatment of neovascular AMD and DME [16]. To date, different protocols for the management of patients with these diseases have been developed. All proposed protocols involve regular treatment assessment based on clinical studies and OCT findings. Currently, OCT is the most informative and widely used method for diagnosing retinal pathology because it enables accurate monitoring during therapy. Based on OCT findings, the current state of the macular area is assessed, and treatment techniques for an individual case are selected.

The increasing number of patients with macular diseases who require regular ophthalmological examinations puts a significant strain on the healthcare system. The need to diagnose a large number of patients in a limited period, evaluate the data obtained, and determine the treatment techniques requires significant labor and time resources, which may cause their shortage. A possible solution to this problem is to develop and implement innovative methods for analyzing ocular images in clinical practice and the use of artificial intelligence (AI)-based technologies [17].

With advancements in AI technology, a whole new area has emerged, which aims at the development and implementation of intelligent systems in routine clinical practice. In Russia, the National AI Development Strategy has been approved until 2030.[1]

In Russia and all over the world, research on creating and validating AI-based software for diagnosing retinal

[1] Decree of the President of the Russian Federation No. 490 dated October 10, 2019, "On the development of artificial intelligence in the Russian Federation." Access: http://www.kremlin.ru/acts/bank/44731

pathology in clinical practice is ongoing. The authors of the Google DeepMind project (UK, USA) examined images obtained in 32 ophthalmology clinics that covered different population groups. The findings of the image analysis may be used to quantify retinal morphology and obtain measurement results for specific pathologies. The company's software is highly efficient in sorting images, nearly the same as specialists or superior. The authors examined 53 pathologies consistent with the national areas of development, presented a novel system capable of high-quality, efficient analysis of clinical OCT images, and offered recommendations. In the future, they plan to focus on a greater number of clinical disorders and expand the scope of their work.

The RetInSight software developed by researchers at the University of Vienna (Austria) under the guidance of Prof. U. Schmidt-Erfurth was designed to monitor the treatment effectiveness of neovascular AMD using AI algorithms. The program is based on the principle of segmenting intraretinal and subretinal fluid and retinal pigment epithelium detachment and dynamically assessing the volumes of these structures [18].

Chicago-based Altris Inc. (USA) launched the Altris AI software designed for automatic analysis of OCT scans. According to the developers, the cloud platform provides rapid analysis and visualization of 100 pathologies and pathological signs, including rare ones. The embedded algorithms can diagnose glaucoma, AMD, DR, and other retinal diseases. Users have access to modules for screening, segmentation/classification, and reporting [19].

B.E. Malyugin et al. [21] focused on creating an algorithm for the automated detection of biomarkers of anti-VEGF therapy effectiveness in patients with AMD. Seven biomarkers were identified, namely, pigment epithelial detachment, pigment epithelium, subretinal fluid, intraretinal fluid, ellipsoid zone, retinal nerve fiber layer, and subretinal hyper-reflective material. The Dice score was 0.8 for retinal pigment epithelial detachment, 0.4 for the pigment epithelium and subretinal fluid, and 0.3–0.15 for other biomarkers. In the future, the authors planned to expand the set of training data and increase the accuracy [20].

AIM

To assess the AI capabilities in diagnosing macular pathology based on structural OCT scans.

MATERIALS AND METHODS

Study design

Structural OCT scans were obtained using an RTVue XR 110-2 OCT scanner (Optovue, USA). To analyze OCT scans, Retina.AI software (Digital Vision Solutions LLC, Russia) was used for processing digital medical images. The single-center, retrospective, observational, sampling-based, single-arm study had a non-inferiority design.

Eligibility criteria

Inclusion criteria:

- Confirmed diagnosis of DME, AMD (dry and exudative), central serous choroidopathy, and vitreomacular traction syndrome (vitreomacular traction, epiretinal membrane, and full-thickness macular hole and lamellar macular hole)
- Central visual acuity loss and suspected macular pathology.

Exclusion criteria:

- OCT scanning is impossible because of the severe lack of clarity of the optical media (corneal opacity, mature cataract, hyphema, hemophthalmos, etc.)
- Patient's inability of visual fixation (nystagmus, Parkinsonism, etc.).

Subgroup analysis

The study included a total of 129 patients, with a mean age of 65.9 years. Women made up 55.8% (n =72), whereas 44.2% were men (n =57). The number of examined eyes was 200, with the following nosological entities:

- DME
- Cystic macular edema
- ARMD (macular neovascularization and retinal drusen)
- Central serous choroidopathy
- Vitreomacular traction syndrome
- Full-thickness macular hole
- Lamellar macular hole
- Epiretinal membrane.

Moreover, eyes without macular pathologies were examined. The distribution by nosological entity is presented in Table 1.

Table 1. Distribution of the study eyes by nosological entity

Diagnosis	No. of eyes
Diabetic macular edema/cystic macular edema	52
Age-related macular degeneration: macular neovascularization	41
Age-related macular degeneration: retinal drusen	40
Central serous choroidopathy	25
Vitreomacular traction syndrome	25
Full-thickness macular hole	23
Lamellar macular hole	25
Epiretinal membrane	72
No pathology	34

Study conditions

This study conducted a comparative clinical analysis of structural OCT scans of patients undergoing examination and treatment at the Federal Research and Clinical Center for Specialized Medical Care and Medical Technologies of the Federal Medical-Biological Agency of Russia and the Moscow Regional Research Clinical Institute named after M.F. Vladimirsky. The study duration was 12 months.

Medical intervention and primary outcome

Structural OCT scans were analyzed by the AI program in two stages. First, the program segmented the biomarkers. Second, it calculated the probable pathology using a differential diagnostic search algorithm. The conclusion resulting from the analysis of OCT scans by the AI program was compared with the clinical opinion of two ophthalmologists.

Ethics review

The study protocol was reviewed by the Ethics Committee of the Federal Research and Clinical Center for Specialized Medical Care and Medical Technologies of the Federal Medical-Biological Agency of Russia, Extract 2 from Protocol No. 11_2022 dated November 29, 2022. The conclusion read as follows: "To approve the retrospective analysis of eye fundus photographs and OCT scans of patients selected from medical databases using Retina.AI software for processing digital images in the diagnosis of eye pathologies by analyzing fundus photographs and structural OCT scans according to TU 58.29.32-001-60003594-2022 on the basis of the Research and Clinical Center for Specialized Medical Care and Medical Technologies of the Federal Medical and Biological Agency of Russia."

Outcome measures and statistical analysis

To evaluate software accuracy, the following parameters were calculated:

- Number of true positives (TP)
- Number of false positives (FP)
- Number of false negatives (FN)
- Number of true negatives (TN).

Based on the presented parameters, sensitivity, specificity, and accuracy were calculated for each nosological entity using the following formulas:

Precision: the proportion of true-positive cases out of the predicted positive cases:

$$\text{Precision} = \frac{TP}{(TP + FP)}$$

Recall/Sensitivity: the proportion of true-positive cases out of all positive cases:

$$\text{Recall} = \frac{TP}{(TP + FN)}$$

Specificity: the proportion of true-negative cases out of all negative cases:

$$\text{Specificity} = \frac{TN}{(TN + FP)}$$ [17]

RESULTS

Study objects (subjects) and primary outcome results

The study used Retina.AI software for processing digital medical images to diagnose pathologies by analyzing structural OCT scans. The study was conducted without patient participation; it only involved the assessment and analysis of clinical data.

During the analysis of OCT scans using the program, the following pathological structures were identified:

- Intraretinal cysts, subretinal fluid
- Retinal pigment epithelium detachment
- Subretinal hyper-reflective material
- Retinal drusen
- Epiretinal membrane
- Vitreomacular traction
- Full-thickness macular hole
- Lamellar macular hole.

The program automatically generated a conclusion based on the identified pathological signs. The general parameters of the method were as follows: sensitivity, 95.16%; specificity, 97.76%; accuracy, 97.38%. Detailed results of the comparative analysis of the conclusions by the AI and ophthalmologists are presented in Table 2.

Fig. 1 shows a structural OCT scan of the macular zone of patient B (54 years old) with type 2 diabetes mellitus. The ophthalmologist's report recorded DME. In the analysis

Table 2. Sensitivity, specificity, and precision of Retina.AI software in diagnosing macular area diseases

Diagnosis	Sensitivity, %	Specificity, %	Precision, %
Diabetic macular edema/cystic macular edema	96.08	97.48	97.14
Macular neovascularization	97.50	97.65	97.62
Age-related macular degeneration: retinal drusen	97.37	96.51	96.67
Central serous choroidopathy	92.59	98.36	97.62
Vitreomacular traction	86.96	97.33	96.19
Full-thickness macular hole	95.65	98.40	98.10
Epiretinal membrane	100.00	97.12	98.10
Lamellar macular hole	95.83	97.85	97.62
No pathology	94.72	97.69	97.25

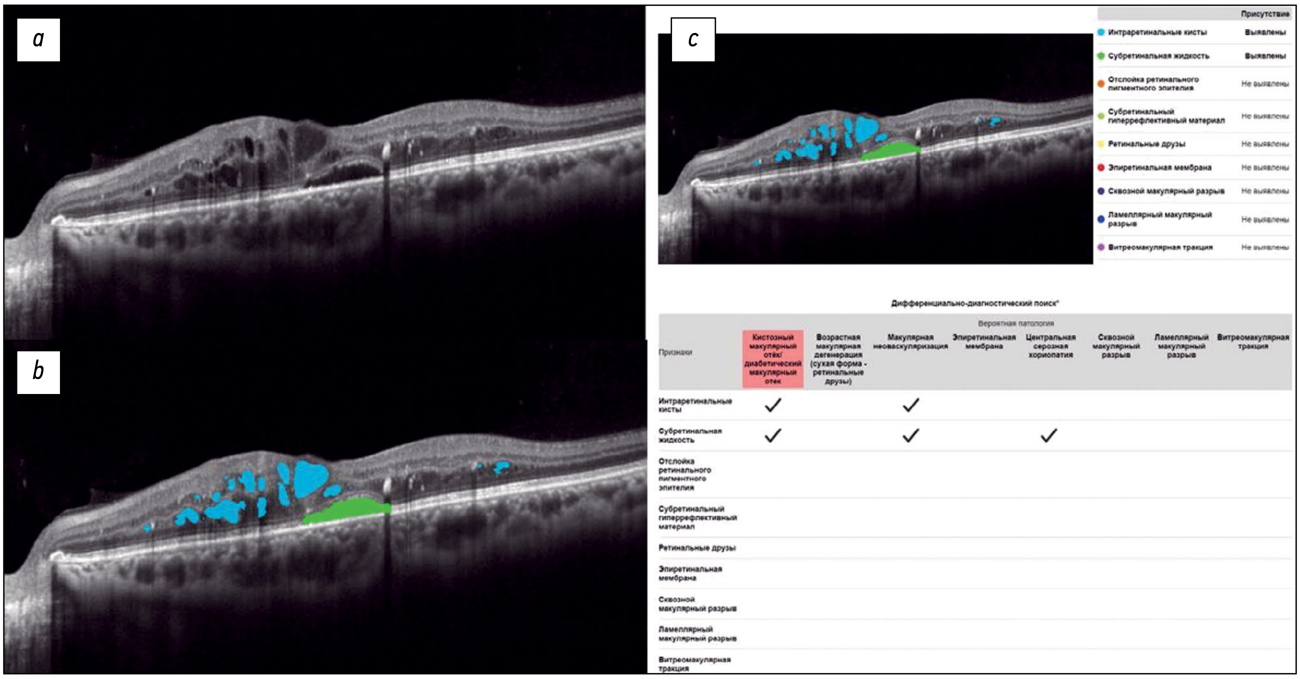

Fig. 1. An example of the optical coherence tomography scan analysis of a patient with diabetic macular edema by the artificial intelligence algorithm: *a* — structural optical coherence tomography scan; *b* — optical coherence tomography scan after segmentation of the pathological features (subretinal fluid — green mask, intraretinal cysts — blue masks); *c* — scan analysis report (the reporting table of the differential diagnostic search, probable pathology is highlighted in red — macular edema).

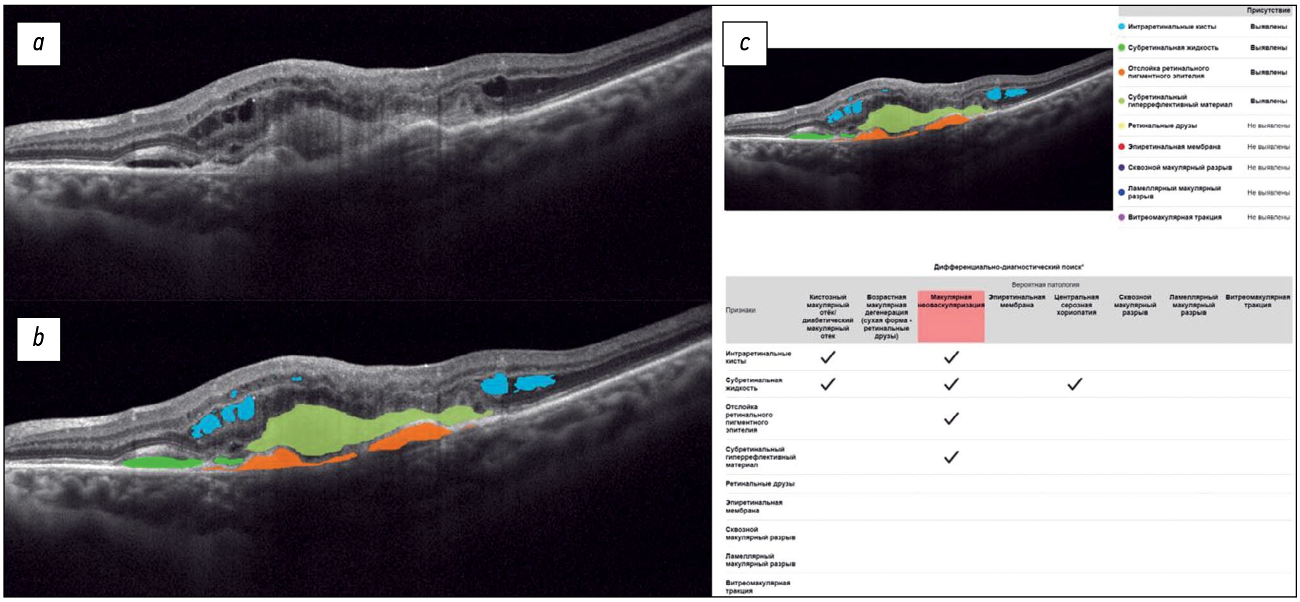

Fig. 2. An example of the optical coherence tomography scan analysis of a patient with exudative age-related macular degeneration by the artificial intelligence algorithm: *a* — structural optical coherence tomography scan; *b* — optical coherence tomography scan after segmentation of the pathological features (subretinal fluid — green mask, intraretinal cysts — blue masks, retinal pigment epithelium detachment — orange mask, subretinal hyperreflective material — yellow mask); *c* — scan analysis report (the reporting table of the differential diagnostic search, probable pathology is highlighted in red — macular neovascularization).

of the structural OCT scan by Retina.AI, the algorithms segmented the following pathological signs: intraretinal cysts, subretinal fluid. In conclusion, the patient was diagnosed with DME.

Fig. 2 shows a structural OCT scan of the macular zone of patient B (68 years old) with exudative AMD. The diagnosis was established by an ophthalmologist. In the analysis of the structural OCT scan by Retina.AI, the algorithm segmented

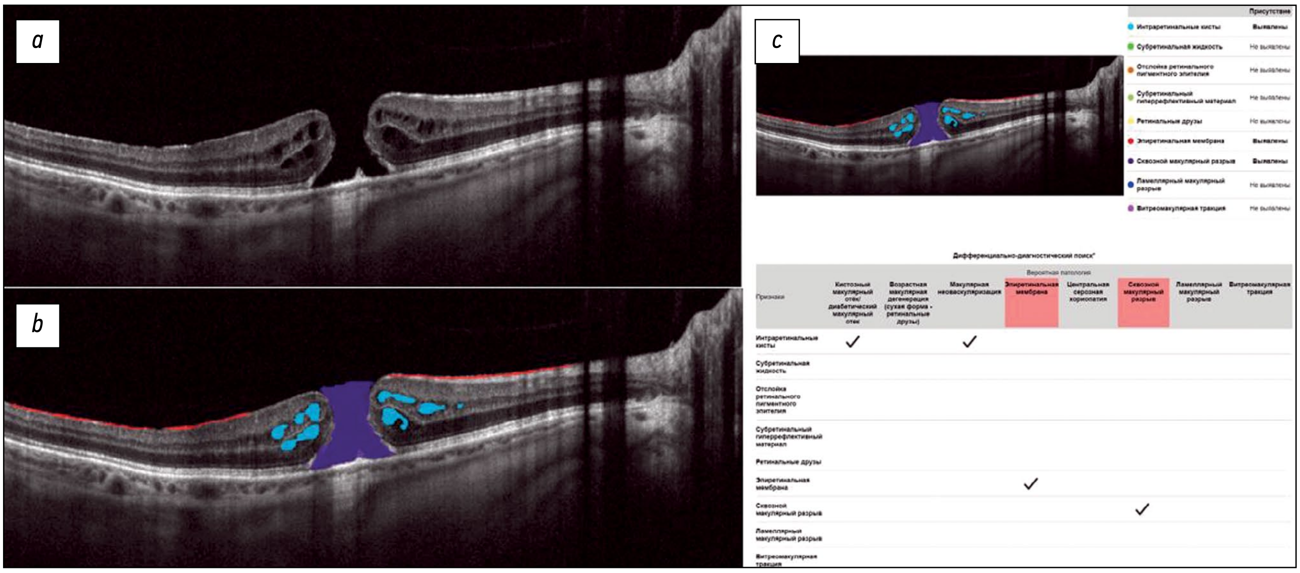

Fig. 3. An example of the optical coherence tomography scan analysis of a patient with macular hole, epiretinal membrane by the artificial intelligence algorithm: *a* — structural optical coherence tomography scan; *b* — optical coherence tomography scan after segmentation of the pathological features (macular hole — violet mask, intraretinal cysts — blue masks, epiretinal membrane — red masks); *c* — scan analysis report (the reporting table of the differential diagnostic search, probable pathology is highlighted in red — macular hole, epiretinal membrane).

the following pathological signs: intraretinal cysts, subretinal fluid, retinal pigment epithelium detachment, and subretinal hyper-reflective material. The program report registered macular neovascularization.

Fig. 3 shows a structural OCT scan of the macular zone of patient K (69 years old) with a full-thickness macular hole diagnosed by an ophthalmologist. In the analysis of the structural OCT scan by Retina.AI, the algorithm segmented the following pathological signs: full-thickness macular hole, intraretinal cysts, and epiretinal membrane. The program report registered a full-thickness macular hole and epiretinal membrane.

Adverse events

No adverse events occurred during the study.

DISCUSSION

Primary outcome summary

During the clinical study, the AI algorithm-based Retina.AI software demonstrated high sensitivity, specificity, and accuracy in diagnosing macular pathology: these parameters exceeded 90% for all diseases, except for vitreomacular traction syndrome, with a sensitivity of 86.96%. The advantage of the software lies in its convenient user interface that highlights the identified pathological structures in an OCT scan, which allows the doctor to additionally double-check the performance of the program and fosters the doctor's trust in the AI technology.

Primary outcome discussion

Practically, one of the most promising areas for introducing AI technologies into clinical practice is screening examinations that require examining a large number of patients and identifying those in need of specialized ophthalmological treatment. AI technologies open up the possibility of delegating some functions to nursing staff and organizing pre-doctor screening to free up the doctor's time for more complex tasks and increase the throughput of the ophthalmologist's office. However, AI technology cannot be viewed as a replacement for an ophthalmologist but as a tool to boost the efficiency of diagnosis and treatment. Implementing AI software may prove troublesome because it requires a stable Internet connection as the platform is cloud-based. For the convenience of continuous operation, developing a desktop application that does not depend on the Internet connection is promising.

Another encouraging area for using AI technologies is on monitoring the pathological process during treatment. In patients with DME and exudative AMD during anti-VEGF therapy, segmentation of intraretinal cysts, subretinal fluid, pigment epithelial detachment, and subretinal hyper-reflective material allows for a dynamic quantitative assessment of the volumes of these structures. At present, the primary quantitative parameters that doctors focus on during treatment include the best-corrected visual acuity, central retinal thickness, and area of the neovascular membrane in patients with AMD as visualized in OCT angiography. New quantitative criteria for assessing the effectiveness of anti-VEGF therapy by ophthalmologists in collaboration with developers of AI algorithms are urgently needed.

However, the technology is limited by the evaluation of a single OCT scan uploaded into the program. Thus, the software must be improved to allow for the analysis of the entire series of images of the same patient in the future.

CONCLUSION

During clinical validation, Retina.AI software based on AI algorithms demonstrated high sensitivity, specificity, and accuracy in the diagnosis of DME, dry and exudative AMD, central serous choroidopathy, and vitreomacular interface disorders based on analysis of structural OCT scans. The Retina.AI platform is a Russian development and is currently available for testing at www.screenretina.ru. However, the conclusion of the program is not a diagnosis and must be clarified by a specialist.

ADDITIONAL INFORMATION

Funding source. This study was not supported by any external sources of funding.

Competing interests. E.A. Katalevskaya and A.Yu. Sizov are part of the software developers. Other authors declare that they have no competing interests.

Authors' contribution. All authors made a substantial contribution to the conception of the work, acquisition, analysis, interpretation of data for the work, drafting and revising the work, final approval of the version to be published and agree to be accountable for all aspects of the work. M.R. Khabazova — literature search and analysis, data analysis, manuscript writing, manuscript editing; E.N. Ponomareva — conducting research, data analysis, manuscript editing; I.A. Loskutov — discussion of the research results, editing; E.A. Katalevskaya — development of the artificial intelligence algorithms, data markup, manuscript editing, literature search and analysis; A.Yu. Sizov — development of the artificial intelligence algorithms, data markup, graphic materials preparation; G.M. Gabaraev — literature search, data analysis.

REFERENCES

1. Report of the 2030 targets on effective coverage of eye care [Internet]. Geneva: World Health Organization. c2024. [cited 2023 Jan 1]. Available from: https://www.who.int/publications/i/item/9789240058002

2. GBD 2019 Blindness and Vision Impairment Collaborators. Causes of blindness and vision impairment in 2020 and trends over 30 years, and prevalence of avoidable blindness in relation to VISION 2020: the Right to Sight: an analysis for the Global Burden of Disease Study. *Lancet Glob Health.* 2021;9(2):144–160. doi: 10.1016/S2214-109X(20)30489-7

3. Samanta A, Aziz AA, Jhingan M, et al. Emerging Therapies in Neovascular Age-Related Macular Degeneration in 2020. *Asia Pac J Ophthalmol (Phila).* 2020;9(3):250–259. doi: 10.1097/APO.0000000000000291

4. Stahl A. The Diagnosis and Treatment of Age-Related Macular Degeneration. *Dtsch Arztebl Int.* 2020;117:513–520. doi: 10.3238/arztebl.2020.0513

5. Teo ZL, Tham YC, Yu M, et al. Global Prevalence of Diabetic Retinopathy and Projection of Burden through 2045: Systematic Review and Meta-analysis. *Ophthalmology.* 2021;128(11):1580–1591. doi: 10.1016/j.ophtha.2021.04.027

6. Schaal S, Kaplan HJ, editors. *Cystoid Macular Edema.* Switzerland: Springer International Publishing; 2017. doi: 10.1007/978-3-319-39766-5

7. Bikbov MM, Fayzrakhmanov RR, Zaynullin RM, et al. Macular oedema as manifestation of diabetic retinopathy. *Diabetes mellitus.* 2017;20(4):263–269. EDN: ZMZAON doi: 10.14341/DM8328

8. Chernykh DV, Chernykh VV, Trunov AN. *Cytokines and growth factors in the pathogenesis of proliferative diabetic retinopathy.* Moscow: Oftal'mologiya; 2017. EDN: ZNDEWH

9. Gupta A, Tripathy K. Central Serous Chorioretinopathy [Internet]. [Updated 2022 Aug 22]. In: StatPearls [Internet]. Treasure Island (FL): StatPearls Publishing, 2022. Available from: https://www.statpearls.com/point-of-care/96027

10. Semeraro F, Morescalchi F, Russo A, et al. Central Serous Chorioretinopathy: Pathogenesis and Management. *Clinical ophthalmology.* 2019;13:2341–2352. doi: 10.2147/OPTH.S220845

11. Oh KT, Lazzaro DR, editors. Macular Hole. [Internet]. Medscape, 2020. [cited 2020 Jan 02]. Available from: https://emedicine.medscape.com/article/1224320-overview#a6

12. Darian-Smith E, Howie AR, Allen PL, et al. Tasmanian macular hole study: whole population-based incidence of full thickness macular hole. *Clinical & Experimental Ophthalmology.* 2016;44(9):812–816. doi: 10.1111/ceo.12801

13. Fung AT, Galvin J, Tran T. Epiretinal membrane: A review. *Clinical & Experimental Ophthalmology.* 2021;49:289–308. doi: 10.1111/ceo.13914

14. Oh KT, Lazzaro DR, editors. Epiretinal Membrane [Internet]. Medscape, 2020. [cited 2020 Jan 02]. Available from: https://emedicine.medscape.com/article/1223882-overview#a4

15. World Health Organization. Regional Office for Europe. Screening for diabetic retinopathy: a short guide. Increase effectiveness, maximize benefits and minimize harm [Internet]. Copenhagen; 2021. [cited 2020 Jan 02]. Available from: https://www.who.int/europe/publications/i/item/9789289055321

16. Qassimi AN, Kozak I, Karam AM, et al. Management of Diabetic Macular Edema: Guidelines from the Emirates Society of Ophthalmology. *Ophthalmology and therapy.* 2022;11:1937–1950. doi: 10.1007/s40123-022-00547-2

17. Katalevskaya EA, Katalevskiy DYu, Tyurikov MI, Velieva IA, Bol'shunov AV. Future of artificial intelligence for the diagnosis and treatment of retinal diseases. *Russian journal of clinical ophthalmology.* 2022;22(1):36–43. EDN: AEBQGU doi: 10.32364/2311-7729-2022-22-1-36-43

18. Schmidt-Erfurth U, Reiter GS, Riedl S, et al. AI-based monitoring of retinal fluid in disease activity and under therapy. *Prog Retin Eye Res.* 2022;86. doi: 10.1016/j.preteyeres.2021.100972

19. Altris.ai [Internet]. United States: Altris Inc. [cited 2022 Jan 01]. Available from: https://www.altris.ai

20. Malyugin BE, Sakhnov SN, Axenova LE, et al. A deep machine learning model development for the biomarkers of the anatomical and functional anti-VEGF therapy outcome detection on retinal OCT images. *Fyodorov Journal of Ophthalmic Surgery.* 2022;(S4):77–84. EDN: OWQLRM doi: 10.25276/0235-4160-2022-4S-77-84

СПИСОК ЛИТЕРАТУРЫ

1. Report of the 2030 targets on effective coverage of eye care [Internet]. Geneva : World Health Organization. c2024. [дата обращения: 1.01.2023]. Доступ по ссылке: https://www.who.int/publications/i/item/9789240058002

2. GBD 2019 Blindness and Vision Impairment Collaborators. Causes of blindness and vision impairment in 2020 and trends over 30 years, and prevalence of avoidable blindness in relation to VISION 2020: the Right to Sight: an analysis for the Global Burden of Disease Study // Lancet Glob Health. 2021. Vol. 9, N 2. P. 144–160. doi: 10.1016/S2214-109X(20)30489-7

3. Samanta A., Aziz A.A., Jhingan M., et al. Emerging Therapies in Neovascular Age-Related Macular Degeneration in 2020 // Asia Pac J Ophthalmol (Phila). 2020. Vol. 9, N 3. P. 250–259. doi: 10.1097/APO.0000000000000291

4. Stahl A. The Diagnosis and Treatment of Age-Related Macular Degeneration // Dtsch Arztebl Int. 2020. Vol. 117. P. 513–520. doi: 10.3238/arztebl.2020.0513

5. Teo Z.L., Tham Y.C., Yu M., et al. Global Prevalence of Diabetic Retinopathy and Projection of Burden through 2045: Systematic Review and Meta-analysis // Ophthalmology. 2021. Vol. 128, N 11. P. 1580–1591. doi: 10.1016/j.ophtha.2021.04.027

6. Schaal S., Kaplan H.J., editors. Cystoid Macular Edema. Switzerland : Springer International Publishing, 2017. doi: 10.1007/978-3-319-39766-5

7. Бикбов М.М., Файзрахманов Р.Р., Зайнуллин Р.М., и др. Макулярный отёк как проявление диабетической ретинопатии // Сахарный диабет. 2017. Т. 20, № 4. С. 263–269. EDN: ZMZAON doi: 10.14341/DM8328

8. Черных Д.В., Черных В.В., Трунов А.Н. Цитокины и факторы роста в патогенезе пролиферативной диабетической ретинопатии. Москва : Офтальмология, 2017. EDN: ZNDEWH

9. Gupta A., Tripathy K. Central Serous Chorioretinopathy [Internet]. [Updated 2022 Aug 22]. In: StatPearls [Internet]. Treasure Island (FL): StatPearls Publishing, 2022. Доступ по ссылке: https://www.statpearls.com/point-of-care/96027

10. Semeraro F., Morescalchi F., Russo A., et al. Central Serous Chorioretinopathy: Pathogenesis and Management // Clinical ophthalmology. 2019. Vol. 13. P. 2341–2352. doi: 10.2147/OPTH.S220845

11. Oh K.T., Lazzaro D.R., editors. Macular Hole. [Internet]. Medscape, 2020. [Дата обращения: 02.01.2020]. Доступ по ссылке: https://emedicine.medscape.com/article/1224320-overview#a6

12. Darian-Smith E., Howie A.R., Allen P.L., et al. Tasmanian macular hole study: whole population-based incidence of full thickness macular hole // Clin Exp Ophthalmol. 2016. Vol. 44, N 9. P. 812–816. doi: 10.1111/ceo.12801

13. Fung A.T., Galvin J., Tran T. Epiretinal membrane: A review // Clin Experiment Ophthalmol. 2021. Vol. 49. P. 289–308. doi: 10.1111/ceo.13914

14. Oh K.T., Lazzaro D.R., editors. Epiretinal Membrane [Internet]. Medscape, 2020. [Дата обращения: 02.01.2020]. Доступ по ссылке: https://emedicine.medscape.com/article/1223882-overview#a4

15. Всемирная организация здравоохранения. Европейское региональное бюро. Скрининг на диабетическую ретинопатию: Повышение эффективности, максимальное увеличение пользы и минимизация вреда, краткое руководство [Internet]. Копенгаген, 2021. [Дата обращения: 02.01.2020]. Доступ по ссылке: https://www.who.int/europe/publications/i/item/9789289055321

16. Qassimi A.N., Kozak I., Karam A.M., et al. Management of Diabetic Macular Edema: Guidelines from the Emirates Society of Ophthalmology // Ophthalmology and therapy. 2022. Vol. 11. P. 1937–1950. doi: 10.1007/s40123-022-00547-2

17. Каталевская Е.А., Каталевский Д.Ю., Тюриков М.И., Велиева И.А., Большунов А.В. Перспективы использования искусственного интеллекта в диагностике и лечении заболеваний сетчатки // РМЖ. Клиническая офтальмология. 2022. Т. 22, № 1. С. 36–43. EDN: AEBQGU doi: 10.32364/2311-7729-2022-22-1-36-43

18. Schmidt-Erfurth U., Reiter G.S., Riedl S., et al. AI-based monitoring of retinal fluid in disease activity and under therapy // Prog Retin Eye Res. 2022. Vol. 86. doi: 10.1016/j.preteyeres.2021.100972

19. Altris.ai [Internet]. United States : Altris Inc. [Дата обращения: 01.01.2022]. Доступ по ссылке: https://www.altris.ai

20. Малюгин Б.Э., Сахнов С.Н., Аксенова Л.Е., и др. Разработка модели глубокого машинного обучения для обнаружения биомаркёров анатомического и функционального исхода анти-VEGF-терапии на ОКТ-изображениях сетчатки // Офтальмохирургия. 2022. № S4. С. 77–84. EDN: OWQLRM doi: 10.25276/0235-4160-2022-4S-77-84

AUTHORS' INFO

*** Margarita R. Khabazova;**
address: 28 Orekhovyi bul'var, 115682 Moscow, Russia;
ORCID: 0000-0002-7770-575X;
eLibrary SPIN: 2736-9089;
e-mail: rita.khabazova@mail.ru

Elena N. Ponomareva;
ORCID: 0009-0001-0828-9844;
eLibrary SPIN: 7868-4425;
e-mail: ponomareva.en@fnkc-fmba.ru

ОБ АВТОРАХ

*** Хабазова Маргарита Робертовна;**
адрес: Российская Федерация, 115682, г. Москва, Ореховый бульвар, д. 28;
ORCID: 0000-0002-7770-575X;
eLibrary SPIN: 2736-9089;
e-mail: rita.khabazova@mail.ru

Пономарева Елена Николаевна;
ORCID: 0009-0001-0828-9844;
eLibrary SPIN: 7868-4425;
e-mail: ponomareva.en@fnkc-fmba.ru

* Corresponding author / Автор, ответственный за переписку

Igor A. Loskutov, MD, Dr. Sci. (Medicine);
ORCID: 0000-0003-0057-3338;
eLibrary SPIN: 5845-6058;
e-mail: loskoutigor@mail.ru

Evgenia A. Katalevskaya, MD, Cand. Sci. (Medicine);
ORCID: 0000-0002-5710-9205;
eLibrary SPIN: 7849-8890;
e-mail: ekatalevskaya@mail.ru

Alexander Yu. Sizov;
ORCID: 0000-0003-3338-4015;
eLibrary SPIN: 4468-1730;
e-mail: sizov_ost_vk@mail.ru

Georgiy M. Gabaraev;
ORCID: 0000-0002-0759-3107;
eLibrary SPIN: 1802-3224;
e-mail: geor_gabaraev1@mail.ru

Лоскутов Игорь Анатольевич, д-р мед. наук;
ORCID: 0000-0003-0057-3338;
eLibrary SPIN: 5845-6058;
e-mail: loskoutigor@mail.ru

Каталевская Евгения Алексеевна, канд. мед. наук;
ORCID: 0000-0002-5710-9205;
eLibrary SPIN: 7849-8890;
e-mail: ekatalevskaya@mail.ru

Сизов Александр Юрьевич;
ORCID: 0000-0003-3338-4015;
eLibrary SPIN: 4468-1730;
e-mail: sizov_ost_vk@mail.ru

Габараев Георгий Малхазович;
ORCID: 0000-0002-0759-3107;
eLibrary SPIN: 1802-3224;
e-mail: geor_gabaraev1@mail.ru

DOI: https://doi.org/10.17816/DD569388

Вклад систем искусственного интеллекта в улучшение выявления аневризм аорты по данным компьютерной томографии грудной клетки

А.В. Соловьёв[1,2], Ю.А. Васильев[1], В.Е. Синицын[1,3,4], А.В. Петряйкин[1], А.В. Владзимирский[1], И.М. Шулькин[1], Д.Е. Шарова[1], Д.С. Семенов[1]

[1] Научно-практический клинический центр диагностики и телемедицинских технологий, Москва, Россия;
[2] Морозовская детская городская клиническая больница, Москва, Россия;
[3] Городская клиническая больница имени И.В. Давыдовского, Москва, Россия;
[4] Московский государственный университет имени М.В. Ломоносова, Москва, Россия

АННОТАЦИЯ

Обоснование. Аневризмы аорты — «тихие убийцы», развиваются без симптомов и могут привести к летальному исходу. Ежегодно заболеваемость аневризмой грудной аорты составляет около 10 случаев на 100 000 человек, а частота разрывов аневризмы — около 1,6 случая. Ранняя диагностика и лечение могут спасти жизнь пациента. Использование технологий искусственного интеллекта может значительно улучшить качество диагностики и предотвратить летальный исход.

Цель — оценить эффективность применения технологий искусственного интеллекта в выявлении аневризм грудного отдела аорты на компьютерной томографии органов грудной клетки и исследовать возможности использования этих технологий в качестве системы поддержки принятия врачебных решений врача-рентгенолога при первичном описании лучевых исследований.

Материалы и методы. Были оценены результаты использования технологий искусственного интеллекта для выявления аневризмы грудной аорты на компьютерной томографии органов грудной клетки без контрастного усиления. Была сформирована выборка из 84 405 случаев обследования пациентов старше 18 лет, из которых отобрано и ретроспективно пересмотрено сосудистыми хирургами Научно-исследовательского института скорой помощи имени Н.В. Склифосовского 86 исследований с подозрением на наличие аневризмы грудного отдела аорты по данным технологий искусственного интеллекта. Эти исследования были также ретроспективно оценены двумя врачами-рентгенологами.
Была сформирована дополнительная выборка из 968 исследований, взятых в случайном порядке из общего числа, для оценки корреляции возраста пациентов и диаметра грудного отдела аорты.

Результаты. Анализ показал, что в 44 исследованиях аневризма была первично выявлена врачом-рентгенологом, в 31 случае аневризмы не были описаны, но технология искусственного интеллекта помогла выявить патологию. Ещё 6 исследований были исключены из выборки, а в 5 случаях были обнаружены ложноположительные результаты анализа. Использование технологий искусственного интеллекта обнаруживает и выделяет патологические изменения аорты на медицинских изображениях, тем самым повышая выявляемость аневризмы грудной аорты при интерпретации результатов компьютерной томографии органов грудной клетки на 41%. При первичном описании лучевых исследований и в ретроспективных исследованиях целесообразно использовать технологии искусственного интеллекта для профилактики пропусков клинически значимых патологий — как в качестве системы поддержки принятия врачебных решений для врача-рентгенолога, так и для повышения выявляемости патологического расширения грудного отдела аорты.
По дополнительной выборке в популяции взрослого населения частота дилатации грудного отдела аорты составила 14,5%, а аневризм грудного отдела аорты —1,2%. Данные также показали возрастную зависимость диаметра грудного отдела аорты для мужчин и женщин.

Заключение. Применение технологий искусственного интеллекта в процессе первичного описания результатов компьютерной томографии органов грудной клетки может повысить выявляемость клинически значимых патологических состояний, таких как аневризма грудного отдела аорты. Расширение ретроспективного скрининга по данным компьютерной томографии органов грудной клетки с использованием технологий искусственного интеллекта может улучшить качество диагностики сопутствующих патологий и предотвратить негативные последствия для пациентов.

Ключевые слова: компьютерная томография; аневризма аорты; искусственный интеллект.

Как цитировать:
Соловьёв А.В., Васильев Ю.А., Синицын В.Е., Петряйкин А.В., Владзимирский А.В., Шулькин И.М., Шарова Д.Е., Семенов Д.С. Вклад систем искусственного интеллекта в улучшение выявления аневризм аорты по данным компьютерной томографии грудной клетки // Digital Diagnostics. 2024. Т. 5, № 1. С. 29–40. DOI: https://doi.org/10.17816/DD569388

Рукопись получена: 19.09.2023 **Рукопись одобрена:** 19.12.2023 **Опубликована online:** 11.03.2024

DOI: https://doi.org/10.17816/DD569388

Improving aortic aneurysm detection with artificial intelligence based on chest computed tomography data

Alexander V. Solovev[1,2], Yuriy A. Vasilev[1], Valentin E. Sinitsyn[1,3,4], Alexey V. Petraikin[1], Anton V. Vladzymyrskyy[1], Igor M. Shulkin[1], Daria E. Sharova[1], Dmitry S. Semenov[1]

[1] Research and Practical Clinical Center for Diagnostics and Telemedicine Technologies, Moscow, Russia;
[2] Morozov Children's Municipal Clinical Hospital, Moscow, Russia;
[3] Clinical City Hospital named after I.V. Davydovsky, Moscow, Russia;
[4] Lomonosov Moscow State University, Moscow, Russia

ABSTRACT

BACKGROUND: Aortic aneurysms are known as "silent killers" because this potentially fatal condition can be asymptomatic. The annual incidence of thoracic aortic aneurysms and ruptures is approximately 10 and 1.6 per 100,000 individuals, respectively. The mortality rate for ruptured aneurysms ranges from 94% to 100%. Early diagnosis and treatment can be life-saving. Artificial intelligence technologies can significantly improve diagnostic accuracy and save the lives of patients with thoracic aortic aneurysms.

AIM: This study aimed to assess the efficacy of artificial intelligence technologies for detecting thoracic aortic aneurysms on chest computed tomography scans, as well as the possibility of using artificial intelligence as a clinical decision support system for radiologists during the primary interpretation of radiological images.

MATERIALS AND METHODS: The results of using artificial intelligence technologies for detecting thoracic aortic aneurysms on non-contrast chest computed tomography scans were evaluated. A sample of 84,405 patients >18 years old was generated, with 86 cases of suspected thoracic aortic aneurysms based on artificial intelligence data selected and retrospectively assessed by radiologists and vascular surgeons. To assess the age distribution of the aortic diameter, an additional sample of 968 cases was randomly selected from the total number.

RESULTS: In 44 cases, aneurysms were initially identified by radiologists, whereas in 31 cases, aneurysms were not detected initially; however, artificial intelligence aided in their detection. Six studies were excluded, and five studies had false-positive results. Artificial intelligence aids in detecting and highlighting aortic pathological changes in medical images, increasing the detection rate of thoracic aortic aneurysms by 41% when interpreting chest computed tomography scans. The use of artificial intelligence technologies for primary interpretations of radiological studies and retrospective assessments is advisable to prevent underdiagnosis of clinically significant pathologies and improve the detection rate of pathological aortic enlargement. In the additional sample, the incidence of thoracic aortic dilation and thoracic aortic aneurysms in adults was 14.5% and 1.2%, respectively. The findings also revealed an age-dependent diameter of the thoracic aorta in both men and women.

CONCLUSION: The use of artificial intelligence technologies in the primary interpretation of chest computed tomography scans can improve the detection rate of clinically significant pathologies such as thoracic aortic aneurysms. Expanding retrospective screening based on chest computed tomography scans using artificial intelligence can improve the diagnosis of concomitant pathologies and prevent negative consequences.

Keywords: computed tomography; aortic aneurysm; artificial intelligence.

To cite this article:
Solovev AV, Vasilev YuA, Sinitsyn VE, Petraikin AV, Vladzymyrskyy AV, Shulkin IM, Sharova DE, Semenov DS. Improving aortic aneurysm detection with artificial intelligence based on chest computed tomography data. *Digital Diagnostics.* 2024;5(1):29–40. DOI: https://doi.org/10.17816/DD569388

Submitted: 19.09.2023 **Accepted:** 19.12.2023 **Published online:** 11.03.2024

DOI: https://doi.org/10.17816/DD569388

人工智能系统对从胸部计算机断层扫描数据中改进主动脉瘤检测的贡献

Alexander V. Solovev[1,2], Yuriy A. Vasilev[1], Valentin E. Sinitsyn[1,3,4], Alexey V. Petraikin[1], Anton V. Vladzymyrskyy[1], Igor M. Shulkin[1], Daria E. Sharova[1], Dmitry S. Semenov[1]

[1] Research and Practical Clinical Center for Diagnostics and Telemedicine Technologies, Moscow, Russia;
[2] Morozov Children's Municipal Clinical Hospital, Moscow, Russia;
[3] Clinical City Hospital named after I.V. Davydovsky, Moscow, Russia;
[4] Lomonosov Moscow State University, Moscow, Russia

摘要

论证。主动脉瘤是“无声杀手”，发病时没有任何症状，而且可能致命。胸主动脉瘤的年发病率约为每10万人10例，动脉瘤破裂的发病率约为1.6例。早期诊断和治疗可以挽救患者的生命。人工智能技术的使用可以大大提高诊断质量，防止死亡。

目的。本研究的目的是评估人工智能技术在胸部计算机断层扫描中检测胸主动脉瘤的有效性，并探讨这些技术作为放射科医生临床决策支持系统在放射学检查初步描述中的可行性。

材料与方法。对使用人工智能技术在无对比度增强的胸部计算机断层扫描中检测胸主动脉瘤的结果进行了评估。研究人员对84405名18岁以上的患者进行了抽样检查。通过人工智能技术筛选出86个疑似胸主动脉瘤的检查。俄罗斯N.V.斯克利福索夫斯基急救研究所的血管外科医生对这些检查结果进行了回顾性分析。两名放射科医生也对这些检查进行了回顾性评估。另外从总数中随机抽取，形成了包括968个检查在内的额外样本以评估患者年龄与胸主动脉直径之间的相关性。

结果。分析表明，在44例检查中，动脉瘤最初是由放射科医生检测到的；在31例检查中，动脉瘤未被描述，但人工智能技术帮助确定了病理。另有6例检查被排除在样本之外，而有5例检查发现了假阳性检测结果。

使用人工智能技术可以检测并突出显示医学图像中主动脉的病理变化。因此，在解读胸部计算机断层扫描结果时发现胸主动脉瘤的概率提高了41%。在放射学研究的初步描述和回顾性研究中，使用人工智能技术来防止遗漏具有临床意义的病理是可行的，既可作为放射科医生的医疗决策支持系统，又可提高胸主动脉病理扩张的可探测性。

在另一个成年人群样本中，胸主动脉扩张的发生率为14.5%，胸主动脉瘤的发生率为1.2%。数据还显示了，男性和女性的胸主动脉直径与年龄有关。

结论。将人工智能技术应用于胸部器官CT结果的初步描述过程中，可以提高对胸主动脉瘤等临床重大病理状态的检测。利用人工智能技术扩大胸部计算机断层扫描的回顾性筛查范围，可提高合并症的诊断质量，避免给患者带来不良后果。

关键词：电子计算机断层扫描；主动脉瘤；人工智能。

引用本文：
Solovev AV, Vasilev YuA, Sinitsyn VE, Petraikin AV, Vladzymyrskyy AV, Shulkin IM, Sharova DE, Semenov DS. 人工智能系统对从胸部计算机断层扫描数据中改进主动脉瘤检测的贡献. *Digital Diagnostics.* 2024;5(1):29–40. DOI: https://doi.org/10.17816/DD569388

收到：19.09.2023 **接受：**19.12.2023 **发布日期：**11.03.2024

BACKGROUND

According to the World Health Organization, cardiovascular diseases and associated disorders are among the leading causes of death [1]. These diseases include aortic aneurysms, which are known as “silent killers.” They are generally asymptomatic and can result in aortic dissection or rupture, which leads to death in 94%–100% of cases [2, 3]. Very few studies have statistically analyzed the prevalence of thoracic aortic aneurysms [4]. In Russia, the incidence of ascending aortic aneurysms ranges from 0.16% to 1.06%. Notably, a recent large epidemiological study on the incidence of thoracic aortic aneurysms in Russia was performed approximately 40 years ago [5], highlighting the need for further studies.

According to autopsy data collected over 10 years in the Filatov City Clinical Hospital No. 15 (Moscow), a thoracic aortic aneurysm was the cause of death in 0.8% of cases, with aneurysms suspected before death in only 11% of these cases [4]. In the USA, aortic aneurysms are the 17th leading cause of cardiovascular-related death, with an annual prevalence of thoracic aortic aneurysms of approximately 10 per 100,000 of population and an aneurysm rupture prevalence of approximately 1.6 per 100,000 of population [6]. In Sweden, thoracic aneurysms and aortic dissections occur in up to 16.3 per 100,000 of population [7]. According to Yale University data, the annual incidence rates of aneurysm ruptures and aortic dissections are 3.6% and 3.7% of the reported cases, respectively [8].

During screening for lung tumors using chest computed tomography (CT), abnormal thoracic aortic dilatation is detected in up to 8.1% of patients aged >50 years [9, 10].

Opportunistic screening is a prospective and retrospective analysis of relevant cases to identify conditions and risk factors in addition to the target pathology. This strategy eliminates the need for repeated examinations, reducing the patient’s radiation exposure [11].

In 2022, more than 647,000 noncontrasted chest CT studies were performed in Moscow. This number of examinations allows for the opportunistic detection of various pathological conditions, including life-threatening ones such as thoracic aortic dilatation (aneurysm) [12].

Since 2020, the world’s largest study has been conducted in Moscow to assess the efficacy and quality of artificial intelligence (AI) technology: “An experiment on the use of innovative computer vision technologies for the analysis of medical images and further use in the healthcare system of the city of Moscow” (Moscow Experiment) [13]. AI technology is used in the test mode in the Moscow Experiment, under the supervision of experts of the Center for Diagnostics and Telemedicine (Moscow). The process includes a continuous quality assessment of the system and adjustments to its operation, calculations of accuracy metrics, and identification of operation errors and other characteristics. Consequently , conditions are created for performing retrospective studies and processing X-ray findings during the primary analysis by a radiologist.

AIM

To assess the efficacy of AI technology in detecting thoracic aortic aneurysms based on chest CT findings and investigate the possibility of using AI technology as a medical decision support system for radiologists during the primary assessment of X-ray findings.

MATERIALS AND METHODS

Study design

A retrospective analysis of 84,405 chest CT scans was performed. Data were derived from the Unified Radiology Information Service of the automated Unified Medical Information Analysis System (ERIS EMIAS) of Moscow between June 1, 2022, and November 30, 2022, and processed using AI technology. The study design is presented in Fig. 1. The total sample included 84,405 patients aged >18 years, from which 86 examinations with a suspected thoracic aortic aneurysm with a maximum diameter of >50 mm were selected using AI technology data. The examinations were selected by vascular surgeons of the Sklifosovsky Institute for Emergency Medicine.

The resulting sample was then reviewed by two radiologists from the Center for Diagnostics and Telemedicine with over 5 years of experience. If the first two radiologists disagreed, an expert with 10 years of experience in radiology acted as an arbitrator and made the final decision on the presence of an aneurysm and its description.

During the review, eleven patients were excluded, specifically because the radiologist did not provide a primary protocol in the ERIS in six patients and the results were classified as false positive after AI data processing (assessment of a nontarget pathology or organ) in five patients. The resulting sample included 75 patients referred for a follow-up examination and treatment.

In addition, 1,000 scans were randomly selected from the total sample of 84,405 examinations to assess the distribution of aortic diameter vs. age. After the exclusion of 32 patients due to missing data on patients’ ages, the resulting sample included 968 patients (433 males and 535 females, 44.7% and 55.3%, respectively).

Inclusion criteria

The inclusion criteria for chest CT scans in the sample for analysis using AI technology during the Moscow Experiment in the Thoracic Aortic Aneurysm area were as follows:

- Outpatients and inpatients (male and female patients) of the institutions forming part of the Moscow Healthcare Department (aged >18 years)
- Examination type: noncontrasted chest CT with ≤3 mm slice thickness
- Availability of chest CT scans in the DICOM format and the radiologist’s protocol in the ERIS EMIAS

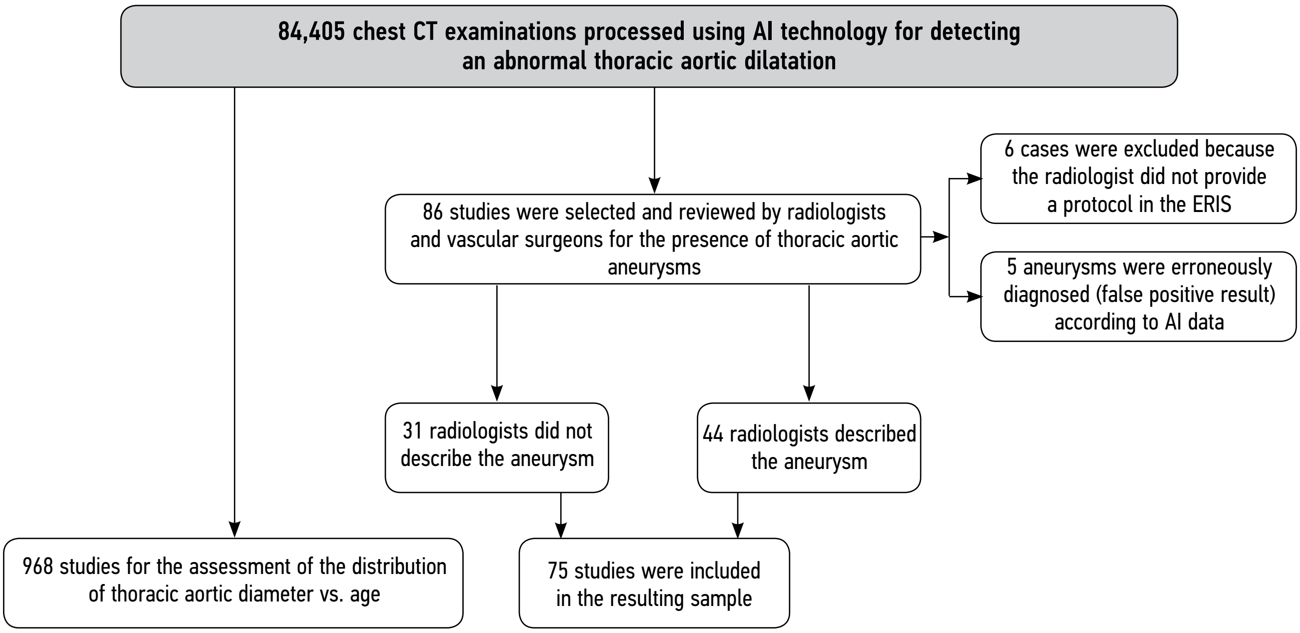

Fig. 1. Study design. AI, artificial intelligence, CT, computed tomography; ERIS, Unified Radiology Information Service.

The exclusion criteria were as follows:
- Patients with surgical hardware (postoperative clamps or plates) creating artifacts in the chest area, including pacemakers
- Contrast enhancement and lung kernel CT
- Absence of chest CT scans in the DICOM format and/or the radiologist's protocol in the ERIS EMIAS.

Study conditions

According to the basic diagnostic requirements, AI technology was used to process examination findings for detecting abnormal thoracic aortic dilatation. These requirements were developed based on the European Society of Cardiology guidelines on the diagnosis and treatment of aortic diseases [14]:
- Ascending aortic dilatation: 40–49 mm
- Ascending aortic aneurysm: ⩾50 mm
- Descending aortic aneurysm: ⩾40 mm [15]

The domestic AI algorithm Chest-IRA (IRA Labs, Russia) was used to automatically determine the thoracic aortic diameter. The accuracy of this AI technology was assessed during the Moscow Experiment, with the following results:
- Area under the ROC curve (AUC): 0.99
- Sensitivity: 0.94
- Specificity: 0.96
- Accuracy: 0.95
- Duration of analysis (one examination): 2.1 min [16]

An example of an AI technology algorithm operation is presented in Fig. 2.

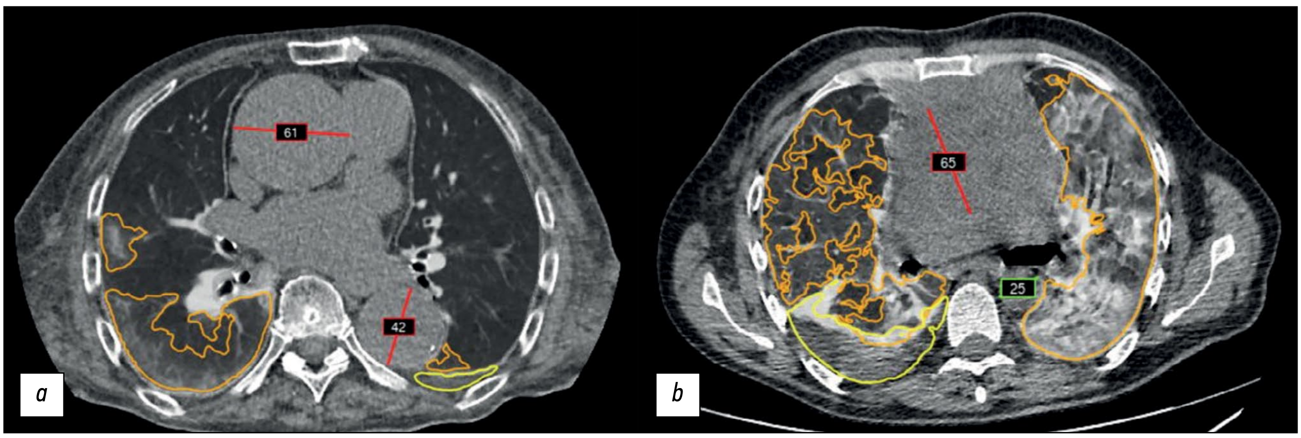

Fig. 2. An example of an algorithm operation of a complex AI-based service to process chest CT findings: *a*: AI technology correctly selected and marked (red line) the suspected ascending and descending thoracic aortic aneurysms; *b*: a false positive result: a mediastinal neoplasm was marked (red line) together with the ascending thoracic aorta; the green frame indicates the diameter of the descending thoracic aorta. This complex AI-based service has additional modules for marking pulmonary infiltrates (orange outline) and pleural effusion (yellow outline).

The retrospective verification of CT scans with suspected thoracic aortic aneurysms in the total sample of 75 studies (maximum diameter: >50 mm) was performed by two radiologists (with >5 years of experience), one expert radiologist, and vascular surgeons (with >10 years of experience). The correctness of AI technology operation in measuring the thoracic aorta in the axial plane was assessed. According to the guidelines of the European Association of Cardiovascular Imaging and the European Society of Cardiology, the physicians measured both the maximum anteroposterior diameter and the perpendicular diameter of the thoracic aorta [17]. All patients in the sample were referred for a follow-up examination to decide on further monitoring or treatment.

The normality of distribution in the groups of patients was assessed using the Shapiro–Wilk test. Given that the distribution was not normal (p <0.001), all subsample values are presented as median [25th percentile; 75th percentile] and minimum/maximum. Between-group comparisons were performed by the Mann–Whitney method.

RESULTS

Primary study results

The AI technology algorithm was used to process 84,405 noncontrasted chest CT scans for detecting abnormal thoracic aortic dilatation. In total, 86 patients (62 male and 24 female patients) with a suspected thoracic aortic aneurysm according to AI technology findings were selected from this sample and retrospectively reviewed by radiologists and vascular surgeons. Of 86 patients, six were excluded from the sample because no protocol was available in the ERIS, and five had a false positive result after AI data processing (assessment of a nontarget pathology or organ, Fig. 2, *b*); these five patients were also excluded from the sample.

The resulting sample included 75 patients: 57 male (66 [59; 73]; 27–87 years) and 18 female patients (62 [59; 74]; 47–87 years). Thoracic aortic aneurysms were described in the primary X-ray protocol in 44 (59%) cases; in 31 (41%) cases, aneurysms were not mentioned in the primary protocol. Thus, AI technology allowed for detecting 31 additional cases of thoracic aortic aneurysms (41%). In this group, the maximum thoracic aortic diameter was 56 [54; 60]: 52–84 mm in male and 57 [54; 63]; 52–87 mm in female patients.

Patients with aortic aneurysms detected using AI technology on chest CT scans were informed and referred for follow-up examinations (echocardiography, CT, or magnetic resonance angiography, and cardiologist or vascular surgeon consultation) to determine the management and treatment strategy.

The follow-up examinations provided additional information: 4 (5.33%) of 75 patients died before the end of diagnostic procedures or surgery, and 3 (4%) patients refused follow-up examinations and treatment. Another 31 (41.33%) patients were lost to follow-up.

In 25 (33.33%) of 37 patients who remained under follow-up and continued treatment, thoracic aortic aneurysm was confirmed (ongoing follow-up); in 12 (16%) patients, the diagnosis was clarified (still being treated by a cardiologist). In 3 patients, the diagnosis of aneurysm was not confirmed after a diagnostic examination; these patients were diagnosed with thoracic aortic dilatation. Moreover, two surgeries (aortic stenting) were performed for aneurysms.

No significant differences in age and thoracic aortic diameter were found between the groups of male and female patients with aneurysms detected using AI technology (p>0.05).

Findings of the second part of the study

Preliminary data on the incidence of aneurysms was obtained in the sample including 968 cases (Fig. 3) randomly

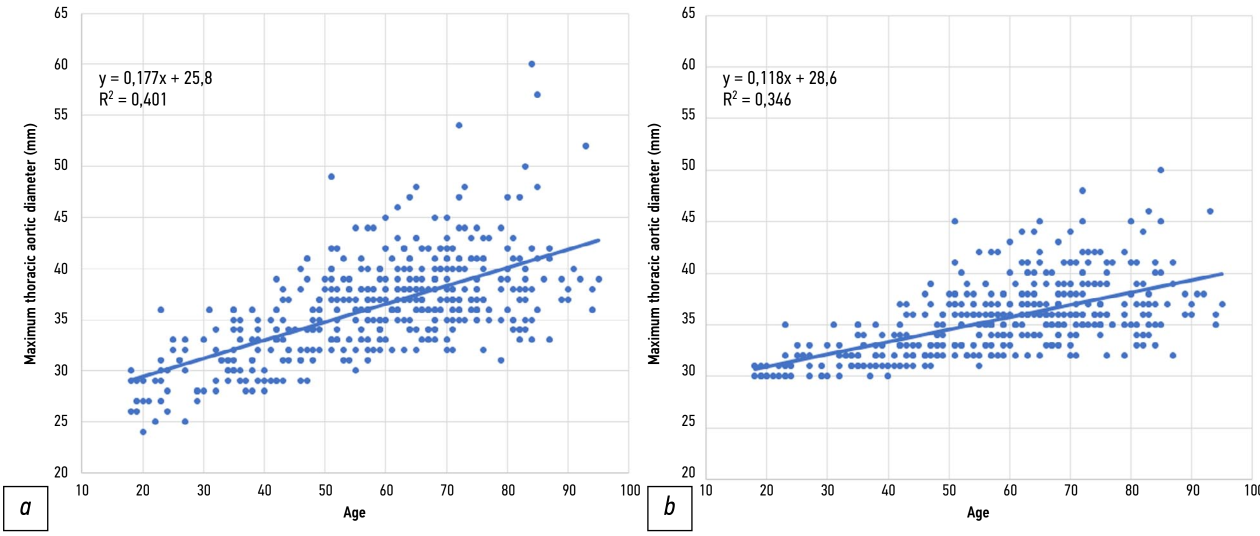

Fig. 3. Plot of the maximum thoracic aortic diameter versus age for the sample including 968 examinations: *a*: male patients; *b*: female patients.

DOI: https://doi.org/10.17816/DD569388

selected from 84,405 cases. In the adult population (aged ⩾18 years), the incidence rates of thoracic aortic dilatation and aneurysms were 14.5% and 1.2%, respectively.

The female patients were 65 [51; 75]; 19–102 years old (n = 535), and the male patients were 60 [47; 71]; 18–95 years old (n = 433). There were slightly more female patients than male patients, reflecting the sex distribution in the total patient population studied. The median age of the female patients (65 years) was slightly higher than that of male patients (60 years), and the interquartile ranges were comparable.

In this group, the thoracic aortic diameter was 34 [31; 37]; 20–50 mm in female patients and 36 [33; 39]; 24–60 mm in male patients.

Significant (p<0.001) differences in age and maximum thoracic aortic diameter were found between the male and female patients. A pronounced association of the thoracic aortic diameter and age was found in male and female patients. In male patients, relative age-related changes in the thoracic aortic diameter are more pronounced at 0.177 mm/year; in female patients, this parameter was 0.118 mm/year.

DISCUSSION

Result summary

The analysis showed no significant differences (p >0.05) in age or maximum thoracic aortic diameter between male and female patients with aortic aneurysms (n = 75). In the sample including 968 patients (randomly selected from the total sample), significant differences (p<0.001) in age and maximum thoracic aortic diameter were found between male and female patients. This highlights the need for age and sex standards to describe the distribution by age. In addition, well-designed studies are necessary for a more comprehensive analysis of the observed trends.

Discussion of study findings

An increase in the detection rate of aneurysms in a retrospective study employing an AI algorithm confirms the efficacy and feasibility of this approach in clinical practice, e.g., as an accessory tool for radiologists during the primary assessment of X-ray findings. However, the software also provided some false positive results. Methods to minimize such errors by monitoring and fine-tuning the algorithm have been reported [20–22].

According to the literature, a positive correlation existed between age and thoracic aortic diameter. Men generally have larger thoracic aortic diameters than women [18], as well as a more pronounced association between age and thoracic aortic diameter [19], which is consistent with the statistical analysis findings in this study.

Physicians are at risk of missing clinically significant conditions for various reasons, including professional burnout (e.g., following the COVID-19 pandemic), increasing workload, and medical personnel shortage. This is another argument in favor of using AI technology as a medical decision support system for radiologists when assessing chest CT scans. AI technology can improve the detection rate and reduce the number of missed clinically significant pathologies [23].

The domestic AI technology used in this study is not the only one in the world, and quality metrics can be used when selecting AI algorithms. Foreign analogs of AI technology are also available for automatic measurement of the thoracic aortic diameter and detection of aneurysms; these solutions allow avoiding errors and can be used in opportunistic screening [24, 25].

According to the literature, AI technology helps radiologists reduce the time spent on detecting pathologies in X-ray images [26, 27].

AI-based solutions are a promising tool for aortic measurements [28]. However, the accuracy of these measurements must be confirmed by further research. This study demonstrates that although AI cannot replace physicians, it can aid radiologists by warning them of potential aortic pathologies, allowing them to avoid missing clinically relevant abnormalities. Radiologists must understand the principle of AI technology operation and possible errors when analyzing study findings [29–33]. Thus, the use of AI in medicine can be a valuable tool in detecting thoracic aortic aneurysms. Accordingly, AI technology must be used to detect abnormal thoracic aortic dilatation during the primary assessment of X-ray findings and in retrospective analysis to reduce the risk of missing clinically significant changes.

CONCLUSIONS

The use of AI technology during the primary assessment of chest CT images and for expanded opportunistic screening may improve the diagnosis of clinically significant pathologies, such as thoracic aortic aneurysms, and prevent unfavorable outcomes. Further optimization of the routing in this patient population requiring urgent medical intervention for timely surgical treatment is crucial. Thus, population reference values for thoracic aortic diameter must be established to adjust the diagnostic criteria for this condition.

ADDITIONAL INFORMATION

Funding source. This article was prepared by the team of authors within the framework of the research work "Opportunistic screening of socially significant and other common diseases" (No. in the Unified State Information System of Accounting: No. 123031400009-1) in accordance with Order of the Department of Health of Moscow from 21.12.2022 No. 1196 "On approval of state tasks, the financial support of which is carried out at the expense of the budget of the city of Moscow state budgetary (autonomous) institutions subordinate to the Department of Health Protection of Moscow, for 2023, 2024 and 2025".

Competing interests. The authors declare that they have no competing interests.

Authors' contribution. All authors made a substantial contribution to the conception of the work, acquisition, analysis, interpretation of data for the work, drafting and revising the work, final approval of the version to be published and agree to be accountable for all aspects of the work. The major contributions are distributed as follows: A.V. Solovev — research conception and design, article writing, editing, and approval of the final manuscript; Yu.A. Vasilev, V.E. Sinitsyn — research conception, final proofreading of the text; A.V. Petraikin, A.V. Vladzymyrskyy — research conception and design, writing, and editing of the text; I.M. Shulkin, D.E. Sharova, D.S. Semenov — research conception, editing, and approval of the final manuscript, advisory support.

REFERENCES

1. The top 10 causes of death [Internet]. World Health Organization. [cited 12 May 2023]. Available from: https://www.who.int/ru/news-room/fact-sheets/detail/the-top-10-causes-of-death

2. Gouveia e Melo R, Silva Duarte G, Lopes A, et al. Incidence and Prevalence of Thoracic Aortic Aneurysms: A Systematic Review and Meta-analysis of Population-Based Studies. *Seminars in thoracic and cardiovascular surgery.* 2022;34(1):1–16. doi: 10.1053/j.semtcvs.2021.02.029

3. Clinical guidelines. Guidelines for the diagnosis and treatment of aortic diseases (2017). *Russian Journal of Cardiology and Cardiovascular Surgery*. 2018;11(1):7–67. EDN: YPAKRP

4. Kuznechevsky FV, Osipov AKh, Evsikov EM, Abramov IS, Otarova SM. Prevalence and clinical features of aorta aneurysm; and dissections: 10-year results of consequent autopsies made at O.M. Filatov city clinical hospital №15. *Russian Journal of Cardiology.* 2004;9(6):5–13. EDN: ISVRYL

5. Irtyuga OB, Voronkina IV, Smagina LV, et al. The frequency to detect of ascending aorta aneurysms and the mechanism of its development according register of the Almazov Federal Heart, Blood and Endocrinology Centre. *Bulletin of Almazov Federal Heart, Blood and Endocrinology Centre.* 2011;(5):73–78. EDN: OWGHOB

6. Lavall D, Schäfers HJ, Böhm M, Laufs U. Aneurysms of the ascending aorta. *Deutsches Arzteblatt international.* 2012;109(13):227–233. doi: 10.3238/arztebl.2012.0227

7. Olsson C, Thelin S, Ståhle E, Ekbom A, Granath F. Thoracic Aortic Aneurysm and Dissection. *Circulation.* 2006;114(24):2611–2618. doi: 10.1161/CIRCULATIONAHA.106.630400

8. Elefteriades JA. Natural history of thoracic aortic aneurysms: indications for surgery, and surgical versus nonsurgical risks. *The Annals of thoracic surgery.* 2002;74(5):1877–1880. doi: 10.1016/s0003-4975(02)04147-4

9. Tsai EB, Chiles C, Carter BW, et al. Incidental Findings on Lung Cancer Screening: Significance and Management. *Seminars in ultrasound, CT, and MR.* 2018;39(3):273–281. doi: 10.1053/j.sult.2018.02.005

10. Chernina VYu, Blokhin IA, Nikolaev AE, et al. *Tactics for the management of incidentalomas. Section 3. Thyroid, pituitary, vasculature and mediastinum.* Moscow: Research and Practical Clinical Center for Diagnostics and Telemedicine; 2019. (In Russ). EDN: WSYSYP

11. Law M. "Opportunistic" Screening. *J Med Screen.* 1994;1(4):208. doi: 10.1177/096914139400100403

12. Kumar Y, Hooda K, Li S, et al. Abdominal aortic aneurysm: pictorial review of common appearances and complications. *Annals of translational medicine.* 2017;5(12):256. doi: 10.21037/atm.2017.04.32

13. Vasilev YuA, Vladzymyrskyy AV, editors. *Computer Vision in Radiologic Diagnostics: the First Stage of the Moscow Experiment.* Moscow: Limited Liability Company Izdatelskie reshenia; 2022. (In Russ). EDN: FOYLXK

14. Erbel R, Aboyans V, Boileau C, Vlachopoulos C. 2014 ESC Guidelines on the diagnosis and treatment of aortic diseases: Document covering acute and chronic aortic diseases of the thoracic and abdominal aorta of the adult. The Task Force for the Diagnosis and Treatment of Aortic Diseases of the European. *European heart journal.* 2014;35(41):2873–2926. doi: 10.1093/eurheartj/ehu281

15. Documents on the Experiment [Internet]. Center for Diagnostics and Telemedicine. [cited 16 June 2023]. Available from: https://mosmed.ai/ai/docs/

16. Chest-IRA [Internet]. Center for Diagnostics and Telemedicine. [cited 16 June 2023]. Available from: https://mosmed.ai/service_catalog/chestira/

17. Evangelista A, Sitges M, Jondeau G, et al. Multimodality imaging in thoracic aortic diseases: a clinical consensus statement from the European Association of Cardiovascular Imaging and the European Society of Cardiology working group on aorta and peripheral vascular diseases. *European Heart Journal Cardiovascular Imaging.* 2023;24(5):e65–e85. doi: 10.1093/ehjci/jead024

18. Etli M, Avnioglu S, Yilmaz H, Karahan O. Investigation of the correlation between cardiac parameters and aortic diameter in patients with ascending aortic aneurysm. *Egyptian Heart Journal.* 2022;74(1):1–7. doi: 10.1186/s43044-022-00238-0

19. Pearce W, Slaughter M, Lemaire S, et al. Aortic diameter as a function of age, gender, and body surface area. *Surgery.* 1993;114(4):691–697.

20. Vasilev YA, Bobrovskaya TM, Arzamasov KM, et al. Medical datasets for machine learning: fundamental principles of standartization and systematization. *Manager Zdravoohranenia.* 2023;4:28–41. EDN: EPGAMD doi: 10.21045/1811-0185-2023-4-28-41

21. Chetverikov SF, Arzamasov KM, Andreichenko AE, et al. Approaches to Sampling for Quality Control of Artificial Intelligence in Biomedical Research. *Modern Technologies in Medicine.* 2023;15(2):19–25. EDN: FUKXYC doi: 10.17691/stm2023.15.2.02

22. Zinchenko VV, Arzamasov KM, Chetverikov SF, et al. Methodology for Conducting Post-Marketing Surveillance of Software as a Medical Device Based on Artificial Intelligence Technologies. *Modern Technologies in Medicine.* 2022;14(5):15–25. doi: 10.17691/stm2022.14.5.02

23. Chernina VY, Belyaev MG, Silin AY, et al. A diagnostic and economic evaluation of the complex artificial intelligence algorithm aimed to detect 10 pathologies on the chest CT images. *medRxiv.* 2023;4. doi: 10.1101/2023.04.19.23288584

24. Macruz FBC, Lu C, Strout J, et al. Quantification of the Thoracic Aorta and Detection of Aneurysm at CT: Development and Validation of a Fully Automatic Methodology. *Radiology: Artificial Intelligence.* 2022;4(2):e210076. doi: 10.1148/ryai.210076

25. Adam C, Fabre D, Mougin J, et al. Pre-surgical and Post-surgical Aortic Aneurysm Maximum Diameter Measurement: Full Automation by Artificial Intelligence. *European Journal*

of Vascular and Endovascular Surgery. 2021;62(6):869–877. doi: 10.1016/j.ejvs.2021.07.013
26. Vladzymyrskyy AV, Kudryavtsev ND, Kozhikhina DD, et al. Effectiveness of using artificial intelligence technologies for dual descriptions of the results of preventive lung examinations. *Profilakticheskaya Meditsina.* 2022;25(7):7–15. doi: 10.17116/profmed2022250717
27. Rodriguez-Ruiz A, Lång K, Gubern-Merida A, et al. Stand-Alone Artificial Intelligence for Breast Cancer Detection in Mammography: Comparison With 101 Radiologists. *Journal of the National Cancer Institute*. 2019;111(9):916–922. doi: 10.1093/jnci/djy222
28. Rueckel J, Reidler P, Fink N, et al. Artificial intelligence assistance improves reporting efficiency of thoracic aortic aneurysm CT follow-up. *European journal of radiology.* 2021;134(134):109424. doi: 10.1016/j.ejrad.2020.109424
29. Tang A, Tam R, Cadrin-Chênevert A, et al. Canadian Association of Radiologists White Paper on Artificial Intelligence in Radiology. *Canadian Association of Radiologists journal.* 2018;69(2):120–135. doi: 10.1016/j.carj.2018.02.002
30. Certificate of state registration of the database № 2023621046/30.03.2023. Vasilev YuA, Turavilova EV, Shul'kin IM, et al. MosMedData: CT scan with signs of abdominal aortic aneurysm. (In Russ). EDN: LXROHZ
31. Aliev AF, Kudryavtsev ND, Petraikin AV, et al. Changing of pulmonary artery diameter in accordance with severity of COVID-19 (assessment based on non-contrast computer tomography). *Digital Diagnostics*. 2021;2(3):249–260. EDN: VTMKCJ doi: 10.17816/DD76726
32. Morozov SP, Shapieva AN, Narkevich BYa, et al. *Informativity of radial diagnostics methods in various pathological conditions of the organism.* Moscow: Research and Practical Clinical Center for Diagnostics and Telemedicine; 2020. (In Russ). EDN: DYEYBT
33. Vasilev YuA, Vladzymyrskyy AV, Bondarchuk DV, et al. Importance of artificial intelligence technologies to prevent defects in radiologist's practice. *Medical doctor and IT.* 2023;(2):16–27. EDN: SYZAOQ doi: 10.25881/18110193_2023_2_16

СПИСОК ЛИТЕРАТУРЫ

1. 10 ведущих причин смерти в мире [Internet]. Всемирная организация здравоохраниения. [дата обращения: 12.05.2023]. Доступ по ссылке: https://www.who.int/ru/news-room/fact-sheets/detail/the-top-10-causes-of-death
2. Gouveia e Melo R., Silva Duarte G., Lopes A., et al. Incidence and Prevalence of Thoracic Aortic Aneurysms: A Systematic Review and Meta-analysis of Population-Based Studies // Seminars in thoracic and cardiovascular surgery. 2022. Vol. 34, N 1. P. 1–16. doi: 10.1053/j.semtcvs.2021.02.029
3. Клинические рекомендации. Рекомендации по диагностике и лечению заболеваний аорты (2017) // Кардиология и сердечно-сосудистая хирургия. 2018. Т. 11, № 1. С. 7–67. EDN: YPAKRP
4. Кузнечевский Ф.В., Осипов А.Х., Евсиков Е.М., Абрамов И.С., Отарова С.М. Распространенность и природа аневризм и расслоений аорты по данным анализа последовательных патологоанатомических вскрытий в течение десяти лет в ГКБ № 15 им. О.М. Филатова // Российский кардиологический журнал. 2004. Т. 9, № 6. С. 5–13. EDN: ISVRYL
5. Иртюга О.Б., Воронкина И.В., Смагина Л.В., и др. Частота выявления аневризмы восходящего отдела аорты и механизм ее развития по данным регистра ФГУ ФЦСКЭ им В.А. Алмазова // Бюллетень Федерального Центра сердца, крови и эндокринологии им. В.А. Алмазова. 2011. № 5. С. 73–78. EDN: OWGHOB
6. Lavall D., Schäfers H.J., Böhm M., Laufs U. Aneurysms of the ascending aorta // Deutsches Arzteblatt international. 2012. Vol. 109, N 13. P. 227–233. doi: 10.3238/arztebl.2012.0227
7. Olsson C., Thelin S., Ståhle E., Ekbom A., Granath F. Thoracic Aortic Aneurysm and Dissection // Circulation. 2006. Vol. 114, N 24. P. 2611–2618. doi: 10.1161/CIRCULATIONAHA.106.630400
8. Elefteriades J.A. Natural history of thoracic aortic aneurysms: indications for surgery, and surgical versus nonsurgical risks // The Annals of thoracic surgery. 2002. Vol. 74, N 5. P. 1877–1880. doi: 10.1016/s0003-4975(02)04147-4
9. Tsai E.B., Chiles C., Carter B.W., et al. Incidental Findings on Lung Cancer Screening: Significance and Management // Seminars in ultrasound, CT, and MR. 2018. Vol. 39, N 3. P. 273–281. doi: 10.1053/j.sult.2018.02.005
10. Чернина В.Ю., Блохин И.А., Николаев А.Е., и др. Тактика ведения инциденталом. Раздел 3. Щитовидная железа, гипофиз, сосуды и средостение. Москва : Государственное бюджетное учреждение здравоохранения города Москвы «Научно-практический клинический центр диагностики и телемедицинских технологий Департамента здравоохранения города Москвы», 2019. EDN: WSYSYP
11. Law M. "Opportunistic" Screening // J Med Screen. 1994. Vol. 1, N 4. P. 208. doi: 10.1177/096914139400100403
12. Kumar Y., Hooda K., Li S., et al. Abdominal aortic aneurysm: pictorial review of common appearances and complications // Annals of translational medicine. 2017. Vol. 5, N 12. P. 256. doi: 10.21037/atm.2017.04.32
13. Компьютерное зрение в лучевой диагностике: первый этап Московского эксперимента / под ред. Ю.А. Васильева, А.В. Владзимирского. Москва : Общество с ограниченной ответственностью «Издательские решения», 2022. EDN: FOYLXK
14. Erbel R., Aboyans V., Boileau C., Vlachopoulos C. 2014 ESC Guidelines on the diagnosis and treatment of aortic diseases: Document covering acute and chronic aortic diseases of the thoracic and abdominal aorta of the adult. The Task Force for the Diagnosis and Treatment of Aortic Diseases of the European // European heart journal. 2014. Vol. 35, N 41. P. 2873–2926. doi: 10.1093/eurheartj/ehu281
15. Документы по Эксперименту [Internet]. Центр диагностики и телемедицины. [дата обращения: 16.06.2023]. Доступ по ссылке: https://mosmed.ai/ai/docs/
16. Chest-IRA [Internet]. Центр диагностики и телемедицины. [дата обращения: 16.06.2023]. Доступ по ссылке: https://mosmed.ai/service_catalog/chestira/
17. Evangelista A., Sitges M., Jondeau G., et al. Multimodality imaging in thoracic aortic diseases: a clinical consensus statement from the European Association of Cardiovascular Imaging and the European Society of Cardiology working group on aorta and peripheral vascular diseases // European Heart Journal Cardiovascular Imaging. 2023. Vol. 24, N 5. P. e65–e85. doi: 10.1093/ehjci/jead024

18. Etli M., Avnioglu S., Yilmaz H., Karahan O. Investigation of the correlation between cardiac parameters and aortic diameter in patients with ascending aortic aneurysm // Egyptian Heart Journal. 2022. Vol. 74, N 1. P. 1–7. doi: 10.1186/s43044-022-00238-0

19. Pearce W., Slaughter M., Lemaire S., et al. Aortic diameter as a function of age, gender, and body surface area // Surgery. 1993. Vol. 114, N 4. P. 691–697.

20. Васильев Ю.А., Бобровская Т.М., Арзамасов К.М, и др. Основополагающие принципы стандартизации и систематизации информации о наборах данных для машинного обучения в медицинской диагностике // Менеджер здравоохранения. 2023. Т. 4. С. 28–41. EDN: EPGAMD doi: 10.21045/1811-0185-2023-4-28-41

21. Четвериков С.Ф., Арзамасов К.М., Андрейченко А.Е., и др. Подходы к формированию выборки для контроля качества работы систем искусственного интеллекта в медико-биологических исследованиях // Современные технологии в медицине. 2023. Т. 15, № 2. С. 19–25. EDN: FUKXYC doi: 10.17691/stm2023.15.2.02

22. Зинченко В.В., Арзамасов К.М., Четвериков С.Ф., и др. Методология проведения пострегистрационного клинического мониторинга для программного обеспечения с применением технологий искусственного интеллекта // Современные технологии в медицине. 2022. Т. 14, № 5. С. 15–25. doi: 10.17691/stm2022.14.5.02

23. Chernina V.Y., Belyaev M.G., Silin A.Y., et al. A diagnostic and economic evaluation of the complex artificial intelligence algorithm aimed to detect 10 pathologies on the chest CT images // medRxiv. 2023. Vol. 4. doi: 10.1101/2023.04.19.23288584

24. Macruz F.B.C., Lu C., Strout J., et al. Quantification of the Thoracic Aorta and Detection of Aneurysm at CT: Development and Validation of a Fully Automatic Methodology // Radiology: Artificial Intelligence. 2022. Vol. 4, N 2. P. e210076. doi: 10.1148/ryai.210076

25. Adam C., Fabre D., Mougin J., et al. Pre-surgical and Post-surgical Aortic Aneurysm Maximum Diameter Measurement: Full Automation by Artificial Intelligence // European Journal of Vascular and Endovascular Surgery. 2021. Vol. 62, N 6. P. 869–877. doi: 10.1016/j.ejvs.2021.07.013

26. Владзимирский А.В., Кудрявцев Н.Д., Кожихина Д.Д., и др. Эффективность применения технологий искусственного интеллекта для двойных описаний результатов профилактических исследований легких // Профилактическая медицина. 2022. Vol. 25, N 7. P. 7–15. doi: 10.17116/profmed2022250717

27. Rodriguez-Ruiz A., Lång K., Gubern-Merida A., et al. Stand-Alone Artificial Intelligence for Breast Cancer Detection in Mammography: Comparison With 101 Radiologists // Journal of the National Cancer Institute. 2019. Vol. 111, N 9. P. 916–922. doi: 10.1093/jnci/djy222

28. Rueckel J., Reidler P., Fink N., et al. Artificial intelligence assistance improves reporting efficiency of thoracic aortic aneurysm CT follow-up // European journal of radiology. 2021. Vol. 134, N 134. P. 109424. doi: 10.1016/j.ejrad.2020.109424

29. Tang A., Tam R., Cadrin-Chênevert A., et al. Canadian Association of Radiologists White Paper on Artificial Intelligence in Radiology // Canadian Association of Radiologists journal. 2018. Vol. 69, N 2. P. 120–135. doi: 10.1016/j.carj.2018.02.002

30. Свидетельство о государственной регистрации базы данных № 2023621046/ 30.03.2023. Васильев Ю.А., Туравилова Е.В., Шулькин И.М., и др. MosMedData: КТ с признаками аневризмы брюшного отдела аорты. EDN: LXROHZ

31. Алиев А.Ф., Кудрявцев Н.Д., Петряйкин А.В., и др. Оценка диаметра лёгочной артерии при различной степени тяжести течения COVID-19 (по данным бесконтрастной компьютерной томографии лёгких) // Digital Diagnostics. 2021. Т. 2, № 3. С. 249–260. EDN: VTMKCJ doi: 10.17816/DD76726

32. Морозов С.П., Шапиева А.Н., Наркевич Б.Я., и др. Информативность методов лучевой диагностики при различных патологических состояниях организма. Москва : Научно-практический клинический центр диагностики и телемедицинских технологий, 2020. EDN: DYEYBT

33. Васильев Ю.А., Владзимирский А.В., Бондарчук Д.В., и др. Значение технологий искусственного интеллекта для профилактики дефектов в работе врача-рентгенолога // Врач и информационные технологии. 2023. № 2. С. 16–27. EDN: SYZAOQ doi: 10.25881/18110193_2023_2_16

AUTHORS' INFO

*** Alexander V. Solovev;**
address: 24-1 Petrovka Str., Moscow, 127051, Russia;
ORCID: 0000-0003-4485-2638;
eLibrary SPIN: 9654-4005;
e-mail: atlantis.92@mail.ru

Yuriy A. Vasilev, MD, Cand. Sci. (Medicine);
ORCID: 0000-0002-0208-5218;
eLibrary SPIN: 4458-5608;
e-mail: VasilevYA1@zdrav.mos.ru

Valentin E. Sinitsyn, MD, Dr. Sci. (Medicine), Professor;
ORCID: 0000-0002-5649-2193;
eLibrary SPIN: 8449-6590;
e-mail: vsini@mail.ru

ОБ АВТОРАХ

*** Соловьёв Александр Владимирович;**
адрес: Россия, 127051, г. Москва, ул. Петровка, д. 24, стр. 1;
ORCID: 0000-0003-4485-2638;
eLibrary SPIN: 9654-4005;
e-mail: atlantis.92@mail.ru

Васильев Юрий Александрович, канд. мед. наук;
ORCID: 0000-0002-0208-5218;
eLibrary SPIN: 4458-5608;
e-mail: VasilevYA1@zdrav.mos.ru

Синицын Валентин Евгеньевич, д-р мед. наук, профессор;
ORCID: 0000-0002-5649-2193;
eLibrary SPIN: 8449-6590;
e-mail: vsini@mail.ru

* Corresponding author / Автор, ответственный за переписку

Alexey V. Petraikin, MD, Dr. Sci. (Medicine);
ORCID: 0000-0003-1694-4682;
eLibrary SPIN: 6193-1656;
e-mail: alexeypetraikin@gmail.com

Anton V. Vladzymyrskyy, MD, Dr. Sci. (Medicine);
ORCID: 0000-0002-2990-7736;
eLibrary SPIN: 3602-7120;
e-mail: VladzimirskijAV@zdrav.mos.ru

Igor M. Shulkin;
ORCID: 0000-0002-7613-5273;
eLibrary SPIN: 5266-0618;
e-mail: ShulkinIM@zdrav.mos.ru

Daria E. Sharova;
ORCID: 0000-0001-5792-3912;
eLibrary SPIN: 1811-7595;
e-mail: SharovaDE@zdrav.mos.ru

Dmitry S. Semenov, Cand. Sci. (Engineering);
ORCID: 0000-0002-4293-2514;
eLibrary SPIN: 2278-7290;
e-mail: SemenovDS4@zdrav.mos.ru

Петряйкин Алексей Владимирович, д-р мед. наук;
ORCID: 0000-0003-1694-4682;
eLibrary SPIN: 6193-1656;
e-mail: alexeypetraikin@gmail.com

Владзимирский Антон Вячеславович, д-р мед. наук;
ORCID: 0000-0002-2990-7736;
eLibrary SPIN: 3602-7120;
e-mail: VladzimirskijAV@zdrav.mos.ru

Шулькин Игорь Михайлович;
ORCID: 0000-0002-7613-5273;
eLibrary SPIN: 5266-0618;
e-mail: ShulkinIM@zdrav.mos.ru

Шарова Дарья Евгеньевна;
ORCID: 0000-0001-5792-3912;
eLibrary SPIN: 1811-7595;
e-mail: SharovaDE@zdrav.mos.ru

Семенов Дмитрий Сергеевич, канд. техн. наук;
ORCID: 0000-0002-4293-2514;
eLibrary SPIN: 2278-7290;
e-mail: SemenovDS4@zdrav.mos.ru

DOI: https://doi.org/10.17816/DD569388

DOI: https://doi.org/10.17816/DD586551

Возможности использования виртуального симулятора «Vimedix 3.2» в процессе обучения по специальности «ультразвуковая диагностика»

В.А. Васильев, С.Н. Кондричина

Петрозаводский государственный университет, Петрозаводск, Россия

АННОТАЦИЯ

Обоснование. В последние годы актуально изменение методик и программ преподавания многих дисциплин, в том числе ультразвуковой диагностики, с включением в них различных виртуальных и симуляционных устройств. Практический опыт использования подобных технологий в процессе обучения достаточно непродолжителен, в связи с этим в отечественной и зарубежной литературе имеются лишь немногочисленные оригинальные работы, посвящённые этой теме.

Цель — определить возможности и алгоритм использования виртуального симулятора ультразвукового исследования в процессе преподавания дисциплины «ультразвуковая диагностика» на основании результатов работы с ним. Оценить преимущества и недостатки применения симулятора в сравнении с традиционной методикой преподавания.

Материалы и методы. Проанализированы результаты применения виртуального тренажёра «Vimedix 3.2» в учебном процессе. На нём проводились симуляции трансабдоминального ультразвукового исследования органов брюшной полости, трансторакальной эхокардиографии, триплексного сканирования магистральных сосудов. В процессе исследования участвовали 26 ординаторов по специальности «ультразвуковая диагностика» и 37 врачей, проходивших обучение на курсах профессиональной переподготовки.

Результаты. Применение виртуального симулятора на начальном этапе в учебном процессе может устранить многие проблемы, с которыми сталкиваются ординаторы и курсанты при обучении на клинических базах. Использование симулятора в процессе тестирования представляется менее предпочтительным, по сравнению с практическим экзаменом с использованием ультразвуковых сканеров и реальных пациентов.

Заключение. Симулятор целесообразно использовать на начальном этапе для отработки методики исследования. Рекомендуется разработка и использование в обучении дополнительных учебно-методических материалов и учебной программы. Преимуществами виртуального симулятора являются комфортность работы на начальном этапе обучения, малое время его освоения, наличие обширной базы данных патологических случаев. Выявленные некритичные недостатки требуют коррекции при дальнейшем обучении в клинике.

Ключевые слова: симуляционное обучение; виртуальный тренажёр; симулятор ультразвуковых исследований; ультразвуковая диагностика.

Как цитировать:
Васильев В.А., Кондричина С.Н. Возможности использования виртуального симулятора «Vimedix 3.2» в процессе обучения по специальности «ультразвуковая диагностика» // Digital Diagnostics. 2024. Т. 5, № 1. С. 41–52. DOI: https://doi.org/10.17816/DD586551

Рукопись получена: 20.09.2023 **Рукопись одобрена:** 18.01.2024 **Опубликована online:** 11.03.2024

DOI: https://doi.org/10.17816/DD586551

Possibilities for using the Vimedix 3.2 virtual simulator to train ultrasound specialists

Valeri A. Vasilev, Svetlana N. Kondrichina

Petrozavodsk State University, Petrozavodsk, Russia

ABSTRACT

BACKGROUND: In recent years, it has been critical to modify training methods and programs in numerous areas, including ultrasound diagnosis, with the use of various virtual and simulation devices. Because practical experience with employing such technologies in the teaching process is limited, there are few original studies on the subject in Russian and foreign literature.

AIM: To determine the possibilities and algorithms for using a virtual ultrasound simulator to train ultrasound specialists based on the results of related work, as well as to assess the benefits and drawbacks of simulators in comparison to conventional teaching methods.

MATERIALS AND METHODS: The results of using the Vimedix 3.2 virtual simulator in the teaching process were analyzed. Simulations of abdominal ultrasound, transthoracic echocardiography, and triplex scanning of major vessels were performed. The study included 26 residents specializing in ultrasound diagnosis and 37 physicians undergoing professional retraining courses.

RESULTS: Using a virtual simulator during the initial stage of training helps eliminate many of the challenges that residents and trainees encounter in clinical practice. The use of a simulator during testing appears to be less beneficial than during a practical examination employing ultrasound scanners and real patients.

CONCLUSION: The use of a simulator at the initial stage is advisable to get familiar with this research methodology. It is recommended to develop and use additional teaching materials and programs in training. The advantages of the virtual simulator include ease of use during the initial stages of training, a steep learning curve, and the availability of an extensive database of pathological cases. The identified noncritical shortcomings require correction during further training in the clinic.

Keywords: simulation training; virtual simulator; ultrasound simulator; ultrasound diagnosis.

To cite this article:
Vasilev VA, Kondrichina SN. Possibilities for using the Vimedix 3.2 virtual simulator to train ultrasound specialists. *Digital Diagnostics.* 2024;5(1):41–52. DOI: https://doi.org/10.17816/DD586551

Submitted: 20.09.2023 **Accepted:** 18.01.2024 **Published online:** 11.03.2024

DOI: https://doi.org/10.17816/DD586551

在“超声诊断”专业教学过程中使用虚拟模拟器“Vimedix 3.2”的可行性

Valeri A. Vasilev, Svetlana N. Kondrichina

Petrozavodsk State University, Petrozavodsk, Russia

摘要

论证。近年来，包括超声诊断在内的许多学科的教学方法和课程发生了变化，教学计划包括在各种虚拟和模拟设备上进行练习。在教学过程中使用此类技术的实践经验相当少，在这方面，国内外文献中有关这一主题的原创作品寥寥无几。

目的。本研究的目的是根据使用虚拟超声模拟器的工作结果，确定在“超声诊断”学科教学过程中使用该模拟器的可行性和算法；评估使用模拟器与传统教学方法相比的优缺点。

材料和方法。分析了在教学过程中使用虚拟模拟器“Vimedix 3.2”的结果，在该模拟器上进行了腹腔器官经腹超声检查、经胸超声心动图检查、大血管的三重扫描。研究的参与者包括26名“超声诊断”专业的住院医师和37名接受过职业进修课程的医生。

结果。在教学过程的初始阶段使用虚拟模拟器可以消除住院医师和学员在临床现场学习时遇到的许多问题。与使用超声波扫描仪和真正患者进行实践考试相比，在测试过程中使用模拟器似乎不太可取。

结论。在初始阶段使用模拟器来练习检查方法是可行的。建议在教学中开发和使用额外的教材和教学计划。虚拟模拟器的优点是在教学初期使用方便，掌握时间短，有大量病例数据库。已发现的非关键缺点需要在临床进一步培训中加以纠正。

关键词：模拟训练；虚拟模拟器；超声模拟器；超声诊断。

引用本文：
Vasilev VA, Kondrichina SN. 在“超声诊断”专业教学过程中使用虚拟模拟器“Vimedix 3.2”的可行性. *Digital Diagnostics*. 2024;5(1):41–52. DOI: https://doi.org/10.17816/DD586551

收到：20.09.2023 **接受：**18.01.2024 **发布日期：**11.03.2024

BACKGROUND

Virtual and simulation technologies have recently increased applications in various areas of medicine, including teaching medical students. Various simulations of real processes have long been used in the training and practice of specialists in numerous areas, and they have been developed for several decades [1–3]. This process is accelerating because of both the widespread digitization of our lives and the active implementation of such technology in clinical practice.

Virtual simulators and augmented reality technologies are increasingly being used in clinical practice, not only for diagnosis but also for therapeutic purposes in areas such as surgery, anesthesia, and resuscitation. These include three-dimensional (3D) anatomy and imaging tables, virtual reality programs for studying human anatomy, and surgical simulators and robots [4–6]. Consequently, digital methods are being used in teaching and knowledge assessment of medical graduates and healthcare professionals undergoing retraining during state certifications and accreditations, including ultrasound diagnostic specialists [1, 7]. The interest in such technologies increased because medical schools and postgraduate education institutions are finding it increasingly difficult to teach some specialties in clinical settings.

These include limitations specific to working in the clinic, such as research place and time constraints [7, 8], shortage of ultrasound machines, lack of mentors, and access issues during quarantine. Other challenges are related to the individuals being examined, including psychological pressure on students during their first interactions with patients, some patients' reluctance to be examined by students [8], lack of patients with the pathology of interest in the clinic, and poor visualization in the so-called "difficult" patients. Moreover, some problems are related to students' theoretical knowledge and level of engagement, which can significantly increase the time for practicing the required skills, which is limited in the clinic. Furthermore, skill building in ultrasound scanning techniques can be challenging because of a lack of understanding of normal and abnormal anatomy. This refers to the proper sensor placement, which can be time-consuming and uncomfortable for the patient.

Thus, changes in the teaching methods and curricula for some specialties in medical schools and the use of modern virtual and simulation devices are necessary. It is especially relevant in training radiology specialists because digital image processing software has long been used in X-ray diagnosis, and specialists must have adequate skills and expertise.

However, the experience of using such technologies in teaching medical students is limited. Consequently, original articles on the subject in both Russian and foreign literature are limited. The majority of these articles emphasize the benefits of simulation technologies in training ultrasound diagnostic specialists [7–10]; however, certain disadvantages exist, particularly in testing and knowledge assessment [7]. Virtually no standardized approaches have been established for simulation training in diagnostic ultrasonography, efficient use of virtual simulators, establishing their role in the educational process and evaluating the results of their use. Data on the development and effectiveness of special training modules and teaching materials aimed at mastering specific types of simulators are limited.

In this regard, we analyzed our experience with modern digital technologies in teaching and knowledge assessment, using an ultrasound simulator as an example. The virtual simulator has been used for 4 years for training of ultrasound diagnostic specialists at the Department of X-ray Diagnostics and Radiation Therapy of the Institute of Medicine of the Petrozavodsk State University. The simulator is intended for first- and second-year residents and physicians during professional retraining. The simulator is used by residents during the final state certification and for primary accreditation of ultrasound diagnostic specialists.

AIM

To determine the possibilities and algorithms for the use of a virtual ultrasound simulator to train ultrasound diagnostic specialists based on the results of using a simulator to assess the benefits and drawbacks of simulators in comparison with conventional teaching methods.

MATERIALS AND METHODS

The results of using a Vimedix 3.2 virtual ultrasound simulator (CAE Healthcare, Canada) in the teaching process were analyzed. This simulator is the most widely available in both the Russian and foreign markets. It includes several mannequins and sensors for practicing ultrasound scanning techniques in various areas and an abnormal case database. The simulator includes an Omen laptop (Hewlett-Packard, USA) with wireless connection, a mouse, a male multipurpose mannequin, an array of ultrasonic convex sensor, and a sensor adapter (Fig. 1).

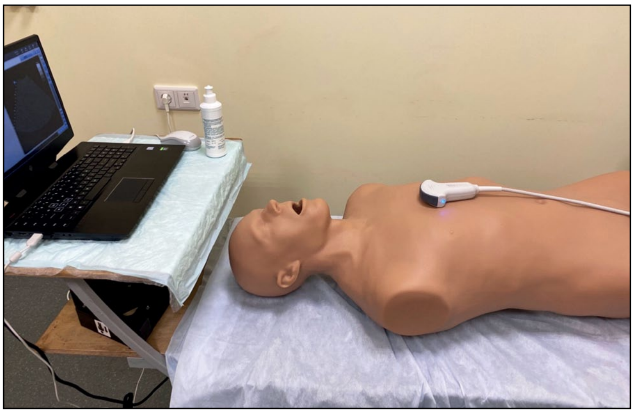

Fig. 1. Vimedix 3.2 virtual ultrasound simulator.

The laptop used comes with original ultrasound simulation software that supports both 2D and 3D/4D anatomical modes with multiplanar reconstruction. Microsoft HoloLens 2 (USA) mixed reality technology allows the user to visualize the anatomical structures of interest in the “live” mode, i.e., in motion. It is used to facilitate navigation in the area of interest by assessing X-ray tomographic images [11, 12] and in the simulator for correct sensor positioning during simulation [13]. In the laptop screen’s workspace, in addition to the 2D image, a separate window displays a 3D/4D animated anatomical image of the organs within the scanning area. Users can control the display of anatomical structures and split the window for better visualization.

The simulator can imitate procedures such as transabdominal ultrasonography, transthoracic echocardiography, and scanning of major vessels. The following scanning modes are available:

- B (2D, B-scan ultrasonography)
- M (A-scan ultrasonography)
- Color Doppler (CD)
- Pulsed wave (PW)

A customized marker system monitors the sensor movement along the mannequin surface, allowing for ultrasound scanning in various positions (dorsal, lateral, etc.). A set of basic tools was used to assess the results, such as length, area, volume, and blood flow velocity measurement in Doppler modes, and calculation of central hemodynamics parameters during echocardiography. A final protocol can be generated based on the scan findings and measurements.

The virtual simulator has a large database of ultrasound images depicting various pathologies of the abdominal organs and cardiovascular system. This allows the user to master ultrasound scanning techniques in various areas, both with normal anatomy and various pathologies. Consequently, during knowledge assessment, the ability of certification candidates to detect and describe various pathological changes using standard protocols can be evaluated.

The study included 26 residents training in diagnostic ultrasonography and 37 physicians undergoing professional retraining in the same discipline. Because the study used categorical data and two answer options, this sample size was sufficient to assess the proposed teaching method and extrapolate the results to all students training in ultrasonography, during the study period and beyond. The results of using the simulator were assessed by personnel of the Department of X-ray Diagnostics and Radiation Therapy and practicing diagnosticians from the institute’s clinical sites who participated in the training and knowledge assessment.

The main parameters for assessing the results of using the virtual simulator were those necessary for organizing and planning the teaching process:

- Time required to master the simulator (including training in running the software and using the interface)
- Ease of learning and psychological comfort
- Ease of handling the sensor and mannequin
- Correct sensor positioning (using anatomic landmarks of the mannequin and the mixed reality technology)

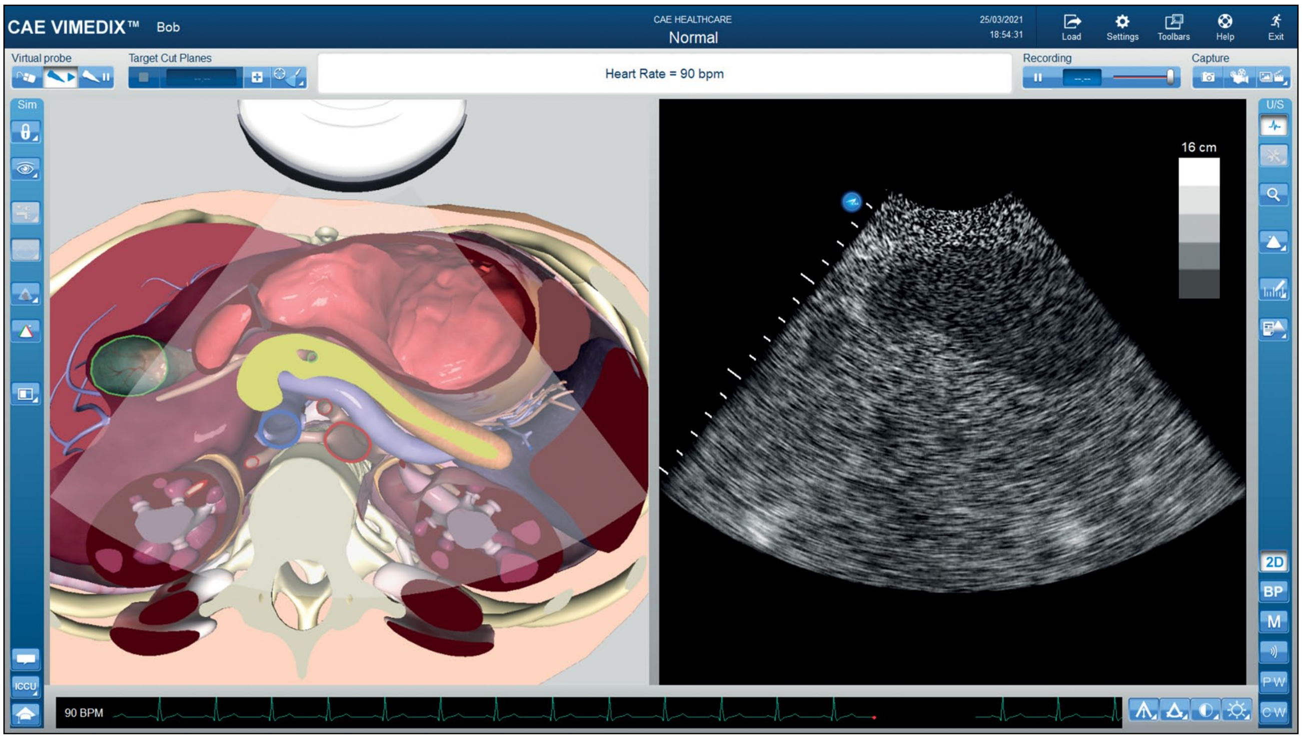

Fig. 2. Simulation program interface in mixed reality and 2D modes.

- Ability of students to use the simulator without assistance
- Need for special teaching materials and modifications of the existing training program.

Residents and students who had previously used ultrasound scanners in the clinic assessed the quality of images created by the simulator and compared it with the quality of the image obtained in a real world setting. Data were collected by an anonymous survey of students using the Likert scale [14] and scoring from 0 to 5 for the proposed questions (Figs. 3 and 4).

During training, the teacher analyzed the work with the equipment using the assessment criteria. At the end of the training course, teachers and mentors working in the clinic used tests to assess the theoretical knowledge and practical skills of the students. The majority of the assessment criteria were subjective, making it difficult to interpret the results. However, this is inherent in ultrasonography, contributing to its high operator dependency. Problems that emerged during training were also recorded, and their causes and solutions were discussed with the students.

Ethical considerations

The study volunteers participating in training and research provide informed consent. Data were acquired using a voluntary anonymous questionnaire survey, and no personal data were collected or processed during the process. This study did not involve any patients.

RESULTS

When assessing the benefits and drawbacks of using a virtual simulator in the training, the simulator was compared with the conventional method, where residents and physicians receive training using an ultrasound scanner in real patients in clinical settings under the supervision of mentors (department staff and practicing physicians). This conventional approach has well-known limitations, particularly in recent years because of the COVID-19 pandemic [15].

All residents and the majority of the students (81%) successfully completed the training with the virtual ultrasound simulator. The success criteria included confident use of the simulator software and interface (running, settings, etc.) and full mastery of ultrasound scanning techniques in various areas (Table 1).

The minimum time required to master the simulator was 2–6 training sessions (2 academic hours each) under the supervision of a department teacher, plus one introductory lecture (1 academic hour, or 45 min). Notably, residents mastered the simulator more quickly than students. This, we believe, is due to their theoretical background (lectures in X-ray diagnosis) and experience in working with ultrasound equipment. For most residents (75%), 2–3 training sessions with a mentor were sufficient, after which they could work without supervision. As for physicians taking professional retraining, older students (aged ⩾ 50 years) required a minimum of 3–4 and a maximum of 6 training sessions to

Questionnaire for residents and students training in diagnostic ultrasonography
The survey is anonymous; you are not required to provide any personal information.
For answers with a gap, please use a scale of 1 to 5, where: 1 = strongly disagree, 2 = disagree, 3 = neither agree or disagree, 4 = agree, and 5 = strongly agree.

For yes/no questions, please select one option.

1. I fully mastered the ultrasound simulator.
Answer:____ (points)
2. I fully mastered the ultrasound scanning technique in specific areas using the ultrasound simulator.
Answer:____ (points)
3. It was easy for me to master the ultrasound simulator.
Answer:____ (points)
4. It was difficult for me to master the ultrasound simulator.
Answer:____ (points)
5. I would prefer the ultrasound simulator when training in diagnostic ultrasonography.
Yes No
6. I would prefer ultrasound scanning in real patients when training in diagnostic ultrasonography.
Yes No
7. It was difficult for me to master the ultrasound simulator software.
Answer:____ (points)
8. My knowledge of computer science is sufficient to confidently use the ultrasound simulator.
Answer:____ (points)
9. My knowledge of computer science is insufficient to confidently use the ultrasound simulator.
Answer:____ (points)

Fig. 3. Questionnaire for residents and students, part 1.

10. For me, training using the ultrasound simulator was more psychologically comfortable than training on real patients in clinical settings.
Answer:____ (points)
11. For me, training on real patients in clinical settings was more psychologically comfortable than training using the ultrasound simulator.
Answer:____ (points)
12. I would prefer the ultrasound simulator for the final testing in diagnostic ultrasonography.
Answer:____ (points)
13. I would prefer real patients in clinical settings for the final testing in diagnostic ultrasonography.
Answer:____ (points)
14. For me, preparing for the final testing using the ultrasound simulator was more psychologically comfortable than training on real patients in the clinical setting.
Answer:____ (points)
15. For me, preparing for the final testing on real patients in clinical settings was more psychologically comfortable than using the ultrasound simulator.
Answer:____ (points)
16. It took me longer to master ultrasound scanning techniques using the ultrasound simulator than training on real patients in the clinical setting.
Yes No
17. It took me longer to master ultrasound scanning techniques when training on real patients in clinical settings than using the ultrasound simulator.
Yes No
18. The images of internal organs on the screen of the ultrasound simulator are not inferior to those of the diagnostic ultrasound systems I have worked with (if you have no such experience, please do not answer this question)
Answer:____ (points)

Comments (please add your opinion on the subjects not addressed in the questionnaire or challenges you encountered when using the ultrasound simulator)

Fig. 4. Questionnaire for residents and students, part 2.

Table 1. Student survey and testing results

	Residents	Physicians
Number of students	26	37
Successful mastery of the simulator	100%	81%
Minimum time required to master the simulator, min	90	135
Psychological comfort during training in diagnostic ultrasonography using the simulator	80%	68%
Psychological comfort during preparation for testing/accreditation using the simulator	90%	75%
Satisfactory quality of simulator images in the M and B modes	95%	95%
Satisfactory quality of simulator images in Doppler modes	90%	89%
Positive opinion on the use of 3D/4D navigation software	100%	100%
Preference for the simulator during final testing and accreditation	100%	90%

master basic skills in using the simulator. Here, problems were encountered because some students (26%) had either zero or rudimentary computer skills. Consequently, they could not independently run laptop software and confidently use the simulator application interface even after completing the training course. To assess the results of using the virtual simulator, task-based tests were performed during the initial accreditation of ultrasound diagnostic specialists (Fig. 5).

When using the simulator to master basic skills in diagnostic ultrasonography, 72% of the students reported more psychological comfort than when training on real patients in clinical settings. This criterion was evaluated only by students who had some actual experience with ultrasound scanners (however limited). Both mentors and students stated that the simulator makes it easier and faster to master ultrasound scanning techniques. However, the stress of the first contact with a patient in a real world setting must be addressed in subsequent practice. This was primarily relevant for residents who had no experience with ultrasound scanning in real patients.

Working on the simulator was effortlessly integrated into the training program because it was placed on the premises of the medical school; thus, we did not have to adjust to the working hours of a healthcare facility. This helps us address the issue of a lack of space and limited time for training in clinical settings. We practiced dividing the students into groups, which allowed us to propose a training schedule convenient for the teacher and students. Accordingly, small groups of up to three students are most suited for simultaneous work on a virtual simulator. This group size is determined by the amount of time taken by one student to master new skills during a training session, as well as the size of the classroom.

Most students rated the image quality in the B and M modes as good (95%) and in the Doppler modes as satisfactory (89%). The assessment criteria included the difficulty in recognizing and interpreting the resulting images and the ability to correlate them with actual anatomical objects. A problem in using Doppler modes was the inability to adjust some of their parameters. Consequently, blood flow in CD and PW modes was only clearly visualized through the heart valves and some portions of the aorta.

All students agreed that an additional window with a mixed reality mode and 3D/4D-live anatomical navigation of the examined area helps in positioning the sensor when examining all areas. It was especially convenient when examining the abdominal organs and the heart [12].

Test to assess the results of mastering ultrasound scanning techniques in the B mode using an ultrasound simulator (option 1, with the MR mode; option 2, without the MR mode).
Testing time: 10 min

1. Turn on the virtual simulator and run the ultrasound simulation program.
2. Place the mannequin in the correct position for scanning ___________________________
2. Display the examined organ in the longitudinal plane ______________________ with/without MR technology.
3. Determine the size measuring points, perform the measurements, and share the findings.
4. Display the examined organ in the transverse plane ______________________ with/without MR technology
5. Determine the size of the measuring points, perform the measurements, and share the findings.
6. Assess the echolucency and echostructure of the organs and share the findings.
7. Assess and describe the contours of the organ.
8. In the case of abnormal changes in the organs, assess them as follows:
   - Location
   - Size
   - Shape
   - Echolucency and echostructure
   - Contours
   - Additional elements (artifacts, etc.)
9. Prepare and share the scanning protocol, including the assessed parameters.

Test to assess the results of mastering ultrasound scanning techniques in the Doppler modes using an ultrasound simulator (option 1, with the MR mode; option 2, without the MR mode).
Testing time: 10 min

1. Turn on the virtual simulator and run the ultrasound simulation program.
2. Place the mannequin in the correct position to scan the heart.
3. Display the heart in the apical five-chamber view in the B mode.
4. Turn on the color flow mapping mode and set the scanned area in the mitral valve region.
5. Display the transmitral flow in the color flow mapping mode, assess its direction and characteristics, and share the findings.
6. Turn on the pulsed wave Doppler mode, set the sample volume above the mitral valve leaflets, and display the transmitral flow spectrum.
7. Measure the velocity, assess the transmitral flow spectrum, and share the findings.
8. Set the scanned area in the color flow mapping mode in the aortic valve region.
9. Display the blood flow in the left ventricular outflow tract in the color flow mapping mode, assess its direction and characteristics, and share the findings.
10. Set the sample volume of the pulsed wave Doppler mode in the left ventricular outflow tract and display the blood flow spectrum.
11. Measure the velocity, assess the blood flow spectrum in the left ventricular outflow tract, and share the findings.
12. Set the sample volume of the pulsed wave Doppler mode in the supravalvular ridge of the aorta and display the blood flow spectrum.
13. Measure the velocity, assess the blood flow spectrum in the supravalvular ridge of the aorta, and share the findings.
14. Prepare and share the conclusion based on the blood flow through the mitral and aortic valves in Doppler modes.

Fig. 5. Tests to assess the results of mastering ultrasound scanning techniques.

In the B mode, an issue with incorrect sensor positioning on the mannequin for some standard projections of the heart (such as apical) was discovered, which will require improvement in the future when practicing on real patients. In these cases, students successfully solved the challenge using the mixed reality system, allowing them to assess accurately the section planes of the organ and the position of the sensor relative to anatomical landmarks.

According to the survey results, 95% (both residents and physicians) favored using the simulator over training on real patients. The mean time spent practicing ultrasound scanning in one area using the simulator was 1–2 training sessions (2 academic hours each). The training included multiple-view scanning with various positions of the mannequin; moreover, the duration was not limited to one scan, which is unavoidable in clinical settings. When our students began using real ultrasound scanners, their skills in ultrasound scanning of various areas were satisfactory, requiring only a quick correction of sensor positioning and the ability to work with “difficult” patients and during specific respiratory phases.

In teaching methodology, it should differ from training in clinical settings under the supervision of mentors. Training in clinical settings includes two main approaches: witnessing the procedure and imitating the mentor’s actions on a patient. Training using a virtual simulator also offers an opportunity for self-learning through trial and error. This approach is more comfortable for students (at least because there are no time constraints or psychological pressures) and can provide better practical results. This training strategy enabled our students to work on the simulator independently and on their schedule. If necessary, the teacher provided consultations remotely via voice and video communications.

Furthermore, the conventional “one mentor, one trainee” approach could be converted to group training at the initial stage, which is more economically viable. The simulator allowed the merging of the theoretical and practical components of the training program in a single training session. Initially, the teacher presents an introductory lecture on a certain topic with a demonstration of the simulator. Then, the students could reinforce their knowledge during practical training (Fig. 6). This approach proved convenient when learning the fundamentals of ultrasound scanning in specific areas and when preparing for testing.

The use of the virtual simulator for knowledge assessment during resident certification and specialist accreditation yielded ambiguous results, requiring further discussion. In several similar studies, the authors emphasize the benefits of using simulators, particularly the lack of stress for certification candidates and conditions close to reality [8, 15]. These findings are consistent with the views of most students (95%), who chose to use the simulator during practical testing. Furthermore, this judgment was consistent before and after testing. However, according to the department staff and mentors, this testing option has more negatives than positives.

Fig. 6. A second-year resident using the simulator.

DISCUSSION

Based on the results obtained with the Vimedix 3.2 virtual simulator, it can be recommended for use at the initial stage of training ultrasound diagnostic specialists. Our experience confirmed the benefits of incorporating virtual and augmented reality technologies into educational programs for medical students and ultrasound training programs as reported previously [8–10, 15]. Virtual simulators are useful for practicing ultrasound scanning techniques in specific areas, positioning the sensor using anatomical landmarks, and learning how to take basic measurements in various modes, including Doppler ones. However, they do not replace clinical experience, but augment it. At subsequent stages, practical skills should be reviewed (and improved) by examining real patients under the supervision of a mentor.

Currently, little information exists on how skills gained through simulation-based training correlate with clinical efficacy or how long they will be maintained [16, 17]. Thus, practical testing is essential in graduates several years after the start of independent work to more accurately assess the efficacy of training. The Objective Structured Assessment of Ultrasound Skills scale can be used for this purpose [18].

To effectively master the simulator, a user manual that addresses topics such as running the application, a user manual for the interface, and step-by-step instructions for specific tasks is necessary. To facilitate self-learning, the teacher should prepare an introductory lecture to familiarize residents and students with the simulator software and demonstrate its capabilities. Accordingly, guidelines for examining specific anatomical areas of the mannequin using a simulator will also be beneficial. To master ultrasound scanning techniques in specific areas, training modules lasting two academic hours proved useful,

DOI: https://doi.org/10.17816/DD586551

with one to demonstrate the techniques and the other for practical training. Because of the varying computer skills of students, the training program can provide two options, with more or less time spent on training in running simulator software.

To fully master the simulator, a minimum of 5–6 training sessions with a teacher covering several scanning areas are required. These could include reviewing the normal anatomy, practicing positioning, various ultrasound modes, and organ assessment parameters. Students can then work independently on their schedule, including with remote supervision from the teacher to address any emerging concerns. Furthermore, using the pathological case database integrated into the software, the virtual simulator can be used for training in the diagnosis of disorders that were not encountered in real patients in clinical settings.

However, the final knowledge assessment should be performed on real patients using ultrasound scanners because this allows assessing the ability of certification candidates to handle specific clinical situations. An optimal, albeit more complex, approach is to perform ultrasound scans in both healthy individuals and patients with a specific condition, for the resident or student to demonstrate to the mentor and accurately describe a standard protocol. Residents and students prefer using a simulator because preparing for and performing the practical test on a simulator is psychologically more comfortable than in clinical settings. Using a simulator does not require much time, patient participation, or clinical equipment; it can be used independently at any time, and students are not stressed.

Conversely, teachers believe that preparing for practical tests is primarily about memorizing certain actions. During testing, experts mainly assess the execution and sequence of certain actions rather than their quality and results. The checklist and remote monitoring system do not allow for a detailed assessment of the accuracy of images obtained by certification candidates and the assignment of additional tasks in the case of doubt. Work with various body types could not be assessed; standardized normal anatomical images in the absence of respiratory movements are assessed, and multiple-view scanning is not performed. The emphasis is more on the existing testing methods and principles rather than the operating principles and capabilities of virtual simulators.

The hardware and software features of the Vimedix 3.2 virtual simulator allow for the appropriate simulation of the primary scanning techniques that an ultrasound specialist should master during training. Accordingly, this simulator can be further improved, and its scope broadened to include training in modern techniques such as ultrasound-guided punctures of various organs and gastrointestinal echoendoscopy.

CONCLUSION

The Vimedix 3.2 simulator is recommended for use at the initial training stage for ultrasound diagnostic specialists to practice ultrasound scanning techniques in various areas, including specific clinical situations. In our opinion, using the simulator for certification and accreditation is currently less preferable than testing on real patients in clinical settings. To use the simulator effectively, additional teaching materials and training modules and reviewing the practical training approaches must be implemented.

The main benefits of using the Vimedix 3.2 virtual simulator for educational purposes are psychological comfort for students, a steep learning curve, possibility to work in a group, an extensive pathological case database, and placement on the premises of the medical school.

The identified drawbacks include the inability to practice skills required to work with real patients, errors in sensor positioning, and inconsistent image quality in the CD mode. These drawbacks are not critical, but they necessitate subsequent adjustments to the acquired skills when working in the clinic.

ADDITIONAL INFORMATION

Funding source. This study was not supported by any external sources of funding.

Competing interests. The authors declare that they have no competing interests.

Authors' contribution. All authors made a substantial contribution to the conception of the work, acquisition, analysis, interpretation of data for the work, drafting and revising the work, final approval of the version to be published and agree to be accountable for all aspects of the work. V.A. Vasiliev — concept and design of the study, data analysis, writing the text of the article; S.N. Kondrichina — collection and processing of materials.

REFERENCES

1. Meller G. A typology of simulators for medical education. *J Digit Imaging.* 1997;10(Suppl. 1):194–196. doi: 10.1007/BF03168699

2. Gaba DM. The future vision of simulation in health care. *Quality and Safety in Health Care.* 2004;13(Suppl. 1):2–10. doi: 10.1136/qshc.2004.009878

3. Alinier G. A typology of educationally focused medical simulation tools. *Medical Teacher.* 2007;29(8):243–250. doi: 10.1080/01421590701551185

4. Gorshkov MD, Nikitenko AI. Review of russian and world experience: usage of virtual simulators in training of endosurgeons. *Virtual'nye tekhnologii v meditsine.* 2009;1(1):15–18. EDN: QBAVGC doi: 10.46594/2687-0037_2009_1_18

5. Gorshkov MD, Fedorov AV. Classification of the simulation equipment. *Virtual'nye tekhnologii v meditsine.* 2012;2(8):23–35. EDN: BJWHJB doi: 10.46594/2687-0037_2012_2_21

6. Svistunov AA, editor. *Simulation training in medicine.* Moscow: Sechenov University Publishing; 2013. (In Russ). EDN: XVVEDZ doi: 10.46594/9785423501099

7. Chalouhi GE, Bernardi V, Gueneuc A, et al. Evaluation of trainees' ability to perform obstetrical ultrasound using simulation: challenges and opportunities. *Am J Obstet Gynecol.* 2016;214(4):525–528. doi: 10.1016/j.ajog.2015.10.932

8. Hani S, Chalouhi G, Lakissian Z, Sharara-Chami R. Introduction of Ultrasound Simulation in Medical Education: Exploratory Study. *JMIR Med Educ.* 2019;5(2):13568. doi: 10.2196/13568

9. Ovsiannikova LS, Shunkova SA, Kespleri EV. The importance of simulation technologies in improving the quality of training of specialists in ultrasound diagnostics. *VI International (76 All-Russian) Scientific and Practical Conference "Topical Issues of Modern Medical Science and Public Health".* 2021;3:642–645.

10. Freundt P, Nourkami-Tutdibi N, Tutdibi E, et al. Controlled Prospective Study on the Use of Systematic Simulator-Based Training with a Virtual, Moving Fetus for Learning Second-Trimester Scan: FESIM III. *Ultraschall Med.* 2023;44(4):e199–e205. doi: 10.1055/a-1984-8320

11. Hatzl J, Böckler D, Hartmann N, et al. Mixed reality for the assessment of aortoiliac anatomy in patients with abdominal aortic aneurysm prior to open and endovascular repair: Feasibility and interobserver agreement. *Vascular.* 2023;31(4):644–653. doi: 10.1177/17085381221081324

12. Kukla P, Maciejewska K, Strojna I, et al. Extended Reality in Diagnostic Imaging-A Literature Review. *Tomography.* 2023;9(3):1071–1082. doi: 10.3390/tomography9030088

13. Vasilev VA, Vasileva AE. 3D/4D anatomical navigation in virtual ultrasound simulators. *Actual issues of fundamental and clinical morphology: Proceedings of the International Scientific and Practical Conference, Tver, October 14, 2022.* 2022:101–105. EDN: TWYHTL

14. Bernstein IH. *Likert Scale Analysis.* Elsevier; 2005. doi: 10.1016/B0-12-369398-5/00104-3

15. Dietrich CF, Lucius C, Nielsen MB, et al. The ultrasound use of simulators, current view, and perspectives: Requirements and technical aspects (WFUMB state of the art paper). *Endosc Ultrasound.* 2023;12(1):38–49. doi: 10.4103/EUS-D-22-00197

16. Almestehi M, Alomaim W, Rainford L, et al. Role of the virtual reality simulator (ScanTrainer) as a multidisciplinary training tool in transvaginal ultrasound: A systematic review and narrative synthesis. *Radiography (Lond).* 2019;25(3):260–268. doi: 10.1016/j.radi.2018.12.009

17. Pezel T, Dreyfus J, Mouhat B, et al. Effectiveness of Simulation-Based Training on Transesophageal Echocardiography Learning: The SIMULATOR Randomized Clinical Trial. *JAMA Cardiol.* 2023;8(3):248–256. doi: 10.1001/jamacardio.2022.5016

18. Tolsgaard MG, Todsen T, Sorensen JL, et al. International multispecialty consensus on how to evaluate ultrasound competence: a Delphi consensus surve. *PLoS One.* 2013;8(2):e57687. doi: 10.1371/journal.pone.0057687

СПИСОК ЛИТЕРАТУРЫ

1. Meller G. A typology of simulators for medical education // J Digit Imaging. 1997. Vol. 10, Suppl. 1. P. 194–196. doi: 10.1007/BF03168699

2. Gaba D.M. The future vision of simulation in health care // Quality and Safety in Health Care. 2004. Vol. 13, Suppl. 1. P. 2–10. doi: 10.1136/qshc.2004.009878

3. Alinier G. A typology of educationally focused medical simulation tools // Medical Teacher. 2007. Vol. 29, N 8. P. 243–250. doi: 10.1080/01421590701551185

4. Горшков М.Д., Никитенко А.И. Применения виртуальных симуляторов в обучении эндохирургов — обзор российского и мирового опыта // Виртуальные технологии в медицине. 2009. Т. 1, № 1. С. 15–18. EDN: QBAVGC doi: 10.46594/2687-0037_2009_1_18

5. Горшков М.Д., Федоров А.В. Классификация симуляционного оборудования // Виртуальные технологии в медицине. 2012. Т. 2, № 8. С. 23–35. EDN: BJWHJB doi: 10.46594/2687-0037_2012_2_21

6. Симуляционное обучение в медицине / под ред. А.А. Свистунова. Москва : Издательство Первого МГМУ им. И.М. Сеченова, 2013. EDN: XVVEDZ doi: 10.46594/9785423501099

7. Chalouhi G.E., Bernardi V., Gueneuc A., et al. Evaluation of trainees' ability to perform obstetrical ultrasound using simulation: challenges and opportunities // Am J Obstet Gynecol. 2016. Vol. 214, N 4. P. 525–528. doi: 10.1016/j.ajog.2015.10.932

8. Hani S., Chalouhi G., Lakissian Z., Sharara-Chami R. Introduction of Ultrasound Simulation in Medical Education: Exploratory Study // JMIR Med Educ. 2019. Vol. 5, N 2. P. 13568. doi: 10.2196/13568

9. Овсянникова Л.С., Шунькова С.А., Кесплери Э.В. Значение симуляционных технологий в повышении качества подготовки специалистов ультразвуковой диагностики // VI Международная (76 Всероссийская) научно-практическая конференция «Актуальные вопросы современной медицинской науки и здравоохранения». 2021. Т. 3. С. 642–645.

10. Freundt P., Nourkami-Tutdibi N., Tutdibi E., et al. Controlled Prospective Study on the Use of Systematic Simulator-Based Training with a Virtual, Moving Fetus for Learning Second-Trimester Scan: FESIM III // Ultraschall Med. 2023. Vol. 44, N 4. P. e199–e205. doi: 10.1055/a-1984-8320

11. Hatzl J., Böckler D., Hartmann N., et al. Mixed reality for the assessment of aortoiliac anatomy in patients with abdominal aortic aneurysm prior to open and endovascular repair: Feasibility and interobserver agreement // Vascular. 2023. Vol. 31, N 4. P. 644–653. doi: 10.1177/17085381221081324

12. Kukla P., Maciejewska K., Strojna I., et al. Extended Reality in Diagnostic Imaging-A Literature Review // Tomography. 2023. Vol. 9, N 3. P. 1071–1082. doi: 10.3390/tomography9030088

13. Васильев В.А., Васильева А.Э. 3D/4D анатомическая навигация в виртуальных симуляторах ультразвукового исследования // Актуальные вопросы фундаментальной и клинической морфологии: Материалы Международной научно-практической конференции, Тверь, 14 октября 2022 года. 2022. С. 101–105. EDN: TWYHTL

14. Bernstein I.H. Likert Scale Analysis. Elsevier, 2005. doi: 10.1016/B0-12-369398-5/00104-3

15. Dietrich C.F., Lucius C., Nielsen M.B., et al. The ultrasound use of simulators, current view, and perspectives: Requirements and technical aspects (WFUMB state of the art paper) // Endosc Ultrasound. 2023. Vol. 12, N 1. P. 38–49. doi: 10.4103/EUS-D-22-00197

16. Almestehi M., Alomaim W., Rainford L., et al. Role of the virtual reality simulator (ScanTrainer) as a multidisciplinary training tool in transvaginal ultrasound: A systematic review and narrative synthesis // Radiography (Lond). 2019. Vol. 25, N 3. P. 260–268. doi: 10.1016/j.radi.2018.12.009

17. Pezel T., Dreyfus J., Mouhat B., et al. Effectiveness of Simulation-Based Training on Transesophageal Echocardiography Learning: The SIMULATOR Randomized Clinical Trial // JAMA Cardiol. 2023. Vol. 8, N 3. P. 248–256. doi: 10.1001/jamacardio.2022.5016

18. Tolsgaard M.G., Todsen T., Sorensen J.L., et al. International multispecialty consensus on how to evaluate ultrasound competence: a Delphi consensus surve // PLoS One. 2013. Vol. 8, N 2. P. e57687. doi: 10.1371/journal.pone.0057687

AUTHORS' INFO

*** Valeri. A. Vasilev,** MD, Cand. Sci. (Medicine), Assistant Professor;
address: 33 Lenin Ave, Petrozavodsk, 185910, Russia;
ORCID: 0000-0001-7164-4274;
eLibrary SPIN: 3582-0940;
e-mail: valerij-vasiljev@list.ru

Svetlana. N. Kondrichina, MD, Cand. Sci. (Medicine), Assistant Professor;
ORCID: 0000-0001-8472-9146;
e-mail: konsvet12@gmail.com

ОБ АВТОРАХ

*** Васильев Валерий Анатольевич,** канд. мед. наук, доцент;
адрес: Россия, 185910, г. Петрозаводск, пр. Ленина, 33;
ORCID: 0000-0001-7164-4274;
eLibrary SPIN: 3582-0940;
e-mail: valerij-vasiljev@list.ru

Кондричина Светлана Николаевна, канд. мед. наук, доцент;
ORCID: 0000-0001-8472-9146;
e-mail: konsvet12@gmail.com

* Corresponding author / Автор, ответственный за переписку

DOI: https://doi.org/10.17816/DD623995

Применение технологии машинного обучения для прогнозирования оптической силы интраокулярных линз: генерализация диагностических данных

А.А. Арзамасцев[1, 2], О.Л. Фабрикантов[2], Н.А. Зенкова[3], С.В. Беликов[2]

[1] Воронежский государственный университет, Воронеж, Россия;
[2] Национальный медицинский исследовательский центр «Межотраслевой научно-технический комплекс “Микрохирургия глаза” имени академика С.Н. Федорова», Тамбов, Россия;
[3] Тамбовский государственный университет имени Г.Р. Державина, Тамбов, Россия

АННОТАЦИЯ

Обоснование. Имплантация современных интраокулярных линз позволяет офтальмологам эффективно решать задачи хирургической реабилитации пациентов с катарактой. Степень улучшения зрительных функций пациента напрямую связана с точностью предоперационного расчёта оптической силы интраокулярных линз. Для расчёта этого показателя используются такие формулы, как SRK II, SRK/T, Hoffer-Q, Holladay II, Haigis, Barrett. Все они хорошо работают для «среднего пациента», однако не являются в достаточной степени адекватными на границах диапазонов входных переменных.

Цель — изучение возможности использования математических моделей, полученных в результате глубокого обучения искусственных нейронных сетей, для генерализации данных и прогнозирования оптической силы современных интраокулярных линз.

Материалы и методы. Обучение моделей, основанных на искусственных нейронных сетях, проводилось на масштабных выборках, в том числе на обезличенных данных пациентов офтальмологической клиники. Данные, предоставленные в 2021 году врачом-офтальмологом К.К. Сырых, отражают результаты как предоперационных, так и послеоперационных наблюдений за пациентами. Исходный файл, использованный для построения модели, основанной на искусственной нейронной сети, включал 455 записей (26 столбцов входных факторов и один столбец выходного фактора) при расчёте интраокулярных линз (дтпр). Для удобного построения моделей использовали программу-симулятор, ранее разработанную авторами.

Результаты. Полученные модели, в отличие от традиционно используемых формул, в гораздо большей степени отражают региональную специфику пациентов. Они также позволяют переобучать и оптимизировать структуру модели на основе вновь поступающих данных, что позволяет учитывать нестационарность объекта. Отличительной особенностью таких моделей, основанных на искусственных нейронных сетях, по сравнению с известными формулами, широко используемыми в хирургическом лечении катаракты, является возможность учёта значительного числа регистрируемых входных величин. Это позволило снизить среднюю относительную погрешность расчётов оптической силы интраокулярных линз с 10–12% до 3,5%.

Заключение. Данное исследование показывает принципиальную возможность генерализации значительного количества эмпирических данных по расчёту оптической силы интраокулярных линз с использованием глубокого обучения моделей искусственных нейронных сетей , которые имеют значительно большее количество входных переменных, чем при использовании традиционных формул и методов. Полученные результаты позволяют построить интеллектуальную экспертную систему с динамическим поступлением новых данных и поэтапным переобучением моделей.

Ключевые слова: искусственный интеллект; медицинские данные; выборка; машинное обучение; интраокулярные линзы.

Как цитировать:
Арзамасцев А.А., Фабрикантов О.Л., Зенкова Н.А., Беликов С.В. Применение технологии машинного обучения для прогнозирования оптической силы интраокулярных линз: генерализация диагностических данных // Digital Diagnostics. 2024. Т. 5, № 1. С. 53–63. DOI: https://doi.org/10.17816/DD623995

Рукопись получена: 28.11.2023 **Рукопись одобрена:** 24.01.2024 **Опубликована online:** 13.03.2024

DOI: https://doi.org/10.17816/DD623995

Machine-learning technology for predicting intraocular lens power: Diagnostic data generalization

Alexander A. Arzamastsev[1, 2], Oleg L. Fabrikantov[2], Natalia A. Zenkova[3], Sergey V. Belikov[2]

[1] Voronezh State University, Voronezh, Russia;
[2] The S. Fyodorov Eye Microsurgery Federal State Institution, Tambov, Russia;
[3] Derzhavin Tambov State University, Tambov, Russia

ABSTRACT

BACKGROUND: The implantation of recent intraocular lens (IOLs) allows ophthalmologists to effectively solve the surgical rehabilitation problems of patients with cataracts. The degree of improvement in the patient's visual function is directly dependent on the accuracy of the preoperative calculation of the optical IOL power. The most famous formulas used to calculate this indicator include SRK II, SRK/T, Hoffer-Q, Holladay II, Haigis, and Barrett. All these work well for an "average patient"; however, they are not adequate at the boundaries of input variable ranges.

AIM: To examine the possibility of using mathematical models obtained by deep learning of artificial neural network (ANN) models to generalize data and predict the optical power of modern IOLs.

MATERIALS AND METHODS: ANN models were trained on large-scale samples, including depersonalized data for patients in the ophthalmology clinic. Data provided in 2021 by ophthalmologist K.K. Syrykh reflect the results of both preoperative and postoperative observations of patients. The source file used to build the ANN model included 455 records (26 columns of input factors and one column for the output factor) for calculating IOL (diopters). To conveniently build ANN models, a simulator program previously developed by the authors was used.

RESULTS: The resulting models, in contrast to the traditionally used formulas, reflect the regional specificity of patients to a much greater extent. They also make it possible to retrain and optimize the structure based on newly received data, which allows us to consider the nonstationarity of objects. A distinctive feature of such ANN models in comparison with the well-known formulas SRK II, SRK/T, Hoffer-Q, Holladay II, Haigis, and Barrett, which are widely used in surgical cataract treatment, is their ability to consider a significant number of recorded input quantities, which reduces the mean relative error in calculating the optical IOL power from 10%–12% to 3.5%.

CONCLUSION: This study reveals the fundamental possibility of generalizing a significant amount of empirical data on calculating the optical IOL power using training ANN models that have a significantly larger number of input variables than those obtained using traditional formulas and methods. The results obtained allow the construction of an intelligent expert system with a continuous flow of new data from a source and a step-by-step retraining of ANN models.

Keywords: artificial intelligence; medical data; dataset; machine learning; intraocular lenses.

To cite this article:
Arzamastsev AA, Fabrikantov OL, Zenkova NA, Belikov SV. Machine-learning technology for predicting intraocular lens power: Diagnostic data generalization. *Digital Diagnostics*. 2024;5(1):53–63. DOI: https://doi.org/10.17816/DD623995

Submitted: 28.11.2023 **Accepted:** 24.01.2024 **Published online:** 13.03.2024

ECO • VECTOR

DOI: https://doi.org/10.17816/DD623995

将机器学习技术应用于眼内镜片光学倍率的预测：诊断数据的归纳

Alexander A. Arzamastsev[1, 2], Oleg L. Fabrikantov[2], Natalia A. Zenkova[3], Sergey V. Belikov[2]

[1] Voronezh State University, Voronezh, Russia;
[2] The S. Fyodorov Eye Microsurgery Federal State Institution, Tambov, Russia;
[3] Derzhavin Tambov State University, Tambov, Russia

摘要

论证。现代眼内镜片的植入使眼科医生能够有效解决白内障患者的手术康复难题。患者视觉功能的改善程度与术前计算眼内镜片光学倍率的准确性直接相关。SRK II、SRK/T、Hoffer-Q、Holladay II、Haigis、Barrett等公式都被用来计算这一指数。所有这些公式对于"中等症患者"来说都很有效。但是，在输入变量范围的极端情况下，它们就不够充分。

目的。本研究的目的是探索使用人工神经网络深度学习衍生的数学模型来归纳数据并预测现代眼内镜片光学倍率的可能性。

材料与方法。基于人工神经网络的模型训练是在大规模样本上进行的，包括来自眼科诊所患者的匿名数据。这些数据由眼科医生K.K.谢雷赫于2021年提供。这些数据反映了患者术前和术后的观察结果。用于建立基于人工神经网络模型的源文件包括455条记录（26列输入因子和1列输出因子），被用于计算眼内镜片（屈光度）。为了方便地建立模型，使用了先前开发的一个模拟程序。

结果。与传统的公式相比，所获得的模型更能反映患者的区域特性。它们还可以根据新获得的数据重新训练和优化模型结构。这样就有可能考虑到对象的非稳定性。与白内障手术中广泛使用的已知公式相比，这种基于人工神经网络模型的一个显著特点是可以考虑大量记录的输入值。这使得计算眼内镜片光学倍率的平均相对误差可以从10-12%降低到3.5%。

结论。本项研究表明，使用人工神经网络模型的深度学习来归纳大量经验数据来计算人工晶状体的光学强度是基本可行的。与使用传统公式和方法相比，这种网络的输入变量数量要大得多。所得结果使得构建新数据动态输入、模型逐步再训练的智能专家系统成为可能。

关键词：人工智能；医疗数据；样本；机器学习；眼内镜片。

引用本文：
Arzamastsev AA, Fabrikantov OL, Zenkova NA, Belikov SV. 将机器学习技术应用于眼内镜片光学倍率的预测：诊断数据的归纳. *Digital Diagnostics*. 2024;5(1):53–63. DOI: https://doi.org/10.17816/DD623995

收到：28.11.2023 **接受：**24.01.2024 **发布日期：**13.03.2024

BACKGROUND

Implantation of recent intraocular lenses (IOLs) allows ophthalmologists to effectively solve the surgical rehabilitation problems of patients with cataracts. However, the degree of improvement in the patient's visual function is directly dependent on the accuracy of the preoperative calculation of the optical IOL power. For this reason, in ophthalmology, different formulas are designed to calculate this indicator. The most famous formulas include SRK II, SRK/T, Hoffer-Q, Holladay II, Haigis, and Barrett [1–7]. All these work well for an "average patient"; however, they are not adequate at the boundaries of input variable ranges. They have other drawbacks such as the following: first, they do not consider the nonstationarity of objects and setup when new empirical data are entered, such as in localization; second, the amount of input factors being considered is clearly insufficient. These circumstances result in many local corrections to the above formulas and their constant adaptation [2, 8].

The outstanding Russian ophthalmologist S.N. Fedorov (1967) is the world's leader in "designing" formulas for calculating the optical IOL power [1, 2]. The most commonly used formulas for calculating the optical IOL power in ophthalmic practice include SRK/T, SRK II, Hoffer-Q, Holladay II, Haigis, and Barrett [3–7]. Several formulas for calculating the optical IOL power appeared in the late 1970s and early 1980s, and they were either theoretical or regressive. Surgeons used to prefer regression formulas, and one of the most successful formulas was the SRK formula developed by J.A. Sanders, D.R. Retzlaff, and M.C. Kraff [3–5].

Currently, there is an unprecedented development of artificial intelligence systems based on artificial neural networks (ANNs), which, with deep learning using large volumes of empirical data, make it possible to build adequate models in nearly any subject area, including biology and medicine [9–12]. Over the past decades, modern ophthalmology centers have created patient data storage that includes tens and hundreds of thousands of digitized indicator records.

In this situation, the construction of an intelligent expert system has clearly become a radical method for solving the problem of preoperative IOL calculation, the core of which would be a mathematical model built using ANN models. Compared with known formulas, such models could be trained based on stored data, which would consider a significantly larger number of relevant input factors and the region-specific nature of patients. A step-by-step retraining of ANN models on newly received data from the storage, and, if necessary, the modification of its structure would ensure its adaptability and solve the problem of considering the nonstationarity of the objects and localization of the model.

The first stage in constructing such an intelligent expert system is to solve the fundamental problem of generalizability of empirical data on a large number of patients using ANN models, identify significant observed input factors, and compare the adequacy of such models with known formulas [1–7].

AIMS

Thus, this study aimed to study the possibility of generalizing a significant amount of empirical data on IOL calculation obtained in one of the ophthalmological centers in Russia as a result of treating patients using a unified ANN model subjected to deep learning, identify the most significant observed input factors that greatly affect the preoperative IOL calculation error, and compare calculation errors made by ANN models and known formulas.

Background error calculation for optical IOL power

Previously, we have compared errors in the use of some formulas based on a significant amount of empirical data provided in an impersonalized form by the Tambov branch of the IRTC "Eye Microsurgery" named after Academician S.N. Fedorov [13]. Initial data were obtained at the end of 2014. The initial number of records was 28,940. Each record contained the following parameters: anonymous patient number, date of surgery, brand and optical power of the implanted IOL, age, eye length, required optical IOL power to correct refractive error and astigmatism (sphere and cylinder), and additional information related to the position of the IOL in the eye. The number of processed records was 11,701, and 17,239 records were not processed for the following reasons: the lens parameters were unknown or data in the fields were incorrect.

The Haigis, Holladay, SRK II, and SRK/T formulas were analyzed as being the closest to empirical data. The values of the mean relative errors in the IOL calculation are presented in Table 1. Fig. 1 shows the correlation dependence of the required and calculated optical IOL power according to these formulas. For the mean optical IOL power, all formulas give results close to the required ones; however, at extreme values, a significant scatter was observed with respect to the required values.

As shown in Fig. 1a, 1b, and 1d, a significant divergence is present in the slope angle of the dependence relative to the diagonal corresponding to the exact calculations. All the investigated formulas use three parameters as input values:

Table 1. Comparison of the IOL power calculation errors using different formulas

Formula	Mean relative error of the IOL calculation,%
Haigis	15.6
Holladay	13.4
SRK II	11.7
SRK/T	12.5

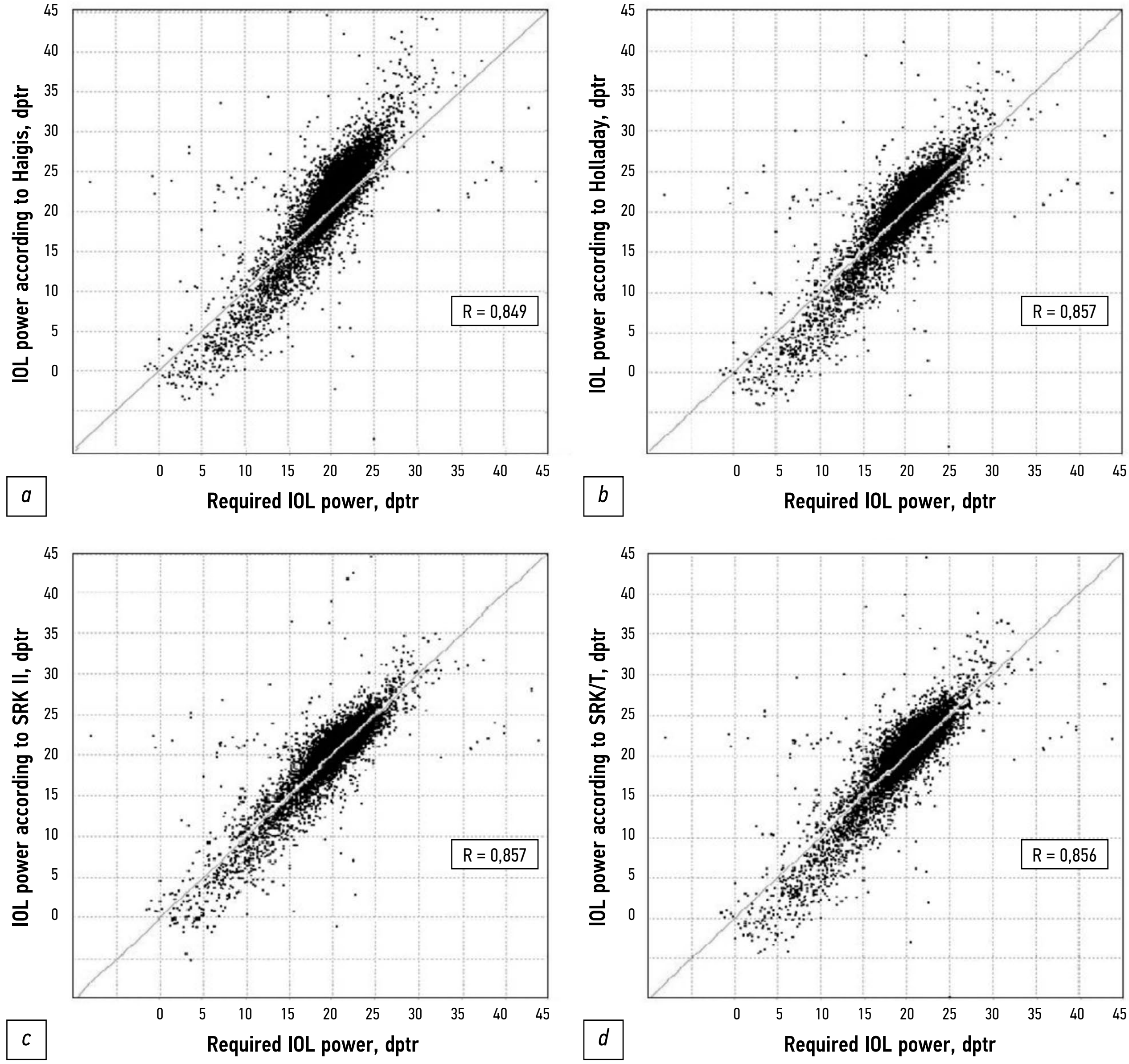

Fig. 1. Correlation dependence of the required optical IOL power along the horizontal axis and the calculated optical IOL power along the vertical axis according to the formulas: *a*) Haigis, *b*) Holladay, *c*) SRK II, and *d*) SRK/T for 11,701 patients. The correlation coefficients are shown in the graphs.

eye length in mm (L), arithmetic mean of the meridians in mm (K), and anterior chamber depth as a lens parameter. This circumstance inevitably suggests the presence of other factors (possibly unobserved), and their effects on the optical IOL power led to the listed features of the calculation.

In the same study [13], we presented an optimized regression formula obtained by minimizing the mean square error for 11,701 patients using nonlinear programing methods. We managed to reduce the mean relative error to 10.6% by introducing a fourth variable. This means that additional input variables and ideally all relevant information about the patient should be considered. In this case, the ideal tool for predicting the optical IOL power is the use of ANN-based models.

A previous study by [14] is most related to our work. The study aimed to describe the use of machine learning in predicting the occurrence of postoperative refraction after cataract surgery and compare the accuracy of the model with formulas for calculating the optical IOL power. The training sample included data from 3331 eyes of 2010 patients. The model coefficients were optimized using data training. The occurrence of postoperative refraction was then predicted using conventional formulas: SRK/T, Haigis, Holladay 1, Hoffer-Q, and Barrett Universal II (BU-II). The absolute errors of some machine-learning methods were lower than those of the formulas. However, no statistically significant difference was found.

The results obtained in [14] appear to be quite expected because the authors did not use additional input parameters. The point is that machine learning and the least squares method, which are usually used for parametric identification of formulas, lead to comparable results. In the present study, we analyze the possibilities of using ANN models to predict the optical IOL power using a much larger number of input quantities.

The work on IOL calculations is sustained because of the need to reduce the IOL calculation error, emergence of data on new factors that were not considered in previous calculations (previously, only four input factors were considered compared with the current 26 input factors), desire to create an adaptive model for IOL calculation, which could consider possible nonstationarity of the incoming data, and the drive to create an expert system with dynamic knowledge acquisition and its step-by-step training based on ANN models.

MATERIALS AND METHODS

In 2021, ophthalmologist K.K. Syrykh provided initial data. They concern depersonalized results of both preoperative and postoperative observations of the patients. The original data file adopted for the construction of the ANN model included 455 entries: 26 columns of input factors (x_1–x_{26}) and one column for the output factor—IOL calculation (diopters), Y. The input variables were as follows: x_1, sex; x_2, visual acuity without correction before surgery; x_3, spherical component of refraction according to visometry data before surgery; x_4, cylindrical component of refraction according to visometry data before surgery; x_5, axis of the cylinder according to visometry data before surgery; x_6, visual acuity with correction before surgery; x_7, axis of the strong meridian of the cornea before surgery; x_8, refraction of the strong meridian of the cornea before surgery; x_9, axis of the weak meridian of the cornea before surgery; x_{10}, refraction of the weak meridian of the cornea before surgery; x_{11}, spherical component of the refraction according to refractometry data before surgery; x_{12}, cylindrical component of the refraction according to refractometry data before surgery; x_{13}, axis of the cylinder according to refractometry data before surgery; x_{14}, length of an eye (optical biometrics, mm); x_{15}, visual acuity without correction after surgery; x_{16} spherical component of the refraction according to visometry data after surgery; x_{17}, cylindrical component of the refraction according to visometry data after surgery; x_{18}, axis of the cylinder according to visometry data after surgery; x_{19}, visual acuity with correction after surgery; x_{20}, axis of the strong meridian of the cornea after surgery; x_{21}, refraction of the strong meridian of the cornea after surgery; x_{22}, axis of the weak meridian of the cornea after surgery; x_{23}, refraction of the weak meridian of the cornea after surgery; x_{24}, spherical component of the refraction according to refractometry data after surgery; x_{25}, cylindrical component of the refraction according to refractometry data after surgery; and x_{26}, axis of the cylinder according to refractometry data after surgery.

For the convenient construction of ANN models, a simulator program previously developed by the authors was used [15].

RESULTS

One of the most complicated points in the development of ANN models is to propose a hypothesis about the structure (architecture) of the network.

The application of the theorems of A.N. Kolmogorov [16, 17] can often lead to an ANN model with a redundant structure. Generally, such a model suits well when representing the output variable at the nodal points; however, it has a weak predictive power.

In [18], we proposed a constructive algorithm that allows us to increase the number of neurons in the hidden layer and the number of hidden layers until certain conditions are reached. In this case, linear, quadratic, cubic, and other transfer functions of neurons are used rather than the commonly used sigmoidal transfer functions. Our approach is based on the expansion of the function of several variables in the Taylor series (1)–(2). Therefore, when expanding a function of many variables in a Taylor series, we must first introduce a differential operator:

$$T^k = \sum_{m=1}^{n} \left(x^{(m)} - x_0^{(m)}\right)^k \frac{\partial^k}{\partial x_k^{(m)}} \tag{1}$$

The expansion of the function $f(x^{(1)}, x^{(2)}, \dots, x^{(n)})$ in the Taylor series takes the following form:

$$\begin{aligned} & f(x^{(1)}, x^{(2)}, \dots, x^{(n)}) = \\ & = f(x_0^{(1)}, x_0^{(2)}, \dots, x_0^{(n)}) + \\ & + \sum {}_{k=1}^{p} \frac{T^k(x^{(1)}, x^{(2)}, \dots, x^{(n)})}{k!} + \\ & + R_p(x^{(1)}, x^{(2)}, \dots, x^{(n)}) \end{aligned} \tag{2}$$

This makes it possible to obtain neural networks with a relatively simple architecture and good approximating (generalizing) and predictive abilities.

The ANN model, built in accordance with formulas (1) and (2), has a layer of input neurons, a functional hidden layer corresponding to several members of the Taylor series, a summing hidden layer, and an output layer. The functional hidden layer contains neurons with transfer functions corresponding to the terms of the Taylor series: linear (first order), quadratic (second order), and cubic (third order). The summing hidden layer contains one linear neuron, and its main function is to calculate the sum of several terms of a series and add a constant value to them. This architecture made it possible to achieve an acceptable accuracy of the ANN model.

DOI: https://doi.org/10.17816/DD623995

The sum of the squared deviations of the model and empirical values was used as the loss function.

When training models based on empirical data, the following optimization methods were chosen: stochastic gradient method, simple gradient method, and gradient-free Gauss–Seidel and Monte Carlo coordinate descent methods, which were used interactively.

The starting point for training the ANN model based on the IOL data was a network consisting of 26 input neurons, one linear neuron in the hidden layer, and one output neuron. Such a construction corresponded to the free and first terms in formulas (1) and (2). Considering the recommendations of previous studies [8–11], the learning process of the model was carried out on 70% of the entire sample, whereas the predictive ability of the ANN model was assessed using the remaining 30% of the sample. Data for training and checking the adequacy of the model were selected from the general table at random using a uniform distribution of random variables.

The results of the training of this simple model are shown in Fig. 2. The true optical power of a given type of IOL to obtain emmetropia in each case was determined as the sum of the optical power of the implanted IOL and the resulting refractive error. The refractive error was calculated by retrospective analysis during the period from 1 to 6 months after surgery.

In terms of the mean relative error, they are comparable with classical formulas; however, in contrast, a linear function of 26 variables is used to predict the optical IOL power. Moreover, the pair correlation coefficient of the calculated and empirical data was 0.71, and the mean relative error was 11.9%.

The coefficients of synaptic connections for the channels of the linear model represent the sensitivity of the channels, and their values can be used to assess their degree of influence on the output variable. The numerical experiments showed that at least 12–15 input factors (available to the ophthalmologist) significantly affect the preoperative calculation of the optical IOL power. Consequently, our assumptions regarding the need to consider a larger number of input quantities to reduce the calculation error were fully confirmed. Significant errors in classical formulas [3–7] can be associated with the presence of a substantial number of input factors that are unobserved in these formulas.

Among the significant factors, the values of some factors (x_{16}, x_{21}, x_{23}, and x_{24}) become known only after surgery. However, these factors correlate well with similar factors, and their values can be obtained before surgery and are therefore well predictable.

Following our algorithm [18], we modified the structure of the ANN model so that along with the linear neuron in the hidden layer, a quadratic neuron was also present. The training of such an ANN model using similar numerical methods of nonlinear programing made it possible to reduce the mean relative error to 5%; thus, previous results were immediately improved by a factor of two. In addition, the pair correlation coefficient increased to 0.97, and the mean relative error was 4.8% (Fig. 3).

Following this logic, we also built a third-order ANN model containing neurons with linear, quadratic, and cubic

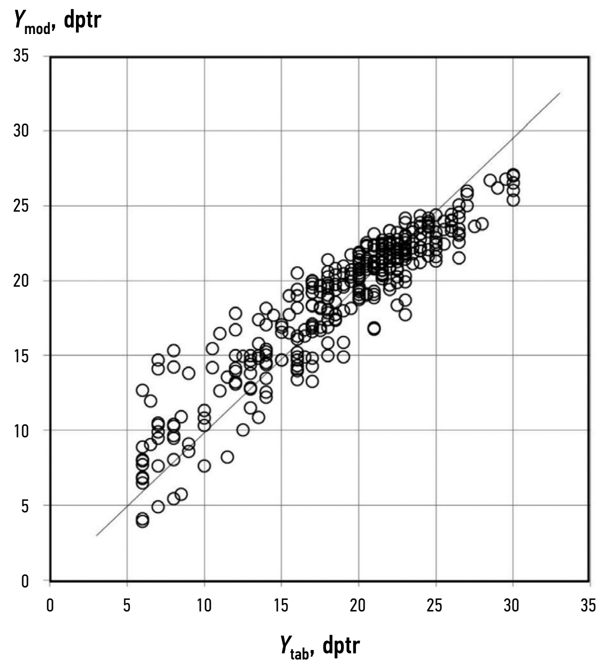

Fig. 2. Correlation of the calculated (Y_{mod}) and empirical data (Y_{tab}) for the first-order ANN model. The pair correlation coefficient is 0.84, and the mean relative error is 11.9%.

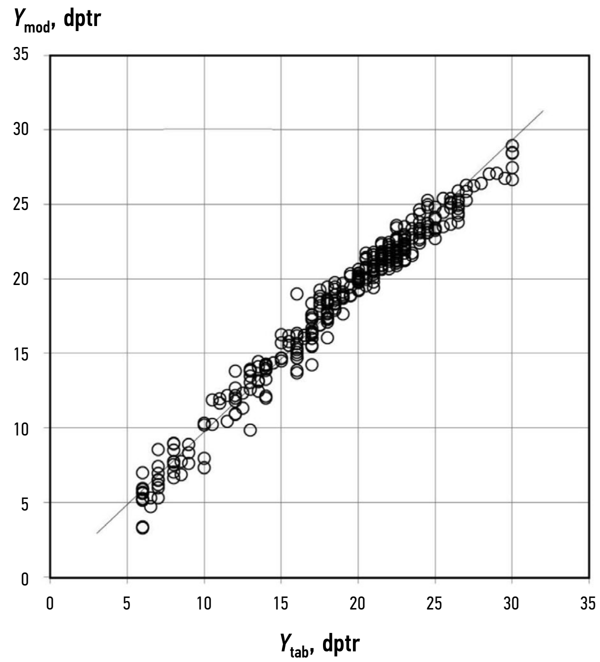

Fig. 3. Correlation of the calculated (Y_{mod}) and empirical data (Y_{tab}) for the second-order ANN model. The pair correlation coefficient is 0.99, and the mean relative error is 4.8%.

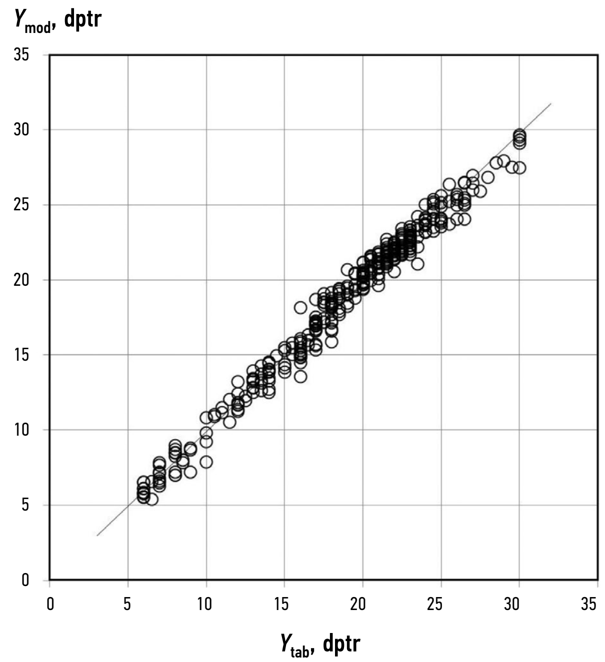

Fig. 4. Correlation of the calculated (Y_{mod}) and empirical data (Y_{tab}) for the third-order ANN model. The pair correlation coefficient is 0.99, and the mean relative error is 3.5%.

transfer functions in the hidden layer. Training the ANN model by similar numerical methods of nonlinear programing made it possible to reduce the mean relative error up to 3.5%, with a pair correlation coefficient of 0.98 (Fig. 4).

The number of degrees of freedom of this ANN model equal to the number of synaptic connections 26 × 3 + 3 = 81 is significantly less than the number of entries in the training set. This circumstance confirms the good generalizability of empirical data on the calculation of the optical IOL power using the third-order ANN model.

Table 2 shows a comparison of various methods for calculating the optical IOL power. Therefore, when using ANN models and a significantly larger number of input variables, the mean relative error of calculations could be reduced by more than two times compared with using traditional methods.

DISCUSSION

The next stage of research should be the collection of a significantly larger amount of data about patients because deep machine-learning methods require significant training samples. Then, the models should be validated on test samples [8–11]. If the system also contains hyperparameters, i.e., the parameters that must be set "from above" and the successful setting of which significantly affects the solution of the problem, then there must also be a third, additional test data sample. The availability of such data will make it possible to build an intelligent expert system for the preoperative calculation of IOLs, some of which are presented in our paper [19].

CONCLUSION

This study has the following findings: (1) The fundamental possibility of generalizing a significant amount of empirical data on calculating the optical IOL power using training ANN models that have a significantly larger number of input variables than when using traditional formulas and methods. The identification of the most significant observed factors that have a significant effect on the target indicator and their inclusion in the ANN model allows the reduction of the calculation error by more than two times. (2) The ability of ANN-based models to generalize data opens up the possibility of creating an intelligent expert system with a dynamic flow of new data and step-by-step deep machine learning of the intelligent core. The main feature of such a system, in comparison with the use of traditional calculation formulas, should be its adaptability, which allows solving the problems of the nonstationarity of an object and localization because of the presence of feedback in it. 3) Currently, the developed ANN model is used in conjunction

Table 2. Comparison of the mean relative calculation errors of the optical IOL power and correlation coefficients of the calculated and empirical data for different methods

Formula and ANN model	Mean relative error, %	Correlation coefficient of the calculated and empirical data
Haigis formula	15,6	0,85
Holladay formula	13,4	0,86
SRK II formula	11,7	0,86
SRK/T formula	12,5	0,86
Linear ANN model	11,9	0,84
Nonlinear second-order ANN model	4,8	0,98
Nonlinear third-order ANN model	3,5	0,99

Note: ANN — artificial neural network

with other calculation tools to preoperatively determine the optical IOL power in the mode of an ophthalmologist assistant.

ADDITIONAL INFO

Funding source. This study was not supported by any external sources of funding.

Competing interests. The authors declare that they have no competing interests.

Authors' contribution. All authors made a substantial contribution to the conception of the work, acquisition, analysis, interpretation of data for the work, drafting and revising the work, final approval of the version to be published and agree to be accountable for all aspects of the work.
A.A. Arzamastsev — research concept, data processing, writing the manuscript, editing the manuscript; O.L. Fabrikantov — research concept, literature analysis, editing the manuscript; N.A. Zenkova — data processing, literature analysis, editing the manuscript; S.V. Belikov — preparing the dataset, searching for publications.

REFERENCES

1. Fyodorov SN, Kolinko AI. Method of calculating the optical power of an intraocular lens. *The Russian Annals of Ophthalmology*. 1967;(4):27–31. (In Russ).

2. Balashevich LI, Danilenko EV. Results in application of the fyodorov's iol power formula for posterior chamber lenses calculation. *Fyodorov Journal of Ophthalmic Surgery.* 2011;(1):34–38. EDN: PXRASV

3. Sanders DR, Kraff MC. Improvement of intraocular lens power calculation using empirical data. *American Intra-Ocular Implant Society Journal.* 1980;6:263–267. doi: 10.1016/s0146-2776(80)80075-9

4. Sanders DR, Retzlaff JA, Kraff MC. Comparison of the SRK II formula and other second-generation formulas. *Journal of Cataract & Refractive Surgery.* 1988;14(2):136–141. doi: 10.1016/s0886-3350(88)80087-7

5. Sanders DR, Retzlaff JA, Kraff MC. Development of the SRK/T IOL power calculation formula. *Journal of Cataract & Refractive Surgery.* 1990;16(3):333–340. doi: 10.1016/s0886-3350(13)80705-5

6. Hoffer KJ. The Hoffer Q formula: a comparison of theoretic and regression formulas. *Journal of Cataract & Refractive Surgery.* 1993;19(6):700–712. doi: 10.1016/s0886-3350(13)80338-0

7. Holladay JT, Prager TC, Ruiz RS, et al. A three-part system for refining intraocular lens power calculation. *Journal of Cataract & Refractive Surgery.* 1988;14(1):17–24. doi: 10.1016/S0886-3350(88)80059-2

8. Pershin KB, Pashinova NF, Tsygankov AYu, Legkhih SL. Choice of IOL Optic Power Calculation Formula in Extremely High Myopia Patients "Excimer" Ophthalmology Centre, Moscow. *Point of view. East - West.* 2016;(1):64–67. EDN: WHCNPF

9. Buduma N, Lokasho N. *Foundations of deep learning. Creating Algorithms for Next Generation Artificial Intelligence.* Moscow: Mann, Ivanov i Ferber; 2020. (In Russ).

10. Foster D. *Generative deep learning. Creative potential of neural networks.* Saint Petersburg: Piter; 2020. (In Russ).

11. Ramsundar B, Istman P, Uolters P, Pande V. *Deep learning in biology and medicine*. Moscow: DMK Press; 2020. (In Russ).

12. Kharrison M. *Machine learning: a pocket guide. A quick guide to structured machine learning methods in Python*. Saint Petersburg: Dialektika LLC; 2020. (In Russ).

13. Arzamastsev AA, Fabrikantov OL, Zenkova NA, Belousov NK. Optimization of Formulae for Intraocular Lenses Calculating. *Tambov University Reports. Series: Natural and Technical Sciences*. 2016;21(1):208–213. EDN: VNWHVZ doi: 10.20310/1810-0198-2016-21-1-208-213

14. Yamauchi T, Tabuchi T, Takase K, Masumoto H. Use of a machine learning method in predicting refraction after cataract surgery. *Journal of Clinical Medicine.* 2021;10(5):1103. doi: 10.3390/jcm10051103

15. Certificate of state registration of the computer program № 2012618141/ 07.09.2012. Arzamastsev AA, Rykov VP, Kryuchin OV. *Artificial neural network simulator with implementation of modular learning principle*. (In Russ).

16. Kolmogorov AN. On the representation of continuous functions of several variables by superpositions of continuous functions of fewer variables. *Doklady Akademii nauk SSSR.* 1956;108(2):179–182. (In Russ).

17. Kolmogorov AN. On the representation of continuous functions of several variables as a superposition of continuous functions of one variable. *Doklady Akademii nauk SSSR.* 1957;114(5):953–956. (In Russ).

18. Arzamaszev AA, Kryuchin OV, Azarova PA, Zenkova NA. The universal program complex for computer simulation on the basis of the artificial neuron network with self-organizing structure. *Tambov University Reports. Series: Natural and Technical Sciences.* 2006;11(4):564–570. EDN: IRMPYX

19. Arzamastsev AA, Zenkova NA, Kazakov NA. Algorithms and methods for extracting knowledge about objects defined by arrays of empirical data using ANN models. *Journal of Physics: Conference Series.* 2021. doi: 10.1088/1742-6596/1902/1/012097

СПИСОК ЛИТЕРАТУРЫ

1. Фёдоров С.Н., Колинко А.И. Методика расчета оптической силы интраокулярной линзы // Вестник офтальмологии. 1967. № 4. С. 27–31.

2. Балашевич Л.И., Даниленко Е.В. Результаты использования формулы С.Н. Фёдорова для расчёта силы заднекамерных интраокулярных линз // Офтальмохирургия. 2011. № 1. С. 34–38. EDN: PXRASV

3. Sanders D.R., Kraff M.C. Improvement of intraocular lens power calculation using empirical data // American Intra-Ocular Implant Society Journal. 1980. Vol. 6. P. 263–267. doi: 10.1016/s0146-2776(80)80075-9

4. Sanders D.R., Retzlaff J.A., Kraff M.C. Comparison of the SRK II formula and other second-generation formulas // Journal of Cataract & Refractive Surgery. 1988. Vol. 14, N 2. P. 136–141. doi: 10.1016/s0886-3350(88)80087-7

5. Sanders D.R., Retzlaff J.A., Kraff M.C. Development of the SRK/T IOL power calculation formula // Journal of Cataract & Refractive Surgery. 1990. Vol. 16, N 3. P. 333–340. doi: 10.1016/s0886-3350(13)80705-5

6. Hoffer K.J. The Hoffer Q formula: a comparison of theoretic and regression formulas // Journal of Cataract & Refractive Surgery. 1993. Vol. 19, N 6. P. 700–712. doi: 10.1016/s0886-3350(13)80338-0

7. Holladay J.T., Prager T.C., Ruiz R.S., et al. A three-part system for refining intraocular lens power calculation // Journal of Cataract & Refractive Surgery. 1988. Vol. 14, N 1. P. 17–24. doi: 10.1016/S0886-3350(88)80059-2

8. Першин К.Б., Пашинова Н.Ф., Цыганков А.Ю., Легких С.Л. Алгоритм выбора формулы для расчета оптической силы ИОЛ при экстремальной миопии // Точка зрения. Восток - Запад. 2016. № 1. С. 64–67. EDN: WHCNPF

9. Будума Н., Локашо Н. Основы глубокого обучения. Создание алгоритмов для искусственного интеллекта следующего поколения. Москва : Манн, Иванов и Фербер, 2020.

10. Фостер Д. Генеративное глубокое обучение. Творческий потенциал нейронных сетей. Санкт-Петербург : Питер, 2020.

11. Рамсундар Б., Истман П., Уолтерс П., Панде В. Глубокое обучение в биологии и медицине. Москва : ДМК Пресс, 2020.

12. Харрисон М. Машинное обучение: карманный справочник. Краткое руководство по методам структурированного машинного обучения на Python. Санкт-Петербург : ООО «Диалектика», 2020.

13. Арзамасцев А.А., Фабрикантов О.Л., Зенкова Н.А., Белоусов Н.К. Оптимизация формул для расчета ИОЛ // Вестник Тамбовского университета. Серия Естественные и технические науки. 2016. Т. 21, № 1. С. 208–213. EDN: VNWHVZ doi: 10.20310/1810-0198-2016-21-1-208-213

14. Yamauchi T., Tabuchi T., Takase K., Masumoto H. Use of a machine learning method in predicting refraction after cataract surgery // Journal of Clinical Medicine. 2021. Vol. 10, N 5. P. 1103. doi: 10.3390/jcm10051103

15. Свидетельство о государственной регистрации программы для ЭВМ № 2012618141/ 07.09.2012. Арзамасцев А.А., Рыков В.П., Крючин О.В. Симулятор искусственной нейронной сети с реализацией модульного принципа обучения.

16. Колмогоров А.Н. О представлении непрерывных функций нескольких переменных суперпозициями непрерывных функций меньшего числа переменных // Доклады Академии наук СССР. 1956. Т. 108, № 2. С. 179–182.

17. Колмогоров А.Н. О представлении непрерывных функций нескольких переменных в виде суперпозиции непрерывных функций одного переменного // Доклады Академии наук СССР. 1957. Т. 114, № 5. С. 953–956.

18. Арзамасцев А.А., Крючин О.В., Азарова П.А., Зенкова Н.А. Универсальный программный комплекс для компьютерного моделирования на основе искусственной нейронной сети с самоорганизацией структуры // Вестник Тамбовского университета. Серия: Естественные и технические науки. 2006. Т. 11, № 4. С. 564–570. EDN: IRMPYX

19. Arzamastsev A.A., Zenkova N.A., Kazakov N.A. Algorithms and methods for extracting knowledge about objects defined by arrays of empirical data using ANN models // Journal of Physics: Conference Series. 2021. doi: 10.1088/1742-6596/1902/1/012097

AUTHORS' INFO

*** Alexander A. Arzamastsev,** Dr. Sci. (Engineering), Professor;
address: 24 Lavrova street, 392000 Tambov, Russia;
ORCID: 0000-0001-6795-2370;
eLibrary SPIN: 4410-6340;
e-mail: arz_sci@mail.ru

Oleg L. Fabrikantov, MD, Dr. Sci. (Medicine), Professor;
ORCID: 0000-0003-0097-991X;
eLibrary SPIN: 9675-9696;
e-mail: fabr-mntk@yandex.ru

Natalia A. Zenkova, Cand. Sci. (Psychology), Assistant Professor;
ORCID: 0000-0002-2325-1924;
eLibrary SPIN: 2266-4168;
e-mail: natulin@mail.ru

Sergey V. Belikov, MD;
ORCID: 0000-0002-4254-3906;
eLibrary SPIN: 5553-8398;
e-mail: pvt.leopold@gmail.com

ОБ АВТОРАХ

*** Арзамасцев Александр Анатольевич,** д-р техн. наук, профессор;
адрес: Россия, 392000, г. Тамбов, ул. Лаврова, д. 24;
ORCID: 0000-0001-6795-2370;
eLibrary SPIN: 4410-6340;
e-mail: arz_sci@mail.ru

Фабрикантов Олег Львович, д-р мед. наук, профессор;
ORCID: 0000-0003-0097-991X;
eLibrary SPIN: 9675-9696;
e-mail: fabr-mntk@yandex.ru

Зенкова Наталья Александровна, канд. психол. наук, доцент;
ORCID: 0000-0002-2325-1924;
eLibrary SPIN: 2266-4168;
e-mail: natulin@mail.ru

Беликов Сергей Вячеславович;
ORCID: 0000-0002-4254-3906;
eLibrary SPIN: 5553-8398;
e-mail: pvt.leopold@gmail.com

* Corresponding author / Автор, ответственный за переписку

DOI: https://doi.org/10.17816/DD624022

Технологии машинного обучения и искусственной нейронной сети в классификации посткератотомической деформации роговицы

Е.К. Цыренжапова[1], О.И. Розанова[1], Т.Н. Юрьева[1, 2, 3], А.А. Иванов[1], И.С. Розанов[4]

[1] Национальный медицинский исследовательский центр «Межотраслевой научно-технический комплекс “Микрохирургия глаза” имени академика С.Н. Фёдорова», Иркутск, Россия;
[2] Иркутский государственный медицинский университет, Иркутск, Россия;
[3] Российская медицинская академия непрерывного профессионального образования, Иркутск, Россия;
[4] ООО «Транснефть-Технологии», Иркутск, Россия

АННОТАЦИЯ

Обоснование. Тщательный анализ как оптических, так и анатомических свойств роговицы у пациентов после перенесённой передней радиальной кератотомии приобретает особое значение в выборе оптической силы интраокулярной линзы при хирургическом лечении катаракты и других видах оптической коррекции. Вариабельность клинической картины посткератотомической деформации определяет необходимость разработки её классификации и является важной задачей современной офтальмологии.

Цель — разработать автоматизированную систему классификации посткератотомической деформации роговицы с использованием машинного обучения и искусственной нейронной сети на основе анализа численных значений топографических карт роговицы.

Материалы и методы. В качестве материала использовались обезличенные результаты анализа медицинской документации 250 пациентов в возрасте от 46 до 76 лет (средний возраст — 59,63±5,95 года). Проведён анализ 500 карт рельеф-топографии передней и задней поверхностей роговицы и 3 этапа машинного обучения классификации посткератотомической деформации.

Результаты. I этап — анализ рельеф-топографии передней и задней поверхностей роговицы — позволил зафиксировать численные значения элевации передней и задней поверхности роговицы в трёх кольцевидных зонах. На II этапе в ходе глубокого машинного обучения была выбрана и создана нейросеть прямого распространения. Установлены 8 вспомогательных параметров, описывающих форму передней и задней поверхностей роговицы. III этап сопровождался получением алгоритмов классификации посткератотомической деформации роговицы в зависимости от соотношения тестовой и обучающей выборок, которое варьировало от 75 до 91%.

Заключение. Разработана искусственная нейронная сеть, успешно решающая задачу классификации типов посткератотомической деформации роговицы с точностью 91%. Установлен потенциал для дальнейшего улучшения качества обучения данной нейронной сети. Применение алгоритмов искусственной нейронной сети может стать полезным инструментом автоматической классификации посткератотомической деформации роговицы у пациентов, перенёсших ранее радиальную кератотомию.

Ключевые слова: передняя радиальная кератотомия; искусственный интеллект; машинное обучение; рельеф-топография роговицы.

Как цитировать:
Цыренжапова Е.К., Розанова О.И., Юрьева Т.Н., Иванов А.А., Розанов И.С. Технологии машинного обучения и искусственной нейронной сети в классификации посткератотомической деформации роговицы // Digital Diagnostics. 2024. Т. 5, № 1. С. 64–74. DOI: https://doi.org/10.17816/DD624022

Рукопись получена: 29.11.2023 **Рукопись одобрена:** 14.02.2024 **Опубликована online:** 11.03.2024

DOI: https://doi.org/10.17816/DD624022

Machine-learning and artificial neural network technologies in the classification of postkeratotomic corneal deformity

Ekaterina K. Tsyrenzhapova[1], Olga I. Rozanova[1], Tatiana N. Iureva[1, 2, 3], Andrey A. Ivanov[1], Ivan S. Rozanov[4]

[1] The S. Fyodorov Eye Microsurgery Federal State Institution, Irkutsk, Russia;
[2] Irkutsk State Medical University, Irkutsk, Russia;
[3] Russian Medical Academy of Continuous Professional Education, Irkutsk, Russia;
[4] LLC Transneft Technology, Irkutsk, Russia

ABSTRACT

BACKGROUND: A thorough analysis of both optical and anatomical properties of the cornea in patients after anterior radial keratotomy is important in choosing the optical power of an intraocular lens in the surgical treatment of cataracts and other types of optical correction. Improving the classification of postkeratotomic corneal deformity is crucial in modern ophthalmology due to its diverse clinical presentation.

AIM: To develop an automated classification system for postkeratotomic corneal deformity using machine learning and artificial neural networks based on the analysis of topographic maps of the cornea.

MATERIALS AND METHODS: Depersonalized data from medical records of 250 patients aged 46–76 (mean, 59.63±5.95) years were analyzed. Moreover, 500 topographic maps of the anterior and posterior surfaces of the cornea were analyzed, and three stages of machine learning for postkeratotomic corneal deformity classification were performed.

RESULTS: Stage I, which involved topography analysis of the anterior and posterior surfaces of the cornea, allowed for the measurement of anterior and posterior corneal elevation in three ring-shaped zones. At stage II, a direct distribution neural network was selected and created during deep machine learning. Eight auxiliary parameters describing the shape of the anterior and posterior surfaces of the cornea were established. In Stage III, classification algorithms for postkeratotomic corneal deformity were developed based on the test-to-training sample ratio, which ranged from 75% to 91%.

CONCLUSION: The proposed artificial neural network classifies postkeratotomic corneal deformity types with an accuracy of 91%. The potential for further improving the training quality of this artificial neural network has been established. Neural network algorithms can become a useful tool for the automatic classification of postkeratotomic corneal deformity in patients after radial keratotomy.

Keywords: anterior radial keratotomy; artificial intelligence; machine learning; corneal topography.

To cite this article:
Tsyrenzhapova EK, Rozanova OI, Iureva TN, Ivanov AA, Rozanov IS. Machine-learning and artificial neural network technologies in the classification of postkeratotomic corneal deformity. *Digital Diagnostics.* 2024;5(1):64–74. DOI: https://doi.org/10.17816/DD624022

Submitted: 29.11.2023 **Accepted:** 14.02.2024 **Published online:** 11.03.2024

ECO•VECTOR

DOI: https://doi.org/10.17816/DD624022

机器学习和人工神经网络技术在角膜切开术后畸形分类中的应用

Ekaterina K. Tsyrenzhapova[1], Olga I. Rozanova[1], Tatiana N. Iureva[1, 2, 3], Andrey A. Ivanov[1], Ivan S. Rozanov[4]

[1] The S. Fyodorov Eye Microsurgery Federal State Institution, Irkutsk, Russia;
[2] Irkutsk State Medical University, Irkutsk, Russia;
[3] Russian Medical Academy of Continuous Professional Education, Irkutsk, Russia;
[4] LLC Transneft Technology, Irkutsk, Russia

摘要

论证。对前放射状角膜切开术后患者角膜的光学和解剖特性进行仔细分析。这对于选择用于白内障手术和其他类型光学矫正的眼内镜片的光学倍率具有特殊意义。角膜切开术后畸形临床表现的多变性决定了有必要对其进行分类，这也是现代眼科学的一项重要任务。

目的。本研究旨在利用机器学习和人工神经网络开发角膜切开术后角膜畸形自动分类系统。该分类系统的开发基于对角膜图形数值的分析。

材料与方法。以250名患者的匿名病历分析结果为材料。患者年龄在46至76岁之间（平均年龄为59.63±5.95岁）。对500张角膜前后表面的图形，对角膜切开术后畸形分类进行了3个阶段的机器学习。

结果。第一阶段是分析角膜前后表面的图形。通过分析记录了角膜前后表面在三个环形区域的隆起数值。在第二阶段，通过深度机器学习选择并建立了一个前馈神经网络，确定了八个辅助参数。这些参数描述了角膜前后表面的形态。在第三阶段根据测试样本和训练样本的比例，获得了角膜切开术后角膜畸形的分类算法，该比例为75%至91%。

结论。开发了一个人工神经网络。成功解决了角膜切开术后角膜畸形类型的分类问题，准确率高达91%。该神经网络的训练质量还有进一步提高的潜力。人工神经网络算法的应用可以成为对曾接受过放射状角膜切开术的患者进行角膜切开术后角膜畸形自动分类的有用工具。

关键词：前放射状角膜切开术；人工智能；机器学习；角膜图形。

引用本文：
Tsyrenzhapova EK, Rozanova OI, Iureva TN, Ivanov AA, Rozanov IS. 机器学习和人工神经网络技术在角膜切开术后畸形分类中的应用. *Digital Diagnostics.* 2024;5(1):64–74. DOI: https://doi.org/10.17816/DD624022

收到：29.11.2023 **接受：**14.02.2024 **发布日期：**11.03.2024

BACKGROUND

More extensive ophthalmological examinations in the diagnosis of eye diseases have significantly increased the healthcare burden, particularly on ophthalmology clinics. Meanwhile, technologies such as deep machine learning and artificial neural networks (ANNs) allow automation of the analysis of the results, increasing the accuracy and speed of abnormality detection, and automating decision-making in clinical practice. In the diagnosis of eye diseases, machine-learning models are most commonly used when assessing fundus images, lens opacities, optic nerve changes in glaucoma, and tonometry data. In addition, machine learning and artificial intelligence are widely used for detecting corneal changes. Studies of corneal disorders have focused on the diagnosis of keratoconus [1–6]. Convolutional neural networks are particularly efficient at pattern recognition and image classification, making these algorithms a smart choice for the automated analysis of color-coded Scheimpflug camera images [7]. V.A. Dos Santos et al. developed and trained the CorneaNet neural network (Austria) for segmenting corneal optical coherence tomography (OCT) images [8]. In Taiwan, B.I. Kuo et al. retrospectively evaluated corneal topography results to develop a deep machine-learning algorithm for detecting keratoconus [9]. S. Shi et al. revealed excellent results in the differential diagnosis of subclinical keratoconus and healthy corneas using machine learning in combination with Scheimpflug camera images and ultrahigh resolution OCT [10]. Several recent studies have shown the effectiveness of methods involving convolutional neural networks in the automated detection of Fuchs' dystrophy as part of an algorithm for classifying corneal endothelium images [11].

Moreover, the number of patients with age-related cataracts and myopia, for which radial keratotomy (RK) was previously performed, is steadily increasing. RK was the first mass-scale refractive surgery, addressing a significant problem at the time: correcting myopia in many patients worldwide. The refractive effect of RK is based on a change in the power of the cornea resulting from a change in the configuration of its central region, which is caused by a local weakening of the biomechanical properties of the cornea at the radial incision site under intraocular pressure. In RK development, it was assumed to result in the uniform flattening of both corneal surfaces, maintaining the ratio of the curvature radii of their circumferences. However, the corneal deformity is influenced by the initial parameters of the eye (biomechanical properties of the cornea, myopia grade, and intraocular pressure), surgical factors (number, depth, and length of incisions, and quality of the surgery), individual characteristics of regenerative processes and scarring, patient's age at surgery, patient's lifestyle, aging processes, etc. These factors explain why the cornea may demonstrate significant deformational changes in the long-term period after RK, which is of particular importance when planning for cataract surgery with intraocular lens (IOL) implantation.

In patients with a previously surgically modified cornea, errors in the analysis of the preoperative optical properties of the cornea may have serious consequences such as refractive errors and poor vision quality after cataract surgery. Therefore, a thorough analysis of the corneal elevation pattern after RK, development of criteria for classifying post-keratotomy corneal deformities (PKCDs), and creation of an automated system for their classification may become the basis for a personalized approach to cataract surgery and increased accuracy of calculating the IOL power in this patient population.

AIM

To develop an automated system for PKCD classification using machine learning and ANNs based on the analysis of numerical values in corneal topography maps.

MATERIALS AND METHODS

Anonymized medical record data of 250 patients aged 46–76 years (mean age, 59.63 ± 5.95 years) who presented to the Irkutsk branch of the S.N. Fyodorov Eye Microsurgery Complex of the Ministry of Health of the Russian Federation between 2020 and 2023 were analyzed. In addition to the standard ophthalmological examination, all patients underwent corneal elevation mapping using Pentacam® HR (Oculus, Germany). In total, 38 parameters of the elevation of the anterior and posterior corneal surfaces and 12 parameters related to the corneal thickness, refractive power, astigmatism, and asphericity values were recorded as characteristics of the optical properties of the cornea. The study was performed in three stages.

Stage I: Analysis of the elevation display maps of the anterior and posterior corneal surfaces

The dataset included 19 numerical values of elevation of both the anterior and posterior corneal surfaces from 500 elevation display maps (Pentacam® 4 Maps Refractive display). The elevation data were recorded in three ring-shaped zones: in the center, at 4 points in the paracentral zone, and at 14 points in the 6-mm peripheral zone. The study was conducted starting from the 90° point and then moving clockwise. A schematic arrangement of topographic points on the corneal elevation map is presented in Fig. 1.

Stage II: Deep-learning architecture and visualization

A personal computer with Windows 10 Operating System, AMD Ryzen™ 7 2700E CPU, and 16 GB RAM was used in the training and testing of the developed architecture. The GPU was not used for model training; all necessary calculations were performed with the CPU. For programming, Python 3.10

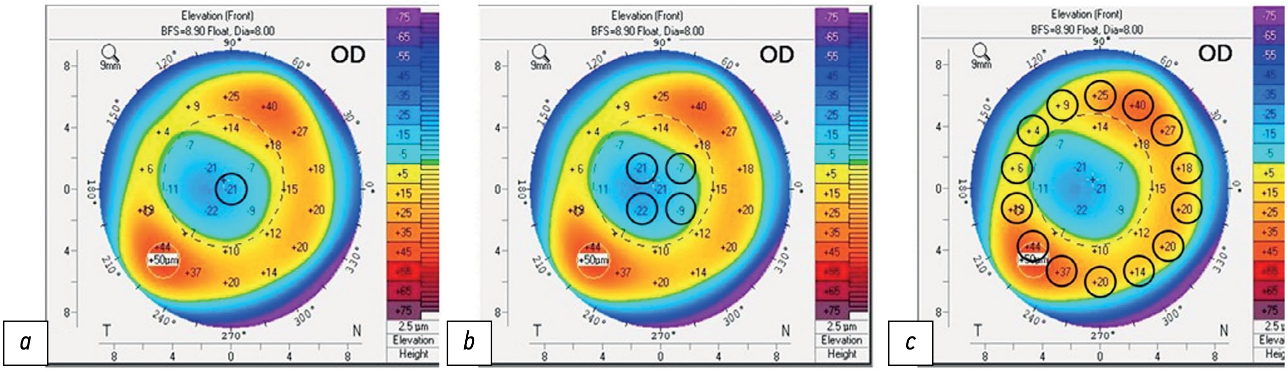

Fig. 1. Corneal surface reference points: *a* — central area; *b* — paracentral area; *c* — 6 mm peripheral area.

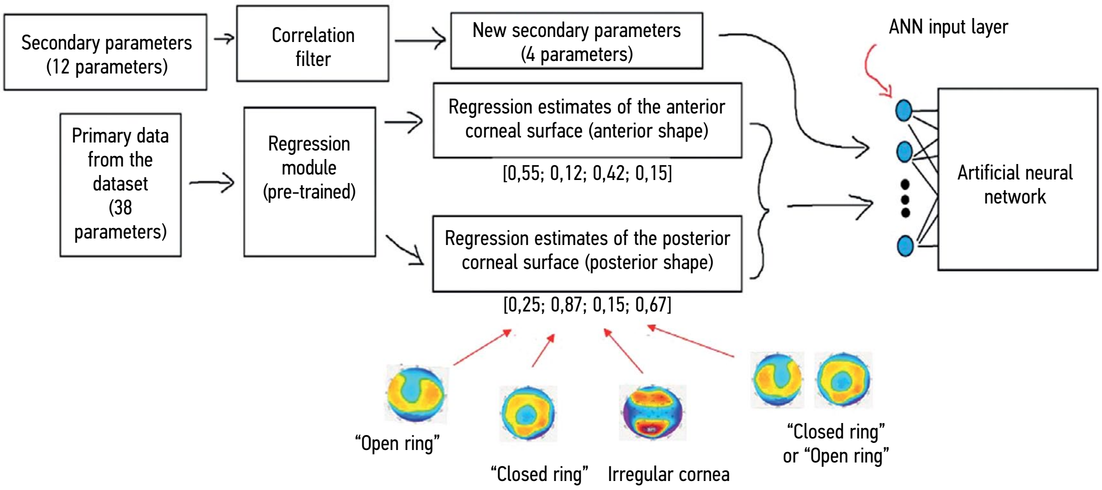

Fig. 2. Dataset processing scheme.

with the Anaconda distribution was used, particularly the tf.keras 2.12.0 library. The Keras API specification was implemented within the TensorFlow framework version 2.0. The key parameter in the dataset was type, which describes the elevation of the anterior and posterior corneal surfaces. The PKCD type was determined based on the elevation display map. Depending on the elevation pattern of the anterior and posterior corneal surfaces, six PKCD types were identified (Table 1) [14].

At this stage, the dataset was optimized, that is, the nature of all parameters was investigated using correlation and regression analyses, and based on the results, uninformative features were excluded (Fig. 2). The type parameter was used solely to test the training of the neural network and was not used as an input parameter.

Stage III: Creation of an ANN

An ANN consists of the input, hidden, and output layers, which are sufficient for classifying an ANN. The number of neurons in the input layer was M = 12 (parameters), and the number of neurons in the output layer was 6 (classes). The number of neurons in the hidden layer was calculated using the following formula: $M = \frac{2}{3} \times N + K$, where N is the number of input neurons and K is the number of output neurons. The objective of this stage was to create an ANN that would work with an input table of features. Fig. 3 presents a schematic of the ANN diagram.

RESULTS

During the neural network development, a simple console interface was created by automatic testing of the training

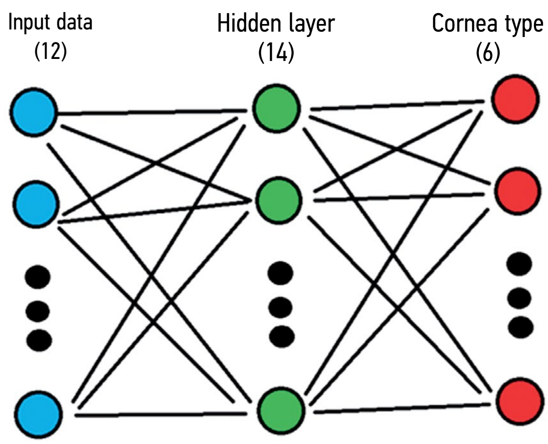

Fig. 3. Diagram of the final-iteration artificial neural network.

Table 1. Classification of postkeratotomic corneal deformities by the elevation pattern of the anterior and posterior corneal surfaces

Deformity type	Anterior corneal elevation pattern	Posterior corneal elevation pattern
1	“Open ring” * 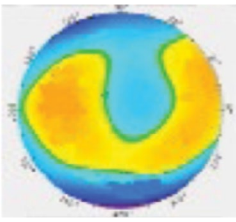	“Open ring” * 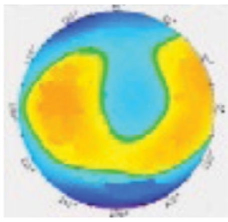
2	“Closed ring” * 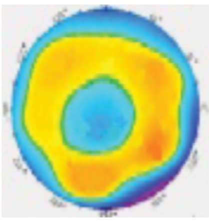	“Open ring” * 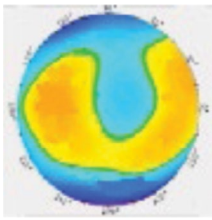
3	“Closed ring” * 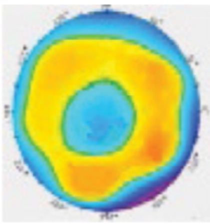	“Closed ring” * 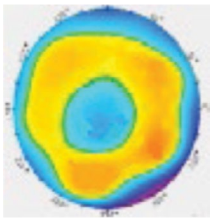
4	“Open ring” * 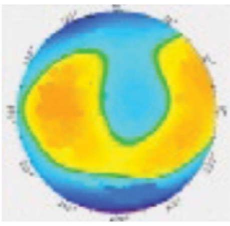	“Closed ring” * 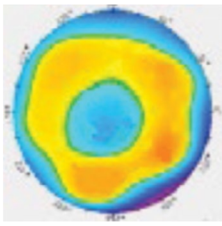
5	Irregular 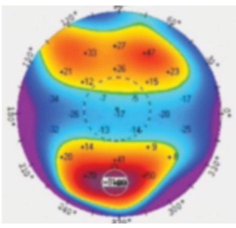	Irregular 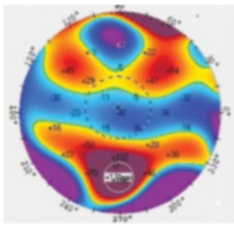
6	“Closed ring” or “Open ring” 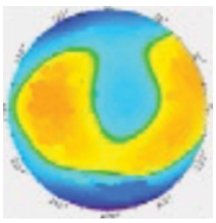 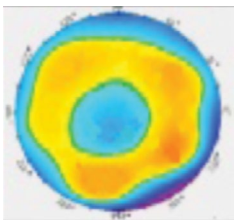	Irregular, with a significant shift of the posterior surface by height (> 80 μm) 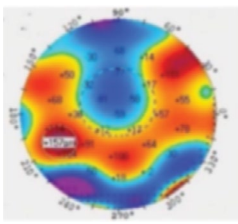

* ≤80 μm elevation

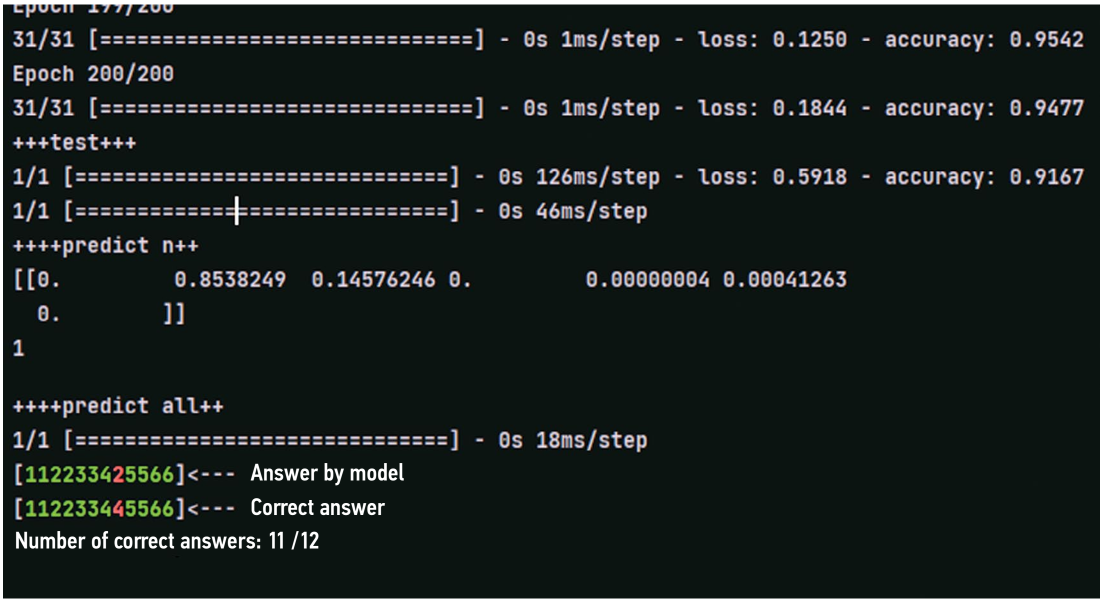

Fig. 4. Interface of the console application for working with the neural network (both the incorrect answer of the neural network and its correction are marked red).

using a test sample (Fig. 4). This interface was used to configure and select the optimal number of epochs. After creating the necessary modules, the cumbersome interface was replaced with a more minimalistic console output. This procedure allows for speeding up the training, reducing complexity, and improving model accuracy.

To more objectively evaluate the effectiveness of neural network training, a model should be trained in batches, and the average performance at each training cycle (i.e., each epoch) was compared. Fig. 5 shows graphs plotted for the average training performance of neural networks before and after optimizing the dataset and excluding noninformative parameters after correlation and regression analyses. Training accelerated significantly after clearing the dataset of homogeneous variables and analyzing the regression estimates. Without the preparation stage, the same process took much longer; however, even the final version of the algorithm did not achieve high training accuracy and stability.

The resulting prototype neural networks did not always determine the corneal deformity type, although they gradually learned to more effectively perform the classification task (Fig. 6).

Frequent errors in PCDR types 4 and 5 are evident (Fig. 6). Because these types are the rarest in the dataset used, this may be indicative of a class imbalance problem. Although the difference between classes and errors in their identification practically disappears by the 200th epoch, errors in identifying types 4 and 5 often appear precisely during training because each new ANN is trained from a random baseline state of neurons. However, the general tendency for the majority of errors being often distributed between types 4 and 5 remains (Fig. 7).

On average, the final-iteration ANN showed 91% (11 out of 12) correct answers by the 200th epoch. However, the test sample was not quite large; as the test sample increased, training performance declined. Types 4 and 5

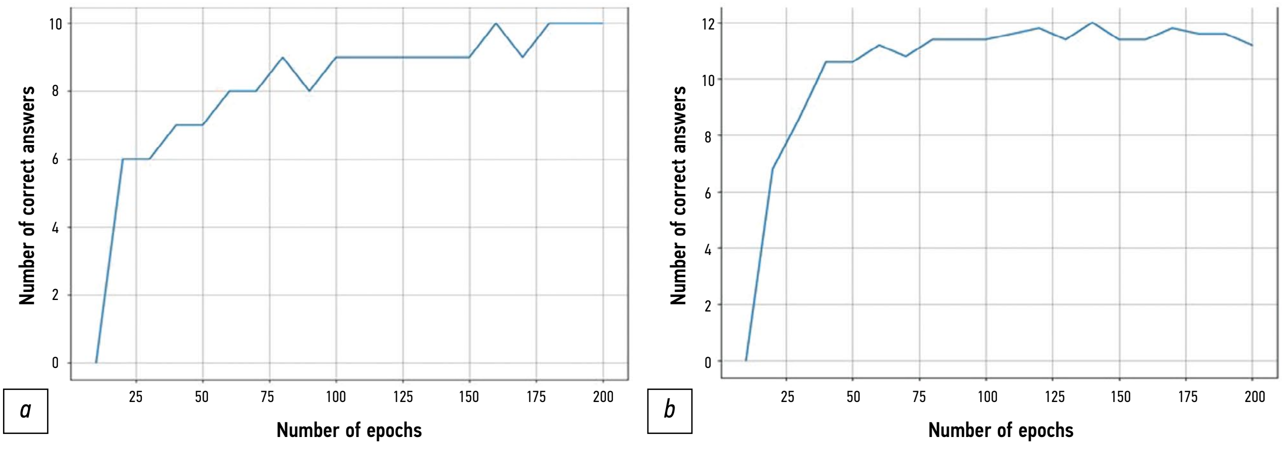

Fig. 5. Training performance vs. number of epochs: *a*, before dataset optimization; *b*, after dataset optimization.

DOI: https://doi.org/10.17816/DD624022

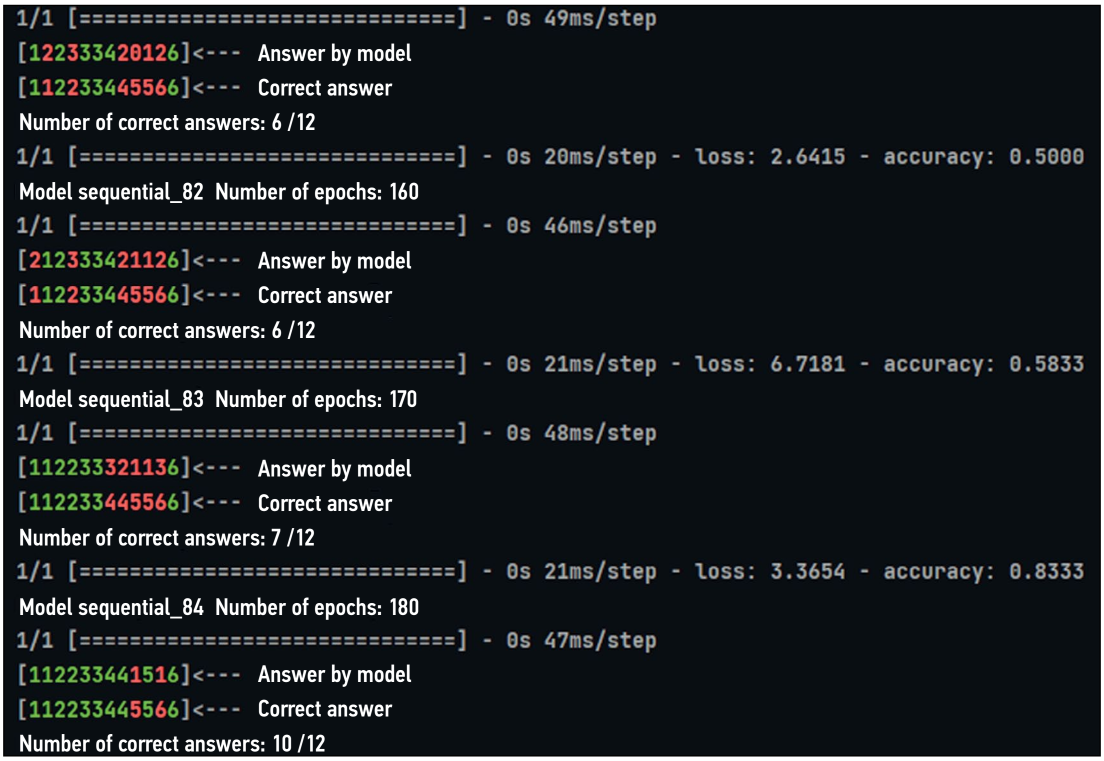

```
1/1 [==============================] - 0s 49ms/step
[122333420126]<--- Answer by model
[112233445566]<--- Correct answer
Number of correct answers: 6 /12
1/1 [==============================] - 0s 20ms/step - loss: 2.6415 - accuracy: 0.5000
Model sequential_82 Number of epochs: 160
1/1 [==============================] - 0s 46ms/step
[212333421126]<--- Answer by model
[112233445566]<--- Correct answer
Number of correct answers: 6 /12
1/1 [==============================] - 0s 21ms/step - loss: 6.7181 - accuracy: 0.5833
Model sequential_83 Number of epochs: 170
1/1 [==============================] - 0s 48ms/step
[112233321136]<--- Answer by model
[112233445566]<--- Correct answer
Number of correct answers: 7 /12
1/1 [==============================] - 0s 21ms/step - loss: 3.3654 - accuracy: 0.8333
Model sequential_84 Number of epochs: 180
1/1 [==============================] - 0s 47ms/step
[112233441516]<--- Answer by model
[112233445566]<--- Correct answer
Number of correct answers: 10 /12
```

Fig. 6. Gradual neural network training and further model test at reference points.

identification was affected by the limited available data. Reducing the sample by two records from each class leads to a 75% decrease in the mean integration rate by the 200th epoch.

DISCUSSION

The study highlights the potential of using ANNs for the diagnostic classification of surgically modified (post-RK) corneal profiles. The data obtained after 200 epochs suggest satisfactory results in the range of 75%–91% for various ratios of test and training samples. However, to reduce classification errors of PKCD types 4 and 5, a greater dataset is necessary. The classification accuracy to some extent correlates with the accuracy of calculations when constructing an ANN, as presented earlier.

For instance, M.C. Arbelaez et al. (2012) examined the effectiveness of support vector machines (SVM) in classifying keratotopographic data in patients with

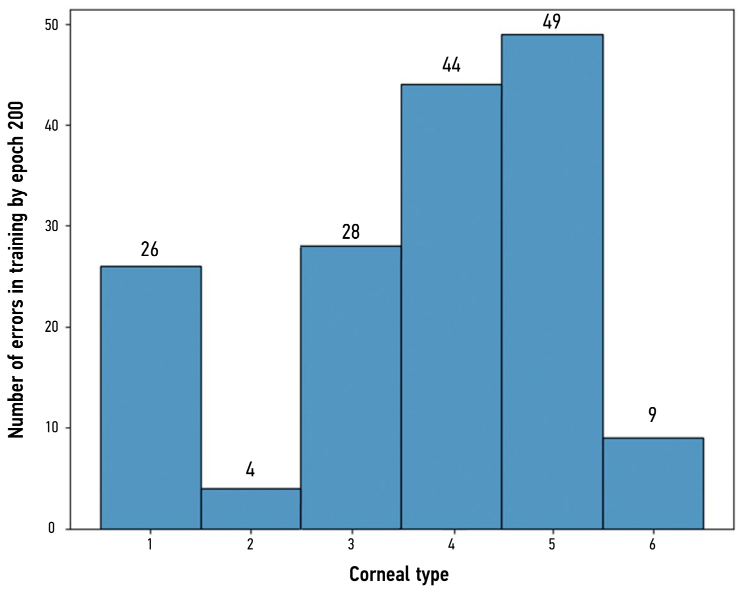

Fig. 7. Distribution of errors in PKCD type identification.

keratoconus. Their study demonstrated high sensitivity and specificity rates of 92.0% and 97.7%, respectively. Compared with analysis of the anterior surface alone, the inclusion of corneal thickness and its anterior and posterior surfaces would significantly improve the detection of subclinical keratoconus [15]. In the study by R. Hidalgo et al. (2016), multiparametric analysis of keratotopographic map data using SVMs demonstrated higher accuracy (i.e., greater area under the ROC curve) than monoparametric analysis (0.922 vs. 0.809). The mean sensitivity and specificity in the overall classification were 89.0% and 95.2%, respectively, and the area under the ROC curve was 0.922 [16].

Our results show that with proper training setup, input data preparation, a larger training sample, and optimal architecture, very high and stable performance in PKCD classification can be achieved. In addition, class imbalance problems must be eliminated because they may affect the quality of ANN training. Although the cross-entropy loss function used significantly minimizes this problem, PKCD types 4 and 5, as the least represented ones, are affected the most and contain the most errors.

The analysis of existing classes within a dataset with independent clustering of entries looks promising because it will eliminate the element of subjectivity in the primary division.

In addition, this study presents the results of ANN development based on an input table of features. However, the data obtained may serve as a basis for the subsequent development of an ANN that directly processes elevation display maps of the cornea.

CONCLUSION

Based on the analysis of numerical values of corneal topographic maps, an ANN that successfully classifies PKCD types with an accuracy of 91% was developed. The potential for further improvement of the training quality of this ANN has been established. Artificial intelligence algorithms may become a helpful tool for the automatic classification of patients with PKCD to ensure timely, high-quality diagnosis and determine further patient management techniques.

ADDITIONAL INFORMATION

Funding source. This study was not supported by any external sources of funding.

Competing interests. The authors declare that they have no competing interests.

Authors' contribution. All authors made a substantial contribution to the conception of the work, acquisition, analysis, interpretation of data for the work, drafting and revising the work, final approval of the version to be published and agree to be accountable for all aspects of the work. O.I. Rozanova — development of the concept and design of the study, writing the text of the article and editing, development of methodology, head of the study; E.K. Tsyrenzhapova — conducting research, writing the text of the article and editing, literature review, preparation and collection of data, preparation of the draft of the article, conducting research, final preparation of the article for publication, statistical data processing and their interpretation; I.S. Rozanov — computer accompaniment of the study; T.N. Iurieva — conducting research, final preparation of the article for publication, statistical data processing and interpretation; A.A. Ivanov — conducting research, literature review, preparation and collection of data, preparation of a draft article.

REFERENCES

1. Issarti I, Consejo A, Jiménez-García M, et al. Computer aided diagnosis for suspect keratoconus detection. *Comput Biol Med.* 2019;109:33–42. doi: 10.1016/j.compbiomed.2019.04.024

2. Chen X, Zhao J, Iselin KC, et al. Keratoconus detection of changes using deep learning of colour-coded maps. *BMJ Open Ophthalmol.* 2021;6(1):e000824. doi: 10.1136/bmjophth-2021-000824

3. Feng R, Xu Z, Zheng X, et al. KerNet: A novel deep learning approach for keratoconus and sub-clinical keratoconus detection based on raw data of the pentacam HR system. *IEEE J Biomed Health Inform.* 2021;25(10):3898–3910. doi: 10.1109/JBHI.2021.3079430

4. Gatinel D. Screening for subclinical keratoconus and prevention of corneal ectasia with SCORE analyzer software. In: Febbraro J-L, Khan HN, Koch DD, editors. *Surgical correction of astigmatism.* Cham: Springer International Publishing; 2018. doi: 10.1007/978-3-319-56565-1_9

5. Ruiz Hidalgo I, Rozema JJ, Saad A, et al. Validation of an objective keratoconus detection system implemented in a scheimpflug tomographer and comparison with other methods. *Cornea.* 2017;36(6):689–695. doi: 10.1097/ICO.0000000000001194

6. Malyugin BE, Sakhnov SN, Axenova LE, Myasnikova VV. Application of artificial intelligence in diagnostics and surgery of keratoconus: a systematic overview. *Fyodorov Journal of Ophthalmic Surgery.* 2022;(1):77–96. EDN: PPQRWZ doi: 10.25276/0235-4160-2022-1-77-96

7. Abdelmotaal H, Mostafa MM, Mostafa ANR, et al. Classification of Color-Coded Scheimpflug Camera Corneal Tomography Images Using Deep Learning. *Transl Vis Sci Technol.* 2020;9(13):30. doi: 10.1167/tvst.9.13.30

8. Dos Santos VA, Schmetterer L, Stegmann H, et al. CorneaNet: fast segmentation of cornea OCT scans of healthy and keratoconic eyes using deep learning. *Biomed Opt Express.* 2019;10(2):622–641. doi:10.1364/BOE.10.000622

9. Kuo BI, Chang WY, Liao TS, et al. Keratoconus Screening Based on Deep Learning Approach of Corneal Topography. *Transl Vis Sci Technol.* 2020;9(2):53. doi:10.1167/tvst.9.2.53

10. Shi C, Wang M, Zhu T, et al. Machine learning helps improve diagnostic ability of subclinical keratoconus using Scheimpflug and OCT imaging modalities. *Eye Vis (Lond).* 2020;7:48. doi: 10.1186/s40662-020-00213-3

11. Shukhaev SV, Mordovtseva EA, Pustozerov EA, Kudlakhmedov SS Application of convolutional neural networks to define Fuchs endothelial dystrophy. *Fyodorov*

Journal of Ophthalmic Surgery. 2022;(S4):70–76. EDN: WEZTKV doi: 10.25276/0235-4160-2022-4S-70-76

12. Obaid HS, Dheyab SA, Sabry SS. The impact of data pre-processing techniques and dimensionality reduction on the accuracy of machine learning. *2019 9th Annu. Inf. Technol. Electromechanical Eng. Microelectron. Conf. IEMECON.* 2019:279–283. doi: 10.1109/IEMECONX.2019.8877011

13. Valdés-Mas MA, Martín-Guerrero JD, Rupérez MJ, et al. A new approach based on Machine Learning for predicting corneal curvature (K1) and astigmatism in patients with keratoconus after intracorneal ring implantation. *Comput Methods Programs Biomed.* 2014;116:39–47. doi: 10.1016/j.cmpb.2014.04.003

14. Patent RUS № RU 2793142 C1/ 29.03.2023. Rozanova OI, Tsyrenzhapova EK, Iureva TN, et al. A method of evaluating the relief of the anterior and posterior corneal surface. (In Russ).

15. Arbelaez MC, Versaci F, Vestri G, et al. Use of a Support Vector Machine for Keratoconus and Subclinical Keratoconus Detection by Topographic and Tomographic Data. *Ophthalmology.* 2012;119(11):2231–2238. doi: 10.1016/j.ophtha.2012.06.005

16. Ruiz Hidalgo I, Rodriguez P, Rozema JJ, et al. Evaluation of a Machine-Learning Classifier for Keratoconus Detection Based on Scheimpflug Tomography. *Cornea.* 2016;35(6):827–832. doi: 10.1097/ico.0000000000000834

СПИСОК ЛИТЕРАТУРЫ

1. Issarti I., Consejo A., Jiménez-García M., et al. Computer aided diagnosis for suspect keratoconus detection // Comput Biol Med. 2019. Vol. 109. P. 33–42. doi: 10.1016/j.compbiomed.2019.04.024

2. Chen X., Zhao J., Iselin K.C., et al. Keratoconus detection of changes using deep learning of colour-coded maps // BMJ Open Ophthalmol. 2021. Vol. 6, N 1. P. e000824. doi: 10.1136/bmjophth-2021-000824

3. Feng R., Xu Z., Zheng X., et al. KerNet: A novel deep learning approach for keratoconus and sub-clinical keratoconus detection based on raw data of the pentacam HR system // IEEE J Biomed Health Inform. 2021. Vol. 25, N 10. P. 3898–3910. doi: 10.1109/JBHI.2021.3079430

4. Gatinel D. Screening for subclinical keratoconus and prevention of corneal ectasia with SCORE analyzer software. In: Febbraro J.-L., Khan H.N., Koch D.D., editors. Surgical correction of astigmatism. Cham: Springer International Publishing, 2018. doi: 10.1007/978-3-319-56565-1_9

5. Ruiz Hidalgo I., Rozema J.J., Saad A., et al. Validation of an objective keratoconus detection system implemented in a scheimpflug tomographer and comparison with other methods // Cornea. 2017. Vol. 36, N 6. P. 689–695. doi: 10.1097/ICO.0000000000001194

6. Малюгин Б.Э., Сахнов С.Н., Аксенова Л.Е., Мясникова В.В. Применение искусственного интеллекта в диагностике и хирургии кератоконуса: систематический обзор // Офтальмохирургия. 2022. № 1. С. 77–96. EDN: PPQRWZ doi: 10.25276/0235-4160-2022-1-77-96

7. Abdelmotaal H., Mostafa M.M., Mostafa A.N.R., et al. Classification of Color-Coded Scheimpflug Camera Corneal Tomography Images Using Deep Learning // Transl Vis Sci Technol. 2020. Vol. 9, N 13. P. 30. doi: 10.1167/tvst.9.13.30

8. Dos Santos V.A., Schmetterer L., Stegmann H., et al. CorneaNet: fast segmentation of cornea OCT scans of healthy and keratoconic eyes using deep learning // Biomed Opt Express. 2019. Vol. 10, N 2. P. 622–641. doi:10.1364/BOE.10.000622

9. Kuo B.I., Chang W.Y., Liao T.S., et al. Keratoconus Screening Based on Deep Learning Approach of Corneal Topography // Transl Vis Sci Technol. 2020. Vol. 9, N 2. P. 53. doi: 10.1167/tvst.9.2.53

10. Shi C., Wang M., Zhu T., et al. Machine learning helps improve diagnostic ability of subclinical keratoconus using Scheimpflug and OCT imaging modalities // Eye Vis (Lond). 2020. Vol. 7. P. 48. doi: 10.1186/s40662-020-00213-3

11. Шухаев С.В., Мордовцева Е.А., Пустозеров Е.А., Кудлахмедов Ш.Ш. Применение сверточных нейронных сетей для определения эндотелиальной дистрофии Фукса // Офтальмохирургия. 2022. № S4. С. 70–76. EDN: WEZTKV doi: 10.25276/0235-4160-2022-4S-70-76

12. Obaid H.S., Dheyab S.A., Sabry S.S. The impact of data pre-processing techniques and dimensionality reduction on the accuracy of machine learning // 2019 9th Annu. Inf. Technol. Electromechanical Eng. Microelectron. Conf. IEMECON. 2019. P. 279–283. doi: 10.1109/IEMECONX.2019.8877011

13. Valdés-Mas M.A., Martín-Guerrero J.D., Rupérez M.J., et al. A new approach based on Machine Learning for predicting corneal curvature (K1) and astigmatism in patients with keratoconus after intracorneal ring implantation // Comput Methods Programs Biomed. 2014. Vol. 116. P. 39–47. doi: 10.1016/j.cmpb.2014.04.003

14. Патент РФ на изобретение № RU 2793142 C1/ 29.03.2023. Розанова О.И., Цыренжапова Е.К., Юрьева Т.Н., и др. Способ оценки рельефа передней и задней поверхности роговицы.

15. Arbelaez M.C., Versaci F., Vestri G., et al. Use of a Support Vector Machine for Keratoconus and Subclinical Keratoconus Detection by Topographic and Tomographic Data // Ophthalmology. 2012. Vol. 119, N 11. P. 2231–2238. doi: 10.1016/j.ophtha.2012.06.005

16. Ruiz Hidalgo I., Rodriguez P., Rozema J.J., et al. Evaluation of a Machine-Learning Classifier for Keratoconus Detection Based on Scheimpflug Tomography // Cornea. 2016. Vol. 35, N 6. P. 827–832. doi: 10.1097/ico.0000000000000834

AUTHORS' INFO

*** Ekaterina K. Tsyrenzhapova,** MD;
address: 337 Lermontov street, 664033, Irkutsk, Russia;
ORCID: 0000-0002-6804-8268;
eLibrary SPIN: 1158-5233;
e-mail: katyakel@mail.ru

Olga I. Rozanova, MD, Dr. Sci. (Medicine);
ORCID: 0000-0003-3139-2409;
eLibrary SPIN: 6557-9123;
e-mail: olgrozanova@gmail.com

Tatiana N. Iureva, MD, Dr. Sci. (Medicine), Professor;
ORCID: 0000-0003-0547-7521;
eLibrary SPIN: 8457-5851;
e-mail: tnyurieva@mail.ru

Andrey A. Ivanov, MD;
ORCID: 0009-0001-4235-9252;
e-mail: ivanov.andrei.med@yandex.ru

Ivan S. Rozanov;
ORCID: 0009-0001-7202-0428;
e-mail: nauka@mntk.irkutsk.ru

ОБ АВТОРАХ

*** Цыренжапова Екатерина Кирилловна;**
адрес: Россия, 664033, г. Иркутск, ул. Лермонтова, 337;
ORCID: 0000-0002-6804-8268;
eLibrary SPIN: 1158-5233;
e-mail: katyakel@mail.ru

Розанова Ольга Ивановна, д-р мед. наук;
ORCID: 0000-0003-3139-2409;
eLibrary SPIN: 6557-9123;
e-mail: olgrozanova@gmail.com

Юрьева Татьяна Николаевна, д-р мед. наук, профессор;
ORCID: 0000-0003-0547-7521;
eLibrary SPIN: 8457-5851;
e-mail: tnyurieva@mail.ru

Иванов Андрей Александрович;
ORCID: 0009-0001-4235-9252;
e-mail: ivanov.andrei.med@yandex.ru

Розанов Иван Сергеевич;
ORCID: 0009-0001-7202-0428;
e-mail: nauka@mntk.irkutsk.ru

* Corresponding author / Автор, ответственный за переписку

DOI: https://doi.org/10.17816/DD623956

Организация диспансерного наблюдения пациентов с патологией макулярной области сетчатки с использованием систем искусственного интеллекта

А.Д. Чупров[1], И.П. Болодурина[2, 3], А.О. Лосицкий[1], А.Ю. Жигалов[2]

[1] Национальный медицинский исследовательский центр «Межотраслевой научно-технический комплекс “Микрохирургия глаза” имени академика С.Н. Федорова», Оренбург, Россия;
[2] Оренбургский государственный университет, Оренбург, Россия;
[3] Оренбургский государственный медицинский университет, Оренбург, Россия

АННОТАЦИЯ

Обоснование. Несмотря на то, что в приказе Министерства здравоохранения Российской Федерации «Об утверждении порядка оказания медицинской помощи взрослому населению при заболеваниях глаза, его придаточного аппарата и орбиты» сказано про оснащение медицинского консультативно-диагностического отделения поликлиники оптическим когерентным томографом, динамическое наблюдение пациентов с патологией сетчатки после начала лечения осуществляется чаще всего в медицинском офтальмологическом центре, что снижает доступность лечения для пациентов со впервые выявленной (первичной) патологией, требующей как можно более раннего начала лечения. Имеющаяся технология нуждается в изменении и интенсификации, в том числе — с применением технологий искусственного интеллекта.

Цель — разработка методических основ организационной технологии диспансерного наблюдения пациентов с патологией заднего отрезка глаза с использованием систем поддержки принятия врачебных решений на основе искусственного интеллекта.

Материалы и методы. Оценка существующей нормативной базы проведена на основе анализа Конституции Российской Федерации, федеральных законов, подзаконной нормативной базы и судебной практики. Создание структурированного медицинского документа описания снимка оптической когерентной томографии проведено с использованием экспертного метода: анкетирования 100 врачей-офтальмологов, имеющих соответствующий уровень образования, в том числе дополнительное профессиональное, занимающихся оказанием медицинских услуг — специализированной медицинской помощи пациентам с патологией заднего отрезка глаза. Структурированный медицинский документ послужил основой для формирования предикторов искусственных нейронных сетей. Обучение нейронных сетей произведено с использованием 60 000 медицинских изображений с помощью метода классификации и сегментации в зависимости от признака.

Результаты. Экспертным методом отобрано и описано 123 бинарных признака, позволяющих описать структуру макулярной области сетчатки в норме и при патологии, из которых выявлено 26 признаков, которые могут быть интерпретированы в качестве предикторов ухудшения клинического течения заболевания.

Заключение. Разработанный классификатор позволил создать и обучить на основе 60 000 медицинских изображений систему поддержки принятия врачебных решений, которая в качестве информационного сервиса, без постановки диагноза, может позволить изменить организацию процесса динамического наблюдения. Формирование маршрутизации пациентов — первичная услуга разработанной системы поддержки принятия врачебных решений. При наличии признаков ухудшения клинической картины предполагается маршрутизация в медицинский офтальмологический центр для оценки динамики и оказания специализированной, в том числе высокотехнологичной, медицинской помощи.

Ключевые слова: система поддержки принятия врачебных решений; искусственный интеллект; оптическая когерентная томография; патология; макула.

Как цитировать:
Чупров А.Д., Болодурина И.П., Лосицкий А.О., Жигалов А.Ю. Организация диспансерного наблюдения пациентов с патологией макулярной области сетчатки с использованием систем искусственного интеллекта // Digital Diagnostics. 2024. Т. 5, № 1. С. 75–84. DOI: https://doi.org/10.17816/DD623956

Рукопись получена: 28.11.2023 **Рукопись одобрена:** 11.03.2024 **Опубликована online:** 15.03.2024

DOI: https://doi.org/10.17816/DD623956

Organizing follow-up care for patients with macular retinal pathologies using artificial intelligence systems

Aleksandr D. Chuprov[1], Irina P. Bolodurina[2, 3], Aleksandr O. Lositskiy[1], Artur Yu. Zhigalov[2]

[1] The S. Fyodorov Eye Microsurgery Federal State Institution, Orenburg, Russia;
[2] Orenburg State University, Orenburg, Russia;
[3] Orenburg State Medical University, Orenburg, Russia

ABSTRACT

BACKGROUND: The Order of the Ministry of Health of Russia “On Approval of the Procedure for the Provision of Medical Care to the Adult Population for Diseases of the Eye, Appendages, and Orbit” provides for equipping consultation and diagnostic departments of outpatient clinics with optical coherence tomographs. However, case follow-up of patients with retinal pathology is most commonly performed in ophthalmology centers, limiting treatment accessibility for patients with primary (newly diagnosed) pathologies requiring immediate treatment initiation. The available approach requires modification and intensification, including the use of artificial intelligence technologies.

AIM: To develop methodological foundations for organizing follow-up care for patients with posterior segment eye diseases using an artificial intelligence-based clinical decision support system.

MATERIALS AND METHODS: The existing regulatory framework was analyzed based on the Constitution of the Russian Federation, federal laws, by-law framework, and judicial practice. A structured medical document describing an optical coherence tomography image was created using an expert method: a survey of 100 ophthalmologists with an appropriate education level, including additional professional training, engaged specialized medical care for patients with posterior segment eye diseases was performed.

RESULTS: Using an expert method, 123 binary features were selected to describe the structure of the macular area of the retina under normal and pathological conditions, with 26 features identified as predictors of a worsening clinical course of the disease.

CONCLUSION: The proposed classifier enabled the creation and training of a medical decision support system based on 60,000 medical images, which, as an information service, without making a diagnosis, can change the case follow-up process. Routing of patients is a primary service of the proposed system. If the clinical picture shows signs of deterioration, a referral to an ophthalmology center is considered to assess the course of the disease and provide specialized services, including high-tech medical care.

Keywords: clinical decision support system; artificial intelligence; optical coherence tomography; pathology; macular.

To cite this article:
Chuprov AD, Bolodurina IP, Lositskiy AO, Zhigalov AYu. Organizing follow-up care for patients with macular retinal pathologies using artificial intelligence systems. *Digital Diagnostics.* 2024;5(1):75–84. DOI: https://doi.org/10.17816/DD623956

Submitted: 28.11.2023 **Accepted:** 11.03.2024 **Published online:** 15.03.2024

ECO•VECTOR

DOI: https://doi.org/10.17816/DD623956

利用人工智能系统组织对视网膜黄斑病变患者的防治观察

Aleksandr D. Chuprov[1], Irina P. Bolodurina[2, 3], Aleksandr O. Lositskiy[1], Artur Yu. Zhigalov[2]

[1] The S. Fyodorov Eye Microsurgery Federal State Institution, Orenburg, Russia;
[2] Orenburg State University, Orenburg, Russia;
[3] Orenburg State Medical University, Orenburg, Russia

摘要

论证。根据俄罗斯联邦卫生部命令《关于向成年居民提供眼部、眼部附属装置和眼眶疾病医疗服务的程序批准》，综合医院的医疗咨询和诊断部门都配备光学相干断层扫描仪。然而，视网膜病变患者在开始治疗后的动态观察通常是在专门眼科医疗中心进行。这就降低了对首次发现（原发性）病变患者的治疗机会，因为这些患者需要尽早开始治疗。需要改变和加强现有技术，包括使用人工智能技术。

目的。本研究旨在利用基于人工智能的医疗决策支持系统，为眼后段病变患者的防治观察组织技术奠定方法论基础。

材料和方法。在对《俄罗斯联邦宪法》、联邦法律、附属法规和司法实践分析的基础上，对现有管理框架进行了评估。使用专家方法编制了描述光学相干断层扫描图像的结构化医学文件：对100名具有适当教育水平的眼科医生进行了问卷调查，包括额外的专业教育。所有医生都从事医疗服务工作，即为眼后段病变患者提供专业医疗服务。结构化医疗文件是形成人工神经网络预测器的基础。利用基于特征的分类和分割方法，使用60000张医学图像对神经网络进行了训练。

结果。通过专家方法选取并描述了123个能够描述正常和病理下视网膜黄斑区结构的二元特征。其中，26个特征被确定为疾病临床过程恶化的预测器。

结论。所开发的分类器可以在60000张医学图像的基础上创建和训练一个医疗决策支持系统。该系统可用作信息服务。它可以在不做出诊断的情况下改变动态观察过程的组织结构。患者路径选择是已开发的医疗决策支持系统的主要服务。如果临床症状有恶化的迹象，患者就会被转诊到眼科医疗中心，以接受动态评估及包括高科技在内的专业医疗服务。

关键词：医疗决策支持系统；人工智能；光学相干断层扫描；病变；黄斑。

引用本文：
Chuprov AD, Bolodurina IP, Lositskiy AO, Zhigalov AYu. 利用人工智能系统组织对视网膜黄斑病变患者的防治观察. *Digital Diagnostics.* 2024;5(1):75–84. DOI: https://doi.org/10.17816/DD623956

收到：28.11.2023 **接受：**11.03.2024 **发布日期：**15.03.2024

BACKGROUND

The National Artificial Intelligence Development Strategy adopted in the Russian Federation determined the artificial intelligence (AI) to be used in increasing the efficiency of organizations.[1] This can be achieved by automating routine (repetitive) production processes and operations.

In accordance with current guidelines, if risk factors for disease progression are present in patients with diabetes mellitus-induced retinal pathology and age-related macular degeneration, regular follow-ups by an ophthalmologist are recommended to monitor changes and start adequate treatment if necessary [1, 2]. Retinal examination using a computer analyzer, i.e., structural optical coherence tomography (OCT), is included in the standard of care for primary specialized medical care of patients with diabetic retinopathy and age-related macular degeneration and is a recurring service.[2] The frequency of doctor visits is determined individually depending on the planned management strategies and clinical signs. According to domestic studies, the minimum number of OCT examinations of the macular retina performed in medical institutions during follow-ups in patients with age-related macular degeneration and diabetic macular edema is 1,629,429 per year.

Foreign analytical studies have shown the willingness of patients to switch to controlled self-medications during follow-up (up to 54% of respondents according to 2019 data, STADA Health Report 2020) and to receive part of the medical services using telemedicine technologies, i.e., without face-to-face visits to a healthcare professional [3–5]. In a study by the Russian Public Opinion Research Center, 48% of Russians are open to follow-up and treatment using telemedicine services [6]. Thus, organizational and clinical prerequisites have been established for the provision of medical services using AI, including the use of telemedicine technologies, for patients who require repeated diagnostic appointments as part of the follow-up for posterior eye segment pathology.

The Order of the Ministry of Health of the Russian Federation dated November 12, 2012, No. 902n, On Approval of the Procedure for the Provision of Medical Care to the Adult Population for Diseases of the Eye, Appendages, and Orbit refers to equipping medical consultative and diagnostic departments of outpatients clinics with optical coherence tomographs. However, patients with retinal pathology most often receive follow-up care in a medical ophthalmology center once they have started treatment, and this reduces the availability of treatment for patients with newly diagnosed pathology, which must be treated the earliest time possible. Existing technologies need changing and intensifying, including through the use of AI technologies.

AIM

To develop the methodological basis for an organizational system for the follow-up of patients with posterior eye segment pathology using AI-based clinical decision support systems (CDSS).

MATERIALS AND METHODS

Content analysis was performed to assess the existing regulatory framework. To create a structured directory, sociological and expert methods were used. Artificial neural networks (ANNs) were trained using segmentation and classification methods.

Study design

The existing regulatory framework was assessed based on an analysis of the Constitution of the Russian Federation, federal laws, sublegislative acts, and judicial practice. The methodology for a structured medical document describing an OCT image was created using an expert method: i.e., 100 ophthalmologists with the appropriate educational level, including advanced professional education, engaged in specialized medical care for patients with posterior segment pathology were included in a survey. The structured medical document was used as the basis for ANN predictors. As a result of annotation, 60,000 medical images were described. For each image, a.json file describes the presence of features after mapping. To analyze and classify binary features in an image, neural networks with the DenseNet121 architecture without pretrained weights were trained. The Mask R-CNN architecture was used for the segmentation task.

Eligibility criteria

A sign was added to the significant factors that indicated disease deterioration when the agreement between respondents reached 70%. A sign was added to the CDSS output when its accuracy (mean sensitivity and specificity) reached a value of ⩾0.7.

Study conditions

A database was constructed based on the anonymized data from clinical studies (retinal examinations using OCT) conducted in the Orenburg and Tambov branches of the S.N. Fyodorov Eye Microsurgery Complex of the Ministry of

[1] Decree of the President of the Russian Federation dated October 10, 2019 No. 490 "On the Development of Artificial Intelligence in the Russian Federation" (together with the "National Artificial Intelligence Development Strategy for the period until 2030"). Access: https://www.consultant.ru/document/cons_doc_LAW_335184/1f32224a00901db9cf44793e9a5e35567a4212c7/ Access date: November 22, 2023.

[2] Order of the Ministry of Health of the Russian Federation dated December 24, 2012, No. 1492n "On Approval of the Standard of Primary Health Care for Diabetic Retinopathy and Diabetic Macular Edema." Access: https://base.garant.ru/70344052/53f89421bbdaf741eb2d1ecc4ddb4c33/ Access date: November 22, 2023.

Health of the Russian Federation. The ANN was trained at the Research Institute of Digital Intelligent Technologies of the Orenburg State University (Russia).

Study duration

Clinical studies (retinal examinations using OCT) were performed between 2015 and 2023. The structured binary classifier directory for describing the macular retina was created in 2022, and the ANNs were trained in 2022–2023.

Medical intervention

For the database, retinal examinations involved OCT scans of the macular retina.

Primary outcome

The methodological basis for the use of AI in the regular follow-up of patients with posterior segment pathology was developed and evaluated.

Subgroup analysis

The follow-up methodology was based on an assessment of the medical care organization and clinical data of patients diagnosed with age-related macular degeneration (ICD-10 code: H 35.3) or diabetic macular edema (ICD-10 code: H 35.8).

Outcome measures

Sensitivity and specificity are statistical parameters of a diagnostic test used to identify patients with pathology and healthy individuals derived from type I and II errors in the binary classification.

Statistical analysis

For the sample size calculation, the minimum volume of the sample study was determined considering the validity criterion and maximum error (product of the confidence interval and specified accuracy).

Statistical procedures included descriptive statistics, calculation of the mean values and relative values, and mathematical modeling. The statistical significance of differences in the studied data according to qualitative characteristics was analyzed through mathematical calculations and subsequently evaluated using Pearson's chi-squared test. Quantitative variables were described during the preliminary assessment for compliance with Gauss's law (normal probability distribution).

RESULTS

Study objects

The study focused on organizing ophthalmological care for the adult population as part of their follow-up for posterior segment pathology. In the content analysis, 22 records were analyzed. The database included 60,000 records of retinal examinations using OCT for which a medical image (scan) and a result interpretation in accordance with the developed binary classifier are available.

Primary outcome results

In accordance with Federal Law dated November 21, 2011, No. 323-FZ "On the Fundamentals of Public Healthcare of Citizens in the Russian Federation," medical care in the Russian Federation was organized and provided:

1) In accordance with the regulations on the organization of medical care by type of medical care
2) In accordance with the procedures for the provision of medical care approved by the authorized federal executive body and mandatory for execution in the territory of the Russian Federation by all medical organizations
3) Based on guidelines
4) Considering the standards of medical care approved by the authorized federal executive body.[3]

In addition, Paragraph 15 of Article 2 of this law defines "attending physician," who is a doctor responsible for organizing and directly providing medical care to a patient during follow-up and treatment. In the provision of primary specialized medical care, certain functions of the attending physician may be delegated to nursing staff in accordance with the approved procedure; however, the provision of primary specialized medical care, including medical services specified in the professional standard of an ophthalmologist, should not be delegated.[4, 5]

Results of imaging studies cannot be interpreted by nursing staff independently when providing medical services. This is only possible with the use of registered medical devices.

CDSSs require registration as a medical device for use by nursing personnel. When used by doctors, they can remain within the legal field of information services because the interpretation of results, diagnosis, and recommendations, including those in follow-up, remain within the competence of the attending physician, regardless of the legal status of the software.

[3] Federal Law "On the Fundamentals of Public Healthcare of Citizens in the Russian Federation" dated November 21, 2011, No. 323-FZ. Access: https://www.consultant.ru/document/cons_doc_LAW_121895/ Access date: November 22, 2023.

[4] Order of the Ministry of Health and Social Development of the Russian Federation dated March 23, 2012, No. 252n "On Approval of the Procedure for Assigning Certain Functions of the Attending Physician to a Paramedic or Midwife by the Head of a Medical Organization when Organizing the Provision of Primary Health Care and Emergency Medical Care for the Direct Provision of Medical Care to the Patient During Follow-up and Treatment, Including the Prescription and Administration of Medications, Including Narcotic Drugs and Psychotropic Drugs." Access: https://base.garant.ru/70170588/ Access date: November 22, 2023.

[5] Order of the Ministry of Health and Social Development of the Russian Federation dated June 5, 2017, No. 470n "On Approval of the Professional Standard for Ophthalmologists." Access: https://docs.cntd.ru/document/436744741 Access date: November 22, 2023.

Using the expert method, 123 binary features that allow describing the structure of healthy and abnormal macular retina were selected and characterized. The features were grouped into sections: general, vitreoretinal and retinal interface, retinal contour, retinal thickness, retinal structures, and choroid. In the survey of experts with appropriate education and professional experience, 75% of the doctors classified only 26 features out of 123 as predictors of worsening conditions in patients with age-related macular degeneration or diabetic macular edema (Table 1).

The selected features directly or indirectly indicated the onset of a pathological process, including neovascularization, which requires specialized and high-tech medical care in tertiary medical institutions (e.g., federal medical organizations). In addition, the features were consistent with the guidelines and current scientific literature describing medical care provision and interpretation of the results of imaging diagnostic studies [7, 8].

The binary classifier was divided into features suitable for use in ANN training by classification and segmentation methods. The ANN training based on 60,000 medical images made it possible to create a CDSS for follow-up in patients with posterior segment pathology. The accuracy of ANN models was assessed using the balanced accuracy metric to correctly account for the heterogeneous distribution of classes in the data. The mean balanced accuracy across features was 81%.

Secondary outcome results

The developed version of the CDSS is in the open-access system: http://retinadeepai.site/. The system recognizes objects to be analyzed as predictors for each of the developed features and allows for the configuration of the analysis of various maps and modes, including those obtained using different devices. The recommended analysis mode is RetinaMap. The service has an ergonomic, intuitive interface

Table 1. Signs of clinical deterioration

Sign	Section
Moderate macular thickness increase (≤500 μm)	Macular thickness
Severe macular thickness increase (>500 μm)	
Focal intraretinal edema identified	Retinal structure
Diffuse intraretinal edema identified	
Cystic intraretinal edema identified	
Abnormality: small (<50 μm) multiple cysts	
Abnormality: medium (50–150 μm) multiple cysts	
Abnormality: large (>150 μm) multiple cysts	
Serous neuroepithelial detachment visualized	
Slit-like neuroepithelial detachment visualized	
Serous RPE detachment visualized	
Dome-shaped RPE detachment	
Flat wave-like RPE detachment visualized	
Flat RPE detachment visualized	
“Tabletop” RPE detachment visualized	
Hemorrhagic RPE detachment visualized	
Fibrovascular RPE detachment visualized	
Double-layer sign visualized	
Highly reflective opacity shadowing deeper layers (subretinal hemorrhage)	
Subretinal fluid visualized	
Hyperreflective focus visualized in inner retinal layers	
Hyperreflective focus visualized in outer retinal layers	
Hyperreflective focus visualized above RPE	
Hyperreflective focus visualized within RPE	
Hyperreflective focus visualized under RPE	
Hyperreflective focus shadowing the underlying layers visualized	

Note: RPE, retinal pigment epithelium.

that makes it possible to upload a report attached to the medical records. The service is not a medical device, but an information service; it does not store or process personal patient data. The service does not make a diagnosis or offer prompts for diagnosis. It describes the structure of the normal and abnormal retina, taking on part of the routine processes of an ophthalmologist during patient follow-ups.

Adverse events

None identified.

DISCUSSION

Currently, several AI-based systems are being developed globally for the early diagnosis of fundus pathology. For example, certain systems detect early signs of diabetic retinopathy using fundus images obtained from stationary and portable fundus cameras: the IDx-DR system (LumineticsCore, USA) and the Retina.AI platform (Digital Vision Solutions LLC, Russia).

In addition, several technological developments aimed at automated analysis of data obtained using medical devices.

- The Retina.AI platform is aimed at analyzing OCT images of the retina and identifying one of the specified syndrome complexes: subretinal fluid, intraretinal cysts, retinal pigment epithelial detachment, subretinal hyperreflective material, epiretinal membrane, retinal drusen, full-thickness macular hole, lamellar macular hole, and vitreomacular traction (https://www.screenretina.com/). Thus, the project is aimed at diagnosing conditions and assessing the course of the process. The project is not registered as a medical device.
- The Altris AI platform (USA) automates the selection of abnormal OCT scans and detection of >70 disorders and pathological signs, including epiretinal fibrosis, intraretinal cystoid fluid, pseudocysts, diffuse edema, fibrovascular detachment of the retinal pigment epithelium, and subretinal hyperreflective material (https://www.altris.ai/). The project aims to diagnose conditions (diseases) and train medical personnel. The project is registered as a medical device in the country of origin (US Food and Drug Administration).

The product we are developing contains a larger number of assessed features (123) and aims not at diagnosis but at changing the organization of the diagnostic and treatment process, i.e., delegating routine work from doctors to nursing staff, reducing research time, and increasing the availability of medical services.

It requires changing the professional standard of nursing staff by including the use of AI-based information services as part of patient follow-up. In addition, in the Order of the Ministry of Health of Russia dated March 15, 2023 No. 168n, “On Approval of the Procedure for Regular Follow-up of Adults,” the regulatory framework must be updated for the regular follow-up of patients with posterior segment pathology to include this pathology.

Primary outcome summary

The methodological basis of the organizational technology for regular follow-up of patients with posterior segment pathology has been developed. A structural classifier for describing the retina has been prepared, and a CDSS has been developed for use in the regular follow-up of this patient population.

Primary outcome discussion

The Order of the Ministry of Health of the Russian Federation dated September 7, 2020, No. 947n, “On Approval of the Procedure for Organizing a Document Flow System in the Field of Healthcare to Manage Medical Electronic Records” defines the procedure for using electronic medical records. To date, several structured electronic medical documents have been developed and approved and are currently used in Russia. The Center for the Development of Structured Electronic Medical Documents is part of the Central Research Institute for Organization and Informatization of Healthcare of the Ministry of Health of the Russian Federation. It ensures the implementation of the tasks of the Ministry of Health of Russia to improve the procedure for organizing document flow in healthcare by developing, updating, and modernizing guidelines for the implementation of structured electronic health records. The developed directory can become the basis for a medical protocol for an imaging study of the retina using OCT.

The accumulation of structured information will contribute to the improvement of the developed CDSS. Using AI-based CDSSs, changing the regulatory framework will help speed up the implementation of the organizational technology for regular follow-up of patients with posterior segment pathology.

Study limitations

The results of the study are intended for follow-up in patients with posterior segment pathology. The results cannot be used in the primary diagnosis of eye, ocular adnexa, and orbit pathologies.

CONCLUSION

In the legal framework of the Russian Federation, some of the physician’s medical functions could not be delegated to nursing staff such as when interpreting the results of a medical examination. For example, in eye, ocular adnexa, and orbital disorders, the professional standard and regulatory framework must be amended. However, no uniform rules have been established for creating a structured electronic medical record containing the results of interpreting a retinal examination using OCT. The proposed classifier made it possible to create and train (based on 60,000 medical images)

DOI: https://doi.org/10.17816/DD623956

a CDSS, which, as an information service not intended for establishing a diagnosis, allows for the reorganization of the follow-up process. The primary service of the developed CDSS is patient routing. If signs of deterioration are observed in the clinical presentation, referral to a medical ophthalmology center is warranted to assess the disease course and provide specialized, including high-tech medical care.

ADDITIONAL INFO

Funding source. This study was not supported by any external sources of funding.

Competing interests. The authors declare that they have no competing interests.

Authors' contribution. All authors made a substantial contribution to the conception of the work, acquisition, analysis, interpretation of data for the work, drafting and revising the work, final approval of the version to be published and agree to be accountable for all aspects of the work. A.D. Chuprov, I.P. Bolodurina — development of the concept, approval of the final version of the manuscript; A.O. Lositskiy — development of methodology, database collection, writing and editing the text of the article; A.Yu. Zhigalov — development of methodology, conducting research.

REFERENCES

1. *Diabetes mellitus: diabetic retinopathy, diabetic macular edema. Clinical guidelines*. ID 115. Approved by the Scientific and Practical Council of the Ministry of Health of the Russian Federation. 2023. Available from: https://cr.minzdrav.gov.ru/recomend/115_2 (In Russ).

2. *Age-related macular degeneration. Clinical guidelines*. ID 114. Approved by the Scientific and Practical Council of the Ministry of Health of the Russian Federation. 2021. Available from: https://cr.minzdrav.gov.ru/recomend/114_2 (In Russ).

3. Health Tech Digital [Internet]. c2018-2024. Digital Therapeutics and Wellness App Users to Reach 1.4 Billion Globally by 2025, as Pandemic Accelerates Regulatory Acceptance. Available from: https://www.healthtechdigital.com/digital-therapeutics-and-wellness-app-users-to-reach-1-4-billion-globally-by-2025-as-pandemic-accelerates-regulatory-acceptance/ Cited 2023 Nov 22.

4. Pugachev PS, Gusev AV, Kobyakova OS, et al. Global trends in the digital transformation of the healthcare industry. *National Health Care (Russia).* 2021;2(2):5–12. EDN: JADWXN doi: 10.47093/2713-069X.2021.2.2.5-12

5. STADA Health Report 2020. Available from: https://www.stada.com/media/5774/stada_healthreport2020_en.pdf Cited 2023 Nov 22.

6. Medvedeva EI, Aleksandrova OA, Kroshilin SV. Telemedicine in modern conditions: the attitude of society and the vector of development. *Economic And Social Changes: Facts, Trends, Forecast,* 2022;15(3):200–222. doi: 10.15838/esc.2022.3.81.11

7. Lumbroso B, Rispoli M. *Retinal OCT. Method of analysis and interpretation.* Neroev VV, Zaitseva OV, editors. Moscow: Aprel'; 2012. (In Russ).

8. Avetisov S, Kats M. Using optical coherent tomography in diagnosis of retinal diseases. (review of literature). *Universum: meditsina i farmakologiya.* 2017;(4(38)):15–26. EDN: YJAYXT

СПИСОК ЛИТЕРАТУРЫ

1. Клинические рекомендации — Сахарный диабет: ретинопатия диабетическая, макулярный отек диабетический. ID 115. Одобрено Научно-практическим Советом Минздрава РФ. 2023. Режим доступа: https://cr.minzdrav.gov.ru/recomend/115_2 Дата обращения: 22.11.2023.

2. Клинические рекомендации — Макулярная дегенерация возрастная. ID 114. Одобрено Научно-практическим Советом Минздрава РФ. 2021. Режим доступа: https://cr.minzdrav.gov.ru/recomend/114_2 Дата обращения: 22.11.2023.

3. Health Tech Digital [Internet]. c2018-2024. Digital Therapeutics and Wellness App Users to Reach 1.4 Billion Globally by 2025, as Pandemic Accelerates Regulatory Acceptance. Доступ по ссылке: https://www.healthtechdigital.com/digital-therapeutics-and-wellness-app-users-to-reach-1-4-billion-globally-by-2025-as-pandemic-accelerates-regulatory-acceptance/ Дата обращения: 22.11.2023.

4. Пугачев П.С., Гусев А.В., Кобякова О.С., и др. Мировые тренды цифровой трансформации отрасли здравоохранения // Национальное здравоохранение. 2021. Т. 2, № 2. С. 5–12. EDN: JADWXN doi: 10.47093/2713-069X.2021.2.2.5-12

5. STADA Health Report 2020. Режим доступа: https://www.stada.com/media/5774/stada_healthreport2020_en.pdf Дата обращения: 22.11.2023.

6. Медведева Е.И., Александрова О.А., Крошилин С.В. Телемедицина в современных условиях: отношение социума и вектор развития // Экономические и социальные перемены: факты, тенденции, прогноз. 2022. Т. 15, № 3. С. 200–222 doi: 10.15838/esc.2022.3.81.11

7. Ламброзо Б., Рисполи М. ОКТ сетчатки. Метод анализа и интерпретации / под ред. В.В. Нероева, О.В. Зайцевой. Москва : Апрель, 2012.

8. Аветисов С.Э., Кац М.В. Использование оптической когерентной томографии в диагностике заболеваний сетчатки (обзор литературы) // Universum: медицина и фармакология. 2017. № 4(38). С. 15–26. EDN: YJAYXT

AUTHORS' INFO

*** Aleksandr O. Lositskiy,** MD, Cand. Sci. (Medicine);
address: 17 Salmyshskaya street, 460047 Orenburg, Russia;
ORCID: 0000-0002-8716-6438;
eLibrary SPIN: 2044-3410;
e-mail: eyedoct@yandex.ru

Aleksandr D. Chuprov, MD, Dr. Sci. (Medicine), Professor;
ORCID: 0000-0001-7011-4220;
e-mail: nauka@ofmntk.ru

Irina P. Bolodurina, Dr. Sci. (Engineering), Professor;
ORCID: 0000-0003-0096-2587;
eLibrary SPIN: 4848-0669;
e-mail: prmat@mail.osu.ru

Artur Yu. Zhigalov;
ORCID: 0000-0003-3208-1629;
eLibrary SPIN: 4692-9037;
e-mail: prmat@mail.osu.ru

ОБ АВТОРАХ

*** Лосицкий Александр Олегович,** канд. мед. наук;
адрес: Россия, 460047, Оренбург, улица Салмышская, д. 17;
ORCID: 0000-0002-8716-6438;
eLibrary SPIN: 2044-3410;
e-mail: eyedoct@yandex.ru

Чупров Александр Дмитриевич, д-р мед. наук, профессор;
ORCID: 0000-0001-7011-4220;
e-mail: nauka@ofmntk.ru

Болодурина Ирина Павловна, д-р техн. наук, профессор;
ORCID: 0000-0003-0096-2587;
eLibrary SPIN: 4848-0669;
e-mail: prmat@mail.osu.ru

Жигалов Артур Юрьевич;
ORCID: 0000-0003-3208-1629;
eLibrary SPIN: 4692-9037;
e-mail: prmat@mail.osu.ru

* Corresponding author / Автор, ответственный за переписку

DOI: https://doi.org/10.17816/DD623196

Применение искусственного интеллекта в диагностике кальцификации артерий

Ю.А. Трусов[1], В.С. Чупахина[2], А.С. Нуркаева[3], Н.А. Яковенко[4], И.В. Абленина[5], Р.Ф. Латыпова[5], А.П. Питке[5], А.А. Язовских[3], А.С. Иванов[3], Д.С. Богатырева[6], У.А. Попова[7], А.Ф. Юзлекбаев[3]

[1] Самарский государственный медицинский университет, Самара, Россия;
[2] Ростовский государственный медицинский университет, Ростов-на-Дону, Россия;
[3] Башкирский государственный медицинский университет, Уфа, Россия;
[4] Первый Московский государственный медицинский университет им. И.М. Сеченова, Москва Россия;
[5] Оренбургский государственный медицинский университет, Оренбург, Россия;
[6] Российский национальный исследовательский медицинский университет им. Н.И. Пирогова, Москва, Россия;
[7] Российский университет медицины, Москва, Россия

АННОТАЦИЯ

Обоснование. Показатели заболеваемости населения Российской Федерации патологиями системы кровообращения за прошедшие два десятилетия постоянно повышались, и с 2000 г. до 2019 г. увеличились в 2,047 раза. Процесс кальцификации сосудов включает отложение солей кальция в стенке артерий, что приводит к ремоделированию сосудистой стенки. Лучевые методы исследования — золотой стандарт диагностики кальцификации сосудов. Однако в связи с возрастающим объёмом данных и необходимостью сокращения времени постановки диагноза неизбежно снижается эффективность работы. Активное развитие и внедрение в клиническую практику искусственного интеллекта открыло перед специалистами возможности для решения этих проблем.

Цель — проанализировать отечественную и зарубежную литературу, посвящённую использованию искусственного интеллекта в диагностике различных типов кальцификации сосудов, а также обобщить прогностическую ценность кальцификации сосудов и оценить аспекты, препятствующие диагностике кальцификации сосудов без применения искусственного интеллекта.

Материалы и методы. Авторы провели поиск публикаций в электронных базах данных PubMed, Web of Science, Google Scholar и eLibrary. Поиск проводился по следующим ключевым словам: «artificial intelligence», «machine learning», «vascular calcification», «искусственный интеллект», «машинное обучение», «кальцификация сосудов». Поиск проводился во временном интервале с момента основания соответствующей базы данных до июля 2023 года.

Результаты. Основная методология включённых в обзор исследований заключалась в сравнении диагностических способностей клиницистов и искусственного интеллекта с применением одних и тех же изображений и последующей оценкой точности, скорости и других показателей. Участки возникновения сосудистых кальцификаций весьма разнообразны, что обусловливает их различную прогностическую ценность.

Заключение. Искусственный интеллект отлично зарекомендовал себя в диагностике сосудистой кальцификации. Помимо повышения точности и эффективности, способности к детализации превосходят возможности ручного метода диагностики. Искусственный интеллект достиг уровня, позволяющего помогать врачам инструментальной диагностики в автоматическом выявлении кальцификации сосудов. Возможности искусственного интеллекта могут способствовать эффективному развитию рентгенологии в будущем.

Ключевые слова: искусственный интеллект; машинное обучение; кальцификация сосудов; рентгенология; диагностическая визуализация.

Как цитировать:

Трусов Ю.А., Чупахина В.С., Нуркаева А.С., Яковенко Н.А., Абленина И.В., Латыпова Р.Ф., Питке А.П., Язовских А.А., Иванов А.С., Богатырева Д.С., Попова У.А., Юзлекбаев А.Ф. Применение искусственного интеллекта в диагностике кальцификации артерий // Digital Diagnostics. 2024. Т. 5, № 1. С. 85–100. DOI: https://doi.org/10.17816/DD623196

Рукопись получена: 10.11.2023 **Рукопись одобрена:** 10.01.2024 **Опубликована online:** 29.01.2024

DOI: https://doi.org/10.17816/DD623196

Use of artificial intelligence in the diagnosis of arterial calcification

Yuri A. Trusov[1], Victoria S. Chupakhina[2], Adilya S. Nurkaeva[3], Natalia A. Yakovenko[4], Irina V. Ablenina[5], Roksana F. Latypova[5], Aleksandra P. Pitke[5], Anastasiya A. Yazovskih[3], Artem S. Ivanov[3], Darya S. Bogatyreva[6], Ulyana A. Popova[7], Azat F. Yuzlekbaev[3]

[1] Samara State Medical University, Samara, Russia;
[2] Rostov State Medical University, Rostov-on-Don, Russia;
[3] Bashkir State Medical University, Ufa, Russia;
[4] Sechenov First Moscow State Medical University, Moscow, Russia;
[5] Orenburg State Medical University, Orenburg, Russia;
[6] Russian National Research Medical University named after N.I. Pirogov, Moscow, Russia;
[7] Russian University of Medicine, Moscow, Russia

ABSTRACT

BACKGROUND: The incidence of circulatory system diseases in the Russian Federation has been steadily increasing during the last two decades, growing 2,047 times between 2000 and 2019. Vascular calcification involves the deposition of calcium salts in the artery wall, which leads to vascular wall remodeling. X-ray imaging is the gold standard for diagnosing of vascular calcification. However, because of the need to process an increasing amount of data in a shorter period of time, the number of diagnostic errors inevitably increases, and work efficiency inevitably decreases. The active development and introduction of artificial intelligence into clinical practice have created opportunities for specialists to address these issues.

AIM: To analyze the national and international literature on the use of artificial intelligence in the diagnosis of various vascular calcifications, summarize the prognostic value of vascular calcification, and evaluate aspects that prevent the diagnosis of vascular calcification without using artificial intelligence.

MATERIALS AND METHODS: A search was performed in PubMed, Web of Science, Google Scholar, and eLibrary. The search was conducted using the following keywords: artificial intelligence, machine learning, vascular calcification, and their analogues in Russian. The search covered the period from inception till July 2023.

RESULTS: The studies included in the review compared the diagnostic abilities of clinicians and artificial intelligence using the same images, with subsequent assessment of the accuracy, speed, and other parameters. The sites of vascular calcification varied, resulting in differences in their prognostic value.

CONCLUSION: Artificial intelligence has proven to be effective in the diagnosis of vascular calcification. In addition to improved accuracy and efficiency, the level of detail is superior to manual diagnosis methods. Artificial intelligence has advanced to the point that imaging specialists can automatically detect vascular calcification. Artificial intelligence can contribute to the successful development of X-ray imaging in the future.

Keywords: artificial intelligence; machine learning; vascular calcification; radiology; diagnostic imaging.

To cite this article:
Trusov YuA, Chupakhina VS, Nurkaeva AS, Yakovenko NA, Ablenina IV, Latypova RF, Pitke AP, Yazovskih AA, Ivanov AS, Bogatyreva DS, Popova UA, Yuzlekbaev AF. Use of artificial intelligence in the diagnosis of arterial calcification. *Digital Diagnostics.* 2024;5(1):85–100. DOI: https://doi.org/10.17816/DD623196

Submitted: 10.11.2023 **Accepted:** 10.01.2024 **Published online:** 29.01.2024

ECO•VECTOR

DOI: https://doi.org/10.17816/DD623196

人工智能在动脉钙化诊断中的应用

Yuri A. Trusov[1], Victoria S. Chupakhina[2], Adilya S. Nurkaeva[3], Natalia A. Yakovenko[4], Irina V. Ablenina[5], Roksana F. Latypova[5], Aleksandra P. Pitke[5], Anastasiya A. Yazovskih[3], Artem S. Ivanov[3], Darya S. Bogatyreva[6], Ulyana A. Popova[7], Azat F. Yuzlekbaev[3]

[1] Samara State Medical University, Samara, Russia;
[2] Rostov State Medical University, Rostov-on-Don, Russia;
[3] Bashkir State Medical University, Ufa, Russia;
[4] Sechenov First Moscow State Medical University, Moscow, Russia;
[5] Orenburg State Medical University, Orenburg, Russia;
[6] Russian National Research Medical University named after N.I. Pirogov, Moscow, Russia;
[7] Russian University of Medicine, Moscow, Russia

摘要

论证。近二十年来，俄罗斯联邦居民循环系统疾病的发病率持续上升。从2000年到2019年，此类疾病的数量增加了2.047倍。血管钙化过程包括钙盐在动脉壁的沉积，这导致血管壁重塑。放射性检查方法是诊断血管钙化的金标准。然而，随着数据量的增加和诊断时间的需要，工作效率不可避免地下降，人工智能的积极发展和应用于临床为专家解决这些问题提供了机会。

目的。本研究的目的是分析国内外关于使用人工智能诊断不同类型血管钙化的文献，同时，总结血管钙化的预后价值，并评估在不使用人工智能的情况下阻碍血管钙化诊断的方面。

材料与方法。在电子数据库PubMed、Web of Science、Google Scholar和eLibrary中搜索了相关出版物。搜索时使用了以下关键词："artificial intelligence"，"machine learning"，"vascular calcification"，"人工智能"、"机器学习"、"血管钙化"。检索时间为相关数据库建立至2023年7月。

结果。综述中包含的研究的主要方法是比较临床医生和人工智能使用相同图片的诊断能力，然后评估准确性、速度和其他指标。血管钙化发生的部位差异很大，这也是其预后价值不同的原因。

结论。事实证明，人工智能在诊断血管钙化方面表现出色。除了提高准确性和效率外，其细节处理能力也超过人工诊断方法。人工智能已经达到了帮助仪器诊断医生自动检测血管钙化的水平。未来，人工智能的能力可以促进放射学的有效发展。

关键词：人工智能；机器学习；血管钙化；放射学；诊断成像。

引用本文：
Trusov YuA, Chupakhina VS, Nurkaeva AS, Yakovenko NA, Ablenina IV, Latypova RF, Pitke AP, Yazovskih AA, Ivanov AS, Bogatyreva DS, Popova UA, Yuzlekbaev AF. 人工智能在动脉钙化诊断中的应用. *Digital Diagnostics.* 2024;5(1):85–100. DOI: https://doi.org/10.17816/DD623196

收到：10.11.2023 **接受：**10.01.2024 **发布日期：**29.01.2024

BACKGROUND

The incidence of circulatory system diseases in the Russian Federation has been steadily increasing in the last two decades, growing 2.047 times between 2000 and 2019 [1]. Vascular calcification involves the deposition of calcium salts in the arterial wall, which leads to vascular wall remodeling [2]. Intimal calcification is focal and associated with atherosclerosis, whereas medial calcification is diffuse and involved in the pathogenesis of conditions such as diabetes mellitus, peripheral artery disease, and chronic kidney disease [3]. X-ray imaging is the gold standard for diagnosing vascular calcifications [4]. However, because of increasing data and the need to reduce the time for diagnosing, work efficiency inevitably decreases [5]. These circumstances necessitate the search for innovative ways to improve the quality of work of imaging specialists.

The active development and introduction of artificial intelligence (AI) into clinical practice have helped specialists address these issues. According to the available literature, until recently, AI was used for X-ray diagnosis of five types of vascular calcifications: coronary artery calcification (CAC), thoracic aorta calcification (TAC), abdominal aorta calcification (AAC), carotid artery calcification (CaAC), and mammary artery calcification (MAC).

This study aimed to analyze the national and international literature on the use of AI in the diagnosis of various vascular calcifications, summarize the prognostic value of vascular calcification, and evaluate aspects that hinder the diagnosis of vascular calcification without using AI.

MATERIALS AND METHODS

A literature search was performed in PubMed, Web of Science, Google Scholar, and eLibrary. The search was conducted using the following keywords: artificial intelligence, machine learning, vascular calcification, and their equivalents in Russian. The search covered the period from database inception till July 2023. The authors reviewed independently the titles and abstracts of the articles and retrieved the full text of relevant publications. Moreover, the reference lists of relevant studies were reviewed.

RESULTS

The studies included in the review compared the diagnostic abilities of clinicians and AI using the same images and subsequently assessed the accuracy, speed, and other parameters.

The sites of vascular calcification vary greatly, resulting in differences in their prognostic value. Table 1 summarizes the prognostic value of vascular calcifications depending on the location.

Coronary artery calcification

The Framingham risk score is a tool for cardiovascular risk assessment, which includes the assessment of risk factors such as age, sex, and blood pressure [7]. However, a large-scale prospective study with 7 years of follow-up found that CACs detected using computed tomography (CT) can improve the risk prognosis obtained using the Framingham risk score alone. In a study with 7.6 years of follow-up, M.H. Criqui et al. demonstrated a good prognostic value of the assessment of CAC severity based on the vascular volume and density [8]. The risk of coronary artery disease (CAD) positively correlated with the CAC volume and negatively correlated with the CAC density [8].

The CAC severity was assessed by multiplying the density of calcified plaques by the area of calcification. The overall CAC was the sum of the results calculated at each level.

Table 1. Prognostic value of vascular calcifications depending on the location

Vascular calcification type	Prognostic value
Coronary artery calcification	– Marker of the severity of coronary artery atherosclerosis – Cardiovascular risk assessment according to the Framingham risk score – CAD predictor – Marker of chemotherapy-induced cardiotoxicity in patients with cancer
Thoracic aorta calcification	– Marker of increased CAD risk – Detection of an increased risk of ischemic stroke – Embolism risk detection
Abdominal aorta calcification	– Detection of obstructive CAD – Prediction of asymptomatic CAD – Marker of congestive heart failure
Carotid artery calcification	– Marker of atherosclerosis of the head and neck blood vessels – Stroke risk detection – Prediction of the risk of cerebrovascular adverse events in young people
Mammary artery calcification	– Detection of the risk of cardiovascular events in women – Association with chronic kidney disease, diabetes mellitus, and bone diseases

Note: CAD, coronary artery disease.

Table 2. Relationship between the severity of coronary artery calcification and the risk for adverse cardiovascular events

Coronary artery calcification assessment	Calcification risk
0	None
1–10	Low
11–100	Moderate
101–400	Moderate to high
>401	High

Generally, older patients represent a major risk group for CAD [1]. However, a 12.5-year study revealed an increased risk for CAD and death among individuals aged 32–46 years, even in cases of mild CAC [9]. These findings suggest that CAC-related information has a high prognostic value for detecting cardiovascular risk in nearly all age groups. Table 2 shows the relationship between CAC severity and risk for adverse cardiovascular events.

Thoracic aorta calcification

TAC is commonly found in patients with hypertension [10]. Furthermore, recurrent evidence has linked TAC to an increased risk for CAD and death [10, 11]. In a study of 2,618 patients, Y. Itani et al. found that TAC was efficient in ischemic stroke risk assessment [12]. In a study of patients with indications for cardiovascular surgery, R. Lee et al. found that preoperative CT screening for TAC can identify high-risk areas and reduce the risk of aortic embolism and stroke [13]. Thus, TAC severity can be used not only to predict the risk of cardiovascular accidents but also to detect cerebrovascular changes.

Abdominal aorta calcification

A study of 58 patients revealed that CT-AAC assessed AAC correlated with CAC severity. In turn, the absence of AAC made it possible to rule out CAD [14]. Moreover, AAC can be used as an additional tool for detecting asymptomatic CAD and an independent risk factor for congestive heart failure [15, 16]. AAC has a significant prognostic value for the skeletal system. Y.Z. Bagger et al. analyzed 2,662 healthy postmenopausal women and reported that AAC correlated with an increased risk of osteoporosis of the proximal femur [17]. Moreover, in a study of 5,994 men aged 65 years, P. Szulc et al. confirmed the correlation between AAC and an increased risk for femoral fracture in older men [18].

Carotid artery calcification

CaAC is an important predictor of cerebrovascular diseases [19]. Intracranial internal carotid artery calcification (ICAC) is an important marker of intracranial hypertension in patients of various ethnicities and strongly correlated with the risk for stroke [19–21]. A study of approximately 2,000 patients revealed that ICAC was common in young people. However, whether ICAC at a young age is similar to that at an older age is unclear and, therefore, may increase the risk of stroke later in life [22].

Mammary artery calcification

Z. Huang et al. analyzed 213 female patients and revealed that MAC correlated with CAC and CAD severity [23]. EV Bochkareva et al. analyzed 4,274 digital mammograms of women aged 40–93 years and found a significant and strong correlation between age and MAC [24]. E.V. Bochkareva et al. also demonstrated that MAC was associated with chronic kidney disease, diabetes mellitus, cerebrovascular diseases, and low bone mineral density [25–27]. Unfortunately, female patients are often unaware of cardiovascular diseases, which pose one of the most serious threats to women's health [28]. Thus, considering the availability of MAC assessment and its diagnostic value in assessing cardiovascular risk in women, imaging specialists should pay close attention to this issue.

Difficulties in imaging diagnosis of vascular calcifications

An analysis of the evolution of X-ray diagnostic services in Russia in 2014–2019 showed that the number of medical images is increasing annually, and imaging specialists have to interpret images every 3–4 s during an 8-h working day [29]. A study of the physical condition of 40 imaging specialists before and after a working day revealed that after working for 1 day, their ability to concentrate decreases dramatically, whereas symptoms of asthenopathy increase [30]. According to available data, 75% of claims concerning the low quality of medical care provided by imaging specialists are related to diagnostic errors [31].

Accurate assessment of the severity of vascular calcifications is difficult. The shape of the calcified foci is variable, and deviations are common. For example, various modifications of CT scans have been used to diagnose CAC [32]; however, they require additional equipment, increasing the economic burden on healthcare facilities and the patient's radiation exposure (which can be reduced if the diagnosis is made by standard methods). Moreover, radiologists do not always assess vascular calcifications detected on CT scans, which could be used for indirect assessment of coronary calcification. Nonetheless, the gold standard is CT with cardiac synchronization and a specified examination area (field of view) [33, 34].

The role of artificial intelligence in the assessment of arterial calcification

CACs

The first automatic assessment of CAC severity using AI was performed in 2007. For each candidate, 64 features were created, and nearest-neighbor clustering was applied. This metric algorithm for automatic object classification or regression had an accuracy of 73.8% [35]. Since then, various approaches to feature development, including spatial and geometric characteristics, have been actively studied [36–38]. Because selecting objects on noncontrast CT scans is technically challenging, recording information from CT scans with the determination of coronary calcification has become a common strategy [39–41]. To assess coronary calcification, electrocardiographic (ECG) synchronization is commonly used to capture images in the diastolic phase, followed by image reconstruction by stitching. A support vector machine-based algorithm achieved a sensitivity of 98.9% and a prognostic value of 94.8% [42]. Such machine-learning (ML) algorithms were actively used until 2016; however, their use was challenging because of the need for manual control [42].

To further improve efficacy, an artificial neural network (ANN) with deep learning (DL) function was selected as the primary option [43]. DL initially demonstrated low efficacy; however, continuous improvement of the ANN allowed for increased efficacy and accurate, automatic scoring [44–51].

In a study on CAC assessment, B.D. de Vos et al. discovered that the results obtained using DL were nearly identical to those calculated manually. The Agatston score (gold standard of CT calcium scoring in clinical practice) was determined in <0.3 s [52].

The U-Net algorithm is an extension of the ANN intended for more efficient learning requiring fewer resources [53]. N. Gogin et al. confirmed the efficacy of DL based on the U-Net architecture, which proved to be extremely close to the performance of other algorithms [46]. U-Net classified the risks correctly in 86% of cases. Notably, U-Net allows uploading images directly without losing pixel information [49].

CT with cardiac synchronization is less widely used globally than CT without ECG [54]. If the reliability of CAC information obtained without ECG increases, the number of CT scans can be reduced, thus decreasing economic expenditures and radiation exposure [55]. Numerous interferences and artifacts significantly lower the accuracy of manual CAC assessment using CT without ECG [56].

AI has played a significant role in CAC diagnosis using CT without ECG. More than a decade ago, I. Isgum et al. found that ML algorithms ensure the Agatston score assessment with an accuracy of 82.2% when using low-dose chest CT [57]. Many researchers have attempted to level out interference and artifacts and reduce the effect of noncalcified components (stents) on the diagnosis. Their developed DL algorithms allowed for increasing the diagnostic value of low-quality images [58, 59]. According to Z. Sun et al., DL algorithms improved the signal-to-noise ratio of low-dose CT by 27.7% and increased the specificity of CAC detection by 41% by eliminating artifacts [60]. Notably, the rate of correct interpretation of CT without ECG was only 70%; however, the correlation coefficient between the results obtained using AI and manual analysis was 0.923 [56].

B. Yacoub et al. revealed that the sensitivity, specificity, and area under the curve (AUC) of CAC detection on noncontrasted chest CT scans using AI were superior to those of manual assessment. This suggests that AI can be superior to human assessment when analyzing CT findings without ECG [34]. In one study, the efficacy of AI in analyzing CT findings without ECG was confirmed at four study sites. All study samples showed high sensitivity and good prognostic value, which increases the quality of the results [61]. The use of AI in diagnosing CAC based on CT findings without ECG is currently considered a reliable method of assessing data.

Notably, researchers have begun to use AI capabilities to diagnose CAC using other devices, such as when assessing chest X-ray images [62]. P.I. Kamel et al. developed a classification of total calcium parameters on chest X-ray images using deep ANN, making it possible to reduce the need for CT in some patients [63]. In this study, the AUC reached 0.73 and 0.7 in the anteroposterior and lateral images, respectively, when detecting CAC. Moreover, a study proposed a neural network that could analyze invasive coronary angiography images within seconds and detect CAC with a F1 of 0.802 [64].

Thoracic aorta calcification

In contrast to CAC, the accuracy of TAC detection on CT scans does not depend on the heart contraction intensity [65]. For example, in a study by I. Isgum et al., the TAC detection rate was 97.9% when using the k-nearest neighbor method, which correlated with manual findings [65]. In recent years, DL made it possible to detect CAC and TAC simultaneously [66]. Similarly, SGM van Velzen et al. used these methods with various CT modalities (including CT with the determination of coronary calcium, low-dose chest CT, and positron-emission CT), with an intraclass correlation coefficient of 0.68–0.98 [67]. Notably, a sensitivity of 98.4% was observed in a study using a convolutional neural network (CNN) for TAC detection, which made it possible not only to detect TAC in the ascending and descending aorta and the aortic arch but also to assess the risk level [68]. Thus, radiologists now routinely employ AI to automatically assess CAC and TAC.

Abdominal aorta calcification

DL advancements made it possible to automatically detect AAC, which was confirmed in two studies [69, 70]. Dual-energy X-ray absorptiometry is a diagnostic tool that assesses the risk for fractures. The increasingly wide use of this method suggests the possibility of automating AAC assessment; however, because of technical difficulties, it is not routinely used for AAC detection. S. Reid et al. classified AAC using a densitometry-based CNN, with a high degree of agreement with manually obtained findings; the Kappa index was 0.71 [69]. CT provides obvious advantages over dual-energy X-ray absorptiometry for the qualitative assessment of aortic calcification. P.M. Graffy et al. effectively implemented automatic detection of AAC using abdominal CT in >9,000 patients; the authors attributed their success to the use of mask region-based CNN [70]. This study also assessed the prevalence of AAC based on quantitative data, which supports the importance of AI.

In summary, AI can be used to automatically quantify AAC; however, available data are extremely limited.

Carotid artery calcification

CT in combination with AI can be used to detect calcification of both extracranial and intracranial internal carotid arteries [71, 72, 73]. G. Bortsova et al. used four DL networks with a structure similar to that of U-Net. The accuracy of ICAC detection was higher than manual assessment, with a sensitivity of 83.8% and a prognostic value of 88% [73]. Manual assessment of CIC necessitates meticulous analysis; moreover, it is prone to errors, with similar probability (e.g., bone calcification). Given this, the excellent accuracy of DL is of great importance.

Magnetic resonance imaging (MRI) can detect the most significant differences between CaAC and other vascular calcifications [71]. In earlier studies, MRI showed low accuracy in detecting calcifications [71]. However, the use of simultaneous noncontrast angiography and intraplaque hemorrhage (SNAP) has improved the ability to detect calcifications using MRI. SNAP inverts all signals by pulse inversion, followed by T1-weighted inversion recovery and a proton density-weighted control scan with dual gradient echo, providing high-quality images of the cranial and cervical spine arteries [74]. Although SNAP effectively detects calcification, it is prone to motion artifacts and has a long acquisition time. Goal-SNAP and quick SNAP can be used to address this issue [75, 76]. In this study, ML algorithms such as random forest are similar to ANNs in terms of calcification detection; however, DL may be more effective in segmenting vascular components, which requires further research.

Mammary artery calcification

MAC is visualized on mammograms; however, calcifications have extremely diverse manifestations. They can be bifurcated, overlapping, or truncated, with varying intensities [77]. As a result, MAC is difficult to quantify manually because of its heterogeneous presentations.

Mammography is an X-ray diagnosis method used for screening and intended for breast cancer detection. It has been included in the scope of preventive medical examination since 2012. In line with the regulations of the Ministry of Health of the Russian Federation, the frequency of this study increases annually.

Several authors have considered the use of DL in this context. Mammograms were divided into sections because the amount of data was too large for direct entry [53]. The 12-layer CNN defines MAC detection as a second-order task [28]. Although it successfully distinguished the presence and absence of MAC, the accuracy of the quantitative assessment was insufficient [28]. Furthermore, data analysis and processing were time-consuming because of the need to process each segment separately. Subsequently, researchers improved the CNN considering the described drawbacks, suggesting the use of a simple contextual U-Net (SCU-Net) and a dense U-Net (DU-Net) [33, 53]. SCU-Net is a simpler version of U-Net that addresses MAC accounting for <1% of the images, resulting in a significant amount of data and preventing the system's efficient training. DU-Net eliminates this problem by considerably improving the efficacy of the CNN, with an accuracy of 91.47% and a sensitivity of 91.22% [53].

In summary, DL used for automatic MAC detection has advanced considerably; however, no public dataset is available for the unification in this field, which necessitates further studies.

DISCUSSION

AI can facilitate and improve the work of imaging specialists regarding vascular calcification by performing preliminary screening and enhancing data processing efficacy.

The accuracy of AI in X-ray diagnosis was determined by AI algorithms and image characteristics. The efficacy of ML and DL algorithms has improved significantly, increasing the diagnostic value of these techniques. As imaging technology evolves, image quality improves, which intensifies the efficiency of diagnosis. AI capabilities depend on the high quality of databases required for training, which can also be useful in creating public databases or testing platforms. Thus, engineers and physicians should work to improve AI diagnostic capabilities based on AI algorithms and image quality.

Although AI has demonstrated good results in five types of vascular calcifications, it also has potential diagnostic value in renal artery calcification, a condition with confirmed prognostic value for hypertension and proteinuria [79]. Moreover, the number of studies on AAC and CaAC is modest, which increases interest in their research. Table 3 provides a comparison of the efficacy of AI in the diagnosis of each type of vascular calcification.

CONCLUSION

Artificial intelligence has proven to be effective in the diagnosis of vascular calcifications. In addition to improved accuracy and efficiency, its level of detail is superior to that of manual diagnosis methods. AI has advanced to the point that imaging specialists can automatically detect vascular calcification. Artificial intelligence can contribute to the successful development of X-ray imaging in the future.

ADDITIONAL INFORMATION

Funding source. This study was not supported by any external sources of funding.

Competing interests. The authors declare that they have no competing interests.

Table 3. Comparison of the efficacy of AI in the diagnosis of five types of vascular calcification

Vascular calcification type	Number of studies	Use of X-ray imaging	Use of CT	Use of MRI	Use of DL
Coronary artery calcification	Large	Yes	Yes	No	Pixel-based and end-to-end DL in combination with GAN reduces the level of noise and artifacts for a reliable automatic assessment of CAC and interpretation of the results
Thoracic aorta calcification	Moderate	No	Yes	No	DL ensures the automatic detection of TAC and CaAC and enables the assessment of the findings in various portions of the aorta
Abdominal aorta calcification	Small, more studies are required	Yes	Yes	No	DL techniques such as the mask region-CNN enable accurate qualitative assessment of AAC when using DEXA and CT
Carotid artery calcification	Small, more studies are required	No	Yes	Yes	The efficacy of DL is similar to that of ML and superior to human performance, with the added possibility of using MRI
Mammary artery calcification	Moderate	Yes	No	No	U-Net, SCU-Net, DU-Net, and other improved DL systems facilitate MAC detection

Note: AAC, abdominal aorta calcification; CAC, coronary artery calcification; CT, computed tomography DEXA, dual-energy X-ray absorptiometry; DL, deep learning; DU-Net, dense U-Net: GAN, generative adversarial network; MAC, mammary artery calcification; ML, machine learning; MRI, magnetic resonance imaging; Mask region-CNN, mask region-based convolutional neural network; SCU-Net, simple contextual U-Net; TAC, thoracic aorta calcification.

Authors' contribution. All authors made a substantial contribution to the conception of the work, acquisition, analysis, interpretation of data for the work, drafting and revising the work, final approval of the version to be published and agree to be accountable for all aspects of the work. Yu.A. Trusov, V.S. Chupakhina — development of the concept and design of the study, scientific revision of the manuscript; A.S. Nurkaeva — data analysis and search, writing the manuscript; N.A. Yakovenko — data analysis, writing the manuscript; I.V. Ablenina — data analysis, editing the text of the manuscript; R.F. Latypova — data analysis, verification and approval of the text; A.P. Pitke — writing a manuscript, obtaining factual data; A.A. Yazovskikh — editing the text of the article, analyzing data; A.S. Ivanov — obtaining data, writing the text of the article; D.S. Bogatyreva — approval of the final version of the manuscript, editing of the text of the article; U.A. Popova — data analysis, participation in the writing of the article; A.F. Yuzlekbayev — analysis and data acquisition.

REFERENCES

1. Sharapova OV, Kicha DI, Gerasimova LI, et al. Map analysis of morbidity and mortality from blood circulatory system diseases of the population of the Russian federation (2010-2019). *Complex Issues of Cardiovascular Diseases.* 2022;11(1):56–68. EDN: ZUQVNA doi: 10.17802/2306-1278-2022-11-1-56-68

2. Mal'kov OA, Govorukhina AA, Burykin YuG, Afineevskaya AYu. The Role of Calcification in the Pathogenesis of Inflammatory Reaction in the Arterial Wall (Exemplified by the Vessels of the Neck and Head in Adults). *Journal of Medical and Biological Research.* 2021;9(4):435–443. EDN: FTSKDS doi: 10.37482/2687-1491-Z081

3. Archakova TV, Nedosugova LV. Factors of vascular calcification in patients with type 2 diabetes mellitus on long-term dialysis. *Diabetes mellitus*. 2020;23(2):125–131. EDN: KPXIVL doi: 10.14341/DM10145

4. Mori H, Torii S, Kutyna M, et al. Coronary Artery Calcification and its Progression: What Does it Really Mean? *JACC Cardiovasc Imaging.* 2018;11(1):127–142. doi: 10.1016/j.jcmg.2017.10.012

5. Yeo KK. Artificial intelligence in cardiology: did it take off? *Russian Journal for Personalized Medicine.* 2022;2(6):16–22. EDN: UIENOT doi: 10.18705/2782-3806-2022-2-6-16-22

6. Karpov OE, Andrikov DA, Maksimenko VA, Hramov AE. Explainable artificial intelligence for medicine. *Medical Doctor and IT.* 2022;(2):4–11. EDN: DTCAWX doi: 10.25881/18110193_2022_2_4

7. Greenland P, LaBree L, Azen SP, et al. Coronary artery calcium score combined with Framingham score for risk prediction in asymptomatic individuals. *JAMA.* 2004;291(2):210–215. doi: 10.1001/jama.291.2.210

8. Criqui MH, Denenberg JO, Ix JH, et al. Calcium density of coronary artery plaque and risk of incident cardiovascular events. *JAMA.* 2014;311(3):271–278. doi: 10.1001/jama.2013.282535

9. Carr JJ, Jacobs DR Jr, Terry JG, et al. Association of Coronary Artery Calcium in Adults Aged 32 to 46 Years With Incident Coronary Heart Disease and Death. *JAMA Cardiol.* 2017;2(4):391–399. doi: 10.1001/jamacardio.2016.5493

10. Khalikov AA, Kuznetsov KO, Iskuzhina LR, Khalikova LV. Forensic aspects of sudden autopsy-negative cardiac death. *Sudebno-Meditsinskaya Ekspertisa.* 2021;64(3):59–63. doi: 10.17116/sudmed20216403159

11. Eisen A, Tenenbaum A, Koren-Morag N, et al. Calcification of the thoracic aorta as detected by spiral computed tomography among stable angina pectoris patients: association with cardiovascular events and death. *Circulation.* 2008;118(13):1328–1334. doi: 10.1161/CIRCULATIONAHA.107.712141

12. Itani Y, Watanabe S, Masuda Y. Relationship between aortic calcification and stroke in a mass screening program using a mobile helical computed tomography unit. *Circ J.* 2006;70(6):733–736. doi: 10.1253/circj.70.733

13. Lee R, Matsutani N, Polimenakos AC, et al. Preoperative noncontrast chest computed tomography identifies potential aortic emboli. *Ann Thorac Surg.* 2007;84(1):38–42. doi: 10.1016/j.athoracsur.2007.03.025

14. Zweig BM, Sheth M, Simpson S, Al-Mallah MH. Association of abdominal aortic calcium with coronary artery calcium and obstructive coronary artery disease: a pilot study. *Int J Cardiovasc Imaging.* 2012;28(2):399–404. doi: 10.1007/s10554-011-9818-1

15. An C, Lee HJ, Lee HS, et al. CT-based abdominal aortic calcification score as a surrogate marker for predicting the presence of asymptomatic coronary artery disease. *Eur Radiol*. 2014;24(10):2491–2498. doi: 10.1007/s00330-014-3298-3

16. Melnikov MV, Zelinskiy VA, Zhorina AS, Chuglova DA. An abdominal aortic calcification in peripheral arterial occlusive disease: risk factors and markers. *Journal of atherosclerosis and dyslipidemias*. 2014;(3):33–38. EDN: SISNRZ

17. Bagger YZ, Tankó LB, Alexandersen P, et al. Radiographic measure of aorta calcification is a site-specific predictor of bone loss and fracture risk at the hip. *J Intern Med.* 2006;259(6):598–605. doi: 10.1111/j.1365-2796.2006.01640.x

18. Szulc P, Blackwell T, Schousboe JT, et al. High hip fracture risk in men with severe aortic calcification: MrOS study. *J Bone Miner Res.* 2014;29(4):968–975. doi: 10.1002/jbmr.2085

19. Lobanova NI, Chicherina EN, Malchikova SV, Maksimchuk-Kolobova NS. Fluid shear stress on the endothelium of the carotid artery wall and coronary artery calcinosis in patients with arterial hypertension. *South Russian Journal of Therapeutic Practice.* 2022;3(3):60–67. EDN: QWCOCH doi: 10.21886/2712-8156-2022-3-3-60-67

20. Kim JT, Yoo SH, Kwon JH, et al. Subtyping of ischemic stroke based on vascular imaging: analysis of 1,167 acute, consecutive patients. *J Clin Neurol.* 2006;2(4):225–230. doi: 10.3988/jcn.2006.2.4.225

21. Wong LK. Global burden of intracranial atherosclerosis. *Int J Stroke.* 2006;1(3):158–159. doi: 10.1111/j.1747-4949.2006.00045.x

22. Kockelkoren R, De Vis JB, de Jong PA, et al. Intracranial Carotid Artery Calcification From Infancy to Old Age. *J Am Coll Cardiol.* 2018;72(5):582–584. doi: 10.1016/j.jacc.2018.05.021

23. Huang Z, Xiao J, Xie Y, et al. The correlation of deep learning-based CAD-RADS evaluated by coronary computed tomography angiography with breast arterial calcification on mammography. *Sci Rep.* 2020;10(1):11532. doi: 10.1038/s41598-020-68378-4

24. Bochkareva EV, Butina EK, Bayramkulova EKh, et al. Prevalence and Severity of Breast Arterial Calcification on Routine Mammography. *Rational Pharmacotherapy in Cardiology.* 2022;18(5):530–535. EDN: HUFTZE doi: 10.20996/1819-6446-2022-09-01

25. Bochkareva EV, Butina EK, Bayramkulova NKh, Drapkina OM. Mammary artery calcinosis and diabetes mellitus: case report and brief literature review. *Profilakticheskaya Meditsina.* 2021;24(9):97–101. EDN: QPQDLT doi: 10.17116/profmed20212409197

26. Bochkareva EV, Butina EK, Savin AS, et al. Breast arteries calcification: a potential surrogate marker for cerebrovascular disease. *Profilakticheskaya Meditsina*. 2020;23(5):164–169. EDN: IRHLDZ doi: 10.17116/profmed202023051164

27. Bochkareva EV, Butina EK, Savin AS, Drapkina OM. Breast artery calcification and osteoporosis in postmenopausal woman: a case report and opinion on the problem. *Cardiovascular Therapy and Prevention*. 2020;19(4):2574. EDN: RTDDQG doi: 10.15829/1728-8800-2020-2574

28. Wang J, Ding H, Bidgoli FA, et al. Detecting Cardiovascular Disease from Mammograms With Deep Learning. *IEEE Trans Med Imaging.* 2017;36(5):1172–1181. doi: 10.1109/TMI.2017.2655486

29. Golubev NA, Ogryzko EV, Tyurina EM, Shelepova EA, Shelekhov PV. Features of the development of the radiation diagnostics service in the Russian Federation for 2014–2019. *Current problems of health care and medical statistics.* 2021;(2):356–376. EDN: EHSADW doi: 10.24412/2312-2935-2021-2-356-376

30. Krupinski EA, Berbaum KS, Caldwell RT, et al. Long radiology workdays reduce detection and accommodation accuracy. *J Am Coll Radiol.* 2010;7(9):698–704. doi: 10.1016/j.jacr.2010.03.004

31. Lee CS, Nagy PG, Weaver SJ, Newman-Toker DE. Cognitive and system factors contributing to diagnostic errors in radiology. *AJR Am J Roentgenol.* 2013;201(3):611–617. doi: 10.2214/AJR.12.10375

32. Nikolaev AE, Shapiev AN, Blokhin IA, et al. New approaches for assessing coronary changes in multi-layer spiral computed tomography. *Russian Journal of Cardiology*. 2019;(12):124–130. EDN: VHYAYK doi: 10.15829/1560-4071-2019-12-124-130

33. Guo X, O'Neill WC, Vey B, et al. SCU-Net: A deep learning method for segmentation and quantification of breast arterial calcifications on mammograms. *Med Phys.* 2021;48(10):5851–5861. doi: 10.1002/mp.15017

34. Yacoub B, Kabakus IM, Schoepf UJ, et al. Performance of an Artificial Intelligence-Based Platform Against Clinical Radiology Reports for the Evaluation of Noncontrast Chest CT. *Acad Radiol.* 2022;29(2):108–117. doi: 10.1016/j.acra.2021.02.007

35. Isgum I, Rutten A, Prokop M, van Ginneken B. Detection of coronary calcifications from computed tomography scans for automated risk assessment of coronary artery disease. *Med Phys.* 2007;34(4):1450–1461. doi: 10.1118/1.2710548

36. Kurkure U, Chittajallu DR, Brunner G, et al. A supervised classification-based method for coronary calcium detection in non-contrast CT. *Int J Cardiovasc Imaging.* 2010;26(7):817–828. doi: 10.1007/s10554-010-9607-2

37. Brunner G, Chittajallu DR, Kurkure U, Kakadiaris IA. Toward the automatic detection of coronary artery calcification in non-contrast computed tomography data. *Int J Cardiovasc Imaging.* 2010;26(7):829–838. doi: 10.1007/s10554-010-9608-1

38. Brunner G, Kurkure U, Chittajallu DR, et al. Toward unsupervised classification of calcified arterial lesions. *Med Image Comput Comput Assist Interv.* 2008;11(1):144-152. doi: 10.1007/978-3-540-85988-8_18

39. Takx RA, de Jong PA, Leiner T, et al. Automated coronary artery calcification scoring in non-gated chest CT: agreement and reliability. *PLoS One.* 2014;9(3):e91239. doi: 10.1371/journal.pone.0091239

40. Wolterink JM, Leiner T, Takx RA, et al. Automatic Coronary Calcium Scoring in Non-Contrast-Enhanced ECG-Triggered Cardiac CT With Ambiguity Detection. *IEEE Trans Med Imaging.* 2015;34(9):1867–1878. doi: 10.1109/TMI.2015.2412651

41. Saur SC, Alkadhi H, Desbiolles L, et al. Automatic detection of calcified coronary plaques in computed tomography data sets. *Med Image Comput Comput Assist Interv.* 2008;11(1):170–177. doi: 10.1007/978-3-540-85988-8_21

42. Yang G, Chen Y, Ning X, et al. Automatic coronary calcium scoring using noncontrast and contrast CT images. *Med Phys.* 2016;43(5):2174. doi: 10.1118/1.4945045

43. Jiang B, Guo N, Ge Y, et al. Development and application of artificial intelligence in cardiac imaging. *Br J Radiol.* 2020;93(1113):20190812. doi: 10.1259/bjr.20190812

44. Shahzad R, van Walsum T, Schaap M, et al. Vessel specific coronary artery calcium scoring: an automatic system. *Acad Radiol.* 2013;20(1):1–9. doi: 10.1016/j.acra.2012.07.018

45. Cano-Espinosa C, González G, Washko GR, et al. Automated Agatston Score Computation in non-ECG Gated CT Scans Using Deep Learning. *Proc SPIE Int Soc Opt Eng.* 2018;10574:105742K. doi: 10.1117/12.2293681

46. Gogin N, Viti M, Nicodème L, et al. Automatic coronary artery calcium scoring from unenhanced-ECG-gated CT using deep learning. *Diagn Interv Imaging.* 2021;102(11):683–690. doi: 10.1016/j.diii.2021.05.004

47. Wolterink JM, Leiner T, de Vos BD, et al. Automatic coronary artery calcium scoring in cardiac CT angiography using paired convolutional neural networks. *Med Image Anal.* 2016;34:123–136. doi: 10.1016/j.media.2016.04.004

48. Wang W, Wang H, Chen Q, et al. Coronary artery calcium score quantification using a deep-learning algorithm. *Clin Radiol.* 2020;75(3):237.e11–237.e16. doi: 10.1016/j.crad.2019.10.012

49. Singh G, Al'Aref SJ, Lee BC, et al. End-to-End, Pixel-Wise Vessel-Specific Coronary and Aortic Calcium Detection and Scoring Using Deep Learning. *Diagnostics (Basel).* 2021;11(2):215. doi: 10.3390/diagnostics11020215

50. Martin SS, van Assen M, Rapaka S, et al. Evaluation of a Deep Learning-Based Automated CT Coronary Artery Calcium Scoring Algorithm. *JACC Cardiovasc Imaging.* 2020;13(1):524–526. doi: 10.1016/j.jcmg.2019.09.015

51. Zhang N, Yang G, Zhang W, et al. Fully automatic framework for comprehensive coronary artery calcium scores analysis on non-contrast cardiac-gated CT scan: Total and vessel-specific quantifications. *Eur J Radiol.* 2021;134:109420. doi: 10.1016/j.ejrad.2020.109420

52. de Vos BD, Wolterink JM, Leiner T, et al. Direct Automatic Coronary Calcium Scoring in Cardiac and Chest CT. I*EEE Trans Med Imaging.* 2019;38(9):2127–2138. doi: 10.1109/TMI.2019.2899534

53. AlGhamdi M, Abdel-Mottaleb M, Collado-Mesa F. DU-Net: Convolutional Network for the Detection of Arterial Calcifications in Mammograms. *IEEE Trans Med Imaging.* 2020;39(10):3240–3249. doi: 10.1109/TMI.2020.2989737

54. Nikolaev AE, Korkunova OA, Khutornoy IV, et al. Comparability of coronary risk assessment methods with chest ultra-LDCT and CT coronography with ECG synchronization. *Medical Visualization.* 2021;25(4):75–92. EDN: CMSGAX doi: 10.24835/1607-0763-1047

55. van Assen M, Martin SS, Varga-Szemes A, et al. Automatic coronary calcium scoring in chest CT using a deep neural network in direct comparison with non-contrast cardiac CT: A validation study. *Eur J Radiol.* 2021;134:109428. doi: 10.1016/j.ejrad.2020.109428

56. Nikolaev AE, Shapiev AN, Blokhin IA. Standardization of coronary artery calcification assessment on contrast-free computed tomograms without ECG synchronization. *Radiology Study.* 2020;3(2):45–52. EDN: VVGXBI

57. Isgum I, Prokop M, Niemeijer M, et al. Automatic coronary calcium scoring in low-dose chest computed tomography. *IEEE Trans Med Imaging.* 2012;31(12):2322–2334. doi: 10.1109/TMI.2012.2216889

58. Wolterink JM, Leiner T, Viergever MA, Isgum I. Generative Adversarial Networks for Noise Reduction in Low-Dose CT. *IEEE Trans Med Imaging.* 2017;36(12):2536–2545. doi: 10.1109/TMI.2017.2708987

59. Klug M, Shemesh J, Green M, et al. A deep-learning method for the denoising of ultra-low dose chest CT in coronary artery calcium score evaluation. *Clin Radiol.* 2022;77(7):509–517. doi: 10.1016/j.crad.2022.03.005

60. Sun Z, Ng CKC. Artificial Intelligence (Enhanced Super-Resolution Generative Adversarial Network) for Calcium Deblooming in Coronary Computed Tomography Angiography: A Feasibility Study. *Diagnostics (Basel).* 2022;12(4):991. doi: 10.3390/diagnostics12040991

61. Eng D, Chute C, Khandwala N, et al. Automated coronary calcium scoring using deep learning with multicenter external validation. *NPJ Digit Med.* 2021;4(1):88. doi: 10.1038/s41746-021-00460-1

62. Morozov SP, Kokina DYu, Pavlov NA, et al. Clinical aspects of using artificial intelligence for the interpretation of chest X-rays. *Tuberculosis and Lung Diseases.* 2021;99(4):58–64. doi: 10.21292/2075-1230-2021-99-4-58-64

63. Kamel PI, Yi PH, Sair HI, Lin CT. Prediction of Coronary Artery Calcium and Cardiovascular Risk on Chest Radiographs Using Deep Learning. *Radiol Cardiothorac Imaging.* 2021;3(3):e200486. doi: 10.1148/ryct.2021200486

64. Du T, Xie L, Zhang H, et al. Training and validation of a deep learning architecture for the automatic analysis of coronary angiography. *EuroIntervention.* 2021;17(1):32–40. doi: 10.4244/EIJ-D-20-00570

65. Isgum I, Rutten A, Prokop M, et al. Automated aortic calcium scoring on low-dose chest computed tomography. *Med Phys.* 2010;37(2):714–723. doi: 10.1118/1.3284211

66. de Vos BD, Lessmann N, de Jong PA, Išgum I. Deep Learning-Quantified Calcium Scores for Automatic Cardiovascular Mortality Prediction at Lung Screening Low-Dose CT. *Radiol Cardiothorac Imaging.* 2021;3(2):e190219. doi: 10.1148/ryct.2021190219

67. van Velzen SGM, Lessmann N, Velthuis BK, et al. Deep Learning for Automatic Calcium Scoring in CT: Validation Using Multiple Cardiac CT and Chest CT Protocols. *Radiology.* 2020;295(1):66–79. doi: 10.1148/radiol.2020191621

68. Guilenea FN, Casciaro ME, Pascaner AF, et al. Thoracic Aorta Calcium Detection and Quantification Using Convolutional Neural Networks in a Large Cohort of Intermediate-Risk Patients. *Tomography.* 2021;7(4):636–649. doi: 10.3390/tomography7040054

69. Reid S, Schousboe JT, Kimelman D, et al. Machine learning for automated abdominal aortic calcification scoring of DXA vertebral fracture assessment images: A pilot study. *Bone.* 2021;148:115943. doi: 10.1016/j.bone.2021.115943

70. Graffy PM, Liu J, O'Connor S, et al. Automated segmentation and quantification of aortic calcification at abdominal CT: application of a deep learning-based algorithm to a longitudinal screening cohort. *Abdom Radiol (NY).* 2019;44(8):2921–2928. doi: 10.1007/s00261-019-02014-2

71. van Engelen A, Niessen WJ, Klein S, et al. Atherosclerotic plaque component segmentation in combined carotid MRI and CTA data incorporating class label uncertainty. *PLoS One.* 2014;9(4):e94840. doi: 10.1371/journal.pone.0094840

72. Onishchenko PS, Klyshnikov KYu, Ovcharenko EA. Artificial neural networks in cardiology: analysis of graphic data. *Bulletin of Siberian Medicine.* 2021;20(4):193–204. EDN: XVBERA doi: 10.20538/1682-0363-2021-4-193-204

73. Bortsova G, Bos D, Dubost F, et al. Automated Segmentation and Volume Measurement of Intracranial Internal Carotid Artery Calcification at Noncontrast CT. *Radiol Artif Intell.* 2021;3(5):e200226. doi: 10.1148/ryai.2021200226

74. Li D, Qiao H, Han Y, et al. Histological validation of simultaneous non-contrast angiography and intraplaque hemorrhage imaging (SNAP) for characterizing carotid intraplaque hemorrhage. *Eur Radiol.* 2021;31(5):3106–3115. doi: 10.1007/s00330-020-07352-0

75. Chen S, Ning J, Zhao X, et al. Fast simultaneous noncontrast angiography and intraplaque hemorrhage (fSNAP) sequence for carotid artery imaging. *Magn Reson Med.* 2017;77(2):753–758. doi: 10.1002/mrm.26111

76. Qi H, Sun J, Qiao H, et al. Carotid Intraplaque Hemorrhage Imaging with Quantitative Vessel Wall T1 Mapping: Technical Development and Initial Experience. *Radiology.* 2018;287(1):276–284. doi: 10.1148/radiol.2017170526

77. Cheng JZ, Cole EB, Pisano ED, Shen D. Detection of arterial calcification in mammograms by random walks. *Inf Process Med Imaging.* 2009;21:713–724. doi: 10.1007/978-3-642-02498-6_59

78. Lomakov SYu. Volumes of mammographic studies in modern conditions of providing preventive measures. *Profilakticheskaya Meditsina*. 2020;23(4):41–44. EDN: OUUINQ doi: 10.17116/profmed20202304141

79. Roseman DA, Hwang SJ, Manders ES, et al. Renal artery calcium, cardiovascular risk factors, and indexes of renal function. *Am J Cardiol.* 2014;113(1):156–161. doi: 10.1016/j.amjcard.2013.09.036

СПИСОК ЛИТЕРАТУРЫ

1. Шарапова О.В., Кича Д.И., Герасимова Л.И., и др. Картографический анализ показателей заболеваемости и смертности от болезней системы кровообращения населения Российской Федерации (2010-2019 гг.) // Комплексные проблемы сердечно-сосудистых заболеваний. 2022. Т. 11, № 1. С. 56–68. EDN: ZUQVNA doi: 10.17802/2306-1278-2022-11-1-56-68

2. Мальков О.А., Говорухина А.А., Бурыкин Ю.Г., Афинеевская А.Ю. Роль кальцификации в патогенезе воспалительной реакции артериальной стенки (на примере сосудов шеи и головы взрослого населения) // Журнал медико-биологических исследований. 2021. Т. 9, № 4. С. 435–443. EDN: FTSKDS doi: 10.37482/2687-1491-Z081

3. Арчакова Т.В., Недосугова Л.В. Факторы кальцификации сосудов у пациентов с сахарным диабетом 2 типа, получающих лечение программным гемодиализом // Сахарный диабет. 2020. Т. 23, № 2. С. 125–131. EDN: KPXIVL doi: 10.14341/DM10145

4. Mori H, Torii S, Kutyna M, et al. Coronary Artery Calcification and its Progression: What Does it Really Mean? // JACC Cardiovasc Imaging. 2018. Vol. 11, N 1. P. 127–142. doi: 10.1016/j.jcmg.2017.10.012

5. Йео К.К. Искусственный интеллект в кардиологии: сработал ли он? // Российский журнал персонализированной медицины. 2022. Т. 2, № 6. С. 16–22. EDN: UIENOT doi: 10.18705/2782-3806-2022-2-6-16-22

6. Карпов О.Э., Андриков Д.А., Максименко В.А., Храмов А.Е. Прозрачный искусственный интеллект для медицины // Врач и информационные технологии. 2022. № 2. С. 4–11. EDN: DTCAWX doi: 10.25881/18110193_2022_2_4

7. Greenland P., LaBree L., Azen S.P., et al. Coronary artery calcium score combined with Framingham score for risk prediction in asymptomatic individuals // JAMA. 2004. Vol. 291, N 2. P. 210–215. doi: 10.1001/jama.291.2.210

8. Criqui M.H., Denenberg J.O., Ix J.H., et al. Calcium density of coronary artery plaque and risk of incident cardiovascular events // JAMA. 2014. Vol. 311, N 3. P. 271–278. doi: 10.1001/jama.2013.282535

9. Carr J.J., Jacobs D.R. Jr, Terry J.G., et al. Association of Coronary Artery Calcium in Adults Aged 32 to 46 Years With Incident Coronary Heart Disease and Death // JAMA Cardiol. 2017. Vol. 2, N 4. P. 391–399. doi: 10.1001/jamacardio.2016.5493

10. Халиков А.А., Кузнецов К.О., Искужина Л.Р., и др. Судебно-медицинские аспекты внезапной аутопсия-отрицательной сердечной смерти // Судебно-медицинская экспертиза. 2021. Т. 64, № 3. С. 59–63. doi: 10.17116/sudmed20216403159

11. Eisen A., Tenenbaum A., Koren-Morag N., et al. Calcification of the thoracic aorta as detected by spiral computed tomography among stable angina pectoris patients: association with cardiovascular events and death // Circulation. 2008. Vol. 118, N 13. P. 1328–1334. doi: 10.1161/CIRCULATIONAHA.107.712141

12. Itani Y., Watanabe S., Masuda Y. Relationship between aortic calcification and stroke in a mass screening program using a mobile helical computed tomography unit // Circ J. 2006. Vol. 70, N 6. P. 733–736. doi: 10.1253/circj.70.733

13. Lee R., Matsutani N., Polimenakos A.C., et al. Preoperative noncontrast chest computed tomography identifies potential aortic emboli // Ann Thorac Surg. 2007. Vol. 84, N 1. P. 38–42. doi: 10.1016/j.athoracsur.2007.03.025

14. Zweig B.M., Sheth M., Simpson S., Al-Mallah M.H. Association of abdominal aortic calcium with coronary artery calcium and obstructive coronary artery disease: a pilot study // Int J Cardiovasc Imaging. 2012. Vol. 28, N 2. P. 399–404. doi: 10.1007/s10554-011-9818-1

15. An C., Lee H.J., Lee H.S., et al. CT-based abdominal aortic calcification score as a surrogate marker for predicting the presence of asymptomatic coronary artery disease // Eur Radiol. 2014. Vol. 24, N 10. P. 2491–2498. doi: 10.1007/s00330-014-3298-3

16. Мельников М.В., Зелинский В.А., Жорина А.С., Чуглова Д.А. Кальцификация абдоминальной аорты при периферическом атеросклерозе: факторы риска и маркёры // Атеросклероз и дислипидемии. 2014. № 3. С. 33–38. EDN: SISNRZ

17. Bagger Y.Z., Tankó L.B., Alexandersen P., et al. Radiographic measure of aorta calcification is a site-specific predictor of bone loss and fracture risk at the hip // J Intern Med. 2006. Vol. 259, N 6. P. 598–605. doi: 10.1111/j.1365-2796.2006.01640.x

18. Szulc P., Blackwell T., Schousboe J.T., et al. High hip fracture risk in men with severe aortic calcification: MrOS study // J Bone Miner Res. 2014. Vol. 29, N 4. P. 968–975. doi: 10.1002/jbmr.2085

19. Лобанова Н.Ю., Чичерина Е.Н., Мальчикова С.В., Максимчук-Колобова Н.С. Напряжение сдвига на эндотелии стенки сонной артерии и кальциноз коронарных артерий у пациентов с гипертонической болезнью // Южно-Российский журнал терапевтической практики. 2022. Т. 3, № 3. С. 60–67. EDN: QWCOCH doi: 10.21886/2712-8156-2022-3-3-60-67

20. Kim J.T., Yoo S.H., Kwon J.H., et al. Subtyping of ischemic stroke based on vascular imaging: analysis of 1,167 acute, consecutive patients // J Clin Neurol. 2006. Vol. 2, N 4. P. 225–230. doi: 10.3988/jcn.2006.2.4.225

21. Wong L.K. Global burden of intracranial atherosclerosis // Int J Stroke. 2006. Vol. 1, N 3. P. 158–159. doi: 10.1111/j.1747-4949.2006.00045.x

22. Kockelkoren R., De Vis J.B., de Jong P.A., et al. Intracranial Carotid Artery Calcification From Infancy to Old Age // J Am Coll Cardiol. 2018. Vol. 72, N 5. P. 582–584. doi: 10.1016/j.jacc.2018.05.021

23. Huang Z., Xiao J., Xie Y., et al. The correlation of deep learning-based CAD-RADS evaluated by coronary computed tomography angiography with breast arterial calcification on mammography // Sci Rep. 2020. Vol. 10, N 1. P. 11532. doi: 10.1038/s41598-020-68378-4

24. Бочкарева Е.В., Бутина Е.К., Байрамкулова Н.Х., и др. Распространенность и степень тяжести кальциноза артерий молочной железы — нового маркёра сердечно-сосудистого риска у женщин // Рациональная Фармакотерапия в Кардиологии. 2022. Т. 18, № 5. С. 530–535. EDN: HUFTZE doi: 10.20996/1819-6446-2022-09-01

25. Бочкарева Е.В., Бутина Е.К., Байрамкулова Н.Х., Драпкина О.М. Кальциноз артерий молочной железы и сахарный диабет: клинический пример и краткий обзор литературы // Профилактическая медицина. 2021. Т. 24, № 9. С. 97–101. EDN: QPQDLT doi: 10.17116/profmed20212409197

26. Бочкарева Е.В., Бутина Е.К., Савин А.С., и др. Кальциноз артерий молочной железы: потенциальный суррогатный маркёр цереброваскулярных заболеваний // Профилактическая медицина. 2020. Т. 23, № 5. С. 164–169. EDN: IRHLDZ doi: 10.17116/profmed202023051164

27. Бочкарева Е.В., Бутина Е.К., Савин А.С., Драпкина О.М. Кальциноз артерий молочной железы и остеопороз у женщины в постменопаузе (клинический случай и мнение по проблеме) // Кардиоваскулярная терапия и профилактика. 2020. Т. 19, № 4. С. 2574. EDN: RTDDQG doi: 10.15829/1728-8800-2020-2574

28. Wang J., Ding H., Bidgoli F.A., et al. Detecting Cardiovascular Disease from Mammograms With Deep Learning // IEEE Trans Med Imaging. 2017. Vol. 36, N 5. P. 1172–1181. doi: 10.1109/TMI.2017.2655486

29. Голубев Н.А., Огрызко Е.В., Тюрина Е.М., Шелепова Е.А., Шелехов П.В. Особенности развития службы лучевой диагностики в Российской Федерации за 2014–2019 года // Современные проблемы здравоохранения и медицинской статистики. 2021. № 2. С. 356–376. EDN: EHSADW doi: 10.24412/2312-2935-2021-2-356-376

30. Krupinski E.A., Berbaum K.S., Caldwell R.T., et al. Long radiology workdays reduce detection and accommodation accuracy // J Am Coll Radiol. 2010. Vol. 7, N 9. P. 698–704. doi: 10.1016/j.jacr.2010.03.004

31. Lee C.S., Nagy P.G., Weaver S.J., Newman-Toker D.E. Cognitive and system factors contributing to diagnostic errors in radiology // AJR Am J Roentgenol. 2013. Vol. 201, N 3. P. 611–617. doi: 10.2214/AJR.12.10375

32. Николаев А.Е., Шапиев А.Н., Блохин И.А., и др. Новые подходы к оценке изменений коронарных артерий при мультиспиральной компьютерной томографии // Российский кардиологический журнал. 2019. № 12. С. 124–130. EDN: VHYAYK doi: 10.15829/1560-4071-2019-12-124-130

33. Guo X., O'Neill W.C., Vey B., et al. SCU-Net: A deep learning method for segmentation and quantification of breast arterial calcifications on mammograms // Med Phys. 2021. Vol. 48, N 10. P. 5851–5861. doi: 10.1002/mp.15017

34. Yacoub B., Kabakus I.M., Schoepf U.J., et al. Performance of an Artificial Intelligence-Based Platform Against Clinical Radiology Reports for the Evaluation of Noncontrast Chest CT // Acad Radiol. 2022. Vol. 29, N 2. P. 108–117. doi: 10.1016/j.acra.2021.02.007

35. Isgum I., Rutten A., Prokop M., van Ginneken B. Detection of coronary calcifications from computed tomography scans for automated risk assessment of coronary artery disease // Med Phys. 2007. Vol. 34, N 4. P. 1450–1461. doi: 10.1118/1.2710548

36. Kurkure U., Chittajallu D.R., Brunner G., et al. A supervised classification-based method for coronary calcium detection in non-contrast CT // Int J Cardiovasc Imaging. 2010. Vol. 26, N 7. P. 817–828. doi: 10.1007/s10554-010-9607-2

37. Brunner G., Chittajallu D.R., Kurkure U., Kakadiaris I.A. Toward the automatic detection of coronary artery calcification in non-contrast computed tomography data // Int J Cardiovasc Imaging. 2010. Vol. 26, N 7. P. 829–838. doi: 10.1007/s10554-010-9608-1

38. Brunner G., Kurkure U., Chittajallu D.R., et al. Toward unsupervised classification of calcified arterial lesions // Med Image Comput Comput Assist Interv. 2008. Vol. 11, N 1. P. 144-152. doi: 10.1007/978-3-540-85988-8_18

39. Takx R.A., de Jong P.A., Leiner T., et al. Automated coronary artery calcification scoring in non-gated chest CT: agreement and reliability // PLoS One. 2014. Vol. 9, N 3. P. e91239. doi: 10.1371/journal.pone.0091239

40. Wolterink J.M., Leiner T., Takx R.A., et al. Automatic Coronary Calcium Scoring in Non-Contrast-Enhanced ECG-Triggered Cardiac CT With Ambiguity Detection // IEEE Trans Med Imaging. 2015. Vol. 34, N 9. P. 1867–1878. doi: 10.1109/TMI.2015.2412651

41. Saur S.C., Alkadhi H., Desbiolles L., et al. Automatic detection of calcified coronary plaques in computed tomography data sets // Med Image Comput Comput Assist Interv. 2008. Vol. 11, N 1. P. 170–177. doi: 10.1007/978-3-540-85988-8_21

42. Yang G., Chen Y., Ning X., et al. Automatic coronary calcium scoring using noncontrast and contrast CT images // Med Phys. 2016. Vol. 43, N 5. P. 2174. doi: 10.1118/1.4945045

43. Jiang B., Guo N., Ge Y., et al. Development and application of artificial intelligence in cardiac imaging // Br J Radiol. 2020. Vol. 93, N 1113. P. 20190812. doi: 10.1259/bjr.20190812

44. Shahzad R., van Walsum T., Schaap M., et al. Vessel specific coronary artery calcium scoring: an automatic system // Acad Radiol. 2013. Vol. 20, N 1. P. 1–9. doi: 10.1016/j.acra.2012.07.018

45. Cano-Espinosa C., González G., Washko G.R., et al. Automated Agatston Score Computation in non-ECG Gated CT Scans Using Deep Learning // Proc SPIE Int Soc Opt Eng. 2018. Vol. 10574. P. 105742K. doi: 10.1117/12.2293681

46. Gogin N., Viti M., Nicodème L., et al. Automatic coronary artery calcium scoring from unenhanced-ECG-gated CT using deep learning // Diagn Interv Imaging. 2021. Vol. 102, N 11. P. 683–690. doi: 10.1016/j.diii.2021.05.004

47. Wolterink J.M., Leiner T., de Vos B.D., et al. Automatic coronary artery calcium scoring in cardiac CT angiography using paired convolutional neural networks // Med Image Anal. 2016. Vol. 34. P. 123–136. doi: 10.1016/j.media.2016.04.004

48. Wang W., Wang H., Chen Q., et al. Coronary artery calcium score quantification using a deep-learning algorithm // Clin Radiol. 2020. Vol. 75, N 3. P. 237.e11–237.e16. doi: 10.1016/j.crad.2019.10.012

49. Singh G., Al'Aref S.J., Lee B.C., et al. End-to-End, Pixel-Wise Vessel-Specific Coronary and Aortic Calcium Detection and Scoring Using Deep Learning // Diagnostics (Basel). 2021. Vol. 11, N 2. P. 215. doi: 10.3390/diagnostics11020215

50. Martin S.S., van Assen M., Rapaka S., et al. Evaluation of a Deep Learning-Based Automated CT Coronary Artery Calcium Scoring Algorithm // JACC Cardiovasc Imaging. 2020. Vol. 13, N 1. P. 524–526. doi: 10.1016/j.jcmg.2019.09.015

51. Zhang N., Yang G., Zhang W., et al. Fully automatic framework for comprehensive coronary artery calcium scores analysis on non-contrast cardiac-gated CT scan: Total and vessel-specific quantifications // Eur J Radiol. 2021. Vol. 134. P. 109420. doi: 10.1016/j.ejrad.2020.109420

52. de Vos B.D., Wolterink J.M., Leiner T., et al. Direct Automatic Coronary Calcium Scoring in Cardiac and Chest CT // IEEE Trans Med Imaging. 2019. Vol. 38, N 9. P. 2127–2138. doi: 10.1109/TMI.2019.2899534

53. AlGhamdi M., Abdel-Mottaleb M., Collado-Mesa F. DU-Net: Convolutional Network for the Detection of Arterial Calcifications in Mammograms // IEEE Trans Med Imaging. 2020. Vol. 39, N 10. P. 3240–3249. doi: 10.1109/TMI.2020.2989737

54. Николаев А.Е., Коркунова О.А., Хуторной И.В., и др. Сопоставимость методик оценки коронарных рисков по данным ультра-НДКТ грудной клетки и КТ-коронарографии с ЭКГ-синхронизацией // Медицинская визуализация. 2021. Т. 25, № 4. С. 75–92. EDN: CMSGAX doi: 10.24835/1607-0763-1047

55. van Assen M., Martin S.S., Varga-Szemes A., et al. Automatic coronary calcium scoring in chest CT using a deep neural network in direct comparison with non-contrast cardiac CT: A validation study // Eur J Radiol. 2021. Vol. 134. P. 109428. doi: 10.1016/j.ejrad.2020.109428

56. Николаев А.Е., Шапиев А.Н., Блохин И.А. Стандартизация оценки кальцификации коронарных артерий на бесконтрастных компьютерных томограммах без ЭКГ-синхронизации // Radiology Study. 2020. Т. 3, № 2. С. 45–52. EDN: VVGXBI

57. Isgum I., Prokop M., Niemeijer M., et al. Automatic coronary calcium scoring in low-dose chest computed tomography // IEEE Trans Med Imaging. 2012. Vol. 31, N 12. P. 2322–2334. doi: 10.1109/TMI.2012.2216889

58. Wolterink J.M., Leiner T., Viergever M.A., Isgum I. Generative Adversarial Networks for Noise Reduction in Low-Dose CT // IEEE Trans Med Imaging. 2017. Vol. 36, N 12. P. 2536–2545. doi: 10.1109/TMI.2017.2708987

59. Klug M., Shemesh J., Green M., et al. A deep-learning method for the denoising of ultra-low dose chest CT in coronary artery calcium score evaluation // Clin Radiol. 2022. Vol. 77, N 7. P. 509–517. doi: 10.1016/j.crad.2022.03.005

60. Sun Z., Ng C.K.C. Artificial Intelligence (Enhanced Super-Resolution Generative Adversarial Network) for Calcium Deblooming in Coronary Computed Tomography Angiography: A Feasibility Study // Diagnostics (Basel). 2022. Vol. 12, N 4. P. 991. doi: 10.3390/diagnostics12040991

61. Eng D., Chute C., Khandwala N., et al. Automated coronary calcium scoring using deep learning with multicenter external validation // NPJ Digit Med. 2021. Vol. 4, N 1. P. 88. doi: 10.1038/s41746-021-00460-1

62. Морозов С.П., Кокина Д.Ю., Павлов Н.А., и др. Клинические аспекты применения искусственного интеллекта для интерпретации рентгенограмм органов грудной клетки // Туберкулез и болезни легких. 2021. Т. 99, № 4. С. 58–64. doi: 10.21292/2075-1230-2021-99-4-58-64

63. Kamel P.I., Yi P.H., Sair H.I., Lin C.T. Prediction of Coronary Artery Calcium and Cardiovascular Risk on Chest Radiographs Using Deep Learning // Radiol Cardiothorac Imaging. 2021. Vol. 3, N 3. P. e200486. doi: 10.1148/ryct.2021200486

64. Du T., Xie L., Zhang H., et al. Training and validation of a deep learning architecture for the automatic analysis of coronary angiography // EuroIntervention. 2021. Vol. 17, N 1. P. 32–40. doi: 10.4244/EIJ-D-20-00570

65. Isgum I., Rutten A., Prokop M., et al. Automated aortic calcium scoring on low-dose chest computed tomography // Med Phys. 2010. Vol. 37, N 2. P. 714–723. doi: 10.1118/1.3284211

66. de Vos B.D., Lessmann N., de Jong P.A., Išgum I. Deep Learning-Quantified Calcium Scores for Automatic Cardiovascular Mortality Prediction at Lung Screening Low-Dose CT // Radiol Cardiothorac Imaging. 2021. Vol. 3, N 2. P. e190219. doi: 10.1148/ryct.2021190219

67. van Velzen S.G.M., Lessmann N., Velthuis B.K., et al. Deep Learning for Automatic Calcium Scoring in CT: Validation Using Multiple Cardiac CT and Chest CT Protocols // Radiology. 2020. Vol. 295, N 1. P. 66–79. doi: 10.1148/radiol.2020191621

68. Guilenea F.N., Casciaro M.E., Pascaner A.F., et al. Thoracic Aorta Calcium Detection and Quantification Using Convolutional Neural Networks in a Large Cohort of Intermediate-Risk Patients // Tomography. 2021. Vol. 7, N 4. P. 636–649. doi: 10.3390/tomography7040054

69. Reid S., Schousboe J.T., Kimelman D., et al. Machine learning for automated abdominal aortic calcification scoring of DXA vertebral fracture assessment images: A pilot study // Bone. 2021. Vol. 148. P. 115943. doi: 10.1016/j.bone.2021.115943

70. Graffy P.M., Liu J., O'Connor S., et al. Automated segmentation and quantification of aortic calcification at abdominal CT: application of a deep learning-based algorithm to a longitudinal screening cohort // Abdom Radiol (NY). 2019. Vol. 44, N 8. P. 2921–2928. doi: 10.1007/s00261-019-02014-2

71. van Engelen A., Niessen W.J., Klein S., et al. Atherosclerotic plaque component segmentation in combined carotid MRI and CTA data incorporating class label uncertainty // PLoS One. 2014. Vol. 9, N 4. P. e94840. doi: 10.1371/journal.pone.0094840

72. Онищенко П.С., Клышников К.Ю., Овчаренко Е.А. Искусственные нейронные сети в кардиологии: анализ графических данных // Бюллетень сибирской медицины. 2021. Т. 20, № 4. С. 193–204. EDN: XVBERA doi: 10.20538/1682-0363-2021-4-193-204

73. Bortsova G., Bos D., Dubost F., et al. Automated Segmentation and Volume Measurement of Intracranial Internal Carotid Artery Calcification at Noncontrast CT // Radiol Artif Intell. 2021. Vol. 3, N 5. P. e200226. doi: 10.1148/ryai.2021200226

74. Li D., Qiao H., Han Y., et al. Histological validation of simultaneous non-contrast angiography and intraplaque hemorrhage imaging (SNAP) for characterizing carotid intraplaque hemorrhage // Eur Radiol. 2021. Vol. 31, N 5. P. 3106–3115. doi: 10.1007/s00330-020-07352-0

75. Chen S., Ning J., Zhao X., et al. Fast simultaneous noncontrast angiography and intraplaque hemorrhage (fSNAP) sequence for carotid artery imaging // Magn Reson Med. 2017. Vol. 77, N 2. P. 753–758. doi: 10.1002/mrm.26111

76. Qi H., Sun J., Qiao H., et al. Carotid Intraplaque Hemorrhage Imaging with Quantitative Vessel Wall T1 Mapping: Technical Development and Initial Experience // Radiology. 2018. Vol. 287, N 1. P. 276–284. doi: 10.1148/radiol.2017170526

77. Cheng J.Z., Cole E.B., Pisano E.D., Shen D. Detection of arterial calcification in mammograms by random walks // Inf Process Med Imaging. 2009. Vol. 21. P. 713–724. doi: 10.1007/978-3-642-02498-6_59

78. Ломаков С.Ю. Объёмы маммографических исследований в современных условиях проведения профилактических мероприятий // Профилактическая медицина. 2020. Т. 23, № 4. С. 41–44. EDN: OUUINQ doi: 10.17116/profmed20202304141

79. Roseman D.A., Hwang S.J., Manders E.S., et al. Renal artery calcium, cardiovascular risk factors, and indexes of renal function // Am J Cardiol. 2014. Vol. 113, N 1. P. 156–161. doi: 10.1016/j.amjcard.2013.09.036

AUTHORS' INFO

*** Adilya S. Nurkaeva;**
address: 45a Zaki Validi str. 450008, Ufa, Russia;
ORCID: 0009-0006-8621-5580;
eLibrary SPIN: 3307-5546;
e-mail: vkomissiya@inbox.ru

Yuri A. Trusov;
ORCID: 0000-0001-6407-3880;
eLibrary SPIN: 3203-5314;
e-mail: yu.a.trusov@samsmu.ru

Victoria S. Chupakhina;
ORCID: 0009-0003-8318-3673;
eLibrary SPIN: 4402-7476;
e-mail: chupalhina@bk.ru

Natalia A. Yakovenko;
ORCID: 0009-0005-6726-9623;
eLibrary SPIN: 4415-2236;
e-mail: tigris2011@yandex.ru

Irina V. Ablenina;
ORCID: 0009-0006-6222-9339;
eLibrary SPIN: 4123-3336;
e-mail: aninelba@gmail.com

Roksana F. Latypova;
ORCID: 0009-0004-5057-6451;
eLibrary SPIN: 3542-3376;
e-mail: roxevansss@gmail.com

Aleksandra P. Pitke;
ORCID: 0009-0002-1111-759X;
eLibrary SPIN: 3726-4213;
e-mail: pitkea00@gmail.com

Anastasiya A. Yazovskih;
ORCID: 0000-0002-3955-0830;
eLibrary SPIN: 3543-5323;
e-mail: anyaz.bgmu@yandex.ru

ОБ АВТОРАХ

*** Нуркаева Адиля Салаватовна;**
адрес: Россия 450008, Уфа, ул. ул. Заки Валиди, 45а;
ORCID: 0009-0006-8621-5580;
eLibrary SPIN: 3307-5546;
e-mail: vkomissiya@inbox.ru

Трусов Юрий Александрович;
ORCID: 0000-0001-6407-3880;
eLibrary SPIN: 3203-5314;
e-mail: yu.a.trusov@samsmu.ru

Чупахина Виктория Сергеевна;
ORCID: 0009-0003-8318-3673;
eLibrary SPIN: 4402-7476;
e-mail: chupalhina@bk.ru

Яковенко Наталья Александровна;
ORCID: 0009-0005-6726-9623;
eLibrary SPIN: 4415-2236;
e-mail: tigris2011@yandex.ru

Абленина Ирина Витальевна;
ORCID: 0009-0006-6222-9339;
eLibrary SPIN: 4123-3336;
e-mail: aninelba@gmail.com

Латыпова Роксана Фанилевна;
ORCID: 0009-0004-5057-6451;
eLibrary SPIN: 3542-3376;
e-mail: roxevansss@gmail.com

Питке Александра Петровна;
ORCID: 0009-0002-1111-759X;
eLibrary SPIN: 3726-4213;
e-mail: pitkea00@gmail.com

Язовских Анастасия Алексеевна;
ORCID: 0000-0002-3955-0830;
eLibrary SPIN: 3543-5323;
e-mail: anyaz.bgmu@yandex.ru

* Corresponding author / Автор, ответственный за переписку

Artem S. Ivanov;
ORCID: 0009-0000-3562-8293;
eLibrary SPIN: 4834-5324;
e-mail: artem.ivanov656@yandex.ru

Darya S. Bogatyreva;
ORCID: 0009-0004-5055-8819;
eLibrary SPIN: 3331-3421;
e-mail: diria1012@yandex.ru

Ulyana A. Popova;
ORCID: 0009-0002-7994-5631;
eLibrary SPIN: 3452-2543;
e-mail: ulyanka.popova.2000@gmail.com

Azat F. Yuzlekbaev;
ORCID: 0009-0002-8799-4732;
eLibrary SPIN: 4812-3213;
e-mail: ztl5@rambler.ru

Иванов Артём Сергеевич;
ORCID: 0009-0000-3562-8293;
eLibrary SPIN: 4834-5324;
e-mail: artem.ivanov656@yandex.ru

Богатырева Дарья Сергеевна;
ORCID: 0009-0004-5055-8819;
eLibrary SPIN: 3331-3421;
e-mail: diria1012@yandex.ru

Попова Ульяна Андреевна;
ORCID: 0009-0002-7994-5631;
eLibrary SPIN: 3452-2543;
e-mail: ulyanka.popova.2000@gmail.com

Юзлекбав Азат Флюрович;
ORCID: 0009-0002-8799-4732;
eLibrary SPIN: 4812-3213;
e-mail: ztl5@rambler.ru

DOI: https://doi.org/10.17816/DD515814

Перспективы применения компьютерного зрения для выявления камней в мочевыделительной системе и новообразований печени и почек на изображениях компьютерной томографии органов брюшной полости и забрюшинного пространства

Ю.А. Васильев[1,2], А.В. Владзимирский[1,3], К.М. Арзамасов[1], Д.У. Шихмурадов[1], А.В. Панкратов[1], И.В. Ульянов[1], Н.Б. Нечаев[1]

[1] Научно-практический клинический центр диагностики и телемедицинских технологий, Москва, Россия;
[2] Национальный медико-хирургический Центр имени Н.И. Пирогова, Москва, Россия;
[3] Первый Московский государственный медицинский университет имени И.М. Сеченова, Москва, Россия

АННОТАЦИЯ

В работе представлен селективный обзор литературы, посвящённый использованию алгоритмов компьютерного зрения для диагностики новообразований печени и почек, а также камней в мочевыделительной системе на изображениях компьютерной томографии органов брюшной полости и забрюшинного пространства.

В обзор были включены статьи, опубликованные за период с 01.01.2020 по 24.04.2023 гг.

В задаче сегментации печени и её новообразований алгоритмы, оперирующие пикселями, показали наибольшие значения параметров диагностической точности (точность достигает 99,6%; коэффициент сходства Дайса — 0,99). Задачи классификации новообразований печени на текущий момент лучше решаются воксельными алгоритмами (точность до 82,5%).

Сегментация почек и их новообразований, а также классификация опухолей почек одинаково хорошо выполняются алгоритмами, анализирующими как пиксели, так и воксели (точность достигает 99,3%, коэффициент сходства Дайса — 0,97).

Алгоритмы компьютерного зрения в настоящее время также способны с высокой степенью точности определять конкременты в мочевыделительной системе размерами от 3 мм (точность достигает 93,0%).

Таким образом, существующие алгоритмы компьютерного зрения позволяют не только эффективно выявлять новообразования печени и почек, а также конкременты в мочевыделительной системе, но и с высокой точностью определять их количественные и качественные характеристики.

Более высокая точность определения вида новообразования может быть достигнута за счёт оценки воксельных данных, поскольку в этом случае алгоритм анализирует новообразование полностью в трёх измерениях, а не только в плоскости одного среза.

Ключевые слова: компьютерная томография; нейронные сети; глубокое машинное обучение; органы брюшной полости; мочекаменная болезнь; образования почек; образования печени.

Как цитировать:

Васильев Ю.А., Владзимирский А.В., Арзамасов К.М., Шихмурадов Д.У., Панкратов А.В., Ульянов И.В., Нечаев Н.Б. Перспективы применения компьютерного зрения для выявления камней в мочевыделительной системе и новообразований печени и почек на изображениях компьютерной томографии органов брюшной полости и забрюшинного пространства // Digital Diagnostics. 2024. Т. 5, № 1. С. 101–119. DOI: https://doi.org/10.17816/DD515814

Рукопись получена: 27.06.2023 **Рукопись одобрена:** 22.12.2023 **Опубликована online:** 11.03.2024

DOI: https://doi.org/10.17816/DD515814

Prospects of using computer vision technology to detect urinary stones and liver and kidney neoplasms on computed tomography images of the abdomen and retroperitoneal space

Yuriy A. Vasilev[1,2], Anton V. Vladzymyrskyy[1,3], Kirill M. Arzamasov[1], David U. Shikhmuradov[1], Andrey V. Pankratov[1], Iliya V. Ulyanov[1], Nikolay B. Nechaev[1]

[1] Research and Practical Clinical Center for Diagnostics and Telemedicine Technologies, Moscow, Russia;
[2] National Medical and Surgical Center Named after N.I. Pirogov, Moscow, Russia;
[3] I.M. Sechenov First Moscow State Medical University, Moscow, Russia

ABSTRACT

The article presents a selective literature review on the use of computer vision algorithms for the diagnosis of liver and kidney neoplasms and urinary stones using computed tomography images of the abdomen and retroperitoneal space. The review included articles published between January 1, 2020, and April 24, 2023. Pixel-based algorithms showed the greatest diagnostic accuracy parameters for segmenting the liver and its neoplasms (accuracy, 99.6%; Dice similarity coefficient, 0.99). Voxel-based algorithms were superior at classifying liver neoplasms (accuracy, 82.5%). Pixel- and voxel-based algorithms fared equally well in segmenting kidneys and their neoplasms, as well as classifying kidney tumors (accuracy, 99.3%; Dice similarity coefficient, 0.97). Computer vision algorithms can detect urinary stones measuring 3 mm or larger with a high degree of accuracy of up to 93.0%. Thus, existing computer vision algorithms not only effectively detect liver and kidney neoplasms and urinary stones but also accurately determine their quantitative and qualitative characteristics. Evaluating voxel data improves the accuracy of neoplasm type determination since the algorithm analyzes the neoplasm in three dimensions rather than only the plane of one slice.

Keywords: computed tomography; neural networks; deep learning; abdomen; urolithiasis; renal neoplasms; liver neoplasms.

To cite this article:
Vasilev YuA, Vladzymyrskyy AV, Arzamasov KM, Shikhmuradov DU, Pankratov AV, Ulyanov IV, Nechaev NB. Prospects of using computer vision technology to detect urinary stones and liver and kidney neoplasms on computed tomography images of the abdomen and retroperitoneal space. *Digital Diagnostics*. 2024;5(1):101–119. DOI: https://doi.org/10.17816/DD515814

Submitted: 27.06.2023 **Accepted:** 22.12.2023 **Published online:** 11.03.2024

DOI: https://doi.org/10.17816/DD515814

计算机视觉在腹部和腹膜后计算机断层扫描图片上检测泌尿系统结石和肝肾肿块的应用前景

Yuriy A. Vasilev[1,2], Anton V. Vladzymyrskyy[1,3], Kirill M. Arzamasov[1], David U. Shikhmuradov[1], Andrey V. Pankratov[1], Iliya V. Ulyanov[1], Nikolay B. Nechaev[1]

[1] Research and Practical Clinical Center for Diagnostics and Telemedicine Technologies, Moscow, Russia;
[2] National Medical and Surgical Center Named after N.I. Pirogov, Moscow, Russia;
[3] I.M. Sechenov First Moscow State Medical University, Moscow, Russia

摘要

本文对计算机视觉算法在腹部和腹膜后计算机断层扫描图片被用于诊断肝肾肿块以及泌尿系统结石的情况进行了有选择性的文献综述。

综述中的文章发表于2020年1月1日至2023年4月24日。

在肝脏及其肿块的分割任务中，使用像素算法显示出最高的诊断准确率参数值（准确率达到99.6%；Dice相似系数为0.99）。目前，基于体素的算法能较好地解决肝肿块分类任务（准确率高达82.5%）。

通过分析像素和体素的算法，肾脏及其肿块的分割和肾肿块的分类同样出色（准确率达到99.3%，Dice相似系数为0.97）。

现在，计算机视觉算法也能高度准确地检测出泌尿系统中3毫米及以上大小的结石（准确率达到93.0%）。

因此，现有的计算机视觉算法不仅能有效检测肝肾肿块以及泌尿系统中的结石，还能高度准确地确定它们的定量和定性特征。

通过评估体素数据，可以提高肿块类检测的准确度。在这种情况下，算法会对整个肿块进行三维分析，而不仅只是在一个切片的平面上进行分析。

关键词：电子计算机断层扫描；神经网络；深度机器学习；腹部器官；泌尿系结石病；肾肿块；肝肿块。

引用本文：
Vasilev YuA, Vladzymyrskyy AV, Arzamasov KM, Shikhmuradov DU, Pankratov AV, Ulyanov IV, Nechaev NB. 计算机视觉在腹部和腹膜后计算机断层扫描图片上检测泌尿系统结石和肝肾肿块的应用前景. *Digital Diagnostics.* 2024;5(1):101–119. DOI: https://doi.org/10.17816/DD515814

收到：27.06.2023 **接受：**22.12.2023 **发布日期：**11.03.2024

INTRODUCTION

X-ray diagnosis has greatly evolved in recent years. In particular, computer vision technology has been actively employed for the interpretation of computed tomography (CT) scans for more accurate and timely diagnosis and reduction of the burden on medical personnel [1–3]. Several artificial intelligence algorithms for the analysis of chest CT scans have already demonstrated high accuracy in specific disease areas (with the area under the receiver operating characteristic curve reaching 0.88) [3].

Moreover, computer vision technology is extensively used in the diagnosis of abdominal pathologies. In the last 5 years, the number of PubMed publications on this topic has increased 12 times, i.e., from 34 in 2018 to 411 in 2022. The dramatic increase in the number of studies could be attributed to increased CT availability to the general population, a relatively broad and growing list of diagnosed disorders, and the high accuracy of their verification using CT scans.

Currently, ready-made computer vision-based solutions are capable of detecting common pathologies such as liver and kidney neoplasms and urinary stones using abdominal and retroperitoneal CT scans [4].

These solutions are based on algorithms that can be classified into two types based on their function:

1. Algorithms identifying (segmenting) organs and their pathologies
2. Algorithms classifying the pathology

The described solutions offer variable levels of diagnostic accuracy, which could be attributed to the architecture of deep-learning networks and computer vision algorithms. Deep machine-learning architectures based on convolutional neural networks are currently most commonly used for classification [5].

This review aimed to assess the diagnostic accuracy and architecture of computer vision algorithms for detecting liver and kidney neoplasms and urinary stones on CT scans, depending on the algorithm function (segmentation or classification).

SEARCH METHODOLOGY

An analytical study was performed: it was a selective literature review of algorithms intended for primary diagnosis of common conditions such as liver and kidney neoplasms and urinary stone disease.

Other common neoplasms, such as pancreatic tumors, can be detected on abdominal and retroperitoneal CT. However, this review focused on liver and kidney neoplasms and urinary stones. If any, few studies have used computer vision technology to detect neoplasms of other organs in these anatomical areas.

The literature search was performed in PubMed (accessed on April 30, 2023) using the following keyword combinations: ["Deep Learning," "Neural Network," "Artificial Intelligence"] + ["Liver Tumor," "Kidney Tumor," "Hepatocellular Carcinoma," "Kidney Stone"] + "Computed Tomography".

A search was also performed in eLibrary, the Russian electronic research library and information analysis system for science citation index (accessed on April 30, 2023), from 2019 to the present using the keywords "Artificial intelligence" + "Computed Tomography". However, the search failed to identify publications on deep-learning algorithms for detecting abdominal and retroperitoneal organ disorders.

The analysis included studies identified in PubMed that used computer vision algorithms for segmentation and classification of pathologies of interest on abdominal and retroperitoneal CT scans, described the deep-learning algorithm architecture, and presented the results of the algorithm performance using one of the following parameters: Dice coefficient for segmentation and accuracy and F1-score or area under the ROC curve (AUC) for classification [6].

The search covered the period from January 1, 2020, to April 24, 2023.

RESULTS

The review included 21 studies, and their findings are presented in Appendix 1. The architecture was analyzed, and diagnostic metrics were assessed in the selected studies. Moreover, these studies were compared with other publicly available articles not included in the analysis.

Liver neoplasms

Contrast-enhanced CT and magnetic resonance imaging (MRI) are currently the most informative methods for the diagnosis of liver neoplasms [7]. CT offers various advantages over MRI, such as equipment availability, expert qualification, testing time, and cost-effectiveness [8]. Contrast enhancement is a common strategy when a liver neoplasm is suspected because non-contrasted scans are less informative. However, in some other diseases, noncontrasted abdominal CT is often performed. The ability of computer vision algorithms to detect liver neoplasms on non-contrasted CT scans may be used for screening for this pathology [9–11].

The U-Net architecture and its modifications (i.e., ResNet blocks) are most widely used for segmentation of the liver and liver neoplasms, with acceptable diagnostic accuracy. H. Rahman et al. demonstrated the best results for the segmentation of the liver and liver neoplasms using ResUNet, with a Dice coefficient of 0.09 and an accuracy of 99.6% [12]. An example of liver neoplasm segmentation is presented in Fig. 1.

Pixel-based (2D image) segmentation algorithms had better diagnostic metrics than voxel-based (3D image) segmentation algorithms [12–18].

In turn, voxel-based algorithms show better diagnostic metrics in liver neoplasm classification. These algorithms

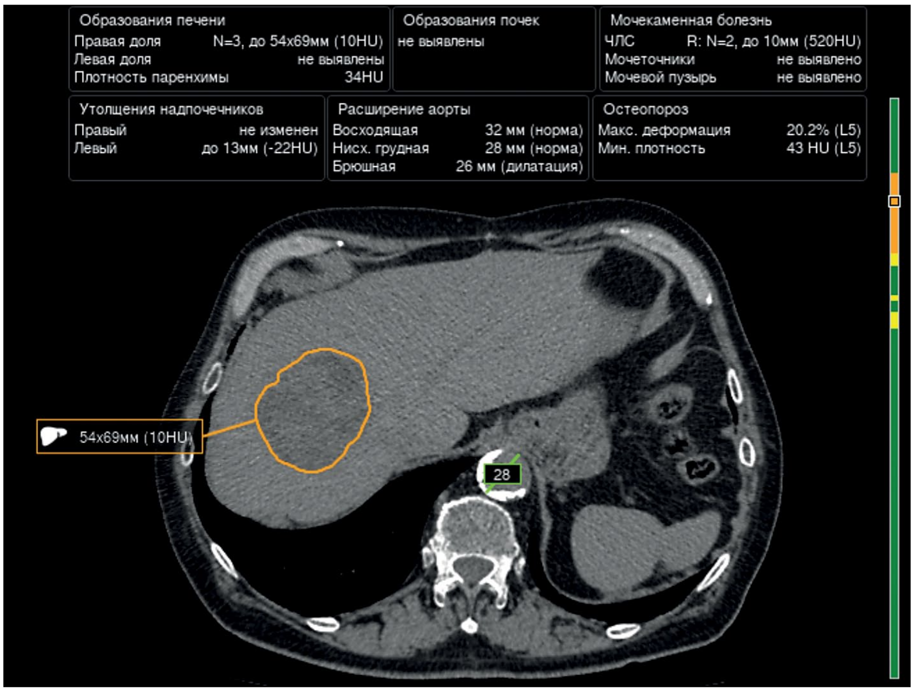

Fig. 1. An example of liver neoplasm segmentation using one of the algorithms.

demonstrate high reliability in distinguishing benign tumors from malignancies (accuracy up to 85.5%). The accuracy of determining a specific type of malignant neoplasms is currently lower at only 73.4% [19, 20].

Despite the development and widespread use of deep machine-learning, some classic machine-learning algorithms (e.g., support vector machine [SVM]) also demonstrate high diagnostic metrics in liver neoplasm classification, with an accuracy of up to 84.6% [19, 21].

The Center for Diagnostics and Telemedicine (Moscow) is currently developing a computer vision algorithm using contrast enhancement for within-class segmentation and differentiation of liver masses. An example is presented in Fig. 2.

Kidney neoplasms

In 27%–50% of cases, kidney neoplasms are asymptomatic and represent random findings [22]. CT allows

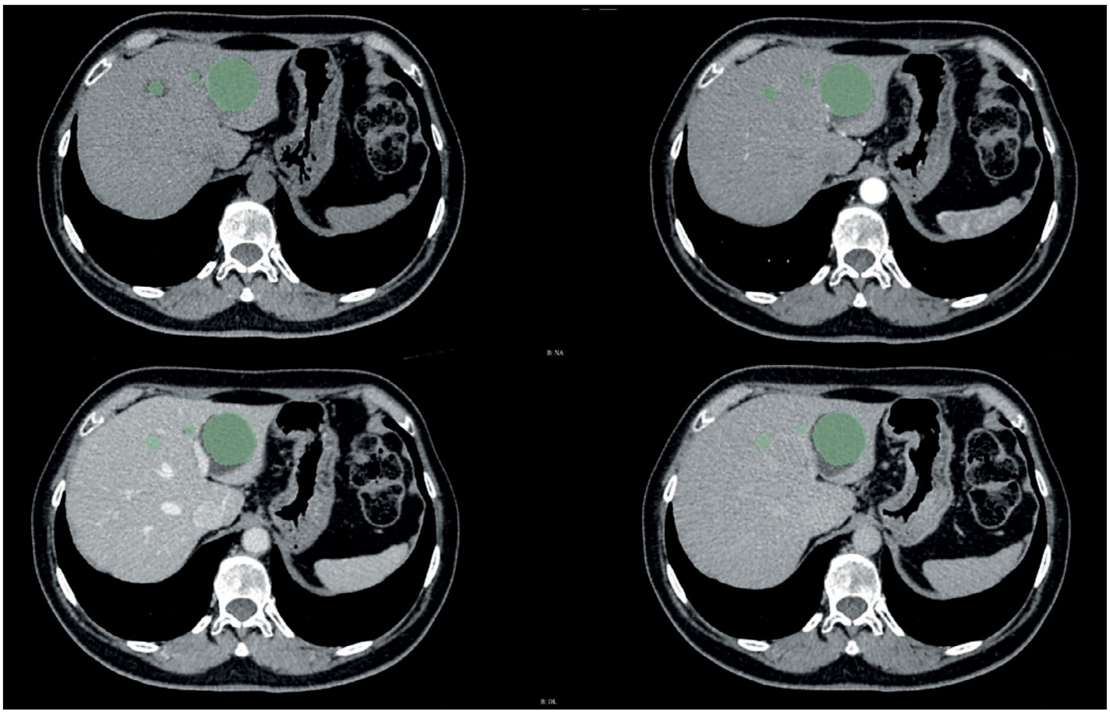

Fig. 2. An example of liver neoplasm segmentation by an algorithm based on a contrast-enhanced CT scan.

for the assessment of the tumor location and size and the relationship between the tumor and renal pelvis and large vessels.

In the analyzed studies, the U-Net architecture and its modifications are most widely employed for the segmentation of the kidneys and kidney neoplasms. The Dice coefficient for kidney segmentation currently reaches 0.97 with the U-Net 3D architecture [23]. The same architecture provided the highest Dice coefficient for kidney tumor and kidney cyst segmentation (0.84 and 0.54, respectively). Thus, the accuracy of kidney neoplasm segmentation is currently inferior to that of kidney segmentation. Moreover, voxel-based architectures demonstrated diagnostic accuracy metrics for the segmentation of the kidneys and kidney neoplasms on CT scans noninferior to those of classic pixel-based algorithms [23–26].

Other architectures (e.g., EffectiveNet) also demonstrate a high Dice coefficient for the segmentation of the kidneys and kidney neoplasms (up to 0.95) [27, 28]. An example of kidney neoplasm segmentation is presented in Fig. 3.

Both classic machine-learning algorithms and deep-learning algorithms are used for the classification of kidney neoplasms [24, 26, 29–31]. Swin transformers architectures have the greatest accuracy (99.3%) [29].

When data are limited, classic machine-learning algorithms and feedforward architectures prove effective [26]. Similarly to the segmentation of the kidneys and kidney neoplasms, the classification performance of voxel-based architectures is noninferior to that of pixel-based architectures [31].

Urinary stone disease

Urinary stone disease is the second most commonly detected urological condition [32]. The incidence and prevalence of urinary stone disease in adults are steadily increasing throughout the Russian Federation. According to N. Gadzhiev et al., the prevalence of urinary stone disease has increased by 35.4% in 15 years, whereas the incidence has reached 16.2% [33].

Retroperitoneal CT is the gold standard for the diagnosis of urinary stone diseases. It allows for the assessment of the location, size, and number of radiopaque urinary stones with sensitivity and specificity of up to 96% and 100%, respectively [34].

The articles showed a direct association between the accuracy of urinary stone detection and the size of urinary stones. The accuracy of convolutional neural network-based algorithms increases with the size of urinary stones [35, 36]. To illustrate, the accuracy rates of detecting urinary stones <1 , 1–2 , and >2 cm were 85%, 89%, and 93%, respectively.

The Swin transformers algorithm has currently the greatest accuracy in urinary stone detection (98%) [29]. An example of urinary stone detection using one of the algorithms is presented in Fig. 4.

The use of computer vision algorithms for the diagnosis of urinary stone diseases can be challenging if small atherosclerotic plaques are present in renal artery walls because their densities are similar to those of urinary stones [36].

Modern deep machine-learning and computer vision technologies allow for the detection of urinary stones measuring ⩾3 mm with low radiation exposure, and urinary stones measuring ⩾5 mm are considered clinically significant [37].

Determining the urinary stone type is one of the most important factors for the future treatment strategy [35, 37]. Numerous CT-based parameters have been employed

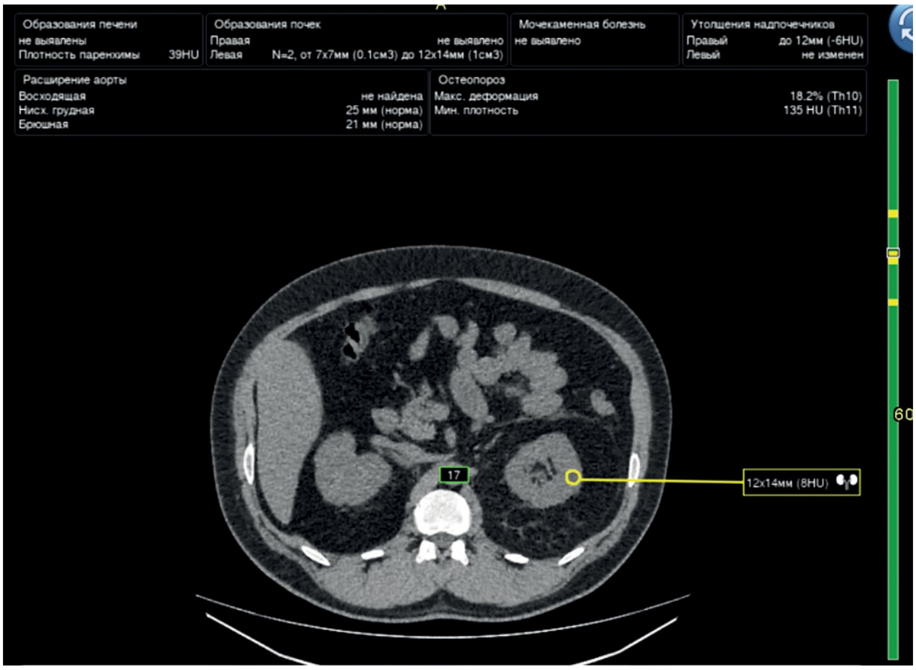

Fig. 3. An example of right kidney neoplasm segmentation.

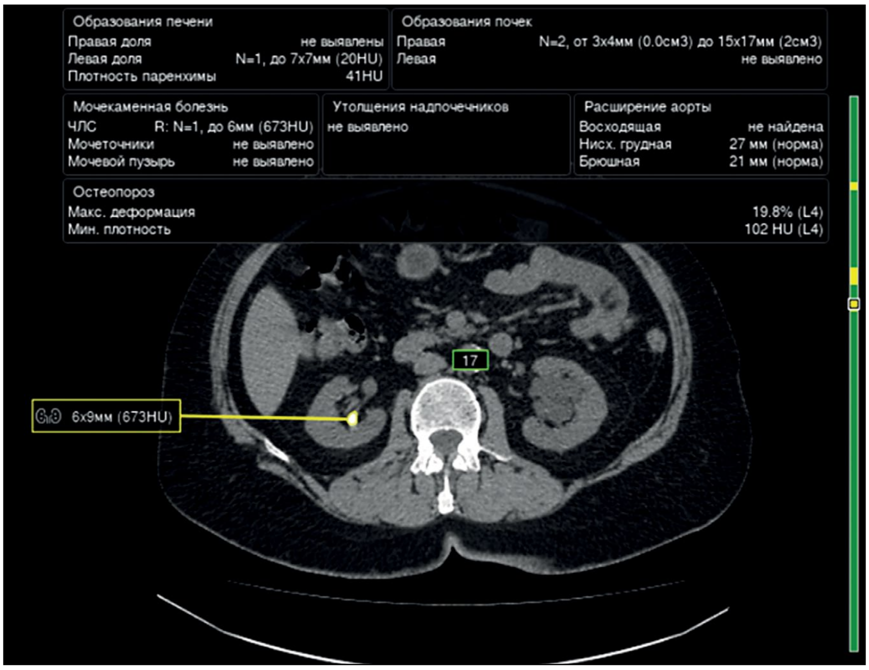

Fig. 4. An example of urinary stone detection using one of the algorithms.

in assessing postoperative prognosis (such as relapse-free disease) and determining the urinary stone type using machine-learning technology [38–41]. Several studies of dual-energy CT confirm that this imaging technique can also be used for assessing the chemical composition of urinary stones [42, 43]. However, this method has several limitations, most notably, its low applicability in routine clinical practice [44].

According to Y. Cui et al., narrowly specialized convolutional neural networks allow for the assessment of urinary stones using the STONE nephrolithometry score, and results were comparable to radiologist opinions [45]. This approach also allows for the assessment of prognossis [46].

DISCUSSION

Several studies have used publicly available datasets, such as LiTS, KiTS'19, and 3D-IRCADb, and most of them include contrast-enhanced CT findings. The datasets of studies using their CT scans mostly included contrast-enhanced CT findings or mixed data.

The analysis revealed that modern deep-learning algorithms provide high accuracy liver segmentation (maximum Dice coefficient, 0.99; mean Dice coefficient, 0.92±0.09) and kidney segmentation (maximum Dice coefficient, 0.97; mean Dice coefficient, 0.94±0.02) on CT scans (Appendix 1).

Pixel-based algorithms show better diagnostic accuracy metrics for liver segmentation (maximum Dice coefficient, 0.99; mean Dice coefficient, 0.97±0.01), whereas voxel-based algorithms are noninferior to pixel-based algorithms for kidney segmentation. This could be attributed to differences in the size and density of these solid organs and the history of algorithm development. Voxel-based algorithms have higher performance requirements. Such computer-based systems have only recently become widely available. Currently, improved pixel-based algorithms are being developed in research centers.

Liver and kidney neoplasm segmentation is less accurate than liver and kidney segmentation, which is primarily due to incomplete neoplasm segmentation. The correct determination of neoplasm borders depends on their growth type and structure; thus, the best segmentation is observed for exophytic heterogeneous neoplasms [23]. This is also why isodense cysts and hemangiomas are segmented with low accuracy [20].

Data preprocessing before using a segmentation algorithm resolves this issue to some extent [27, 28]. K. Yildirim et al. found that analyzing alternative CT slices, such as sagittal or coronal, using deep machine-learning algorithms also contributes to the accuracy of pathology detection [47].

According to the literature review, voxel-based algorithms are more suitable for neoplasm classification than pixel-based algorithms because the structure of the tumor is indicative of its nature [19, 26, 31]. Deep-learning technology provides highly accurate classification of benign and malignant abdominal neoplasms [19, 20, 31].

The completeness of segmentation is critical for the accuracy of subsequent classification. Currently, a combination of two-dimensional algorithms can be used for segmentation and a combination of three-dimensional (3D) algorithms for classification [19, 24]. Moreover, a combination of deep- and classic machine-learning algorithms (including gradient boosting) can improve diagnostic metrics [19]. The studies analyzed used two types of combinations of these algorithms. L. Yang et al. and M. Shehata et al. proposed creating features by algorithmic methods and using them in a feedforward network [30, 31]. Meanwhile, E. Trivizakis et al. and X.L. Zhu et al. proposed creating features using deep-learning networks and classifying them using classic machine-learning algorithms [19, 26].

Equally important is using a transformer architecture for neoplasm classification; however, its application is limited by the availability of training data. Obtaining high metrics when using transformer architectures requires significantly more training data than with high accuracy neural networks [29].

The studies analyzed used conventional quality assessment metrics for deep machine-learning algorithms. However, the research methodology varied among studies, making comparative assessment of diagnostic accuracy difficult. Most authors did not provide the 95% confidence interval for diagnostic accuracy parameters, which was an additional limitation and prevented assessment of the significance of differences between metrics obtained using different neural network architectures and approaches. A standardized assessment can be useful in determining algorithms with the best results [48]. Some of the analyzed studies also had small samples.

Another possible use of deep machine-learning algorithms is to improve the quality of low-dose CT scans. For example, F.R. Schwartz et al. proposed using deep machine-learning algorithms for data interpolation and reconstruction in DECT [49–51]. This approach allows for the acquisition of high-energy CT scans with a low radiation exposure.

Thus, computer vision algorithms have already demonstrated good diagnostic accuracy parameters in detecting urinary stones and liver and kidney neoplasms on CT scans. The next goal is to implement computer vision technology in healthcare facilities for more accurate and timely diagnosis and reduction of the burden on medical personnel. More large-scale, well-designed prospective studies are warranted to assess the efficacy of artificial intelligence-based software in detecting abdominal neoplasms during screening and for their qualitative and quantitative assessment with subsequent verification of the results.

CONCLUSION

Existing computer vision systems for assessing abdominal and retroperitoneal CT scans effectively detect liver and kidney neoplasms and urinary stones. Moreover, these systems allow for the accurate determination of their quantitative and qualitative parameters. Further technological advancements will improve 3D deep-learning algorithms and their diagnostic accuracy, ensuring more accurate results, particularly for multiclass classification. Voxel data can provide a more accurate determination of the pathology type because, in this case, algorithms ensure the 3D analysis of neoplasms rather than a single-slice analysis.

A more thorough analysis of data obtained using computer vision technology can be used to determine the effectiveness of contrast-enhanced CT scans. Methods for improving CT scan quality will make it possible to take scans only during specific phases (e.g., arterial and excretory phases) depending on the study purposes, reducing the effective radiation dose.

ADDITIONAL INFORMATION

Funding source. This article was prepared by a group of authors as a part of the research and development effort titled "Evidence-based methodologies for sustainable development of artificial intelligence in medical imaging" (USIS No. 123031500004-5) in accordance with Order No. 1196 dated December 21, 2022 "On Approval of State Assignments Funded by means of Allocations from the Budget of the City of Moscow to the State Budgetary (Autonomous) Institutions Subordinate to the Moscow Health Care Department, for 2023 and the Planned Period of 2024 and 2025" issued by the Moscow Health Care Department.

Competing interests. The authors declare that they have no competing interests.

Authors' contribution. All authors made a substantial contribution to the conception of the work, acquisition, analysis, interpretation of data for the work, drafting and revising the work, final approval of the version to be published and agree to be accountable for all aspects of the work. Yu.A. Vasiliev, A.V. Vladzimirsky, K.M. Arzamasov — research concept; N.B. Nechaev — writing the text of the article; D.W. Shikhmuradov, A.V. Pankratov, I.V. Ulyanov — data analysis.

REFERENCES

1. Iliashenko OY, Lukyanchenko EL. Possibilities of using computer vision for data analytics in medicine. *Izvestiya of Saratov University. Mathematics. Mechanics. Informatics.* 2022;22(2):224–232. EDN: MCSLKQ doi: 10.18500/1816-9791-2022-22-2-224-232

2. Alekseeva MG, Zubov AI, Novikov MYu. Artificial intelligence in medicine. *Meždunarodnyj naučno-issledovatel'skij žurnal.* 2022;7(121):10–13. EDN: JMMMDF doi: 10.23670/IRJ.2022.121.7.038

3. Gusev AV, Vladzymyrskyy AV, Sharova DE, Arzamasov KM, Khramov AE. Evolution of research and development in the field of artificial intelligence technologies for healthcare in the Russian Federation: results of 2021. *Digital Diagnostics.* 2022;3(3):178–194. EDN: KHWQWZ doi: 10.17816/DD107367

4. Wang L, Wang H, Huang Y, et al. Trends in the application of deep learning networks in medical image analysis: Evolution between 2012 and 2020. *Eur J Radiol.* 2022;146:110069. doi: 10.1016/j.ejrad.2021.110069

5. Alrefai N, Ibrahim O. AI Deep learning-based cancer classification for microarray data: A systematic review. *Journal of Theoretical and Applied Information Technology.* 2021;99:2312–2332. doi: 10.5281/zenodo.6126510

6. *Clinical trials of artificial intelligence systems (radiation diagnostics).* Vasil'ev YuA, Vladzymyrskyy AV, Sharova DE, editors. Moscow: GBUZ «NPKTs DiT DZM»; 2023. EDN: PUIJLD

7. Lee J, Kim KW, Kim SY, et al. Automatic detection method of hepatocellular carcinomas using the non-rigid registration method of multi-phase liver CT images. *J Xray Sci Technol.* 2015;23(3):275–288. doi: 10.3233/XST-150487

8. Patel BN, Boltyenkov AT, Martinez MG, et al. Cost-effectiveness of dual-energy CT versus multiphasic single-energy CT and MRI for characterization of incidental indeterminate renal lesions. *Abdom Radiol (NY).* 2020;45(6):1896–1906. doi: 10.1007/s00261-019-02380-x

9. Marrero JA, Kulik LM, Sirlin CB, et al. Diagnosis, Staging, and Management of Hepatocellular Carcinoma: 2018 Practice Guidance by the American Association for the Study of Liver Diseases. *Hepatology.* 2018;68(2):723–750. doi: 10.1002/hep.29913

10. Ayuso C, Rimola J, Vilana R, et al. Diagnosis and staging of hepatocellular carcinoma (HCC): current guidelines. *Eur J Radiol.* 2018;101:72–81. doi: 10.1016/j.ejrad.2018.01.025

11. *Liver cancer (hepatocellular). Clinical guidelines.* ID 1. Approved by the Scientific and Practical Council of the Ministry of Health of the Russian Federation. 2022. Available from: https://cr.minzdrav.gov.ru/schema/1_3 (In Russ)

12. Rahman H, Bukht TFN, Imran A, et al. A Deep Learning Approach for Liver and Tumor Segmentation in CT Images Using ResUNet. *Bioengineering (Basel).* 2022;9(8):368. doi: 10.3390/bioengineering9080368

13. Maqsood M, Bukhari M, Ali Z, et al. A Residual-Learning-Based Multi-Scale Parallel-Convolutions- Assisted Efficient CAD System for Liver Tumor Detection. *Mathematics.* 2021;9(10):1133. doi: 10.3390/math9101133

14. Khan RA, Luo Y, Wu FX. RMS-UNet: Residual multi-scale UNet for liver and lesion segmentation. *Artif Intell Med.* 2022;124:102231. doi: 10.1016/j.artmed.2021.102231

15. Affane A, Kucharski A, Chapuis P, et al. Segmentation of Liver Anatomy by Combining 3D U-Net Approaches. *Applied Sciences.* 2021;11(11):4895. doi: 10.3390/app11114895

16. Han X, Wu X, Wang S, et al. Automated segmentation of liver segment on portal venous phase MR images using a 3D convolutional neural network. *Insights Imaging.* 2022;13(1):26. doi: 10.1186/s13244-022-01163-1

17. Wang J, Zhang X, Guo L, et al. Multi-scale attention and deep supervision-based 3D UNet for automatic liver segmentation from CT. *Math Biosci Eng.* 2023;20(1):1297–1316. doi: 10.3934/mbe.2023059

18. Kashala KG, Song Y, Liu Z. Optimization of FireNet for Liver Lesion Classification. *Electronics.* 2020;9(8):1237. doi: 10.3390/electronics9081237

19. Trivizakis E, Manikis GC, Nikiforaki K, et al. Extending 2-D Convolutional Neural Networks to 3-D for Advancing Deep Learning Cancer Classification With Application to MRI Liver Tumor Differentiation. *IEEE J Biomed Health Inform.* 2019;23(3):923–930. doi: 10.1109/JBHI.2018.2886276

20. Zhou J, Wang W, Lei B, et al. Automatic Detection and Classification of Focal Liver Lesions Based on Deep Convolutional Neural Networks: A Preliminary Study. *Front Oncol.* 2021;10:581210. doi: 10.3389/fonc.2020.581210

21. Rela M, Rao SN, Patil RR. Performance analysis of liver tumor classification using machine learning algorithms. *International Journal of Advanced Technology and Engineering Exploration.* 2022;9(86):143–154. doi: 10.19101/IJATEE.2021.87465

22. Oberai A, Varghese B, Cen S, et al. Deep learning based classification of solid lipid-poor contrast enhancing renal masses using contrast enhanced CT. *Br J Radiol.* 2020;93(1111):20200002. doi: 10.1259/bjr.20200002

23. Lin Z, Cui Y, Liu J, et al. Automated segmentation of kidney and renal mass and automated detection of renal mass in CT urography using 3D U-Net-based deep convolutional neural network. *Eur Radiol.* 2021;31(7):5021–5031. doi: 10.1007/s00330-020-07608-9

24. Toda N, Hashimoto M, Arita Y, et al. Deep Learning Algorithm for Fully Automated Detection of Small (≤4 cm) Renal Cell Carcinoma in Contrast-Enhanced Computed Tomography Using a Multicenter Database. *Invest Radiol.* 2022;57(5):327–333. doi: 10.1097/RLI.0000000000000842

25. Ding Y, Chen Z, Wang Z, et al. Three-dimensional deep neural network for automatic delineation of cervical cancer in planning computed tomography images. *J Appl Clin Med Phys.* 2022;23(4):e13566. doi: 10.1002/acm2.13566

26. Zhu XL, Shen HB, Sun H, et al. Improving segmentation and classification of renal tumors in small sample 3D CT images using transfer learning with convolutional neural networks. *Int J Comput Assist Radiol Surg.* 2022;17(7):1303–1311. doi: 10.1007/s11548-022-02587-2

27. Hsiao CH, Sun TL, Lin PC, et al. A deep learning-based precision volume calculation approach for kidney and tumor segmentation on computed tomography images. *Comput Methods Programs Biomed.* 2022;221:106861. doi: 10.1016/j.cmpb.2022.106861

28. Hsiao CH, Lin PC, Chung LA, et al. A deep learning-based precision and automatic kidney segmentation system using efficient feature pyramid networks in computed tomography images. *Comput Methods Programs Biomed.* 2022;221:106854. doi: 10.1016/j.cmpb.2022.106854

29. Islam MN, Hasan M, Hossain MK, et al. Vision transformer and explainable transfer learning models for auto detection of kidney cyst, stone and tumor from CT-radiography. *Sci Rep.* 2022;12(1):11440. doi: 10.1038/s41598-022-15634-4

30. Yang L, Gao L, Arefan D, et al. A CT-based radiomics model for predicting renal capsule invasion in renal cell carcinoma. *BMC Med Imaging.* 2022;22(1):15. doi: 10.1186/s12880-022-00741-5

31. Shehata M, Alksas A, Abouelkheir RT, et al. A Comprehensive Computer-Assisted Diagnosis System for Early Assessment of Renal Cancer Tumors. *Sensors (Basel).* 2021;21(14):4928. doi: 10.3390/s21144928

32. Kulikovskiy VF, Shkodkin SV, Batishchev SA, et al. Modern research and thinking about the epidemiology and pathogenesis of urolithiasis. *Nauchnyi rezul'tat. Meditsina i farmatsiya.* 2016;2(4):4–12. EDN: NSGAXL doi: 10.18413/2313-8955-2016-2-4-4-12

33. Gadzhiev N, Prosyannikov M, Malkhasyan V, et al. Urolithiasis prevalence in the Russian Federation: analysis of trends over a 15-year period. *World J Urol.* 2021.Vol. 39(10):3939–3944. doi: 10.1007/s00345-021-03729-y

34. *Urology. Russian Clinical Recommendations.* Alyaev YuG, Glybochko PV, Pushkar' DYu, editors. Moscow: GEOTARMedia; 2016. (In Russ).

35. Caglayan A, Horsanali MO, Kocadurdu K, et al. Deep learning model-assisted detection of kidney stones on computed tomography. *Int Braz J Urol.* 2022;48(5):830–839. doi: 10.1590/S1677-5538.IBJU.2022.0132

36. Elton DC, Turkbey EB, Pickhardt PJ, Summers RM. A deep learning system for automated kidney stone detection and volumetric segmentation on noncontrast CT scans. *Med Phys.* 2022;49(4):2545–2554. doi: 10.1002/mp.15518

37. He Z, An L, Chang Z, Wu W. Comment on "Deep learning computer vision algorithm for detecting kidney stone composition". *World J Urol.* 2021;39(1):291. doi: 10.1007/s00345-020-03181-4

38. Doyle PW, Kavoussi NL. Machine learning applications to enhance patient specific care for urologic surgery. *World J Urol.* 2022;40(3):679–686. doi: 10.1007/s00345-021-03738-x

39. Neymark AI, Neymark BA, Ershov AV, et al. The use of intelligent analysis (IA) in determining the tactics of treating patients with nephrolithiasis. *Urologia Journal.* 2023;(3915603231162881). doi: 10.1177/03915603231162881

40. Kadlec AO, Ohlander S, Hotaling J, et al. Nonlinear logistic regression model for outcomes after endourologic procedures: a novel predictor. *Urolithiasis.* 2014;42(4):323–330. doi: 10.1007/s00240-014-0656-1

41. Black KM, Law H, Aldoukhi A, et al. Deep learning computer vision algorithm for detecting kidney stone composition. *BJU Int.* 2020;125(6):920–924. doi: 10.1111/bju.15035

42. Zhang GM, Sun H, Xue HD, et al. Prospective prediction of the major component of urinary stone composition with dual-source dual-energy CT in vivo. *Clin Radiol.* 2016;71(11):1178–1183. doi: 10.1016/j.crad.2016.07.012

43. Chaytor RJ, Rajbabu K, Jones PA, McKnight L. Determining the composition of urinary tract calculi using stone-targeted dual-energy CT: evaluation of a low-dose scanning protocol in a clinical environment. *Br J Radiol.* 2016;89(1067):20160408. doi: 10.1259/bjr.20160408

44. Kapanadze LB, Serova NS, Rudenko VI. Application of dual-energy computer tomography in diagnostics of urolithiasis. *REJR.* 2017;7(3):165–173. EDN: ZWBLYL doi: 10.21569/2222-7415-2017-7-3-165-173

45. Cui Y, Sun Z, Ma S, et al. Automatic Detection and Scoring of Kidney Stones on Noncontrast CT Images Using S.T.O.N.E. Nephrolithometry: Combined Deep Learning and Thresholding Methods. *Mol Imaging Biol.* 2021;23(3):436–445. doi: 10.1007/s11307-020-01554-0

46. Okhunov Z, Friedlander JI, George AK, et al. S.T.O.N.E. nephrolithometry: novel surgical classification system for kidney calculi. *Urology.* 2013;81(6):1154–1159. doi: 10.1016/j.urology.2012.10.083

47. Yildirim K, Bozdag PG, Talo M, et al. Deep learning model for automated kidney stone detection using coronal CT images. *Comput Biol Med.* 2021;135:104569. doi: 10.1016/j.compbiomed.2021.104569

48. Kodenko MR, Reshetnikov RV, Makarova TA. Modification of quality assessment tool for artificial intelligence diagnostic test accuracy studies (QUADAS-CAD). *Digital Diagnostics.* 2022;3(1S):4–5. EDN: KNBHOJ doi: 10.17816/DD105567

49. Schwartz FR, Clark DP, Ding Y, Ramirez-Giraldo JC. Evaluating renal lesions using deep-learning based extension of dual-energy FoV in dual-source CT-A retrospective pilot study. *Eur J Radiol.* 2021;139:109734. doi: 10.1016/j.ejrad.2021.109734

50. Li W, Diao K, Wen Y, et al. High-strength deep learning image reconstruction in coronary CT angiography at 70-kVp tube voltage significantly improves image quality and reduces both radiation and contrast doses. *Eur Radiol.* 2022;32(5):2912–2920. doi: 10.1007/s00330-021-08424-5

51. Bae JS, Lee JM, Kim SW, et al. Low-contrast-dose liver CT using low monoenergetic images with deep learning-based denoising for assessing hepatocellular carcinoma: a randomized controlled noninferiority trial. *Eur Radiol.* 2023;33(6):4344–4354. doi: 10.1007/s00330-022-09298-x

СПИСОК ЛИТЕРАТУРЫ

1. Ильяшенко О.Ю., Лукьянченко Е.Л. Возможности применения компьютерного зрения для аналитики данных в медицине // Известия Саратовского университета. Новая серия. Серия : Математика. Механика. Информатика. 2022. Т. 22, № 2. С. 224–232. EDN: MCSLKQ doi: 10.18500/1816-9791-2022-22-2-224-232

2. Алексеева М.Г., Зубов А.И., Новиков М.Ю. Искусственный интеллект в медицине // Международный научно-исследовательский журнал. 2022. Т. 7, № 121. С. 10–13. EDN: JMMMDF doi: 10.23670/IRJ.2022.121.7.038

3. Гусев А.В., Владзимирский А.В., Шарова Д.Е., Арзамасов К.М., Храмов А.Е. Развитие исследований и разработок в сфере технологий искусственного интеллекта для здравоохранения в Российской Федерации: итоги 2021 года // Digital Diagnostics. 2022. Т. 3, № 3. С. 178–194. EDN: KHWQWZ doi: 10.17816/DD107367

4. Wang L., Wang H., Huang Y., et al. Trends in the application of deep learning networks in medical image analysis: Evolution between 2012 and 2020 // Eur J Radiol. 2022. Vol. 146. P. 110069. doi: 10.1016/j.ejrad.2021.110069

5. Alrefai N., Ibrahim O. AI Deep learning-based cancer classification for microarray data: A systematic review // Journal of Theoretical and Applied Information Technology. 2021. Vol. 99. P. 2312–2332. doi: 10.5281/zenodo.6126510

6. Клинические испытания систем искусственного интеллекта (лучевая диагностика) / под ред. Ю.А. Васильева, А.В. Владзимирского, Д.Е. Шаровой, и др. Москва : ГБУЗ «НПКЦ ДиТ ДЗМ», 2023. EDN: PUIJLD

7. Lee J., Kim K.W., Kim S.Y., et al. Automatic detection method of hepatocellular carcinomas using the non-rigid registration method of multi-phase liver CT images // J Xray Sci Technol. 2015. Vol. 23, N 3. P. 275–288. doi: 10.3233/XST-150487

8. Patel B.N., Boltyenkov A.T., Martinez M.G., et al. Cost-effectiveness of dual-energy CT versus multiphasic single-energy CT and MRI for characterization of incidental indeterminate renal lesions // Abdom Radiol (NY). 2020. Vol. 45, N 6. P. 1896–1906. doi: 10.1007/s00261-019-02380-x

9. Marrero J.A., Kulik L.M., Sirlin C.B., et al. Diagnosis, Staging, and Management of Hepatocellular Carcinoma: 2018 Practice Guidance by the American Association for the Study of

Liver Diseases // Hepatology. 2018. Vol. 68, N 2. P. 723–750. doi: 10.1002/hep.29913

10. Ayuso C., Rimola J., Vilana R., et al. Diagnosis and staging of hepatocellular carcinoma (HCC): current guidelines // Eur J Radiol. 2018. Vol. 101. P. 72–81. doi: 10.1016/j.ejrad.2018.01.025

11. Клинические рекомендации — Рак печени (гепатоцеллюлярный). ID 1. Одобрено Научно-практическим Советом Минздрава РФ. 2022. Режим доступа: https://cr.minzdrav.gov.ru/schema/1_3 Дата обращения: 03.04.2023

12. Rahman H., Bukht T.F.N., Imran A., et al. A Deep Learning Approach for Liver and Tumor Segmentation in CT Images Using ResUNet // Bioengineering (Basel). 2022. Vol. 9, N 8. P. 368. doi: 10.3390/bioengineering9080368

13. Maqsood M., Bukhari M., Ali Z., et al. A Residual-Learning-Based Multi-Scale Parallel-Convolutions- Assisted Efficient CAD System for Liver Tumor Detection // Mathematics. 2021. Vol. 9, N 10. P. 1133. doi: 10.3390/math9101133

14. Khan R.A., Luo Y., Wu F.X. RMS-UNet: Residual multi-scale UNet for liver and lesion segmentation // Artif Intell Med. 2022. Vol. 124. P. 102231. doi: 10.1016/j.artmed.2021.102231

15. Affane A., Kucharski A., Chapuis P., et al. Segmentation of Liver Anatomy by Combining 3D U-Net Approaches // Applied Sciences. 2021. Vol. 11, N 11. P. 4895. doi: 10.3390/app11114895

16. Han X., Wu X., Wang S., et al. Automated segmentation of liver segment on portal venous phase MR images using a 3D convolutional neural network // Insights Imaging. 2022. Vol. 13, N 1. P. 26. doi: 10.1186/s13244-022-01163-1

17. Wang J., Zhang X., Guo L., et al. Multi-scale attention and deep supervision-based 3D UNet for automatic liver segmentation from CT // Math Biosci Eng. 2023. Vol. 20, N 1. P. 1297–1316. doi: 10.3934/mbe.2023059

18. Kashala K.G., Song Y., Liu Z. Optimization of FireNet for Liver Lesion Classification // Electronics. 2020. Vol. 9, N 8. P. 1237. doi: 10.3390/electronics9081237

19. Trivizakis E., Manikis G.C., Nikiforaki K., et al. Extending 2-D Convolutional Neural Networks to 3-D for Advancing Deep Learning Cancer Classification With Application to MRI Liver Tumor Differentiation // IEEE J Biomed Health Inform. 2019. Vol. 23, N 3. P. 923–930. doi: 10.1109/JBHI.2018.2886276

20. Zhou J., Wang W., Lei B., et al. Automatic Detection and Classification of Focal Liver Lesions Based on Deep Convolutional Neural Networks: A Preliminary Study // Front Oncol. 2021. Vol. 10. P. 581210. doi: 10.3389/fonc.2020.581210

21. Rela M., Rao S.N., Patil R.R. Performance analysis of liver tumor classification using machine learning algorithms // International Journal of Advanced Technology and Engineering Exploration. 2022. Vol. 9, N 86. P. 143–154. doi: 10.19101/IJATEE.2021.87465

22. Oberai A., Varghese B., Cen S., et al. Deep learning based classification of solid lipid-poor contrast enhancing renal masses using contrast enhanced CT // Br J Radiol. 2020. Vol. 93, N 1111. P. 20200002. doi: 10.1259/bjr.20200002

23. Lin Z., Cui Y., Liu J., et al. Automated segmentation of kidney and renal mass and automated detection of renal mass in CT urography using 3D U-Net-based deep convolutional neural network // Eur Radiol. 2021. Vol. 31, N 7. P. 5021–5031. doi: 10.1007/s00330-020-07608-9

24. Toda N., Hashimoto M., Arita Y., et al. Deep Learning Algorithm for Fully Automated Detection of Small (≤4 cm) Renal Cell Carcinoma in Contrast-Enhanced Computed Tomography Using a Multicenter Database // Invest Radiol. 2022. Vol. 57, N 5. P. 327–333. doi: 10.1097/RLI.0000000000000842

25. Ding Y., Chen Z., Wang Z., et al. Three-dimensional deep neural network for automatic delineation of cervical cancer in planning computed tomography images // J Appl Clin Med Phys. 2022. Vol. 23, N 4. P. e13566. doi: 10.1002/acm2.13566

26. Zhu X.L., Shen H.B., Sun H., et al. Improving segmentation and classification of renal tumors in small sample 3D CT images using transfer learning with convolutional neural networks // Int J Comput Assist Radiol Surg. 2022. Vol. 17, N 7. P. 1303–1311. doi: 10.1007/s11548-022-02587-2

27. Hsiao C.H., Sun T.L., Lin P.C., et al. A deep learning-based precision volume calculation approach for kidney and tumor segmentation on computed tomography images // Comput Methods Programs Biomed. 2022. Vol. 221. P. 106861. doi: 10.1016/j.cmpb.2022.106861

28. Hsiao C.H., Lin P.C., Chung L.A., et al. A deep learning-based precision and automatic kidney segmentation system using efficient feature pyramid networks in computed tomography images // Comput Methods Programs Biomed. 2022. Vol. 221. P. 106854. doi: 10.1016/j.cmpb.2022.106854

29. Islam M.N., Hasan M., Hossain M.K., et al. Vision transformer and explainable transfer learning models for auto detection of kidney cyst, stone and tumor from CT-radiography // Sci Rep. 2022. Vol. 12, N 1. P. 11440. doi: 10.1038/s41598-022-15634-4

30. Yang L., Gao L., Arefan D., et al. A CT-based radiomics model for predicting renal capsule invasion in renal cell carcinoma // BMC Med Imaging. 2022. Vol. 22, N 1. P. 15. doi: 10.1186/s12880-022-00741-5

31. Shehata M., Alksas A., Abouelkheir R.T., et al. A Comprehensive Computer-Assisted Diagnosis System for Early Assessment of Renal Cancer Tumors // Sensors (Basel). 2021. Vol. 21, N 14. P. 4928. doi: 10.3390/s21144928

32. Куликовский В.Ф., Шкодкин С.В., Батищев С.А., и др. Современные представления о эпидемиологии и патогенезе уролитиаза // Научный результат. Медицина и фармация. 2016. Т. 2, № 4. С. 4–12. EDN: NSGAXL doi: 10.18413/2313-8955-2016-2-4-4-12

33. Gadzhiev N., Prosyannikov M., Malkhasyan V., et al. Urolithiasis prevalence in the Russian Federation: analysis of trends over a 15-year period // World J Urol. 2021.Vol. 39, N 10. P. 3939–3944. doi: 10.1007/s00345-021-03729-y

34. Урология. Российские клинические рекомендации / под ред. Ю.Г. Аляева, П.В. Глыбочко, Д.Ю. Пушкаря. Москва : ГЭОТАРМедиа, 2016.

35. Caglayan A., Horsanali M.O., Kocadurdu K., et al. Deep learning model-assisted detection of kidney stones on computed tomography // Int Braz J Urol. 2022. Vol. 48, N 5. P. 830–839. doi: 10.1590/S1677-5538.IBJU.2022.0132

36. Elton D.C., Turkbey E.B., Pickhardt P.J., Summers R.M. A deep learning system for automated kidney stone detection and volumetric segmentation on noncontrast CT scans // Med Phys. 2022. Vol. 49, N 4. P. 2545–2554. doi: 10.1002/mp.15518
37. He Z., An L., Chang Z., Wu W. Comment on "Deep learning computer vision algorithm for detecting kidney stone composition" // World J Urol. 2021. Vol. 39, N 1. P. 291. doi: 10.1007/s00345-020-03181-4
38. Doyle P.W., Kavoussi N.L. Machine learning applications to enhance patient specific care for urologic surgery // World J Urol. 2022. Vol. 40, N 3. P. 679–686. doi: 10.1007/s00345-021-03738-x
39. Neymark A.I., Neymark B.A., Ershov A.V., et al. The use of intelligent analysis (IA) in determining the tactics of treating patients with nephrolithiasis // Urologia Journal. 2023. N 3915603231162881. doi: 10.1177/03915603231162881
40. Kadlec A.O., Ohlander S., Hotaling J., et al. Nonlinear logistic regression model for outcomes after endourologic procedures: a novel predictor // Urolithiasis. 2014. Vol. 42, N 4. P. 323–330. doi: 10.1007/s00240-014-0656-1
41. Black K.M., Law H., Aldoukhi A., et al. Deep learning computer vision algorithm for detecting kidney stone composition // BJU Int. 2020. Vol. 125, N 6. P. 920–924. doi: 10.1111/bju.15035
42. Zhang G.M., Sun H., Xue H.D., et al. Prospective prediction of the major component of urinary stone composition with dual-source dual-energy CT in vivo // Clin Radiol. 2016. Vol. 71, N 11. P. 1178–1183. doi: 10.1016/j.crad.2016.07.012
43. Chaytor R.J., Rajbabu K., Jones P.A., McKnight L. Determining the composition of urinary tract calculi using stone-targeted dual-energy CT: evaluation of a low-dose scanning protocol in a clinical environment // Br J Radiol. 2016. Vol. 89, N 1067. P. 20160408. doi: 10.1259/bjr.20160408
44. Капанадзе Л.Б., Серова Н.С., Руденко В.И. Аспекты применения двухэнергетической компьютерной томографии в диагностике мочекаменной болезни // REJR. 2017. Т. 7, № 3. С. 165–173. EDN: ZWBLYL doi: 10.21569/2222-7415-2017-7-3-165-173
45. Cui Y., Sun Z., Ma S., et al. Automatic Detection and Scoring of Kidney Stones on Noncontrast CT Images Using S.T.O.N.E. Nephrolithometry: Combined Deep Learning and Thresholding Methods // Mol Imaging Biol. 2021. Vol. 23, N 3. P. 436–445. doi: 10.1007/s11307-020-01554-0
46. Okhunov Z., Friedlander J.I., George A.K., et al. S.T.O.N.E. nephrolithometry: novel surgical classification system for kidney calculi // Urology. 2013. Vol. 81, N 6. P. 1154–1159. doi: 10.1016/j.urology.2012.10.083
47. Yildirim K., Bozdag P.G., Talo M., et al. Deep learning model for automated kidney stone detection using coronal CT images // Comput Biol Med. 2021. Vol. 135. P. 104569. doi: 10.1016/j.compbiomed.2021.104569
48. Коденко М.Р., Решетников Р.В., Макарова Т.А. Инструмент оценки качества исследований диагностической точности алгоритмов искусственного интеллекта (QUADAS-CAD) // Digital Diagnostics. 2022. Т. 3, № 1S. С. 4–5. EDN: KNBHOJ doi: 10.17816/DD105567
49. Schwartz F.R., Clark D.P., Ding Y., Ramirez-Giraldo J.C. Evaluating renal lesions using deep-learning based extension of dual-energy FoV in dual-source CT-A retrospective pilot study // Eur J Radiol. 2021. Vol. 139. P. 109734. doi: 10.1016/j.ejrad.2021.109734
50. Li W., Diao K., Wen Y., et al. High-strength deep learning image reconstruction in coronary CT angiography at 70-kVp tube voltage significantly improves image quality and reduces both radiation and contrast doses // Eur Radiol. 2022. Vol. 32, N 5. P. 2912–2920. doi: 10.1007/s00330-021-08424-5
51. Bae J.S., Lee J.M., Kim S.W., et al. Low-contrast-dose liver CT using low monoenergetic images with deep learning-based denoising for assessing hepatocellular carcinoma: a randomized controlled noninferiority trial // Eur Radiol. 2023. Vol. 33, N 6. P. 4344–4354. doi: 10.1007/s00330-022-09298-x

AUTHORS' INFO

*** Nikolay B. Nechaev,** MD, Cand. Sci. (Medicine);
address: 24-1 Petrovka Str., Moscow, 127051, Russia;
ORCID: 0009-0007-9219-7726;
eLibrary SPIN: 3232-1545;
e-mail: NechaevNB@zdrav.mos.ru

Yuriy A. Vasilev, MD, Cand. Sci. (Medicine);
ORCID: 0000-0002-0208-5218;
eLibrary SPIN: 4458-5608;
e-mail: npcmr@zdrav.mos.ru

Anton V. Vladzymyrskyy, MD, Dr. Sci. (Medicine), Professor;
ORCID: 0000-0002-2990-7736;
eLibrary SPIN: 3602-7120;
e-mail: VladzimirskijAV@zdrav.mos.ru

ОБ АВТОРАХ

*** Нечаев Николай Борисович,** канд. мед. наук;
адрес: Россия, 127051, г. Москва, ул. Петровка, д. 24, стр. 1;
ORCID: 0009-0007-9219-7726;
eLibrary SPIN: 3232-1545;
e-mail: NechaevNB@zdrav.mos.ru

Васильев Юрий Александрович, канд. мед. наук;
ORCID: 0000-0002-0208-5218;
eLibrary SPIN: 4458-5608;
e-mail: npcmr@zdrav.mos.ru

Владзимирский Антон Вячеславович, д-р мед. наук, профессор;
ORCID: 0000-0002-2990-7736;
eLibrary SPIN: 3602-7120;
e-mail: VladzimirskijAV@zdrav.mos.ru

* Corresponding author / Автор, ответственный за переписку

Kirill M. Arzamasov, MD, Cand. Sci. (Medicine);
ORCID: 0000-0001-7786-0349;
eLibrary SPIN: 3160-8062;
e-mail: ArzamasovKM@zdrav.mos.ru

David U. Shikhmuradov, MD;
ORCID: 0000-0003-1597-5786;
eLibrary SPIN: 9641-0913;
e-mail: ShikhmuradovDU@zdrav.mos.ru

Andrey V. Pankratov, MD;
ORCID: 0009-0008-4741-4530;
e-mail: PankratovAV3@zdrav.mos.ru

Iliya V. Ulyanov, MD;
ORCID: 0000-0002-8330-6069;
eLibrary SPIN: 5898-3242;
e-mail: UlyanovIV2@zdrav.mos.ru

Nikolay B. Nechaev, MD, Cand. Sci. (Medicine);
ORCID: 0009-0007-9219-7726;
eLibrary SPIN: 3232-1545;
e-mail: NechaevNB@zdrav.mos.ru

Арзамасов Кирилл Михайлович, канд. мед. наук;
ORCID: 0000-0001-7786-0349;
eLibrary SPIN: 3160-8062;
e-mail: ArzamasovKM@zdrav.mos.ru

Шихмурадов Давид Уружбегович;
ORCID: 0000-0003-1597-5786;
eLibrary SPIN: 9641-0913;
e-mail: ShikhmuradovDU@zdrav.mos.ru

Панкратов Андрей Вячеславович;
ORCID: 0009-0008-4741-4530;
e-mail: PankratovAV3@zdrav.mos.ru

Ульянов Илья Владимирович;
ORCID: 0000-0002-8330-6069;
eLibrary SPIN: 5898-3242;
e-mail: UlyanovIV2@zdrav.mos.ru

Нечаев Николай Борисович, канд. мед. наук;
ORCID: 0009-0007-9219-7726;
eLibrary SPIN: 3232-1545;
e-mail: NechaevNB@zdrav.mos.ru

Appendix 1

Table 1. Architectures and diagnostic metrics of deep machine-learning algorithms for detecting abdominal pathologies by imaging

1	2	3	4	5
Purpose	**Authors, year**	**Sample size**	**Architecture**	**Claimed diagnostic accuracy parameters**
Segmentation of the liver and its structures	M. Maqsood et al., 2021 [13]	4 studies	ResUNet with multiscale parallel convolution blocks after Res blocks	Segmentation of the liver – Dice coefficient: 0.77 – Accuracy: 93%
	R.Z. Khan et al., 2022 [14]	3 studies (Dircadb) 19 studies (LiTS) 4 studies (Silver07) 1 study (Chaos)	ResUNet basic block: three sequential Conv2D layers with kernel-based convolution expansion (three expansion rates: 1, 2, and 4)	1) Segmentation of the liver Dice's coefficients: – 0.97 for the Dircadb dataset – 0.97 for the LiTS dataset – 0.97 for the Sliver07 dataset – 0.95 for the Chaos dataset 2) Segmentation of liver neoplasms Dice coefficients: – 0.92 for the Dircadb dataset – 0.87 for the LiTS dataset
	H. Rahman et al., 2022 [12]	4 studies	Sequential use of ResUNet for liver segmentation, with subsequent use of the findings in another ResUNet for neoplasm segmentation	Segmentation of the liver and liver neoplasms: – Dice coefficient: 0.99 – Accuracy: 99.6%
	A. Affane et al., 2021 [15]	1 study	Three 3D U-Net modifications: 1) 3D U-Net and classic network 2) 3D MultiRes U-Net. The resolution path block is used before skip connection. Inside the Conv block: three linked 3D convolutions, 3×3×3 (first, 32 filters; remainder, 16 filters each), which are pooled, normalized, and summed up with input data processed using Conv3D (1 × 1 × 1, 64 filters). This is followed by sigmoid activation. 3) 3D Dense U-Net: with residual pooling after each Conv layer	Segmentation of the liver Dice coefficients: – 0.86 for the 3D MultiRes U-Net – 0.84 for the 3D Dense U-Net – 0.73 for the 3D U-Net
	J. Wang et al., 2023 [17]	8 studies (Dircadb) 15 studies (LiTS)	3D MAD-UNet: Long-short skip connection (LSSC) and attention module are used for all decoder levels.	Segmentation of liver neoplasms Dice coefficients: – 0.96 for the 3D U-Net + LSSC + MA with the LiTS dataset – 0.96 for the 3D U-Net + LSSC + MA with the Dircadb dataset – 0.92 for the 3D U-Net with the LiTS dataset – 0.89 for the 3D U-Net with the Dircadb dataset

Table 1. Continued

1	2	3	4	5
Classification of liver neoplasms by nosological entities	K.G. Kashala et al., 2020 [18]	250 studies	Modified SqeezeNet model with a bypass after blocks 2, 4, 6, and 8, and Conv2D (1 × 1) before pooling expand blocks	– Accuracy: 81.8% – F1-score: 0.80
	J. Zhou et al., 2021 [20]	154 studies	2.5D Faster R-CNN was used for segmentation. 3D ResNet-18 (Conv3D-based modification) was used for classification.	– Accuracy: 82.5% for distinguishing between benign/ malignant neoplasms – Accuracy: 73.4% for detecting one of the six conditions (hepatocellular carcinoma, cholangiocarcinoma, metastasis, hemangioma, hyperplasia, and cyst)
	M. Rela et al., 2022 [21]	14 studies	Support vectors method, k-nearest neighbors method	1) Support vectors method – Accuracy: 84.6% – F1-score: 0.80 2) k-nearest neighbors method – Accuracy: 76.92% – F1-score: 0.76
Segmentation of the kidneys and kidney neoplasms	Y. Ding et al., 2022 [25]	30 studies	– U-Net – V-Net, a modification using ResNet blocks for 3D images	Segmentation of the kidneys: 1) Dice coefficient for the left kidney – 0.93 for U-Net – 0.92 for V-Net 2) Dice coefficient for the right kidney – 0.91 for U-Net – 0.92 for V-Net
	Z. Lin et al., 2021 [23]	66 studies	3D U-Net	1) Segmentation of the kidneys – Dice coefficient: 0.97 2) Segmentation of kidney neoplasms – Dice coefficient: 0.84 3) Segmentation of kidney cysts – Dice coefficient: 0.54

Table 1. Continued

1	2	3	4	5
Segmentation of the kidneys and kidney neoplasms	C.H. Hsiao et al., 2022 [27]	90 studies	U-Net with ResNet-41 or EffectiveNet architectures used as encoder blocks	Segmentation of the kidneys 1) Dice coefficient (data with preprocessing and U-Net with an encoder) – 0.96 for EfficientNet-B7 – 0.95 for ResNet-41 – 0.95 for EfficientNet-B4 – 0.95 for EfficientNet-B4, fine-tuning 2) Dice coefficient (data without preprocessing and U-Net with an encoder) – 0.95 for EfficientNet-B4, fine-tuning – 0.93 for ResNet-41 – 0.29 for EfficientNet-B4 – 0,27 for EfficientNet-B7 3) Segmentation of kidney neoplasms Dice coefficient: 0.41 (EfficientNet-B5)
	C.H. Hsiao et al., 2022 [28]	56 studies (KiTS19)	EffectiveNet-B5 (encoder); Feature pyramid network (decoder)	Segmentation of the kidneys and kidney neoplasms Dice coefficient: 0.95
Segmentation and classification of kidney neoplasms by nosological entities	M.H. Islam et al., 2022 [29]	~1,000 scans	Six architectures – Modified VGG16 – Inception v3 – ResNet50 – EANet – Swin Transformers – CCT	Classification of kidney neoplasms 1) VGG16 architecture – Accuracy: 98.2% – Mean F1-score: 0.98 – Mean AUC: 0.99 2) Inception v3 architecture – Accuracy: 61.6% – Mean F1-score: 0.59 – Mean AUC: 0.85 3) ResNet50 architecture – Accuracy: 73.8% – Mean F1-score: 0.74 – Mean AUC: 0.93 4) EANet architecture: – Accuracy: 77.0% – Mean F1-score: 0.77 – Mean AUC: 0.96 5) Swin Transformers architecture – Accuracy: 99.3% – Mean F1-score: 0.99 – Mean AUC: 0.99 6) CCT architecture – Accuracy: 96.5% – Mean F1-score: 0.97 – Mean AUC: 0.99

Table 1. Continued

1	2	3	4	5
Segmentation and classification of kidney neoplasms by nosological entities	Toda N. et al., 2022 [24]	132 studies	2D U-Net for kidney segmentation 3D U-Net for neoplasm segmentation and classification	Classification of kidney neoplasms – Accuracy: 87.5% – AUC: 0.93
	Zhu X.L. et al., 2022 [26]	20 studies	FS-net: source data were entered into a fine-tuned 3D U-Net. The resulting mask was pooled with the source data and entered into the fine-tuned 3D U-Net. Segmented kidney and kidney area data were received from the resulting mask. A texture analysis of the segmented data was performed to create features. A fine-tuned 3D U-Net was used for the kidney area to create features. The resulting features were used in the support vectors method.	1) Segmentation of the kidneys –Dice coefficient: 0.97 (KiTS19) – Dice coefficient: 0.97 (own dataset) 2) Segmentation of kidney neoplasms – Dice coefficient: 0.79 (KiTS19) – Dice coefficient: 0.77 (own dataset)
Classification of kidney neoplasms and their characteristics	L. Yang et al., 2022 [30]	120 studies	Features were created for manually segmented kidneys using the Pyradiomiocs library. A feedforward network was used for the features.	Classification of kidney neoplasms: AUC: – 0.76 in the pre-contrast phase – 0.79 in the corticomedullary phase – 0.77 in the nephrographic phase
	M. Shehata et al., 2021 [31]	–	The following features were created for manually segmented kidneys with a neoplasm: morphological (shape assessment), textural, and functional. A feedforward network was used for the features to classify them as benign or malignant. A feedforward network was used for malignant features to distinguish between clear cell and nonclear cell cancer	Classification of benign vs. malignant kidney neoplasms – F1-score: 0.98 Classification of kidney cancer – Accuracy: 89.6%
Urinary stone detection by CT	A. Caglayan et al., 2022 [35]	–	xResNet50	Urinary stones <1 cm – Accuracy: 85% – F1-score: 0.85 Urinary stones 1–2 cm – Accuracy: 89% – F1-score: 0.89 Urinary stones >2 cm – Accuracy: 93% – F1-score: 0.93

Table 1. End

1	2	3	4	5
Urinary stone detection by CT	C. Daniel et al., 2022 [36]	90 studies	3D U-Net for kidney segmentation, noise reduction, and cropping the area of interest; 13-layer 3D CNN for classification	– AUC: 0.95 – Specificity: 0.91
	Y. Cui et al., 2021 [45]	117 studies	Sequential use of 3D U-Net architectures for kidney segmentation. The obtained data were used in five 3D U-Net architectures, each intended to classify one STONE score parameter.	Segmentation of the kidneys and sinuses – Dice coefficient: 0.93 Urinary stone detection – Accuracy: 90.3% – AUC: 0.96
	K. Yildirim et al., 2021 [47]	100 studies	xResNet50	– Accuracy: 97% – F1-score: 0.97

DOI: https://doi.org/10.17816/DD625319

Эпистемический статус искусственного интеллекта в медицинских практиках: этические вызовы

А.В. Баева

Московский государственный университет имени М.В. Ломоносова, Москва, Россия

АННОТАЦИЯ

В современных научных исследованиях в последнее время всё чаще появляются дискуссии о том, что в связи с развитием технологий искусственного интеллекта встают вопросы об объективности, правдоподобности и достоверности знания, а также о том, не заменят ли эти технологии фигуру эксперта как ту инстанцию, которая до сих пор выступала гарантом объективности и центром принятия решений. Современные историки науки Л. Дастон и П. Галисон в своей книге, посвящённой истории научной объективности, говорят о сменяемости «эпистемических добродетелей», в качестве одной из которых с определённого момента утвердилась и объективность. При этом выдвижение той или иной добродетели, регулирующей научную самость, то есть выступающей нормативным принципом для учёного при выборе способа видения и научной практики, зависит от принятия решений в трудных случаях, требующих воли и ограничения самости. В этом смысле эпистемология соединяется с этикой: учёный, руководствуясь определёнными моральными принципами, отдаёт предпочтение тому или иному способу поведения, выбирая, например, не более точное изображение, сделанное от руки, а неретушированную фотографию, возможно, нечёткую, но полученную механически, а значит — более объективную и свободную от какой-либо примеси субъективности. В этой связи небезынтересным представляется эпистемический статус современных технологий на основе искусственного интеллекта, которые всё больше берут на себя функции научной самости, в том числе и в части оказания влияния на принятие конечных решений и получение объективного знания. Так, например, в области медицины роботизированные аппараты уже оказывают существенную поддержку: им передаётся часть функций, например, врача первого звена для сбора и анализа стандартизированных данных о пациенте и диагностики. Есть предположение, что в ближайшее время всё больше обязанностей будет передаваться искусственному интеллекту: обработка данных, разработка новых лекарств и способов лечения, налаживание дистанционного взаимодействия с пациентом и др. Значит ли это, что научная самость может быть заменена алгоритмами на основе искусственного интеллекта, а на смену объективности придёт другая эпистемическая добродетель, окончательно разрывающая связь этики и эпистемологии, — этот вопрос нуждается в исследовании.

Ключевые слова: современные научные практики; объективность; эпистемическая добродетель; научная самость; технологии на основе искусственного интеллекта.

Как цитировать:
Баева А.В. Эпистемический статус искусственного интеллекта в медицинских практиках: этические вызовы // Digital Diagnostics. 2024. Т. 5, № 1. С. 120–132. DOI: https://doi.org/10.17816/DD625319

Рукопись получена: 26.12.2023 **Рукопись одобрена:** 13.02.2024 **Опубликована online:** 11.03.2024

ЭКО-ВЕКТОР

DOI: https://doi.org/10.17816/DD625319

Epistemic status of artificial intelligence in medical practice: Ethical challenges

Angelina V. Baeva

Lomonosov Moscow State University, Moscow, Russia

ABSTRACT

Advances in artificial intelligence have raised controversy in modern scientific research regarding the objectivity, plausibility, and reliability of knowledge, and whether these technologies will replace the expert figure as the authority that has so far served as a guarantor of objectivity and the center of decision-making. In their book on the history of scientific objectivity, modern historians of science L. Duston and P. Galison discuss the interchangeability of "epistemic virtues," which now include objectivity. Moreover, selecting one or another virtue governing the scientific self, i.e., serving as a normative principle for a scientist when adopting a perspective or scientific practice, depends on making decisions in difficult cases that require will and self-restriction. In this sense, epistemology and ethics are intertwined: a scientist, guided by certain moral principles, prefers one or another course of action, such as choosing not a more accurate hand-drawn image but an unretouched photograph, perhaps fuzzy, but obtained mechanically, which means it is more objective and free of subjectivity. In this regard, the epistemic standing of modern artificial intelligence technologies, which increasingly perform the functions of the scientific self, including influencing ultimate decision-making and obtaining objective knowledge, is intriguing. For example, in medicine, robotic devices considerable support and are assigned some of the responsibilities of a primary care physician, such as collecting and analyzing standardized patient data and diagnosis. It is expected that artificial intelligence will take on more tasks such as data processing, development of new drugs and treatment methods, and remote interaction with patients. It remains to be seen whether this implies that the scientific self can be replaced by artificial intelligence algorithms and another epistemic virtue will replace objectivity, thus breaking the link between ethics and epistemology.

Keywords: modern scientific practices; objectivity; epistemic virtue; scientific self; artificial intelligence technologies.

To cite this article:
Baeva AV. Epistemic status of artificial intelligence in medical practice: Ethical challenges. *Digital Diagnostics.* 2024;5(1):120–132. DOI: https://doi.org/10.17816/DD625319

Submitted: 26.12.2023 **Accepted:** 13.02.2024 **Published online:** 11.03.2024

DOI: https://doi.org/10.17816/DD625319

人工智能在医疗实践中的认识论地位：伦理挑战

Angelina V. Baeva

Lomonosov Moscow State University, Moscow, Russia

摘要

最近，在现代科学研究中越来越多地讨论认为，随着人工智能技术的发展，知识的客观性、可信度和可靠性出现了问题，以及这些技术是否会取代专家的问题。科迄今为止，专家一直是客观性的保证和决策中心。现代科学史学家L. Daston和P. Galison在他们关于科学客观性历史的著作中谈到了“认识论美德”的更迭。客观性从某个时刻就确立为其中之一。美德是科学家选择理解方式和科学实践的规范性原则。管理科学信念的特定美德的弘扬过程取决于科学家在需要意志和信念限制的困难情况下做出的决策。从这个意义上说，认识论与伦理学是相通的。科学家在某些道德原则的指导下，倾向于这样或那样的行为方式。例如，科学家选择一张未经修饰的照片，而不是更精确的手绘图像。照片可能模糊不清，但它是通过机械方式获得的，这意味着这样的照片更加客观，未受到任何主观因素的影响。在这方面，以人工智能为基础的现代技术的认识论地位很有意思。这些人工智能技术越来越多地承担科学信念的功能，包括在影响最终决策和获取客观知识方面。例如，在医学领域，机器人设备已经开始提供重要的支持。一些功能被转移到这些机器上，例如一线医生收集和分析病人标准数据的功能和诊断功能。有一种假设认为，在不久的将来，越来越多的职责将移交给人工智能：数据处理、新药物和新疗法的开发、与病人建立远程互动等等。这是否意味着科学可能会被基于人工智能的算法所取代，客观性将被另一种最终打破伦理学与认识论之间联系的认识论美德所取代。这是一个需要探讨的问题。

关键词：现代科学实践；客观性；认识论美德；科学信念；基于人工智能的技术。

引用本文：
Baeva AV. 人工智能在医疗实践中的认识论地位：伦理挑战. *Digital Diagnostics.* 2024;5(1):120–132. DOI: https://doi.org/10.17816/DD625319

收到：26.12.2023 **接受：**13.02.2024 **发布日期：**11.03.2024

INTRODUCTION

The integration of artificial intelligence (AI) technologies into modern scientific practices, especially within the medical field[1], poses significant questions for researchers. Among these questions are the epistemic nature of AI and the ethical challenges it presents. Clarifying the epistemic nature of AI becomes significant as its widespread adoption in scientific practice raises concerns about how technological agency may threaten the decision-making authority of healthcare professionals (HCPs) and challenges the traditional notion of objectivity as a fundamental virtue in scientific inquiry.[2]

In a notable study exploring the historical concept of objectivity, L. Daston and P. Galison [1] used specific material scientific practices, particularly the creation of visual images for scientific atlases. Their study showed that throughout history, objectivity as an epistemic virtue has rested on two main aspects: epistemic virtues (especially objectivity) and visuality.

"Delving into distinct forms of scientific perception places two crucial questions at the forefront: What practices are needed to produce this kind of image? What practices foster the development of a scientific persona capable of such a perception? The history of scientific vision consistently demands this double motion, toward the evolution of an epistemology centered on imagery, on one hand, and toward the ethical refinement of the scientific individual, on the other. Fidelity to nature has always borne a triple responsibility: visual, epistemological, and ethical. However, what unfolds when fidelity itself is abandoned and nature blends with the artifact? We concluded by glimpsing into contemporary scientific atlases: depictions in which creation is synonymous with observation" [1]. These two aspects are intertwined through particular methodologies of visualizing the functional elements of science.[3]

Through alterations in imagery and practices, various epistemic virtues are exemplified. In this respect, the challenge posed by the evolution of visualization through digital and AI technologies impacts both the epistemological virtue of objectivity and the scientific persona. In current scientific discourse, various methods of visualization (including diagrams, maps, photographs, and the creation of atlases) have become dispensable, forming an integral part of argumentation. Concurrently, visualization transcends illustration; it becomes a form of research facilitated by the capabilities of modern digital technologies. A paradigm shift is underway in how science is perceived and practiced, characterized by a transition from representation to presentation. Manipulating the observed object or phenomena now equates to manipulating a visual representation. Computer modeling and imaging represent the subsequent revolutionary frontiers in science following observation and experimentation. In this context, a pressing question emerges regarding the present and prospective state of objectivity as an epistemic virtue in the era of digitization and scientific innovation, where technology and engineering play a significant role in knowledge production, shifting from discovering facts to inventing them. What are the emergent scientific methodologies? Does the evolution of virtues necessitate a re-evaluation of the underlying aims and goods associated with specific practices? Can we define the scientific persona in terms beyond virtues, and how might the incorporation of AI technology reshape it?

MODERN SCIENTIFIC PRACTICES: MATERIALITY AND EPISTEMIC STATUS OF ARTIFACTS

Contemporary scientific practices blur traditional boundaries between objectivity and subjectivity, the abstract and concrete, and the discovered and constructed. Artifacts have played a significant role in shaping scientific knowledge and influencing its main characteristics, notably objectivity, which is now viewed not as an abstract scientific quality detached from the observer but as intimately intertwined with subjective engagement. Advancements in technology have

[1] When we speak of modern scientific practices, we are referring to a fundamentally complicated and empirically diverse scientific space that includes not only propositional knowledge production modes, but also various non-propositional forms using graphs, diagrams, visual images, etc. A research project by A. Mol is one of the most striking examples of how scientific practice not only recognizes its object, but also creates it in practice. This study is dedicated to the multiplicity of medical practice ontology, using the example of the implementation of diseases such as atherosclerosis in branched practices [2].

[2] Objectivity, viewed as an epistemic virtue, emerges during a particular historical phases characterized by intricate coordination between the observer and the practice of observation. It manifests through district visual practices and visualization technologies, as epistemic virtues are cultivated as stable traits in specific research methodologies, thereby shaping a unique scientific identity. Each manifestation of the scientific self-pursues a particular good, implying that sustainable practices are those capable of fostering the evolution of epistemic virtues.

[3] In the second half of the 19th century, the concept of "speaking for nature itself" emerged as a fundamental principle driving a new form of scientific objectivity. Concerned about human interference between nature and science, French physiologist Etienne-Jules Marais and his contemporaries, who studied many visual methods of science, turned to mechanical image reproduction to eliminate potential biases. Employing polygraphs, photographs, and other technologies, they attempt to create atlases that served as the definitive guides of observable science, similar to a scientific Bible. These atlases revolutionized discussions surrounding scientific objectivity [3]. Atlases serves as functional tool for visual sciences by training the observer to recognize certain objects as exemplary (commonly referred to as typical) and to perceive them in a certain manner. In instances where atlases present images captured through new instruments (such as X-ray atlases from the early 20th century), the entire field associated with atlas necessitates a fresh interpretive approach. Even in disciplines where other senses are essential, atlases rely on visuals, as they play a crucial role in refining observational skills [3].

led to the emergence of technical artifacts,[4] constructed in scientific laboratories, and endowed with novel properties crucial for knowledge creation. Beyond their utilitarian function, the materiality of artifacts emerges as a critical aspect. Unlike idealized entities, artifacts are rooted in the real world, embedded within cultural environments, historical periods, and social practices, rendering them intentionally connected (ontologically, rather than causally) to the processes involved in their interaction. Through the act of creation, humans reshape and refine nature, generating new objects that serve as tools for conceptualizing idealizations and understanding the world. Technical artifacts employed in scientific endeavors possess distinctive characteristics and functionalities, constituting integral elements essential for maintaining scientific knowledge stability. Consequently, artifacts can be understood as components within a system imbued with "material," capable of embodying culture-specific meanings, mechanisms for production, processes of learning and interpretation, and catalysts for cultural evolution. In essence, artifacts hold ontological significance, embodying the essence of culture in ways that transcend mere representation and contribute profoundly to the dynamics of knowledge creation and transformation [4].

The artificial nature of an object cannot be fully understood in isolation from contextual elements such as other objects, relationships, and operational frameworks; these elements collectively unveil the object's essence as an artifact. As M. Polanyi suggests, the presence of a tool, or the tool itself, transcends mere mechanical adequacy; it assumes a role similar to an extension of the human body, seamlessly integrated into our physicality or expanding our bodily capabilities through incorporation. M. Lynch further elaborates on this notion, referring to Polanyi's concept as "interiorization" [6], the process through which a physical tool becomes an integral part of our embodied experience. The dichotomy between "objective" and "constructed" realities emerges within laboratory-driven scientific practices, where the distinction between artifact and natural objectivity is a subject of intense scrutiny and debate.[5]

Lynch's analysis of artifacts in scientific practices distinguishes between positive and negative artifacts. Positive artifacts are characterized by their external manifestation, such as a blemish on a microscope slide. They form part of the subjective conditions of observation, relying on the instrumental conditions of perception. Lynch outlines several key characteristics of these artifacts. First, they are tangible and visible, making them accessible for examination. Second, they are prevalent and reproducible, often presenting routine challenges encountered in creating technical images. Furthermore, once recognized as artifacts, they can be effectively separated from appropriately constructed image features like those in an electron micrograph. However, the detection of such artifacts prompts consideration of whether they should be acknowledged and integrated into subsequent analyses and research endeavors.

However, Lynch highlights certain challenges associated with adopting an "ethnographic" focus on artifacts within laboratory settings. First, he observes that the artifacts presented as examples in reports exclude all potential artificial elements within the studies. This selective presentation may distort the understanding of what constitutes an artifact. Second, what is artificial is often determined by how it is presented in the reporting records. For example, a neural ultrastructure can be represented as an analytical dataset. This dataset assumes the status of an artifact within the field of neural entities accessible through analysis. The presentation format of the artifact may be characterized by the two-dimensionality of the photograph; black and white textural variations that delineate the forms of the photographed phenomenon; and sequencing photographic series to depict a continuous sequence of events [6]. Recording can be viewed as a means of visualizing an otherwise imperceptible phenomenon. However, in numerous instances, artifacts have been discovered in laboratory reports detailing previously unanticipated phenomena. These artifacts emerged as discoveries, representing new phenomena in previously unexplored areas. These are what Lynch referred to as situational or negative artifacts. In any case, Lynch notes that instances of such artifacts evolving into discoveries imply that the outcome of an observation or experiment is greatly influenced by the conditions under which it is conducted.

Lynch provides an illustrative example of the discovery of the microglia phenomenon as an artifact, elucidating the interplay between positive and negative artifacts within scientific practices [6]. Its "incredibility" stemmed not from empirical impossibility but from being an isolated occurrence among a more credible alternative narrative. The theoretical

[4] "Artifacts are objects intentionally made to serve a given purpose; natural objects come into being without intervention of any agents. Artifacts inherently possess intended functions, while natural objects do not" [5]. On the one hand, artifacts are commonly understood as objects created for specific purpose , distinct from natural objects. On the other hand, modern epistemology studies rightly highlight that a technical artifact can be not only artificially designed but also a completely natural, living organism used to address certain challenges. In such instances, we must acknowledge that an artifact's defining characteristic is not solely its artificiality but rather its use in human cognitive endeavors. Functionality stands as one of its core properties. "An artifact includes a vaccine, hadron collider, and poking stick. These objects are all connected to the human life-world, defining them as technical artifacts" [4].

[5] Karl Popper observes that "objectivity is closely linked with the social aspect of the scientific method, emphasizing that science and scientific objectivity emerge not solely from an individual scientist's effort to remain "objective" but from the collaborative yet adverse cooperation of numerous scientists. Scientific objectivity can be understood as the intersubjectivity of the scientific method. However, this social aspect of science is often neglected by those identifying as sociologists of knowledge" [6].

framework that gave particular significance to the capillary microglia (via a series of close-up images) resulted from a deeper investigation into the phenomenon than would otherwise have occurred. The microglia photograph posed challenges not only because it contradicted a laboratory assumption regarding microglia in brain physiology but also due to the presence of a competing assumption documented within the photo. Not only did the appearance of microglial cells in the laboratory version of brain physiology lack a clear explanation, but it also served as potential evidence for an alternative explanation. The depiction of microglia within capillaries reflects an unconscious construct more than an accurate representation of reality [6].

In this instance, the example of an artifact did not manifest in a tangible, positive sense. The actual appearance of the phenomenon was not the primary issue; rather, the challenge stemmed from a different interpretation of materiality. Axon sprouting showed a material extension in a direction contrary to what had been widely accepted as indisputable among laboratory researchers, sparking a challenge based on an alternative material argument [6]. This artifact became evident within a specific discourse regarding sprouting axons, leading to controversy. In scenarios like this, where conflicting viewpoints clash, the artifact assumes a role that is more similar to an "antithing" rather than a concrete object. Artifacts transcend being mere "things;" they can also represent opportunities that emerge in contrast to established expectations. These characteristics were often noted by their absence rather than presence observations (such as spots, stains, and blurring in photographs, which could be interpreted as "intrusions").[6] In this context, the artifacts arose within the realm of uncertainty.

Negative artifacts are not viewed as intrusions, distortions, or specific defects in the observed field but rather as the absence of the expected results or effects. In the context of negative artifacts, the lack of a positive result from an experiment or observation implies the adequacy of the laboratory procedures undertaken, allowing for an examination of any factors that may have contributed to the achieved result. Failure caused by uncertainty prompts an investigation into why the desired result was not achieved. Lynch considered the uncertainty associated with such negative results as an essential addition to the technical framework necessary for achieving objectivity [6]. The implications of failure vary depending on the local circumstances, with some instances being attributed to approximately objective factors.

In research endeavors aiming to minimize subjective errors, positive artifacts manifest as intrusions within the visual domain of a natural phenomenon. Conversely, negative artifacts signify the ongoing search for an elusive object, highlighting the investigation process itself. However, mere search efforts are not enough to avoid errors; achieving success requires controlling circumstances to achieve the desired result. Negative artifacts represent the potential existence of "hidden" elements, much like the artifacts themselves, which conceal their presence until technical modifications unveil their existence during testing. Consequently, negative artifacts set the stage for actualizing previously unforeseen objects under specific circumstances. When errors occur, they are attributed to subjective factors hindering the accurate representation of the object itself. Furthermore, tools and equipment have imperfections, defects, and associated errors. As elaborated below, the materiality inherent in scientific practices profoundly influences the attainment of scientific objectivity and bestows epistemic significance upon the technologies utilized in its attainment.

MODERN MEDICAL PRACTICES: DISTRIBUTED AGENCY AND THE EPISTEMIC STATUS OF AI

The rejection of the traditional cognitive subject–object model within scientific research, marked by the "material turn," attributes all aspects of the research process and its outcome (i.e., scientific knowledge) to social characteristics. "Forgetting artifacts (in the sense of tangible objects) has led to the creation of another kind of artifact (in the sense of an illusion): a society sustained solely by social constructs" [7]. As a result, the knowledge we obtain is determined by the social processes involved in its production. This acquired knowledge represents the final result of the scientist's work. In classical science, knowledge acquires a logical form because it aligns with the object studied. However, in contemporary practice, knowledge attains scientific status not only because of its logical correspondence with reality but also due to its functional utility within society as an artifact. This functional success often marks the social processes involved in its production. The scientist's role is not merely detached from the research object but involves a specific form of subjectivity characterized by submission to the object's resistance to complete control. This dynamic creates a sense of scientific subjectlessness in which the scientist is an evaluator of an ever-present object but lacks ultimate authority in its judgment. B. Latour argues that within the realm of science, there is no concept of authoritative finality found in legal proceedings ("the authority of the adjudicated case (*res judicata*)" [8]. However, he introduces the notion of an independent hybrid entity as a third party in decision-making processes. These hybrids serve as representatives speaking on behalf of scientists who, in turn, speak on

[6] For example, Galileo's experimental method, in contrast to Bacon's empirical approach, facilitates the integration of speculative frameworks and empirical models through technical engagement act. Simultaneously, the observation of sunspots through a telescope had to be justified as a product of observation rather than an artifact generated by the telescope itself.

behalf of "things" or objects under study. In this context, the scientist's role shifts from attempting to dominate the object to enabling it to express itself ("make it speak"). The facts play a dual role; they represent what they speak about and determine the truth of their statements [8; p. 82].[7]

For Latour, science is not just discourse; it is primarily a network of practices for fact production. In the context of understanding science as technoscience, where technology and engineering are not merely applied to science but are integral to development, AI occupies a unique epistemic status as an agent (or actor) that cannot be excluded from the scientific practice where it operates. Consequently, the question of innovation in science during the digital age is closely related to how scientific identity is evolving. What actions must scientists take to nurture science, and how does objectivity as an epistemic principle fare in today's landscape? By the end of the 20th century, the emergence of new technologies and a hybridized approach to scientific inquiry relegated what was once considered a method of representing nature to a secondary role. The integration of natural elements and human-made artifacts in the scientific realm, particularly in creating images at the atomic scale, shifts the focus from representation to presentation strategies.[8] Within the context of nanotechnology's evolution from the 20th to the 21st century, Daston and Galison introduced the concept of "image-as-tool" to describe a new approach to scientific visualization. This conceptual shift redefines modern scientific images; and transcends mere representations to become active tools for manipulating and exploring the depicted objects.[9] In this sense, the most profound change, delineating the shift from representative to representational strategies, unfolds precisely within the domain of the scientific self. In this amalgamation of disciplines, the delineation between the scientist and engineer, once sharply defined, gradually fades. As this convergence solidifies into a unified scientific-engineering identity, a new perspective on images emerges. No longer mere representations, these images assume an active role as tools that are seamlessly integrated into the scientific apparatus. They are similar to computer screens that reveal the intricate maneuvers of a robot performing surgery from a remote location, adjustments made to satellites orbiting in space, the processes involved in chemical reactions, or the delicate task of defusing a bomb [1]. Modern scientific practices, especially those driven by AI, increasingly seek to minimize human subjectivity[10] in creating and observing objective images. This trend extends to the point of potentially eradicating the human self from the process to prevent any potential interference or misinterpretation of the observed phenomenon. This prompts a critical question: are these new technologies posing a threat to the traditional scientific self, historically guided by objectivity as an epistemic virtue? Moreover, are we witnessing the emergence of new epistemic regimes that break the link between ethics and epistemology? Alternatively, could algorithms replacing human agency in scientific endeavors be the new custodians of epistemic virtues?

For example, the image of a disciplined, meticulous observer who refrains from intervening in the process but only impartially records and accurately interprets observed phenomena embodies the essence of the "objective" scientist.

[7] It is no coincidence that the realms of law and science are closely linked; they both share a common virtue, impartiality, achieved through meticulous distance and precision. Each area has its unique language and mode of thinking. For example, Latour suggests viewing the Council of State as a laboratory in the search for objectivity pursued by scientists. "The role of the *conseiller du gouvernement* is similar to that of a scientist to the extent that they speak and publish under their own name; similarly, scientist all possess elements similar to the *conseiller du gouvernement*, seeing themselves as enlightening the world. The *conseiller du gouvernement* is, thus a strange and complex hybrid, embodying the sovereignty of *lex animata*, law incarnated in a person, yet their declarations bind only themselves <...> the *conseiller du gouvernemen*t is a unique exemplar of producing objections, or, of objectivity" [8]. The fundamental link between legal and scientific endeavors lies in the art of manipulation of texts and records in a broader sense.

[8] This transition is characterized by the following state: "On one side are the older atlases that aimed, through representation, at fidelity to nature. Capturing nature accurately on the page might align with the 18th-century concept of truth-to-nature, yet it could also adhere to 19th century's mechanical objectivity or 20th-century trained judgment. On the other side are the newer forms of image galleries that serves as presentations, where the presentational strategy can include either new entities (such as rearranged nanotubes, DNA strands, or diodes) or the presentations' explicit embrace of deliberate enhancements to clarify, persuade, delight—and sometimes, market" [1]. O.E. Stolyarova notes that by highlighting these two strategies (representational and presentational) Daston and Galison implicitly create an ontology of "collective formation" [9], with epistemological implications that, using I. Hacking terminology , involve intervention as the formation of the new rather than the reproduction of the existing. This pragmatically interpreted constructivism imposes an ontological framework on our theorizing and practice, shaping what is termed as "second nature." In modern epistemology, the concept of the subject is evolving; the disembodied subject is giving way to the embodied subject. The outcomes of the embodied subject's engagement with the world no longer merely yield subjective images of an objective reality but rather artifacts that, according to Latour, expand our capacities and connect us with other individuals and social groups, thereby changing our needs.

[9] The ability of modern scientists to manipulate nanoobjects and their nanoimages is in itself amazing. However, equally surprising is the fact that "produced by an atomic force microscope that measures the force between a tiny probe and a surface over which the probe scans, [these figures are] not intended to depict a "natural" phenomenon. Instead, this and similar haptic images are part and parcel of the fabrication process itself" [1].

[10] Note that the desire to minimize the self not only goes along with the desire to minimize subjectivity and thus errors related to the human factor, but "makes some routine procedures unnecessary for HCPs. The reduction of time and material costs is another important advantage of using AI in medicine" [10].

To achieve objective (i.e., to uphold the epistemic virtue of objectivity), it was not simply about advancing scientific knowledge, but primarily about relinquishing personal biases and desires, such as refraining from altering a photograph. In this context, a change in epistemic virtues is not just a change in scientific practices but a also change in the ethical guidelines that guide a scientist's behavior. However, as observed by Daston and Galison, "Yet these three virtues all served, each in its way, a common goal: what we have called a faithful representation of nature" [1]. In the 20th century, traditional methods of representing nature, which seemed self-evident, were pushed into the background with the emergence of new technologies. This shift also transformed and significantly broadened scientific identity, now acknowledging neural networks and AI-based technologies as essential non-negotiable elements in decision-making processes.[11]

As visual representation in scientific endeavors is increasingly interconnected with computers and computational formats, their digital materiality requires a special approach.[12] In the not-so-distant past, as the 20th century transitioned into the 21st century, there was a belief that the role of the scientist-observer would eventually be supplanted by enhanced algorithms and imaging technologies devoid of human intervention. However, the creation of new digital atlases, in contrast with earlier brain mapping methods, now imposes new requirements on exercising control and limiting personal biases in pursuit of what is termed "digital objectivity"[13] [12]. Digital scans are integral to a complex infrastructure that provides visual knowledge in a manner distinctly different from merely assessing mechanically generated objective representations by an observer. Alongside the objective perspective, a relational viewpoint becomes imperative, treating the image as a dataset intertwined with the object under investigation. Within the realm of big data in science, the pursuit of delivering intricate and exhaustive data representations often results in a selective reflection of significant information. This selectivity is largely shaped by the technologies and platforms used for data collection, as well as the fundamental ontological perspectives guiding the data. In essence, the data suggest a selective view that is tuned certainly and limited to the use of certain tools [13].

Emerging methodologies in data analysis, such as advances in machine learning, computer vision, and innovative visualization techniques, are revolutionizing modern scientific investigations. In fields like nanoscience, where the emphasis lies on discovering and exploring new phenomena, a unique form of visualization is crucial to capture these phenomena effectively. However, the question of whether a new mode of representation is emerging may not have a straightforward answer; there could be uncertainty regarding the novelty of such methods. Nevertheless, there is no doubt that in fields like nanotechnology and other dynamic scientific fields, strict adherence to replicating the exact properties of the study object is no longer the dominant requirement for the object under study. Digital atlases, beyond attaining mechanical objectivity through scanning and visualization technologies, "are shaped by the deployment of computer-supported statistical and quantitative tools, serving as additional means for validation and ensuring objectivity" [12]. In these contexts, the assumption is that digital imaging can promote the epistemic ideal of objectivity by using automated processes, thereby reducing the need for human intervention in data processing.

Finally, the evolution of scientific value manifests itself in the transformation of the epistemic virtue of objectivity. Initially rooted in the historical ideal of science, objectivity now assumes a new form as a scientific value, intertwined with the pursuit of refining artifacts toward a more instrumental image. This transition from representation to presentation becomes a turning point in the history of visual practices and objectivity, highlighting the coupling of representation practices with their construction process; the accuracy of photographic images does not delegate objectivity to technology as a desire to minimize subjectivity.[14]

Introducing AI-based technologies and computer vision aims to standardize image streams for primary and automated defects and pathology detection, as well as upscale screening programs. For example, a biomedical

[11] For example, observing and visualizing using digital atlases of the brain is mainly done behind a computer monitor [11]. This implies changing the relationship between the observer, the object observed, the technologies used, and the institutional arrangements that enable the practice of surveillance. A digital atlas, in contrast to the atlases discussed by Daston and Galison, takes on the characteristics of a tool that is not so much a representative as a presenter, since it can both represent and be used to improve representations.

[12] For example, a brain scan result is not a static snapshot, and some of Daston and Galison's assumptions about mechanical objectivity do not directly apply to brain scans [11]. Advances in computer technology have integrated brain scans into a digital and networked context, leading to brain scans less representative but more presentative.

[13] During the 1990s, known as the Decade of the Brain, numerous digital and electronic resources were developed to facilitate the organization and integration of various neuroscience sub-fields. This approach, termed neuroinformatics, aims to rationalize and integrate sub-fields. In the process of developing atlases, the definition of objective neuroscientific knowledge undergoes significant redefinition. This redefinitions influenced by the technological possibilities of these tools and the standardization constraints inherent in projects involving multiple measurements. The term "digital objectivity" is proposed to describe a specific configuration of ideals, methodologies, and cognitive objects in modern cyberscience [12].

[14] For example, R. Buiani details cases where technology falls short in detecting significant differences, prompting researchers to manually enhance, highlight, and organize image elements [14].

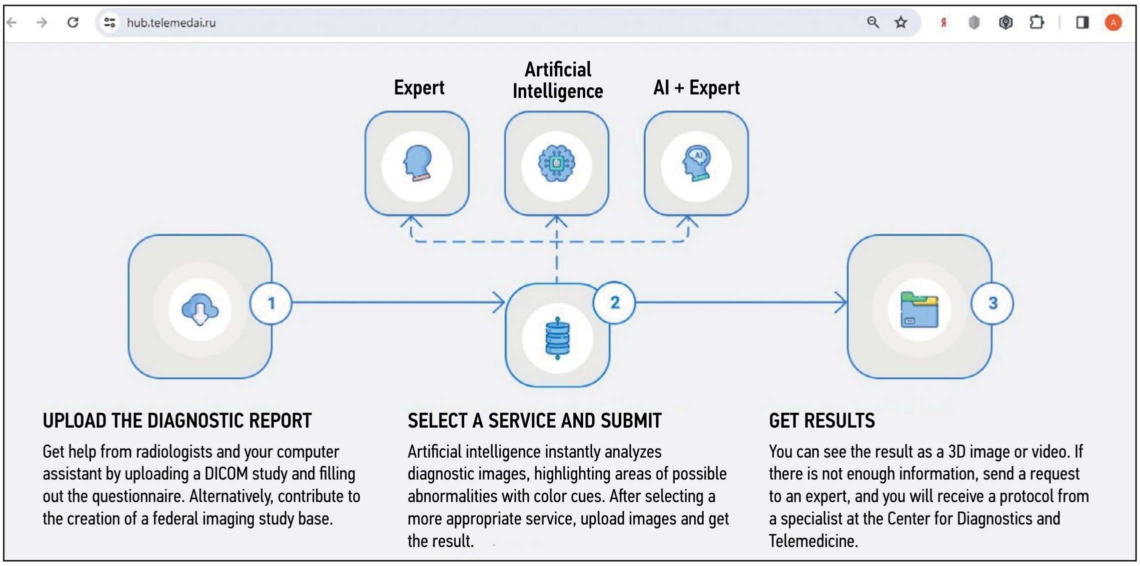

Fig. 1. Screenshot of the project page for a telemedicine platform for HCPs describing the examination process.

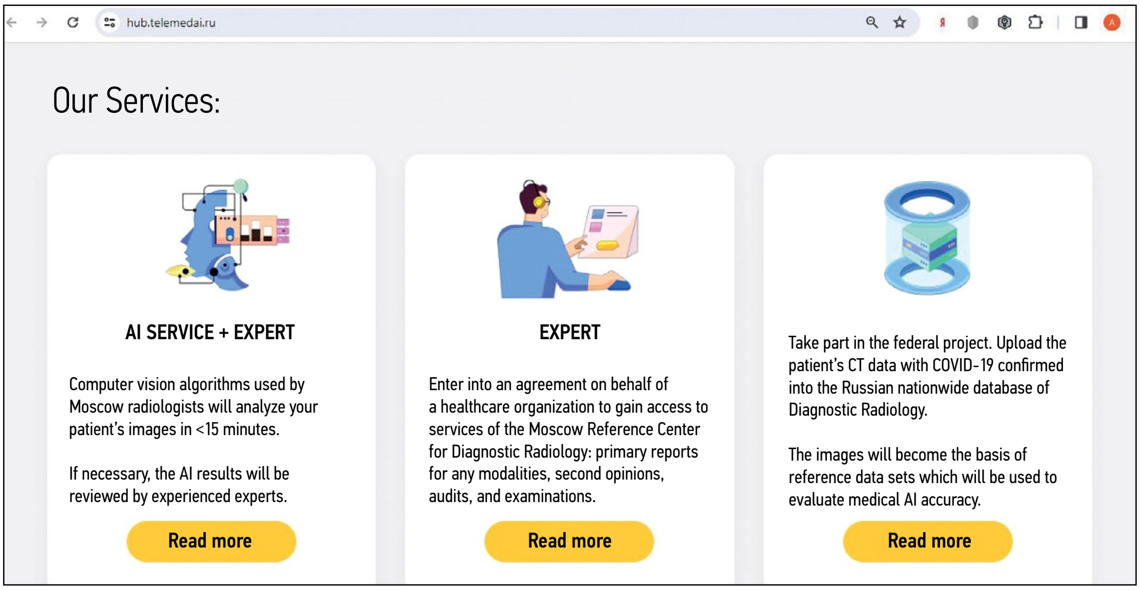

Fig. 2. Screenshot of the project page for a telemedicine platform for HCPs describing the services provided.

image analysis service in Moscow explores using AI data analysis for decision support in healthcare.[15] This service minimizes diagnostic error risks but does not eliminate false positives. HCPs are integral to the process but work alongside AI in a hybrid model. HCPs' objectivity in decision-making hinges on data analysis from the service. Initially, however, HCPs' expert opinion is not required, only becoming necessary if the AI results are unsatisfactory. Computer vision algorithms analyze images, reviewed by experts if necessary (Fig. 1 and 2).

ETHICAL CHALLENGES: PROS AND CONS OF AGENCY AND THE SUBJECTIVITY OF AI

AI-based robots are already providing significant assistance to both HCPs and patients in diagnosis, therapy, and surgery. Russia has embraced robotic medical systems, as exemplified by the Assisted Surgical Technologies robotic surgeon.[16] In therapy, a preliminary diagnosis is traditionally made by a primary care physician. However, robots are already doing this job; special

[15] The study includes three projects: Experiment on the Use of Innovative Computer Vision Technologies for Medical Image Analysis and Further Application in the Moscow Healthcare System; HUB AI Consultant (service for automatic X-ray analysis for HCPs), and Speech Recognition Technologies in Healthcare using an AI-based technology for automatic conversion of spoken speech to text to help HCPs to voice control a workstation and dictate diagnostic findings instead of typing them manually [15].

[16] https://new.fips.ru/registers-doc-view/fips_servlet?DB=RUPAT&DocNumber=2715400&TypeFile=html [Accessed 09 February 2024].

sensors placed on the patient's body gather all the information and transmit it to the HCP in case of abnormalities. The system can diagnose in place of an HCP. The Russian RoboScan diagnostic system performs automated ultrasound scanning.

The proper use of neural networks in medical practice, such as detecting pulmonary COVID-19 lesions, helps in reducing tomography's radiation dose. A pre-trained neural network model acts as an expert,[17] enhancing objectivity by standardizing data collection, initial diagnosis, and, sometimes, preliminary decisions. This shift reduces the burden on HCPs, allowing them to focus on data analysis, interpretation, and conclusion. Increasingly, HCPs delegate responsibilities to AI, including data processing, diagnosis, treatment planning, patient interaction, and decision-making. However, this trend prompts questions about AI's potential to completely replace HCPs and the ethical challenges that may arise [15-16].

What are the consequences of misdiagnosis or failure to detect a pathology, and who bears the responsibility for these decisions? Russia stands among the pioneers globally in recognizing the risks and threats, delineated in the AI Code of Ethics [17], as threats to human rights and freedoms, associated with the digitization and application of AI technologies within the medical field. These threats to discrimination, loss of privacy, loss of control over AI, potential harm to individuals stemming from AI errors, and misuse of AI. For example, the Russian Service for Surveillance in Healthcare recently suspended the use of a system designed to analyze computed tomography images, known as Botkin.AI, citing concerns over "the threat to the life and health of citizens."[18]

The traditional domain of decision-making, once the sole purview of human experts, is now shifting toward AI systems. Given that achieving a Technosphere similar to nature necessitates delegating decision-making authority to technical systems, this trend is expected to continue over the next 10–20 years.[19] Concurrently, the digital transformation of modern medicine is occurring not only at a procedural level but also at the communicative interface, where HCPs and patients may find themselves separated by technological barriers. Indeed, digital technologies usher in an era of expanded network space, significantly augmenting the potential to bride and surpass existing, notable geographical boundaries between HCPs and patients. This paradigm shift also opens avenues for the potential replacement and displacement of expert HCPs from their traditional professional domains, yet, among these transformations, opportunities have emerged to form a networked collective expert subject through digital laboratories and multidisciplinary discussions [19].

The inclination toward substituting and partially displacing the expert functions of the HCP with quasi-expert functions using digital technologies indicates a new form of communication. This shift moves from the traditional dynamic between an expert (medical professional) and a layman (a nonspecialist patient) to a hybrid model of "doctor plus software to patient" and, in the long run, to a "software to patient" communicative model. This evolution challenges the expert status of HCPs, transferring the role of possessing absolute or near-absolute knowledge to digital programs. Although this model is technocentric, it also, to some extent, becomes patient-centered by leveling the physician's role [19; pp. 166–167]. The delegation of expert functions to technologies reflects a broader trend aimed at mitigating diagnostic errors by HCPs. The higher accuracy of AI in diagnosing pathology or predicting disease risks fuels the desire to substitute expert functions with algorithms. Consequently, decision support systems claim to be not merely human tools but full-fledged actors performing complex procedures. This progression diminishes irreparable biases. Technology assumes the responsibility of making judgments about the reality it perceives [19; pp. 167–168]. In this context, it is foreseeable that if the trend persists to limit human involvement in favor of AI, we will inevitably confront the need to view AI-based technologies not merely as tools but as entities with full agency and subjectivity, accompanied by their advantages and drawbacks.

ADDITIONAL INFORMATION

Funding source. This article was not supported by any external sources of funding.

Competing interests. The author declares that she has no competing interests.

[17] "The proposed method reduces the total number of X-ray projections and the radiation dose required for COVID-19 detection without significantly affecting the prediction accuracy. The proposed protocol was evaluated on 163 patients from the COVID-CTset dataset and achieved an average dose reduction of 15.1%, while the average reduction in prediction accuracy was only 1.9%. Pareto optimality was improved compared to the fixed protocol" [16].

[18] https://www.kommersant.ru/doc/6350252 [Accessed 09 February 2024].

[19] No comprehensive studies have yet explored the perspectives of HCPs and patients regarding their the implementation of AI into medical practice. However, a recent public opinion survey, the first of its kind to assess HCPs' interest in using AI in medicine and healthcare while also identifying challenges and prospects, reached an optimistic conclusion. According to the survey, "Russian HCPs are supportive of AI in medicine. Most respondents believe that AI will not replace them in the future but will instead serve as valuable tool for optimizing organizational processes, research, and diseases diagnosis." According to the report, several potential challenges in using AI were highlighted by respondents. These include concerns about the lack of flexibility and limited applicability in controversial situations (cited by 64% and 60% of respondents, respectively). Additionally, 56% believe that decision-making using AI could be challenging when there is no sufficient information available for analysis. One-third of HCPs expressed worry about the involvement of specialists with limited experience in AI. Notably, 89% of respondents believe that HCPs should be actively participate in the development of AI for medicine and healthcare. Interesting, only 20 respondents (6.6%) agreed that AI could replace them at work. However, a significant majority (76%) of respondents believe that in the future, doctors who use AI will replace those who do not" [18].

REFERENCES

1. Daston L, Galison P. *Objectivity.* Ivanov KV, editor. Moscow: Novoe literaturnoe obozrenie; 2018. (In Russ). EDN: PIXKTY

2. Mol A. *The body multiple ontology in medical practice.* Gavrilenko SM, Pisarev AA, editors. Perm: Gile Press; 2017. EDN: LJXRPN

3. Daston L, Galison P. The Image of Objectivity. *Representations.* 1992;(40):81–128. doi: 10.2307/2928741

4. Maslanov EV. Artifact: culture and nature. In: *Epistemology today. ideas, problems, discussions.* Kasavin IT, Alekseeva DA, Antonovskii AYu, et al, editors. N. Novgorod: Lobachevsky State University of Nizhni Novgorod; 2018. P:295–299. EDN: ELYPTC

5. Baker LR. Ontological significance of artifacts. In: *Ontologies of artifacts: the interaction of "natural" and "artificial" components of the lifeworld.* Stolyarova OE, editor. Moscow: Izdatel'skii Dom «Delo» RANKhiGS; 2012. P:18–33. (In Russ).

6. Lynch M. *Art and Artifact in Laboratory Science: A Study of Shop Work and Shop Talk in a Research Laboratory.* London/Boston/Melbourne: Routledge & Kegan Paul; 1985.

7. Latour B, Vakhshtain V, Smirnov A. On interobjectivity. *Russian sociological review.* 2007;6(2):79–96. (In Russ). EDN: JWURYH

8. Latour B. Scientific objects and legal objectivity. *Kul'tivator.* 2011;(2):74–95. (In Russ).

9. Stolyarova OE. The historical context of science: material culture and ontologies. *Epistemology and philosophy of science.* 2011;30(4):32–50. (In Russ). EDN: OPDQIX

10. Alekseeva MG, Zubov AI, Novikov MYu. Artificial intelligence in medicine. *International Research Journal.* 2022;(7(121)):10–13. EDN: JMMMDF doi: 10.23670/IRJ.2022.121.7.038

11. Beaulieu A, de Rijcke S. Networked Neuroscience: Brain Scans and Visual Knowing at the Intersection of Atlases and Databases. Coopmans C, Woolgar S, editors. In: *Representation in Scientific Practice Revisited*. Coopmans C, Vertesi J, Lynch M, Woolgar S, editors. Cambridge: MIT Press; 2014. P:131–152. doi: 10.7551/mitpress/9780262525381.003.0007

12. Beaulieu A. Voxels in the Brain: Neuroscience, Informatics and Changing Notions of Objectivity. *Social Studies of Science.* 2001;31(5):635–680. doi: 10.1177/030631201031005001

13. Kitchin R. Big data, new epistemologies and paradigm shifts. *Sociology: methodology, methods, mathematical modeling (4M).* 2017;(44):111–152. EDN: YMAFTQ

14. Buiani R. Innovation and Compliance in Making and Perceiving the Scientific Visualization of Viruses. *Canadian Journal of Communication.* 2014;39(4):539–556. doi: 10.22230/cjc.2014v39n4a2738

15. Center for diagnostics and telemedicine [Internet]. Moscow; c2013-2023 [cited 2023 Nov 29]. Available from: https://mosmed.ai/

16. Bulatov KB, Ingacheva AS, Gilmanov MI, et al. Reducing radiation dose for NN-based COVID-19 detection in helical chest CT using real-time monitored reconstruction. *Expert Systems with Applications.* 2023;229 Part A. doi: 10.1016/j.eswa.2023.120425

17. AI ethics code [Internet]. AI Alliance Russia, c2020-2024 [cited 2024 Feb 9]. Available from: https://ethics.a-ai.ru/

18. Orlova IA, Akopyan ZhA, Plisyuk AG, et al. Opinion research among Russian Physicians on the application of technologies using artificial intelligence in the field of medicine and health care. *BMC Health Services Research.* 2023;23(1):749. doi: 10.1186/s12913-023-09493-6

19. Popova OV. Digitalization and transformation of medicine: problems and prospects for development. In: *Modern problems of socio-technical-anthroposphere: a collective monograph.* Budanov VG, editor. Kursk: Universitetskaya kniga; 2022. P:153–171. (In Russ).

СПИСОК ЛИТЕРАТУРЫ

1. Дастон Л., Галисон П. Объективность / под ред. К.В. Иванова. Москва: Новое литературное обозрение, 2018. EDN: PIXKTY

2. Мол А. Множественное тело: Онтология в медицинской практике / под ред. С.М. Гавриленко, А.А. Писарева. Пермь : Гиле Пресс, 2017. EDN: LJXRPN

3. Daston L., Galison P. The Image of Objectivity // Representations. 1992. N 40. P. 81–128. doi: 10.2307/2928741

4. Масланов Е.В. Артефакт: культура и природа. В: Эпистемология сегодня. Идеи, проблемы, дискуссии / под ред. И.Т. Касавина, Д.А. Алексеевой, А.Ю. Антоновского, и др. Н. Новгород : Национальный исследовательский Нижегородский государственный госуниверситет им. Н.И. Лобачевского, 2018. С. 295–299. EDN: ELYPTC

5. Бейкер Л.Р. Онтологическая значимость артефактов. В: Онтологии артефактов: взаимодействие «естественных» и «искусственных» компонентов жизненного мира / под ред. О.Е. Столяровой. Москва : Издательский дом «Дело» РАНХиГС, 2012. С. 18–33.

6. Lynch M. Art and Artifact in Laboratory Science: A Study of Shop Work and Shop Talk in a Research Laboratory. London/Boston/Melbourne : Routledge & Kegan Paul, 1985.

7. Латур Б., Вахштайн В., Смирнов А. Об интеробъективности // Социологическое обозрение. 2007. Т. 6, № 2. С. 79–96. EDN: JWURYH

8. Латур Б. Научные объекты и правовая объективность // Культиватор. 2011. № 2. С. 74–95.

9. Столярова О.Е. Исторический контекст науки: материальная культура и онтологии // Эпистемология и философия науки. 2011. Т. 30, № 4. С. 32–50. EDN: OPDQIX

10. Алексеева М.Г., Зубов А.И., Новиков М.Ю. Искусственный интеллект в медицине // Международный научно-исследовательский журнал. 2022. № 7 (121). С. 10–13. EDN: JMMMDF doi: 10.23670/IRJ.2022.121.7.038

11. Beaulieu A., de Rijcke S. Networked Neuroscience: Brain Scans and Visual Knowing at the Intersection of Atlases and Databases. Coopmans C., Woolgar S., editors. In: Representation in Scientific Practice Revisited. Coopmans C., Vertesi J., Lynch M., Woolgar S., editors. Cambridge : MIT Press, 2014. P. 131–152. doi: 10.7551/mitpress/9780262525381.003.0007

12. Beaulieu A. Voxels in the Brain: Neuroscience, Informatics and Changing Notions of Objectivity // Social Studies of Science. 2001. Vol. 31, N 5. P. 635–680. doi: 10.1177/030631201031005001

13. Китчин Р. Большие данные, новые эпистемологии и смена парадигм // Социология: методология, методы, математическое моделирование. 2017. № 44. С. 111–152. EDN: YMAFTQ

14. Buiani R. Innovation and Compliance in Making and Perceiving the Scientific Visualization of Viruses. Canadian

Journal of Communication. 2014. Vol. 39, N 4. P. 539–556. doi: 10.22230/cjc.2014v39n4a2738
15. Центр диагностики и телемедицины [Internet]. Москва; c2013-2023 [дата обращения: 29.11.2023]. Доступ по ссылке: https://mosmed.ai/
16. Bulatov K.B., Ingacheva A.S., Gilmanov M.I., et al. Reducing radiation dose for NN-based COVID-19 detection in helical chest CT using real-time monitored reconstruction // Expert Systems with Applications. 2023. Vol. 229 Part A. doi: 10.1016/j.eswa.2023.120425
17. Кодекс этики в сфере ИИ [Internet]. AI Alliance Russia, c2020-2024 [дата обращения: 09.02.2024]. Доступ по ссылке: https://ethics.a-ai.ru/
18. Orlova I.A., Akopyan Zh.A., Plisyuk A.G., et al. Opinion research among Russian Physicians on the application of technologies using artificial intelligence in the field of medicine and health care // BMC Health Services Research. 2023. Vol. 23, N 1. P. 749. doi: 10.1186/s12913-023-09493-6
19. Попова О.В. Цифровизация и трансформация медицины: проблемы и перспективы развития. В: Современные проблемы социо-техно-антропосферы: коллективная монография / под ред. В.Г. Буданова. Курск : Университетская книга, 2022. С. 153–171.

AUTHOR'S INFO

Angelina V. Baeva, Cand. Sci. (Philosophy);
address: 27-4 Lomonosovsky Prospekt,
119192, Moscow, Russia;
ORCID: 0009-0005-5871-6217;
eLibrary SPIN: 2951-1427;
e-mail: a-baeva93@mail.ru

ОБ АВТОРЕ

Баева Ангелина Викторовна, канд. философ. наук;
адрес: Россия, 119192, Москва,
Ломоносовский проспект, д. 27, к. 4;
ORCID: 0009-0005-5871-6217;
eLibrary SPIN: 2951-1427;
e-mail: a-baeva93@mail.ru